ABSTRACT

Title of Document: CUCURBIT[N]URIL ANALOGUES

Jason Alan Lagona, Ph.D., 2005

Directed By: Professor Lyle D. Isaacs,
Department of Chemistry and Biochemistry

Molecular recognition and self-assembly in aqueous solution have experienced rapid growth in recent years. The use of α-, β-, and γ-cyclodextrins, calixarenes, and cyclophanes have served as the platforms for molecular recognition in aqueous solution. Recently, the investigation of an alternative platform based on cucurbituril has become the focus of several research groups. The rigid structure and capability of forming complexes with molecules and ions through hydrophobic, ion-dipole and hydrogen-bonding interactions make cucurbituril an attractive candidate as a synthetic receptor as well as a building block for the construction of supramolecular architectures.

However, before cucurbituril can be used to supplant the more common platforms as the molecule of choice for molecular recognition and self-assembly in aqueous solution, several advances must be made: 1) cucurbiturils must become available in a variety of sizes, 2) their solubility must be improved, and 3) synthetic procedures must be advanced to include the ability to selectively generate specific cucurbituril homologues, derivatives, and analogues.

Herein, the synthesis of cucurbit[n]uril analogues is presented with control over their size, shape, and solubility. These CB[5], CB[6], and CB[7] analogues all contain bis(phthalhydrazide) walls which are incorporated into the macrocycle. The tailor-made synthesis of these CB[n] analogues proceeds by the condensation of the appropriate bis(electrophile) with bis(phthalhydrazide) which delivers the CB[6] and CB[7] analogues in good yield whereas the CB[5] analogue is formed in low yield. To help rationalize the high yields obtained in these macrocyclization reactions, we performed mechanistic studies of model methylene bridged glycoluril dimers.

The molecular recognition properties of a water soluble cucurbit[6]uril analogue in aqueous buffer toward a variety of guests including alkanediamines, aromatics, amino acids, and nucleobases were studied by fluorescence spectroscopy. For the alkanediamines studied, as the length of the alkane is increased between the amines, the association constants also increase. The CB[6] analogue is capable of forming strong complexes with guests containing aromatic rings with association constants (K_a) ranging from 10^2 to 10^6 M^{-1} due to the favorable π-π interactions that occur between the host and the aromatic portion of the guest while encapsulated in its hydrophobic cavity.

CUCURBIT[N]URIL ANALOGUES

By

Jason Alan Lagona

Dissertation submitted to the Faculty of the Graduate School of the
University of Maryland, College Park, in partial fulfillment
of the requirements for the degree of
Doctor of Philosophy
2005

Advisory Committee:
Associate Professor Lyle Isaacs, Chair
Professor Philip DeShong
Professor Daniel Falvey
Professor Steven Rokita
Associate Professor Sheryl Ehrman, Dean's Representative

Dedication

To my parents, Teresa and Richard,
my brother, Tristan,
my cats, Romeo and Juliet,
and especially my wife, Miriam.

Acknowledgement

I would like to express my sincere appreciation to Professor Lyle Isaacs for his help and guidance throughout the course of the research presented in this dissertation. I also have to thank Dr. Dariusz Witt for his patience while teaching me how to become a technically skilled synthetic organic chemist. Without their help and guidance, this accomplishment would have never been possible.

I would like to thank my parents for their support and encouragement when things were getting unbearable and providing a place to stay during the Fire of June 2005.

I would like to thank the rest of my family for their support as well as the friends I met during the past ten years at the University of Maryland. Cheers and good luck!

Most importantly, I would like to thank my wife for providing endless support, both emotionally and financially. Thanks for putting up with me during these five long years (and thanks for the R32).

Table of Contents

List of Tables

Chapter 1

Chapter 3

List of Figures

Chapter 1

Chapter 2

Chapter 3

List of Schemes

Chapter 1

Chapter 2

List of Abbreviations

Ac	acetyl
anh.	anhydrous
aq.	aqueous
Bn	benzyl
br. s	broad singlet
Bu	butyl
calcd	calculated
conc	concentrated
cy	cyclohexyl
d	doublet
dec	decomposition
DMSO	dimethyl sulfoxide
EI	electron ionization
equiv	equivalent(s)
ESI	electrospray ionization
Et	ethyl
Et_2O	diethyl ether
EtOAc	ethyl acetate
FAB	fast atom bombardment
h	hour(s)
HR-MS	high resolution mass spectrometry

Hz	hertz
IR	infrared
J	coupling constant
m	multiplet
m	meta
M^+	molecular ion
m/z	mass-to-charge ratio
MHz	megahertz
min	minute(s)
M.p.	melting point
MS	mass spectrometry
NMR	nuclear magnetic resonance
o	ortho
OAc	acetate
p	para
Ph	phenyl
PTSA	*p*-toluenesulfonic acid
R_f	retention factor
RT	room temperature
TFA	trifluoroacetic acid
TLC	thin layer chromatography
TMSP	trimethylsilylpropionic acid

I. Chapter 1: Cucurbit[6]uril and Its Homologues

1.1 Introduction

In 1905 – contemporaneous with the pioneering work of Schardinger on the cyclodextrins – Behrend reported that the condensation of glycoluril and formaldehyde in concentrated HCl yields an insoluble polymeric substance now known as Behrend's polymer.[1] Behrend was able to obtain a crystalline substance in good yield (40 – 70%) by recrystallization from concentrated H_2SO_4 and demonstrated its ability to form co-crystals (complexes) with a variety of substances including $KMnO_4$, $AgNO_3$, H_2PtCl_6, $NaAuCl_4$, Congo Red and Methylene Blue. The constitution of this substance remained unclear until 1981 when Mock reinvestigated Behrend's report and disclosed the remarkable macrocyclic structure comprising six glycoluril units and twelve methylene bridges and dubbed it cucurbituril in recognition of its resemblance to a pumpkin which is a prominent member of the *cucurbitaceae* family (Figure 1).[2] We refer to cucurbituril as cucurbit[6]uril and abbreviate this as CB[6] to distinguish it from cucurbit[n]uril (CB[n]) homologues containing a different number of glycoluril units.

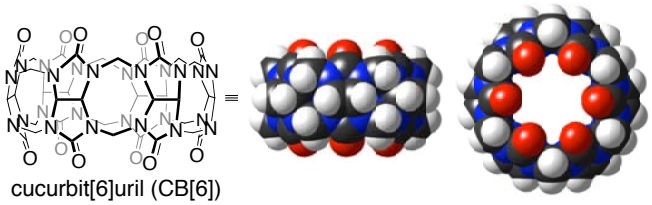

Figure 1. Chemical structure of CB[6] along with side and top views of a space filling model. Color coding: C gray, H white, N blue, O red.

In contrast to the host-guest chemistry of α-, β-, and γ-cyclodextrin which has developed steadily over the past century, the supramolecular chemistry of CB[6] only began to develop in the 1980's and 1990's due to the pioneering work of Mock,[3] Buschmann,[4] and Kim.[5,6] Interest in the CB[n] family has increased dramatically in the new millennium following the preparation of four new CB[n] homologues (CB[5], CB[7], CB[8], and CB[10]•CB[5]) by the groups of Kim and Day.[7-9] CB[5] – CB[8] are now even commercially available. This increase in interest in the CB[n] family correlates with the great advances in many areas of fundamental and applied science – chemistry, biology, materials science, and nanotechnology – that rely on the ability to employ and control non-covalent interactions between molecules. Consequently, CB[6] and the CB[n] family has been the focus of numerous reviews[3,5,6,10-29] and the subject of a number of patents.[21,30-43]

The pioneering work of Lehn, Cram, and Pedersen brought host-guest and supramolecular chemistry to the forefront of contemporary science.[44-46] The scientific insights gained from fundamental studies of non-covalent interactions have been of practical value in a wide range of applications including chromatographic stationary phases, sequestration of contaminants from solution, and the development of catalysts, chemical sensors, and new drugs. All of these applications require the availability of low molecular weight receptors,[47-49] natural or non-natural oligomers and polymers,[50,51] or solid state materials[52-54] that interact with their analytes in high affinity, highly selective binding processes. In response, supramolecular chemists have designed, synthesized, and evaluated the recognition properties of a wide variety

of non-natural receptors – including cyclodextrins, calixarenes, cyclophanes, crown ethers, and many others – that display remarkable affinity and selectivity (Figure 2).[47-49] Amongst these non-natural receptors, α-, β-, and γ-cyclodextrin remain the recognition platform of choice for industrial applications – despite a range of potential limitations which include low affinity, low selectivity, and challenges in their selective functionalization – because they are commercially available and inexpensive.

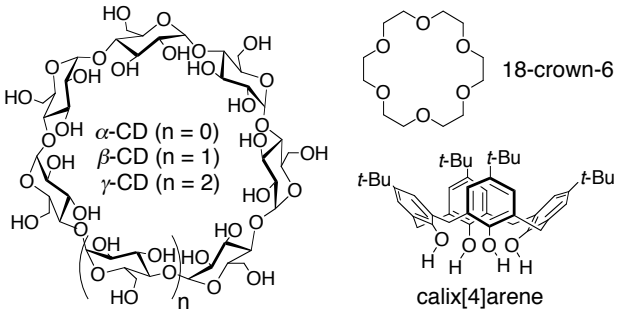

Figure 2. Chemical structures of α-, β-, and γ-cyclodextrin, 18-crown-6, and a calix[4]arene.

In this chapter, we trace the development of the supramolecular chemistry of CB[6] from its early days when it was plagued by issues including poor solubility in aqueous and organic media, a lack of a homologous series of different sized hosts (e.g. CB[n]), and an inability to access CB[n] derivatives and analogues by tailor-made synthetic procedures to the present day when the CB[n] family is emerging as a premiere platform for fundamental and applied molecular recognition and self-assembly studies. We, and others, believe that the CB[n] family is even poised to compete with the cyclodextrins as the platform of choice in industrial-scale applications. Today, the CB[n] family has overcome all of these early issues and

currently possesses a confluence of properties that suggest their high potential in nanotechnology as components of molecular machines. These properties now include: 1) commercial availability in four different sizes, 2) high affinity binding interactions, 3) high selectivity of binding, 4) synthetic control over size, shape, and functional group placement, 5) high structural integrity, 6) solubility in both organic and aqueous solution, and 7) control over the molecular recognition processes by suitable electrochemical, photochemical, and chemical stimuli.

The organization of this chapter is as follows. First, we begin with a discussion of the synthesis of CB[n] and review some of their fundamental chemical and physical properties. Second, we present the recognition properties of the CB[n] family. In this section we emphasize the behavior of the most widely studied cucurbit[n]uril, CB[6], with an emphasis on those aspects of its recognition behavior – protonation, metal binding, selectivity based on size, shape and charge, and the mechanism of binding – that are likely to apply universally to the CB[n] family. Third, we discuss the use of chemical, photochemical, and electrochemical stimuli to control recognition processes within CB[n]. Finally, we discuss some applications of the CB[n] family in areas including catalysis, self-assembled monolayers, waste stream remediation, DNA binding, and gene transfection.

1.2 Synthesis of CB[n]

In the condensation of glycoluril (**I-1**) and formaldehyde, neither Behrend nor Mock detected any macrocyclic compounds (homologues) composed of a different number of glycoluril rings (e.g. CB[5], CB[7], and CB[8]). It was not until nearly 20

years later when this reaction was conducted under milder, kinetically controlled conditions by the groups of Kim and Day that CB[5] – CB[8] and CB[5]@CB[10] were detected and isolated (Scheme 1).[7-9,55]

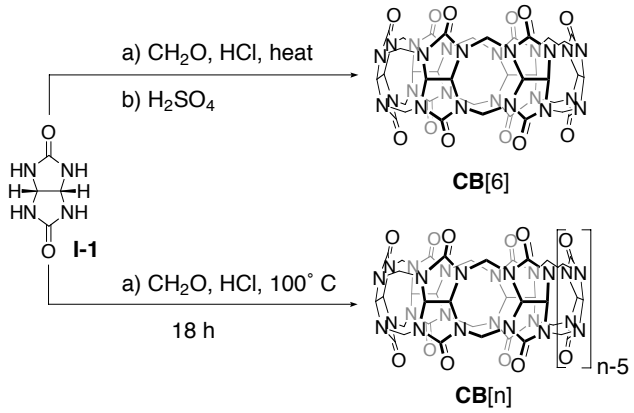

Scheme 1. Synthesis of CB[6] under forcing conditions and a mixture of CB[5] – CB[10] under milder conditions.

1.3 Fundamental Properties of CB[n]

The section highlights several of the fundamental physical and chemical properties of the CB[n] family.

1.3.1 Dimensions

CB[5] – CB[10] are cyclic methylene bridged glycoluril oligomers whose shape resembles a pumpkin. Figure 3 shows the X-ray crystal structures for CB[5], CB[6], CB[7], CB[8], and CB[5]@CB[10]. The cavity of CB[6] in the solid state contains three H-bonded H_2O molecules which can be released upon guest binding.

The defining features of CB[5] – CB[10] are their two ureidyl-carbonyl rimmed portals that provide entry to their hydrophobic cavity.[56] Similar to the cyclodextrins, the various CB[n] have a common depth (9.1 Å), but their equatorial widths, annular widths, and volumes vary systematically with ring size (Table 1). Note that the portals guarding the entry to CB[n] are ≈ 2 Å narrower than the cavity itself. These narrow portals result in constrictive binding that produce significant steric barriers to guest association and dissociation.[57] The cavity sizes available in the CB[n] family span and exceed those available with the cyclodextrins (Table 1).

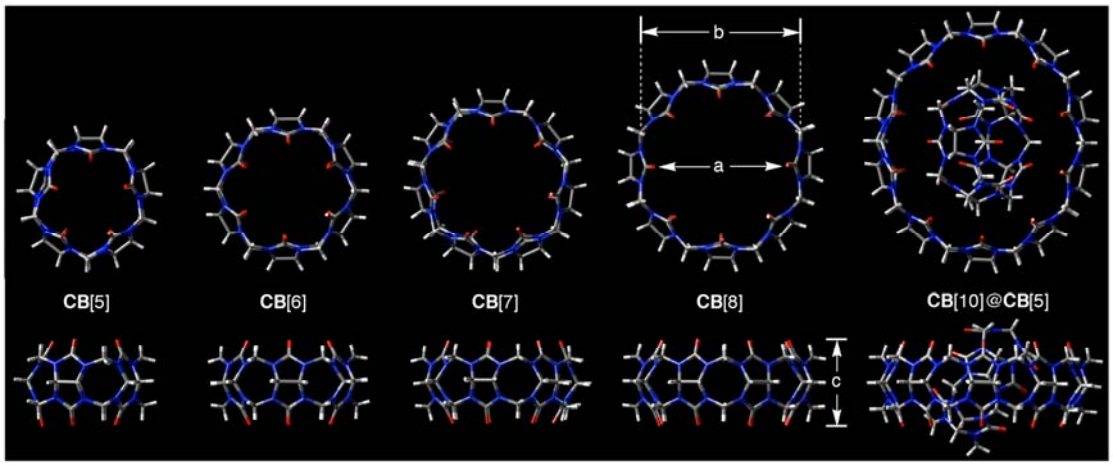

Figure 3. Top and side views of the X-ray crystal structures of CB[5],[7] CB[6],[2] CB[7],[7] CB[8],[7] and CB[5]@CB[10].[9] The various CB[n] are drawn to scale.

Table 1: Dimensions and physical properties of CB[n] and the cyclodextrins.

	MW	a (Å)[a)]	b (Å)[a)]	c (Å)[a)]	Volume (Å^3)	Solubility (H_2O, mM)	Stability (°C)	pK_a
CB[5]	830	2.4[5]	4.4[5]	9.1[5]	82[5]	20 – 30[5]	> 420[5]	–
CB[6]	996	3.9[5]	5.8[5]	9.1[5]	164[5]	0.018[58]	425[59]	3.02[60]
CB[7]	1163	5.4[5]	7.3[5]	9.1[5]	279[5]	20 – 30[5]	370[5]	–
CB[8]	1329	6.9[5]	8.8[5]	9.1[5]	479[5]	< 0.01[5]	> 420[5]	–
CB[10][b)]	1661	9.0–11.0	10.7–12.6	9.1	–	–	–	–
α-CD	972	4.7[61]	5.3[61]	7.9[61]	174[61]	149[61]	297[62]	12.332[61]
β-CD	1135	6.0[61]	6.5[61]	7.9[61]	262[61]	16[61]	314[62]	12.202[61]
γ-CD	1297	7.5[61]	8.3[61]	7.9[61]	427[61]	178[61]	293[62]	12.081[61]

a) The values quoted for a, b, and c for CB[n] taken into account the van der Waals radii of the relevant atoms, b) Determined from the X-ray structure of the CB[5]@CB[10] complex[9].

1.3.2 Solubility, Acidity, and Stability

One of the potential limitations of the CB[n] family is their relatively poor solubility in water; CB[6] and CB[8] are essentially insoluble, whereas CB[5] and CB[7] possess modest and excellent solubility in water, respectively (Table 1). The solubility of the CB[n] family is generally lower than the cyclodextrins. Just like urea

itself, however, the carbonyl-lined portals of CB[n] are weak bases; the pK_a of the conjugate acid of CB[6] is 3.02. Although the pK_a values for CB[5], CB[7], and CB[8] have not been measured, they are likely to be similar to CB[6]. Accordingly, the solubility of CB[5] – CB[8] increase dramatically in concentrated aqueous acid (e.g. CB[6] = 61 mM in 1:1 aq. HCO_2H; CB[5] ≈ 60 mM, CB[7] ≈ 700 mM, and CB[8] ≈ 1.5 mM in 3 M HCl).[63-65] One of the outstanding features of CB[5] – CB[8] is their high thermal stability measured by thermal gravimetric analysis which exceeds 370 ˚C in all cases.

1.3.3 Electrostatic Potential

Electrostatic effects can play a crucial role in molecular recognition events in both aqueous and organic solution.[66] Figure 4 shows the electrostatic potentials of β-CD and CB[7]. Obviously, the electrostatic potential at the portals and within the cavity of CB[7] is significantly more negative than β-CD. This difference in electrostatic potential has significant consequences for their recognition behavior; the CB[n] exhibit a pronounced preference to interact with cationic rather than neutral or anionic guests whereas β-CD prefers to bind to neutral or anionic rather than cationic guests.

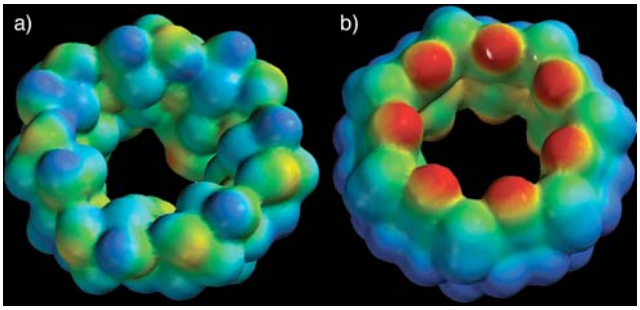

Figure 4. Electrostatic potential maps for a) β-CD and b) CB[7]. The red to blue color range spans –80 to 40 kcal mol^{-1}. Adapted from Kim and co-workers.[5]

1.4 Host-Guest Chemistry of CB[6]

This section compares and contrasts the recognition properties of CB[6] with α-CD and 18-crown-6 and presents a series of lessons learned from CB[6] chemistry that can be generalized to the CB[n] family.

1.4.1 A Brief Comparison of CB[6], α-, β-, and γ-Cyclodextrin, and 18-Crown-6 Complexation Thermodynamics

Houk recently reviewed the binding affinities for a wide variety of systems including synthetic host-guest, antibody-antigen, receptor-drug, and enzyme-substrate complexes.[67] The average binding affinity for 1257 α-, β-, and γ-CD complexes[68] (K_a = $10^{2.5\pm1.1}$ M^{-1}) is an order of magnitude smaller and more narrowly distributed than when 973 synthetic host-guest pairs in water are considered (K_a = $10^{3.4\pm1.6}$ M^{-1}). A similar analysis using the 56 CB[6]•guest pairs reported by Mock[69] yields K_a = $10^{3.8\pm1.5}$ M^{-1}. Table 2 compares the affinity of α-CD and CB[6] toward a series of

alcohols; the alcohols are modest guests for both hosts. Despite its preference to interact with positively charged guests (*vide infra*), CB[6] binds more tightly to the alcohols (except hexanol) than does α-CD although it does so in a non-selective manner. In general, CB[6] binds with higher affinity and higher selectivity toward its guest than do the cyclodextrins. A similar comparison between the affinity of CB[6] and 18-crown-6 toward several monovalent and divalent cations is given in Table 3. CB[6] shows higher affinity than 18-crown-6 toward all cations except Ba^{2+} whose radius is a good match for the cavity of 18-crown-6. These examples are intended to illustrate that the binding ability of CB[6] generally equals or exceeds those of other well known host molecules like cyclodextrins and crown ethers.

Table 2: Calorimetrically determined log K_a values for CB[6] (1:1 HCO_2H:H_2O, 25 °C) and α-CD (H_2O) binding to alcohols.[70,71]

	CH_3CH_2OH	$CH_3(CH_2)_2OH$	$CH_3(CH_2)_3OH$	$CH_3(CH_2)_4OH$	$CH_3(CH_2)_5OH$
CB[6]	2.64	2.61	2.53	2.73	2.71
α-CD	0.99	1.46	1.91	2.51	2.90

Table 3: Calorimetrically determined log K_a values for CB[6] (1:1 HCO_2H:H_2O, 25 °C) and 18-crown-6 with monovalent and divalent cations and for Ba^{2+} as a function of solvent composition.[63,72]

	HCO_2H:H_2O	Li^+	Na^+	K^+	Rb^+	Ca^{2+}	Sr^{2+}	Ba^{2+}
CB[6]	50:50	2.38	3.23	2.79	2.68	2.80	3.18	2.83
	40:60							3.50
	30:70							4.13
	25:75							4.39
	0:100							5.23
18-C-6	0:100	–	0.80	2.03	1.56	< 0.5	2.72	3.87

1.4.2 Lessons Learned from CB[6]

Compared to CB[6] which recently celebrated its 100th birthday, the supramolecular chemistry of the 5 year-olds CB[5], CB[7], CB[8], and CB[10] are relatively undeveloped. While these CB[n] homologues promise much new chemistry, many of the basic lessons learned in studies of CB[6] can, we hypothesize, be transferred to CB[n]. This section presents those lessons from a largely mechanistic viewpoint. Accordingly, Scheme 2 depicts a comprehensive mechanism for the interaction of CB[6] with protons, metal ions, amines, and ammonium ions.

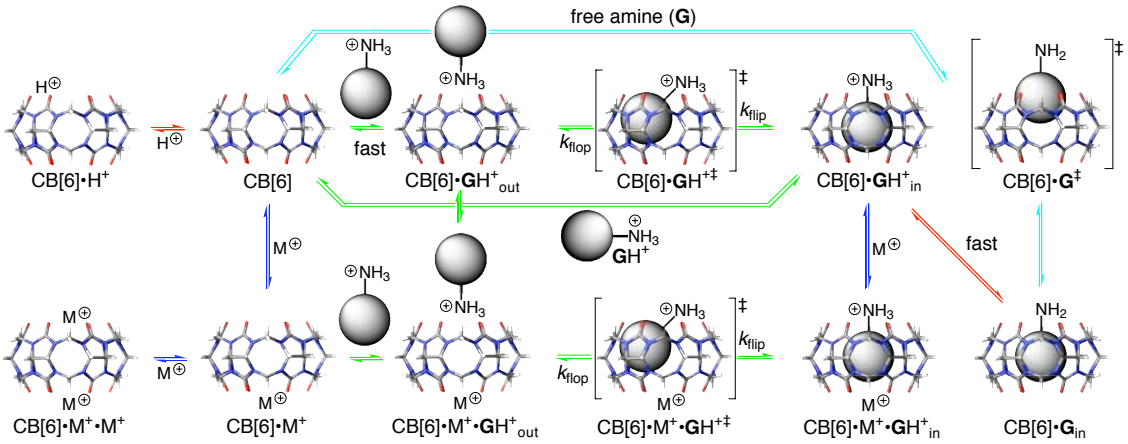

Scheme 2. Comprehensive mechanistic scheme for CB[6] recognition chemistry. Arrow color coding: Red: protonation, Blue: cation binding, Green: ammonium ion binding, Aqua: amine binding.

1.4.3 CB[6] Binds Protons at its Carbonyl Lined Portals

As mentioned above, CB[6] is a weak base that can be protonated in moderately acidic media (pK_a = 3.02). Accordingly, when binding studies are conducted with CB[6] in strongly acidic media (e.g. 1:1 HCO_2H:H_2O) H^+ competes with guest binding (Scheme 2, red equilibria). Comparisons between binding constants measured in different media must, therefore, be treated with caution.

1.4.4 CB[6] Binds Metal Ions at its Carbonyl Lined Portals

Given that CB[6] binds H^+ at its ureidyl carbonyl portals, it is perhaps unsurprising that CB[6] also binds alkali metal, alkaline earth, transition metal, and lanthanide cations in homogenous solution (Scheme 2, blue equilibria).[4,60,63,64,73-76]

Table 3 shows the binding constants determined by Buschmann for CB[6] with a variety of monovalent and divalent cations. Selectivity between the different cations is less than 10-fold. The low selectivity observed and the lack of a simple trend in log K_a values is attributed to a mismatch between the ionic radii of cations and the annular radius of the relatively rigid CB[6] ionophore (1.95 Å). The metal binding equilibria (Scheme 2, blue equilibria) are in competition with protonation (red equilibrium). Accordingly, as the acidity of the solution is increased the observed log K_a values for metal binding should decrease. Table 3 documents the 2.4 unit decrease in log K_a observed for CB[6]•Ba^{2+} upon changing the medium from water to 50:50 water:HCO_2H.

1.4.5 CB[6] Binds Preferentially to Positively Charged Organic Guests Driven by Ion-Dipole Interactions

In their pioneering work, Mock and co-workers observed that alkylammonium ions bind tightly to CB[6] in 1:1 aq. HCO_2H and measured binding constants ranging from 10^1 – 10^7 M^{-1} by a series of ^1H NMR competition experiments, a selection of which (NH_3, and **I-2** – **I-14**) are given in Table 4.[2,69,77-79] Buschmann and co-workers have measured the corresponding thermodynamic parameters (ΔH and ΔS).[80] Mock's experiments were facilitated by two unusual characteristics of host-guest complexes of CB[6]. First, the interior of CB[6] constitutes a ^1H NMR shielding region and upfield shifts of 1 ppm are common; the regions just outside the carbonyl portals are weakly deshielding. Second, dynamic exchange processes between free and bound

guest are often slow on the chemical shift time scale allowing a direct observation of free and bound guest simultaneously. To establish the importance of ion-dipole interactions relative to hydrogen bonds in the formation of CB[6] complexes (Figure 5), Mock considered the relative binding affinities of **I-2** – **I-4** (Table 4, entries 2 – 4). "Formal replacement of the terminal hydrogen of *n*-hexylamine with another amino group enhances binding 1200-fold. … However, replacement of this hydrogen by a *hydroxyl* group contributes nothing to the stabilization of the complex. … While the alcohol (and ammonium ions) may be hydrogen bonded in the complex, in the absence of CB[6] they would also be fully hydrogen bonded. … The consequential feature of ammonium ions is that they are *charged*. … Hence, it is our understanding that the high specificity for ammonium ions is largely an electrostatic *ion-dipole attraction*."[69] The preference of CB[6] for charged guests will transfer to the other CB[n], but the relative importance of electrostatic interactions versus the hydrophobic effect may change as cavity size increases. Blatov recently developed a computational technique based on crystallographic data to identify good guests for each member of the CB[n] family.[81]

Table 4: Association constants measured for CB[6] with a variety of amines in 1:1 H_2O:HCO_2H at 40 ˚C.

Entry	Amine	K_a (M^{-1})
1	NH_3	83
2	$H_2N(CH_2)_6H$ (**I-2**)	2300
3	$H_2N(CH_2)_6OH$ (**I-3**)	1200
4	$H_2N(CH_2)_6NH_2$ (**I-4**)	2800000
5	c-$(CH_2)_2CHCH_2NH_2$ (**I-5**)	15000
6	c-$(CH_2)_3CHCH_2NH_2$ (**I-6**)	370000
7	c-$(CH_2)_4CHCH_2NH_2$ (**I-7**)	330000
8	c-$(CH_2)_5CHCH_2NH_2$ (**I-8**)	80[a)], 110000[b)]
9	4-$MeC_6H_4CH_2NH_2$ (**I-9**)	320
10	3-$MeC_6H_4CH_2NH_2$ (**I-10**)	n.d.
11	2-$MeC_6H_4CH_2NH_2$ (**I-11**)	n.d.
12	$H_2N(CH_2)_5NH_2$ (**I-12**)	2400000
13	$H_2N(CH_2)_2S(CH_2)_2NH_2$ (**I-13**)	420000
14	$H_2N(CH_2)_2O(CH_2)_2NH_2$ (**I-14**)	5300

a)[82], b) Measured for the hydrochloride salt in D_2O.[57] n.d. = no binding detected.

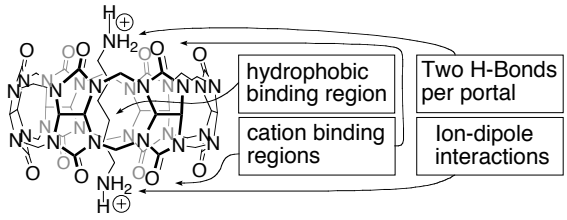

Figure 5. Depiction of the different binding regions of CB[6] and the geometry of the complex between CB[6] and hexanediammonium.

1.4.6 CB[6] Displays Length, Size, Shape and Functional Group Selectivity

The relative rigidity of CB[6] and the close juxtaposition of two binding regions that favor positively charged groups with one that favors hydrophobic residues imparts high selectivity to CB[6] binding processes (Figure 5). For example, Mock found that alkylamines and alkanediamines exhibit length dependent selectivity for CB[6]. Figure 6 shows a plot of log K_a versus chain length. CB[6] prefers butylamine relative to propylamine (8-fold) and pentylamine (4-fold) whereas 1,5-pentanediamine and 1,6-hexanediamine are preferentially bound relative to 1,4-butanediamine (15-fold) and 1,7-heptanediamine (64-fold). These high selectivities have been used to construct molecular switches (*vide infra*). CB[6] is also size selective. For example, CB[6] forms tight complexes with **I-6** and **I-7** whereas the 3- and 6-membered ring analogs **I-5** and **I-8** are rejected by CB[6] (Table 4, entries 5 – 8). Similarly, CB[6] selects guests based on shape. For example, even though **I-7** and **I-9** have similar included volumes (86 Å^3 versus 89 Å^3), the former binds 1000-fold more tightly (Table 4, entries 7 and 9).[57] Similarly, **I-9** is included within CB[6] whereas the ortho and meta isomers **I-10** and **I-11** are not bound (Table

4, entries 9 – 11). Lastly, CB[6] displays functional group selectivity. For example, **I-12** binds 6-fold more tightly than **I-13** which in turn binds 79-fold more tightly than **I-14** (Table 4, entries 12 – 14). Mock attributes this trend "to a solvation effect operating primarily on the uncomplexed guest; oxygen has greater intrinsic hydrophilicity than does sulfur, and a methylene group is more hydrophobic than is a thioether linkage."[69]

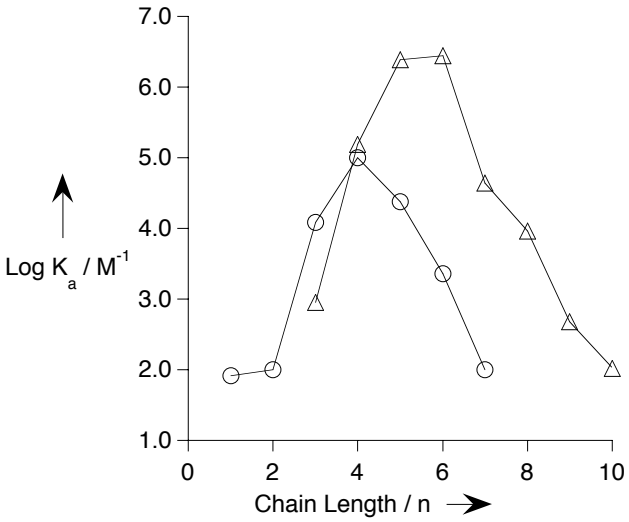

Figure 6. Plot of binding constant (log K_a) versus chain length (n) for $H(CH_2)_nNH_3^+$ (o) and $^+H_3N(CH_2)_nNH_3^+$ (Δ).

1.4.7 The Recognition Properties of CB[6] Can Be Conveniently Studied in Saline Solution

One of the major challenges that has faced the CB[n] family is their poor solubility in aqueous and organic solution. For this reason, the majority of quantitative studies of binding with CB[6] have used 1:1 aq. HCO_2H as solvent. As early as 1992, it was known that CB[6] binds to alkali and alkaline earth cations in

pure water and increases its concentration at saturation.[60] It was not until 1996, however, when Kim's group reported that the solubilization of CB[6] in aqueous saline solution allows the study of guest binding in neutral water that the full importance of this discovery was realized.[83] For example, the solubility of CB[6] increases dramatically in 0.2 M Na_2SO_4 (66 mM), LiCl (0.94 mM), KCl (37 mM), CsCl (59 mM), and $CaCl_2$ (70 mM). The X-ray crystal structure of CB[6]•Na_4•$(H_2O)_{17}$•$(SO_4)_2$•THF revealed that the sodium ions act as lids that result in the encapsulation of THF (Scheme 3). Even more remarkably, the addition of CF_3CO_2H releases THF from the CB[6]•THF complex (K_a = 510 M^{-1}) by competitive binding;[84] the process can be reversed by the addition of Na_2CO_3. In a related paper, Kim showed that the lids are not merely innocent bystanders; Cs^+ lidded CB[6] actively participates in the binding of THF by cesium–oxygen coordination interactions.[85] Despite the reduced binding constants due to competition present with metal ions in solution, these pioneering studies showed that CB[n] supramolecular chemistry would not be limited to strongly acidic conditions. Currently, many workers employ the hydrochloride salts of suitable guests for their investigations since the resulting complexes are rendered water soluble in the absence of competing H^+ or M^+.

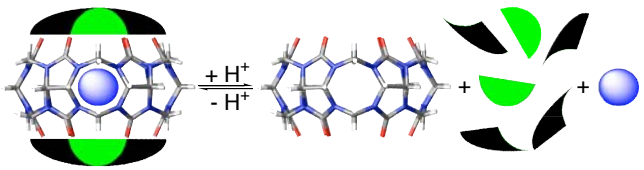

Scheme 3. Lidding and delidding of CB[6]. Legend: blue sphere, THF; green hemispheres, Na^+, black wedges, H_2O.

1.5 Host-Guest Properties of the Individual Homologues

1.5.1 CB[5] and $Me_{10}CB[5]$

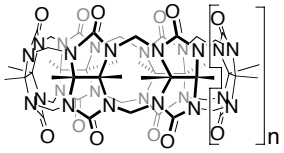

$Me_{10}CB[5]$ (n = 0)

The supramolecular chemistry of CB[5] and $Me_{10}CB[5]$[86] (*vide infra*) is controlled by the narrow carbonyl lined portals which provide entry to a cavity of low volume. Consequently, much of the supramolecular chemistry of CB[5] has been limited to proton, metal, and ammonium binding at their portals.[64,65,73,74,76,87] Bradshaw, Izatt, and co-workers studied the ability of $Me_{10}CB[5]$ in 1:1 aq. HCO_2H to bind monovalent and divalent cations and found a remarkably high selectivity toward Pb^{2+} ($> 10^{5.5}$).[76] Somewhat surprisingly, CB[5] itself does not display a similar Pb^{2+} selectivity.[73] CB[5] and $Me_{10}CB[5]$ form weak host-guest complexes with α-, β-, and γ-cyclodextrins ($K_a \approx 10$).[58] Recently, Tao and co-workers disclosed that hexamethylene tetramine is capable of lidding CB[5].[88] The most remarkable property of CB[5] and $Me_{10}CB[5]$ is their ability to bind gases[89] (e.g. Kr, Xe, N_2, O_2, Ar, N_2O, NO, CO, CO_2, and CH_4) and small solvents (e.g. CH_3OH and CH_3CN) which was observed by Dearden[87,90,91] in mass spectrometric investigations, by Miyahara[92] in aqueous solution and the solid state, and discussed by Day[33] and Miyahara[40] in the patent literature. Miyahara demonstrated the reversible sorption and desorption of gas by solid $Me_{10}CB[5]$ with capacities up to 40 mL g^{-1} (N_2O).

These results suggest that Me_{10}CB[5] and CB[5] may be of practical utility in the reducing the level of NOx gases from air.

1.5.2 CB[6]

The pioneering work of Buschmann has established equilibrium constants and in many cases the enthalpic (ΔH) and entropic (ΔS) contributions to ΔG for CB[6] binding to ω-amino acids and ω-amino alcohols,[93] aliphatic alcohols, acids, and nitriles,[70] bipyridine derivatives,[94] aromatic compounds,[95,96] non-ionic surfactants and poly(ethylene glycols),[96] cyclodextrins,[58] diamides,[97] and α-amino acids and dipeptides.[98] Just like for CB[6]•M^+ complexes, the values of K_a measured for organic guests complexes to CB[6] in aq. HCO_2H increase as the percentage of HCO_2H decreases due to reduced competitive protonation of CB[6].[99] Knoche studied the complexation of azobenzenes with CB[6].[4,100] Bartik studied the binding of the neutral guests Xe, THF, and CF_3CO_2H in CB[6] by ^{129}Xe, ^{19}F, and ^1H NMR spectroscopy.[84,101] Dearden's group has studied the formation and dissociation of CB[6] pseudorotaxanes and the corresponding exclusion complexes in the gas phase.[87] The groups of Wagner and Buschmann have shown that CB[6] enhances the fluorescence of 1,6- and 2,8-anilinonapthalene sulfonates in solution and the solid state.[102-104] Recently, Wu showed that CB[6] also binds diazonium compounds.[105]

1.5.3 CB[7]

CB[7] is slightly more voluminous than β-CD (Table 1); accordingly, CB[7] can bind a wider range of guests than CB[6] or CB[5]. CB[7] binds a variety of positively charged aromatics including adamantanes and bicyclooctanes,[5,88,106,107] naphthalene,[7,108,109] stilbene,[110] viologen,[111-115] *o*-carborane,[116] ferrocene,[5,117] and cobaltocene[117] derivatives (**I-15** – **I-25**). CB[7] also binds metal complexes **I-26**[118], **I-27**,[5,38] and related compounds[119,120] which suggests the use of CB[7] to reduce toxicity in cancer treatment. A number of elegant studies by Kaifer and co-workers have demonstrated that many of the unusual properties of CB[6] are retained by CB[7]. For example, Ong and Kaifer determined the values of K_a for CB[7]•**I-20a** in 0 – 0.2 M NaCl and 0 – 0.2 M $CaCl_2$ and demonstrated that Na^+ and Ca^{2+} cations compete with **I-20a** for CB[7] binding which reduces K_a by 9–40 fold.[114] In two elegant studies, Kaifer showed that the CB[7] bead resides can reside in different locations along guests containing multiple binding sites (e.g. CB[7]•**I-20a** – CB[7]•**I-20g**).[115,121] CB[7] resides on the longer butyl and hexyl chains of **I-20c** and **I-20d** whereas it resides on the viologen nucleus of derivatives that contain shorter (**I-20a** and **I-20b**) or hydrophilic residues (**I-20e** and **I-20f**). These results imply that CB[7] retains the highly selective binding properties noted above for CB[6]. CB[7] forms a pseudorotaxane with **I-20i**. Nau and co-workers have used CB[7]•2,3-diazabicyclo[2.2.2]oct-2-ene to document that the polarizability of the CB[7] cavity is extremely low[122,123] and to distinguish between mechanistic alternatives in fluorescence quenching studies.[55,124] Wagner and co-workers have studied the enhancement in fluorescence observed upon binding of anilinonapthalene sulfonates

by CB[7].[108] CB[7] was recently reported to form a weak 1:2 exclusion complex with C_{60} by high-speed vibration milling.[125] Most recently, CB[7] has been used as an additive to separate positional isomers by capillary electrophoresis.[126]

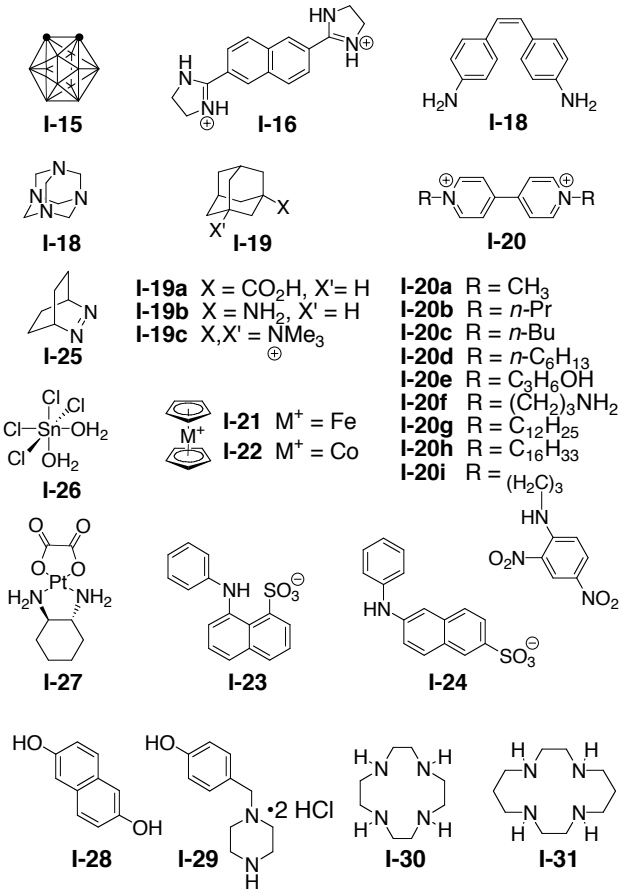

1.5.4 CB[8]

The cavity of CB[8] is similar in terms of volume to γ-CD, but is less conformationally flexible. CB[8] behaves like the big brother of CB[5] – CB[7] in many ways, but also exhibits more complex recognition behavior. Just like CB[5] – CB[7], CB[8] prefers to bind to positively charged guests by ion-dipole interactions.[7,127] CB[8] readily binds single guest molecules that partially (CB[8]•**I-20a**, K_a = 1.1 × 10^5 M^{-1}) or completely (CB[8]•**I-19b**) fill its cavity. In contrast to

CB[5] – CB[7], the voluminous cavity of CB[8] is capable of simultaneously binding *two* aromatic rings (Figure 7). For example, CB[8] readily forms termolecular complex CB[8]•**I-16**•**I-16**.[7,128] Even more strikingly, when CB[8] and **I-16** are mixed in a 1:1 ratio, a mixture of CB[8] and CB[8]•**I-16**$_2$ is formed which demonstrates cooperativity between the binding of the first and second aromatic rings. Kim and co-workers have also demonstrated the selective formation of a hetero termolecular complex CB[8]•**I-20a**•**I-28** which results in enhanced charge transfer interactions between **I-20a** and **I-28** in the complex.[129] Kim has used this recognition motif to control intramolecular folding processes[130] and in the formation of vesicles.[131] More recently, Tao has shown that aromatic piperazine derivatives form a mixture of 1:1 and 1:2 complexes with CB[8] (e.g. CB[8]•**I-29** and CB[8]•**I-29**$_2$).[132] Similarly, Fedin recently reported the crystal structure of the CB[8]•(PhPO(OH)$_2$)$_2$ complex.[133] CB[8] is even capable of encapsulating cyclen (**I-30**) or cyclam (**I-31**). Even more remarkably, CB[8]•**I-30** and CB[8]•**I-31** can be metalated by treatment with Cu^{II} or Zn^{II} which results in macrocycle within macrocycle complexes that resemble the Russian Matrioshka dolls.[134]

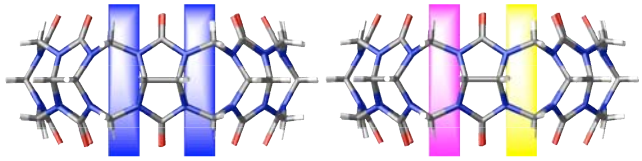

Figure 7. Schematic depictions of termolecular complexes CB[8]•**I-16**•**I-16** and CB[8]•**I-20a**•**I-28**.

1.5.5 CB[10]

Day and co-workers successfully isolated CB[10] as its CB[5]@CB[10] complex (Figure 3). The structure of this remarkable complex was established by X-ray crystallography which demonstrated its resemblance to a gyroscope.[9] Despite the fact that it was not possible to isolate free CB[10] by removal of CB[5], chemical exchange between free and bound CB[5] was demonstrated through the use of ^{13}C labeled CB[5]. Such molecular gyroscopes and the related molecular ball bearing[116] (CB[7]•**I-15**) are potential components of future molecular machines.

1.6 Control Over the Recognition Processes Within CB[n]

The creation of molecular machines[135] by self-assembly processes is currently of great scientific interest. One of the most fundamental molecular machines is a molecular switch that can toggle between two different states by appropriate environmental stimuli (e.g. chemical, electrochemical, or photochemical). The CB[n] family is ideally suited for such applications due to the high affinity, highly selective binding processes that occur within their cavities.

1.6.1 Chemical Control – Molecular Switches

An early example of a molecular switch was published by Mock in 1990 wherein CB[6] is induced to shuttle along a triamine string by changes in pH that

result in changes in the protonation state of the aniline N-atom (Scheme 4).[136] At values of pH below the pK_a of the anilinium (pK_a = 6.73), the CB[6] bead resides in the hexanediammonium region with its higher binding constant (CB[6]•**I-32**); above the pK_a, the bead moves to the still fully protonated butanediammonium region (CB[6]•**I-33)**. Kim and co-workers have reported CB[6] rotaxane based molecular switches with UV/Vis and fluorescence outputs,[137] that can be actuated by changes in pH but requires both pH and heat to be turned off,[138] and that undergo a slow transformation from the kinetic to the thermodynamically more stable rotaxane.[139]

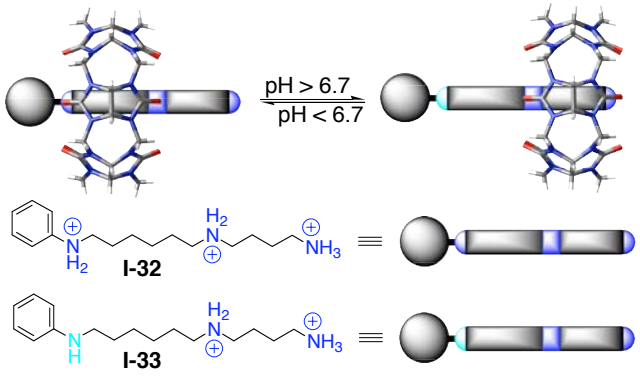

Scheme 4. CB[6] based molecular switch.

1.6.2 Photochemical Control

As mentioned above, the ability of the two carbonyl lined portals of the CB[n] family to orient two guests within their cavity results in opportunities to accelerate and control chemical reactions. For example, Kim and co-workers found that CB[8] binds two equivalents of (*E*)-**I-34**.[140] Irradiation of CB[8]•**I-34**•**I-34** (300 nm, 30 min.) results in the formation of CB[8]•*syn*-**I-35** and only a trace of CB[8]•*anti*-**I-35** (Scheme 5). In the absence of CB[8], (*E*)-**I-34** does not dimerize but does undergo

photoisomerization to (*Z*)-**I-34**. Upon addition of base, free **I-36** is released. The dimerization of (*E*)-**I-34** within γ-CD is slower and less stereoselective (80:20 *syn:anti)*. CB[8] accelerates and controls the stereochemistry of the [2+2] photoreaction. In a related example, Kim found that a solution of CB[7] and (*E*)-**I-34** forms the complex CB[7]•(*E*)-**I-34** which, upon irradiation (350 nm) converts nearly quantitatively to CB[7]•(*Z*)-**I-34**. Remarkably, CB[7]•(*Z*)-**I-34** is stable at room temperature for 30 days.[110] This result demonstrates that CB[7] is able to control the otherwise unfavorable equilibrium between CB[7]•(*E*)-**I-34** and CB[7]•(*Z*)-**I-34**.

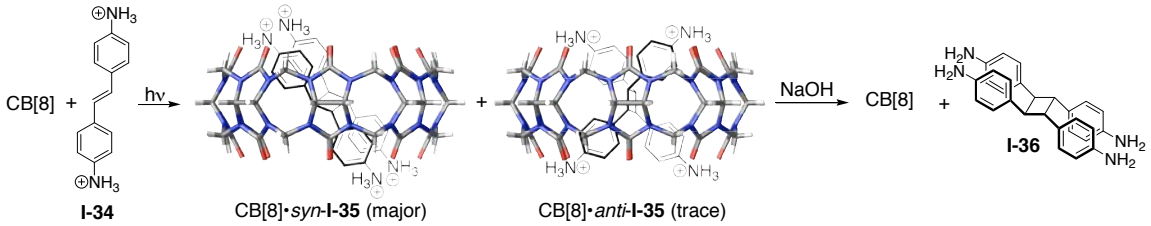

Scheme 5. 2+2 photoaddition reaction mediated by CB[8].

1.6.3 Electrochemical Control

As described above, the CB[n] family displays a marked preference to interact with positively charged guest species. For example, the groups of Kim[111] and Kaifer,[112] studied the interaction of CB[7] with **I-20a**$^{2+}$ (K_a = 2 × 10^5 M^{-1}) and its reduced forms **I-20a**$^{\bullet+}$ (K_a = 8.5 × 10^4 M^{-1}) and **I-20a**^{0} (K_a = 2.5 × 10^2 M^{-1}) by electrochemical measurements. Two unusual observations were made: 1) the presence of CB[7] prevents the dimerization of **I-20a**$^{\bullet+}$ and 2) the reduction of **I-20a**$^{\bullet+}$ occurs by a direct electron transfer pathway. Related observations were made by

Kaifer for the CB[7]•**I-21** and CB[7]•**I-22** complexes ($K_a \geq 10^6$ M^{-1}).[117] The cavity of CB[8] is large enough to accommodate two flat aromatic rings, provided they possess complementary electrostatic profiles (e.g. charge transfer complex CB[8]•**I-20a**•**I-28**). Very interestingly, Kim found that CB[8] binds a single molecule of **I-20a**$^{2+}$ (CB[8]•**I-20a**$^{2+}$, K_a = 1.1 × 10^5 M^{-1}); upon electrochemical reduction, however, the complex undergoes disproportionation to form a mixture of CB[8] and CB[8]•**I-20a**$^{\bullet+}$•**I-20a**$^{\bullet+}$.[127] The presence of CB[8] enhances the dimerization of **I-20a**$^{\bullet+}$ by a factor of 10^5. Electrochemistry allows quantitative control of stoichiometry within CB[8]! The dimerization of tetrathiafulvalene radical cation is also promoted by CB[8].[141] Armed with this knowledge, Kim's group prepared dimeric viologen **I-37**$^{4+}$. Compound **I-37** forms a stable 1:1 complex with CB[8] (CB[8]•**I-37**$^{4+}$, K_a = 2.3 × 10^5 M^{-1}) where the CB[8] bead resides mainly on the hexamethylene spacer (Scheme 7). Upon electrochemical reduction (or light induced chemical reduction with $Ru^{II}(bpy)_3$) a folding process takes places which results in the formation of molecular loop CB[8]•**I-37**$^{2+}$ which displays dramatically reduced dimensions relative to CB[8]•**I-37**$^{4+}$ (e.g. 28 × 18 Å versus 15 × 18 Å). The observed large changes in size and shape may be useful in the design of molecular actuators.

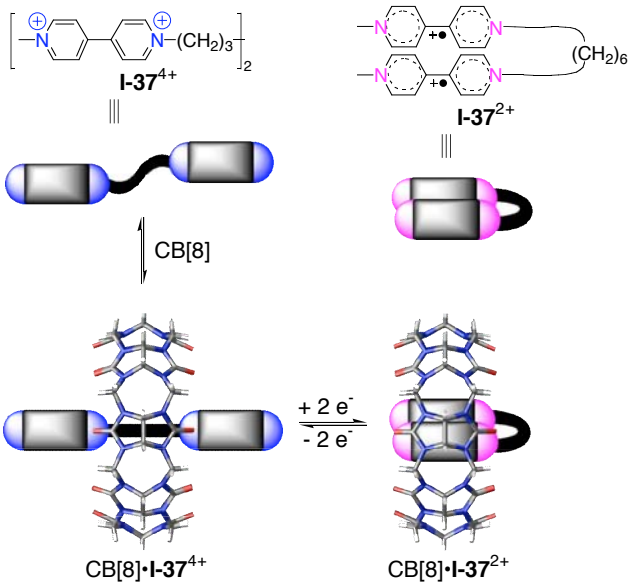

Scheme 6. A [2]pseudorotaxane based molecular machine.

1.7 Applications of the CB[n] Family

The outstanding recognition properties of the CB[n] family have lead to their use in numerous applications, some of which are highlighted in this section.

1.7.1 Catalysis

A long standing challenge in supramolecular chemistry has been the design of catalysts. Mock's group recognized that CB[6] was ideally suited for this purpose due to the presence of two carbonyl lined portals that can potentially recognize two ammonium ion substrates forming a termolecular complex that orients and compresses those substrates for chemical reaction.[142,143] Mock and co-workers

studied the dipolar cycloaddition between azide **I-38** and alkyne **I-39** catalyzed by CB[6] in an elegant example of click-chemistry (Scheme 7).[144] They find that the CB[6] catalyzed reaction of **I-38** and **I-39** is a rare example of what is known as "the Pauling principle of catalysis, which states that the complementarity between an enzyme and the *transition state* for its conducted reaction ought to be greater than that between enzyme and the reactants".[142] Remarkably, CB[6] accelerates this reaction by a factor of 5.5×10^4 compared to the bimolecular reaction and renders it highly regioselective. The reaction also displays several features that are commonly observed in enzymatic reactions, namely: 1) saturation behavior at high [**I-38**] and [**I-39**], 2) rate limiting product release from CB[6]•**I-40**, 3) substrate inhibition by the formation of non-productive termolecular complex CB[6]•**I-38**•**I-38**, and 4) competitive inhibition by non-reactive substrate analogs. Steinke's research group has used the CB[6] promoted dipolar cycloadditon of azides and terminal acetylenes for the preparation of catalytically self-threading rotaxanes,[145,146] [2], [3], and [4]rotaxanes and pseudorotaxanes,[147] and oligotriazoles.[148]

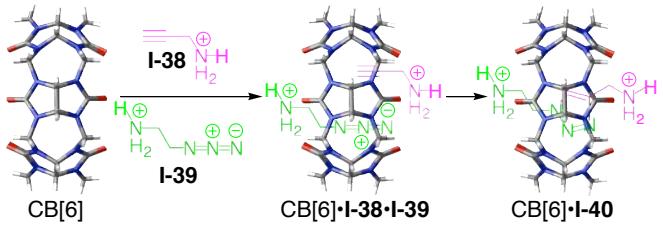

Scheme 7. Catalysis of a 3+2 dipolar cycloaddition inside CB[6].

1.7.2 Self-Assembled Monolayers

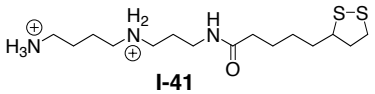

I-41

To realize the full potential of pseudo(rotaxanes) as components of molecular machines, it is necessary to develop methods for their immobilization on solid substrates. Kim has reported the functionalization of a gold surface with the pseudorotaxane CB[6]•**I-41**.[149] SAM's comprising CB[6]•**I-41** undergo reversible dethreading and rethreading of the CB[6] beads upon treatment with 0.1 M NaOH followed by CB[6] as monitored by surface plasmon resonance. Cyclic voltametry measurements indicate that the SAM formed by pseudorotaxane CB[6]•**I-41** constitutes an effective barrier to redox processes involving $[Fe(CN)_6]^{3-}$; after dethreading, a quasireversible redox wave is observed. This reversible gating behavior may have application in the design of surface bound molecular machines. More recently, Kim and co-workers have reported a surface initiated supramolecular polymer based on CB[8] stabilized charge transfer interactions (Scheme 8). An aqueous solution containing CB[8] and thiol **I-42** results in the formation of pseudorotaxane CB[8]•**I-42**; dipping a gold substrate in this solution results in the formation of a self-assembled monolayer. Supramolecular polymerization from the CB[8]•**I-42** SAM was initiated by immersing the substrate in a solution containing CB[8] and **I-43**. The course of the reversible supramolecular polymerization could be monitored by FT-IR, SPR, and AFM and controlled by certain variables (time and concentration). On average, the polymer consists of four CB[8] beads per chain.[149]

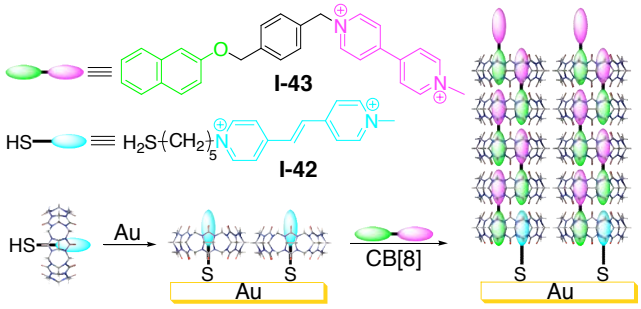

Scheme 8. Formation of pseudorotaxane CB[8]•**I-42** on Au and formation of surface bound supramolecular polymer based on CB[8] stabilized charge transfer interactions.

1.7.3 Textile Waste Stream Remediation

The application of CB[6] toward the complexation of indicator dyes (e.g. congo red and methylene blue) was published by Behrend in 1905. Since then, the groups of Buschmann[30,31,99,150-165] and Karcher,[166-170] have studied the ability of CB[6] to effectively remove heavy metals, chromates and dichromate, aromatic substances, acid dyes, direct dyes, reactive dyes, from textile waste streams, quantified the influence of key variables (e.g. pH, temperature, salts, and surfactants) on the process, and studied methods for regeneration of the solid phase. Taketsuji found that Behrend's polymer was more efficient in these applications than CB[6].[34,171,172] Major issues that need to be resolved include loading levels, the covalent attachment of CB[6] to solid phases suitable for use in fixed bed filters, and cost.

1.7.4 DNA Binding and Gene Transfection

Nakamura and Kim investigated a non-covalent approach to selectively deliver CB[6] to DNA.[173] The concept is illustrated in Scheme 9. Compound **I-44** contains acridine and tetramine regions which function as DNA intercalator and CB[6] binding elements, respectively. Mixing DNA, CB[6], and **I-44** results in termolecular complex formation (DNA•**I-44**•CB[6]) as monitored by gel electrophoresis. The DNA•**I-44**•CB[6] complex partially protects supercoiled DNA against cleavage by the restriction enzyme *Ban*II. In a complementary study, Kim and co-workers demonstrated that G3, G4, and G5 poly(propyleneimine) dendrimers bearing diaminobutane moieties (PPI-DAB) for CB[6] binding functions as a gene delivery carrier.[174] The PPI-DAB•CB[6] conjugates have low cytotoxicity and successfully transfect Vero 76 and 293 cells with efficiencies only 10-fold lower than poly(ethyleneimine) which is one of the most potent gene transfer carriers.

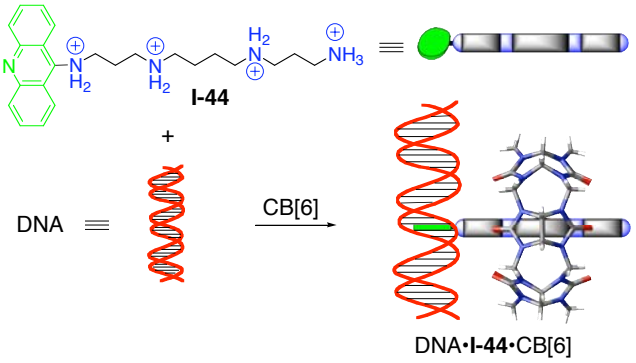

Scheme 9. Intercalation of acridine spermine rotaxane CB[6]•**I-44** into DNA. The components are not drawn to scale.

1.8 Conclusion

Cucurbit[6]uril is celebrating its 100th birthday this year! It was only in 1981 at age 76, that the structure of this unusual macrocycle was elucidated by Mock and co-workers. In their early pioneering work, Mock and co-workers demonstrated that CB[6] displays: 1) remarkably high affinity for alkanediammonium ions due to ion-dipole interactions and the hydrophobic effect, 2) size, shape, and functional group selectivity, 3) unusually slow kinetics of association and dissociation, and 4) even behaves as an enzyme mimic! CB[6] was clearly a talented host, but a series of perceived problems limited the scope of applications to which it could be applied. Compared to α-, β-, and γ-cyclodextrin with their good solubility in aqueous solution, their commercial availability in a variety of sizes, their well-known chemical functionalization, and their affinity toward a wide variety of species, CB[6] was not in a position to challenge the cyclodextrins as the recognition platform of choice for studies of molecular recognition in aqueous solution.

In the intervening time, all of these perceived issues have been either partially or fully resolved which has dramatically expanded the range of applications to which the CB[n] family can be applied. For example, the solubility of CB[6] increases dramatically in the presence of salts which allows their recognition and self-assembly processes to be studied in neutral aqueous solution. It was not until the turn of the millennium, however, that the CB[n] family expanded dramatically with the preparation of CB[5], CB[7], CB[8], and CB[10]•CB[5] by Kim and Day. The recognition properties of these new CB[n] homologues – which are now

commercially available – parallel and exceed those of CB[6]. Recognition processes within CB[6], CB[7], and CB[8] are subject to efficient chemical, electrochemical, and photochemical control. These attributes along with the detailed knowledge of the mechanism of formation and dissociation of CB[6] complexes has lead to the application of the CB[n] family in areas as diverse as gas purification, catalysis, molecular machines, waste stream remediation, supramolecular polymers, self-assembling, self-assembled monolayers, and even gene transfection.

II. Chapter 2: Cucurbit[n]uril Analogues: Synthetic and Mechanistic Studies

2.1 Introduction

2.1.1 CB[n] Homologues

CB[6] is a macrocyclic cavitand comprising six glycoluril units linked through twelve methylene bridges which defines a hydrophobic cavity guarded by two carbonyl fringed portals. The unusual recognition properties of CB[n] have been delineated by the pioneering work of Mock,[3] Buschmann,[4] and Kim.[5,6] CB[6] has the ability to encapsulate guests in its hydrophobic cavity due to a combination of noncovalent interactions including the hydrophobic effect, ion-dipole interactions, and hydrogen bonding. The high selectivity exhibited by CB[6] is due to the relative rigidity of the macrocycle which allows for guests of an appropriate size, shape, and chemical functionality to bind tightly. The formation of these CB[6]•guest complexes is easily detected by ^{1}H NMR, UV/Vis, and isothermal titration calorimetry. In this chapter, we incorporate fluorescent bis(phthalhydrazide) walls into CB[n] analogues which allows the sensitive detection ($K_a > 10^6$ M^{-1}) of host-guest complexation by fluorescence titrations.[175,176] The outstanding recognition properties of the CB[n] family[177] has resulted in numerous intriguing applications including molecular switches,[136] catalysis,[110,140,142,143,146,178] water purification in textile industries,[157] polyrotaxanes,[179-181] ion-channels,[182] self-assembling dendrimers,[183] as components of molecular machines,[9,57] and advanced separations technologies.[184,185]

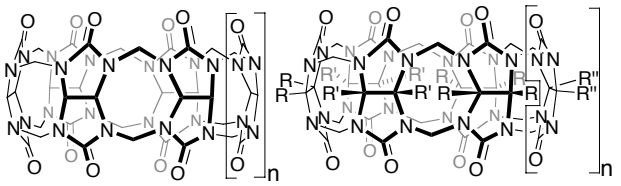

CB[5] (n = 0)
CB[6] (n = 1)
CB[7] (n = 2)
CB[8] (n = 3)

$(HO)_{10}$**CB**[5] (R = R' = R'' = OH, n = 0)
$(HO)_{12}$**CB**[6] (R = R' = R'' = OH, n = 1)
Ph_2**CB**[1,5] (R = R' = H, R'' = Ph, n = 1)
Me_6**CB**[3,3] (R = H, R' = R'' = Me, n = 1)
Cy_5**CB**[5] (R = R' = $(CH_2)_4$, n = 0)
Cy_6**CB**[6] (R = R' = R'' = $(CH_2)_4$, n = 1)

When we began our work in this area, the range of applications to which CB[6] could be applied was limited by a series of issues: 1) poor solubility in aqueous and organic solution, 2) the lack of synthetic procedures to allow the preparation of CB[6] homologues, CB[n] derivatives and CB[n] analogues,[186] and 3) the inability to change the binding selectivity of the macrocycles by incorporation of groups that define the cavity. In the intervening time, several of these issues have been alleviated either partially or fully. For example, when the condensation reaction was performed under milder conditions, the formation of CB[5], CB[7], CB[8], and CB[10] were isolated along with CB[6] as the major product.[7,8] The improved solubility of CB[7] and the spacious cavity of CB[8] gave rise to new opportunities in supramolecular chemistry.[108,110,112,114-116,140]

2.1.2 CB[n] Derivatives

Two approaches have been reported for the preparation of CB[n] derivatives with enhanced solubility in water and organic solvents. The first involves the condensation of glycoluril derivatives – either alone or in combination with glycoluril – with formaldehyde under acidic conditions. This approach has resulted in the

synthesis of several persubstituted CB[n] derivatives including $Cy_5CB[5]$ and $Cy_6CB[6]$[187] as well as the partially substituted CB[n] derivatives $Ph_2CB[1,5]$[188] and $Me_6CB[3,3]$.[189] In pioneering work, Kim recently demonstrated a second approach – the direct functionalization of CB[n] – which delivered perhydroxylated CB[n] derivatives including $(HO)_{10}CB[5]$ and $(HO)_{12}CB[6]$.[190]

2.1.3 S- and C-Shaped Methylene Bridged Glycoluril Dimers

Our approach to the synthesis of CB[n] derivatives and analogues relied on the identification of the methylene bridged glycoluril dimer structure as the fundamental building blocks of the CB[n] family. Our studies have focused, therefore, on methods for the preparation and interconversion of methylene bridged glycoluril dimers. We discovered that suitable combinations of nucleophilic and electrophilic glycoluril building blocks result in the selective formation of heterodimers as a mixture of S-shaped and C-shaped diastereomers.[191,192] To rationalize the selective formation of C-shaped heterodimers, we studied the mechanism of the interconversion of **II-1** and **II-2**. We discovered that the S-shaped to C-shaped isomerization was an intramolecular process that occurs with retention of configuration (Scheme 1). The implications of these studies toward CB[n] synthesis were manifold. For example, we hypothesized that suitable combinations of glycoluril N-H compounds (e.g. **II-3**) and glycoluril bis(cyclic ethers) (e.g. **II-4**) would deliver control over size, shape, and functionalization pattern in CB[n] forming reactions. Herein, we present a full report on the preparation of functionalized CB[n]

analogues[186] with solubility in aqueous solutions and organic solvents through a tailor-made approach as well as mechanistic studies which lead to insights on the stability and formation pathways of CB[n] analogues. These new CB[n] analogues are potentially useful in applications such as fluorescence based sensors,[55,175,176] catalysis,[140,142] cation and molecular transport,[182] in self-sorting systems,[106,193,194] and as components of molecular machines.[195]

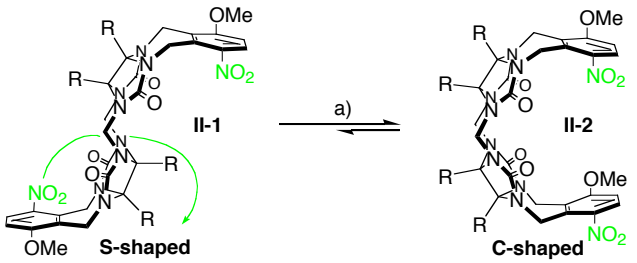

Scheme 1. S- to C-shaped isomerization reaction (R = CO_2Et). Conditions: a) PTSA, $(ClCH_2)_2$, reflux.

2.2 Results and Discussion

2.2.1 Oligomerization Reactions

In order to access a series of bis(cyclic ether) electrophilic building blocks to test our mechanistically guided hypotheses, we performed the condensation of **II-3** with paraformaldehyde in 1,2-dichloroethane in the presence of *p*-toluenesulfonic acid (PTSA) for 2 h at reflux. The bis(cyclic ether) monomer **II-4** was isolated as the major product along with oligomeric bis(cyclic ethers) (**II-5** – **II-9**) (Scheme 2). These compounds could be readily separated by column chromatography and their structures were elucidated by ^{1}H NMR spectroscopy. For example, **II-7** shows 2-

diastereotopic N-CH_2-N resonances whereas **II-5** shows a single resonance for these protons. Compound **II-7** can also be isolated in pure form in gram quantities by washing the crude material with ethyl acetate followed by recrystallization from acetonitrile.

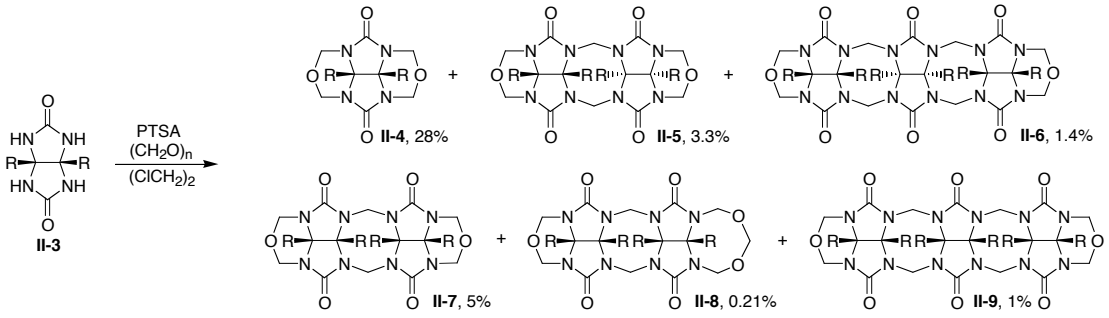

Scheme 2. Controlled oligomerization of **II-3**. R = CO_2Et.

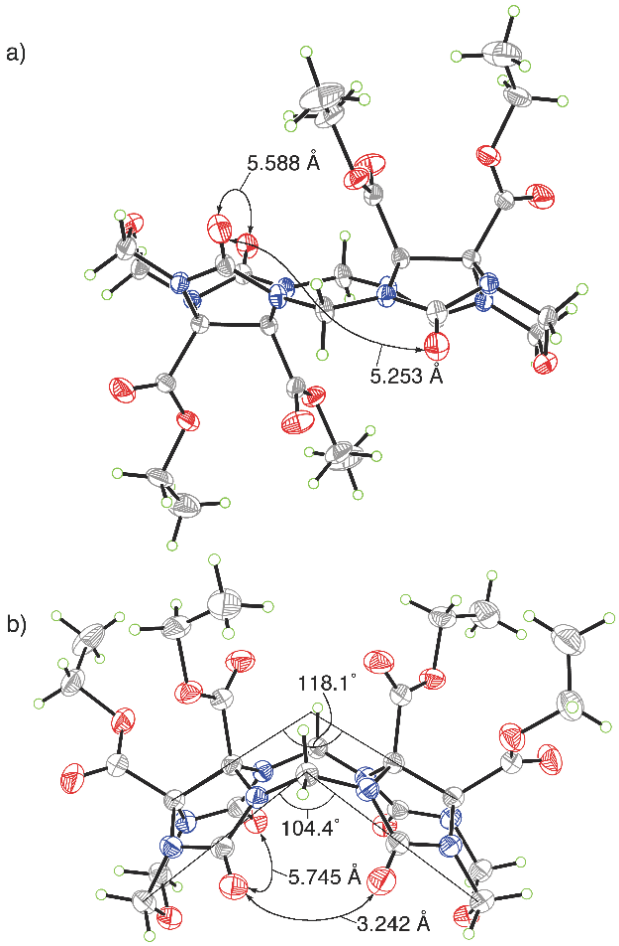

Figure 1. ORTEP plots of the X-ray crystal structures of: a) **II-5** and b) **II-7** with 50% probability ellipsoids and selected distances and angles. Solvent molecules have been omitted for clarity. Color coding: C gray, H green, N blue, O red.

2.2.2 X-ray Crystal Structures of Building Blocks **II-5** and **II-7**

We also confirmed our spectroscopic assignment of the structure of **II-5** and **II-7** by X-ray crystallography (Figure 1). The X-ray structure of **II-5** establishes the relative configuration of the glycolurils rings which gives the S-shape to the molecule. This S-shaped stereochemistry between the two glycoluril rings is not

conducive to forming macrocyclic CB[n] derivatives or analogues unless isomerization to the C-shape occurs concomitantly. Compound **II-7** possesses a C-shape which can be seen in the X-ray crystal structure. The glycoluril rings display both sets of R groups (CO_2Et) on the same face of the molecule which gives the molecule a curvature that promotes the formation of macrocycles. From Figure 1, it is evident that the O•••O distances from the carbonyls in the same glycoluril are relatively similar for **II-5** and **II-7**, but the O•••O distances for the carbonyls in the adjacent glycolurils differ by about 2 Å which can be explained by the directionality incorporated into the shape of glycoluril. When the oligomer is in the S-shape (**II-5**) the carbonyls on the adjacent glycolurils point in opposite directions whereas in the oligomer in the C-shape (**II-7**), the carbonyls on the adjacent glycolurils point in the same direction and begin to define the C=O portals characteristic of the CB[n] family. Although we were unable to isolate tetrameric and higher oligomers, they could be detected by electrospray mass spectrometry.

In an attempt to optimize the reaction conditions of the condensation in order to isolate a higher yield of **II-7** and **II-9** relative to **II-4**, we varied the time of the reaction as well as the ratio of paraformaldehyde to **II-3**. At longer reaction times (> 2 h), **II-4** was indeed reacting but only resulted in the formation of longer oligomers as was evidenced by three broad peaks in the ^{1}H NMR spectrum at ≈ 5.8 ppm and ≈ 4.5 ppm (diasterotopic methylene C-H's indicative of C-shaped glycoluril connections) as well as ≈ 5.3 ppm (methylene C-H's indicative of S-shaped glycoluril

connections). We have not been able to further enhance the yield of building blocks **II-7** and **II-9**.

With C-shaped electrophilic bis(cyclic ether) building blocks **II-4** and **II-7** in hand we set out to synthesize new CB[n] derivatives and analogues by heterodimerization reactions. We hypothesized that the dimer **II-7** and trimer **II-9**, which were already in the thermodynamically favored C-shaped form, would undergo cleaner macrocyclization relative to the S-shaped dimer **II-5** and trimer **II-6**, which do not possess the preorganized shape required for macrocycle formation.

We investigated the macrocyclization of the building blocks under a variety of conditions including refluxing bis(cyclic ethers) (**II-4**, **II-7**, or **II-9**) alone or a combination of bis(cyclic ethers) (**II-4** and **II-7**, **II-7** and **II-9**) in $(ClCH_2)_2$ with PTSA for 1 day or longer at different bis(cyclic ether) and PTSA concentrations.[196] We also investigated the condensation of **II-3** with **II-4**, **II-3** with **II-7**, and **II-3** with **II-9** in hopes of isolating new CB[n] derivatives.[189,197] Unfortunately, we did not detect any doublets at ≈ 5.8 ppm and ≈ 4.5 ppm with coupling constants ≈ 16 Hz in the crude ^{1}H NMR spectrum which would indicate the formation of new methylene bridges required for the formation of CB[n]. Other evidence of the absence of CB[n] formation in the crude reaction mixture was the presence of characteristic doublets at ≈ 5.5 ppm and ≈ 4.7 ppm with coupling constants ≈ 11 Hz, which are due to the diastereotopic methylene C-H's from **II-4**, that do not completely disappear during

the reaction. We hypothesize that the anhydrous acidic conditions employed – to avoid potential saponification of the CO_2Et groups – slows down the S- to C-shaped isomerization of trimeric and higher oligomers which results in oligomer formation rather than macrocyclization.[8,191]

2.2.3 Heterocyclization

In order to circumvent the problem of oligomerization of **II-4**, **II-7**, and **II-9** we resorted to the synthesis of a nucleophilic dimer which could undergo heterodimerization with the bis(cyclic ether) building blocks. For this purpose, we heated **II-7** with 3,5-dimethylphenol (**II-10**) in CF_3CO_2H which gave **II-11** in 63% yield (Scheme 3). We chose **II-10** as the reagent in this deprotection reaction because the *meta*-positions on the aromatic ring are blocked which prevents 7-membered ring formation and promotes removal of the CH_2 bridges from **II-7**.[198] Compound **II-11** has the same curvature as **II-7**, but now possesses four potentially nucleophilic ureidyl N-H groups that can be used to form new methylene bridges in the synthesis of CB[n]. Our initial hypothesis was that the reaction between **II-7** and **II-11** under anhydrous acidic conditions would yield CB[n] with multiples of two (CB[6], CB[8], CB[10], etc.) glycoluril rings by a heterocyclization process which could be monitored by ^{1}H NMR analysis. If the formation of macrocycles occurred, we would expect to see a new set of doublets with coupling constants of ≈ 16 Hz at ≈ 5.8 ppm and ≈ 4.5 ppm in the ^{1}H NMR spectrum. Despite several attempts under a variety of different conditions (acid, concentration, ratios, etc.), we could not obtain any

evidence for the formation of macrocyclic CB[n] by ^{1}H NMR analysis. We consistently observed either oligomerization or decomposition. We hypothesize that the S- to C-shaped isomerization of compounds containing three or more glycoluril units is not possible under the anhydrous reaction conditions resulting in the formation of linear oligomers rather than macrocycles.[8,186,191] Due to our inability to use either **II-7** or **II-11** in the tailor-made synthesis of CB[n] derivatives with enhanced properties, we decided to search for other nucleophilic partners that might undergo selective heterodimerization reactions with the bis(cyclic ether) building blocks to ultimately deliver *CB[n] analogues*.

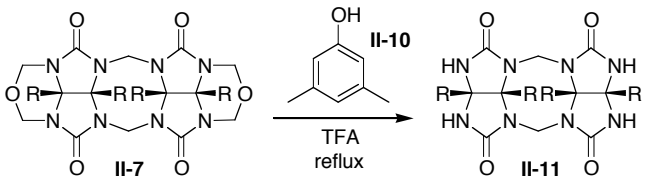

Scheme 3. Bis(cyclic ether) deprotection (R = CO_2Et, 63%).

2.2.4 Gycoluril Surrogates

Through serendipity, we discovered that **II-12** and **II-13** undergo rapid, highly selective heterodimerization yielding **II-14** in 69% yield (Scheme 4). We attribute this result to the enhanced nucleophilicity of the hydrazide N-H groups present in **II-13** due to the α-effect. After obtaining this result, we were interested in studying the reactivity of other hydrazides. For example, condensation of **II-15** with **II-12** in TFA gave **II-16** in 55% yield (Scheme 4). We were able to perform this condensation reaction in TFA due to the increased solubility of **II-15**. Interestingly,

if **II-16** is submitted to PTSA/$(ClCH_2)_2$ at reflux with 1 equiv. of **II-13**, a replacement reaction is observed which delivers **II-14** in 81% yield. This result indicates that **II-13** is a superior partner in these reactions, presumably because it sacrifices less resonance energy upon condensation and suggests that CH_2-bridges between glycoluril and phthalhydrazide rings form reversibly.

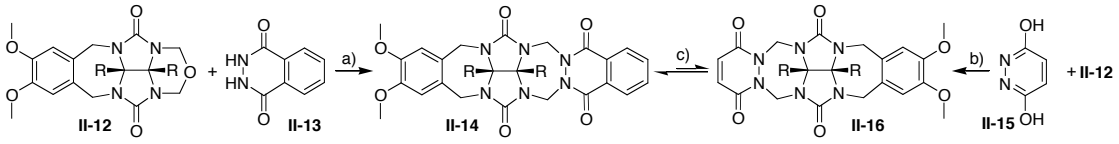

Scheme 4. Glycoluril surrogates **II-13** and **II-15**. Conditions: a) PTSA, $(ClCH_2)_2$, reflux, 69%; b) TFA, reflux, 55%; c) 1 equiv. **II-13**, PTSA, $(ClCH_2)_2$, reflux, 81%. R = CO_2Et.

2.2.5 CB[n] Analogues

2.2.5.1 Synthesis

To allow for potential macrocycle formation, we synthesized bis(phthalhydrazide) **II-17** by the reaction of pyromellitic anhydride with hydrazine in acetic acid at reflux.[199] Compound **II-17**, which is planar, does not result in S- and C-shaped diastereomers upon reaction with **II-7**, which is expected to favor macrocyclization relative to oligomerization. Unfortunately, the solubility of **II-17** is poor in all common organic solvents (< 1 mg/mL in $CHCl_3$, CH_3CN, $(ClCH_2)_2$, PhH, and TFA). After much experimentation, we found that **II-17** is soluble in hot, anhydrous $MeSO_3H$.[200] Accordingly, we attempted the condensation reaction of **II-7**

with **II-17** (Scheme 5). We were delighted to observe a remarkably clean ^{1}H NMR spectrum of the crude reaction mixture. Pure CB[6] analogue **II-18** could be obtained in 78% yield simply by washing the crude solid with H_2O and acetone. Next, we condensed the monomeric building block (**II-4**) with **II-17** to give the CB[5] analogue **II-19** although in much lower isolated yield (6%). Finally, we investigated the condensation of **II-9** with **II-17** in hope of forming a CB[8] analogue by a four component macrocyclization. Once again, the crude reaction mixture was remarkably clean and we were able to isolate a single compound by SiO_2 chromatography in 67% yield.[201] Surprisingly, however, the new compound proved to be CB[7] analogue (±)-**II-20** formed by the condensation of 2 equiv. **II-9** with 1 equiv. **II-17**. This new macrocycle possesses several unusual structural features: 1) it is chiral and racemic due to its C_2-symmetry, 2) it contains a single methylene bridge between the 2 equivalents of **9**, and 3) this methylene group is directed into the cavity of (±)-**II-20**.

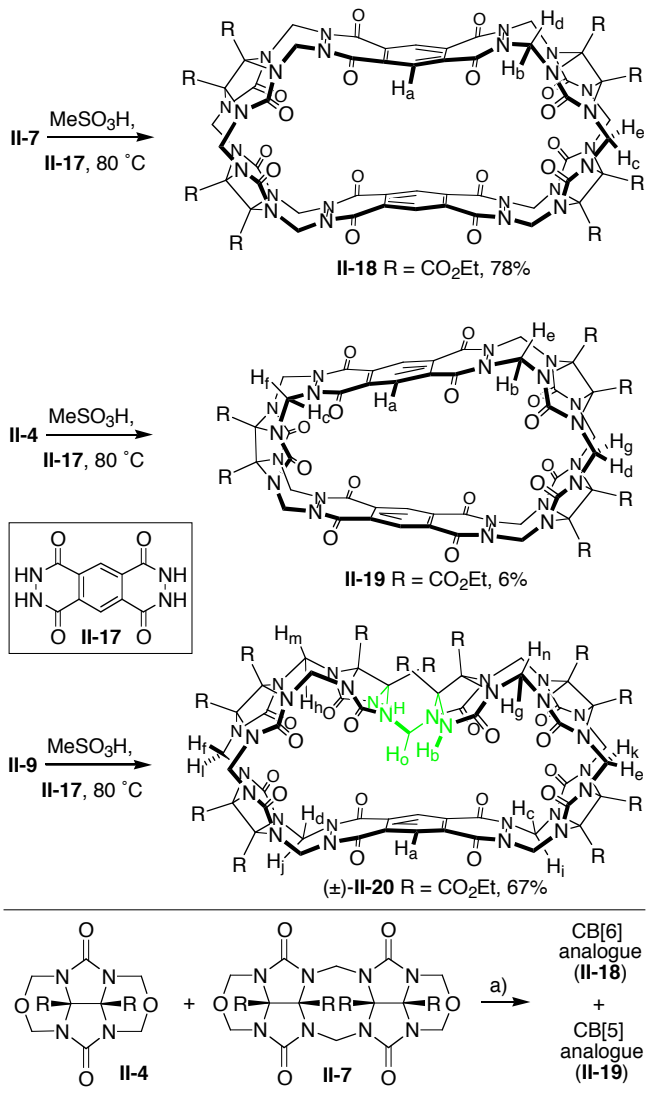

Scheme 5. Synthesis of CB[n] analogues (R = CO_2Et). Conditions: a) **II-17**, $MeSO_3H$, 80 ˚C.

In order to understand the reasons behind the low yield obtained for CB[5] **II-19**, we carried out the three component macrocyclization (**II-4** + **II-7** + **II-17**) shown in Scheme 5. In contrast to the low yield obtained with **II-4** and **II-17**, analysis of the crude ^{1}H NMR spectrum for the three component macrocyclization indicated a clean formation of a 1:1 mixture of **II-18** and **II-19**. Unfortunately, we were unable to

separate this mixture into its components. Apparently, the need to form methylene bridges *between glycolurils* – a process that is quite slow relative to the formation of methylene bridges between glycolurils and phthalhydrazide rings – in the macrocyclization of **II-4** and **II-17** alone is obviated by the use of **II-4**, **II-7**, and **II-17**. Consequently, a larger fraction of material undergoes macrocyclization rather than oligomerization in the three component reaction. Although we were delighted with the formation of CB[5], CB[6], and CB[7] analogues (**II-18** – **II-20**), we were disappointed by their relatively low solubility in both aqueous and organic solvents. Whereas TFA and DMSO are excellent solvents for the $–CO_2Et$ substituted CB[n] analogues their solubilities in CH_3CN were only modest (1-2 mM).

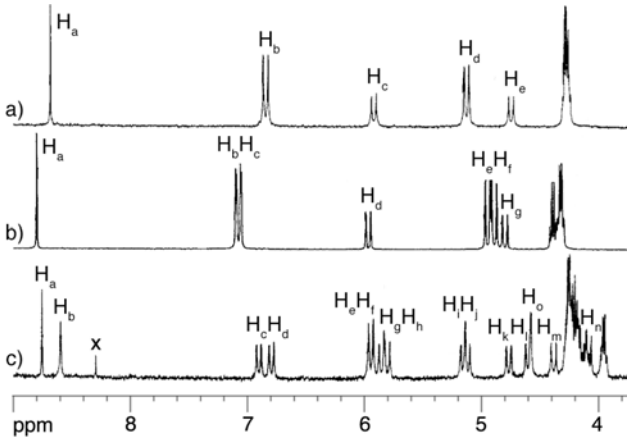

Figure 2. Portion of the ^{1}H NMR spectra (298 K, 400 MHz) recorded for: a) **II-18** in DMSO-d_6, b) **II-19** in CD_3CN, c) (±)-**II-20** in DMSO-d_6. × = $CHCl_3$ in DMSO-d_6. The unlabeled resonances come from the $CO_2CH_2CH_3$ groups.

2.2.5.2 ^{1}H NMR Spectral Characterization

The ^{1}H NMR spectra of **II-18**, **II-19**, and (±)-**II-20** are shown in Figure 2 using the labeling from Scheme 5. The aromatic proton H_a is the furthest downfield

in all cases. The spectrum for **II-18** has the fewest resonances for the methylene protons due to its D_{2h}-symmetry (Figure 2a). The diastereotopic protons H_b and H_d are on the methylene bridges connecting the bis(phthalhydrazide) and the glycoluril. The diastereotopic protons H_c and H_e resonate at chemical shifts similar to CB[n] methylene bridges because they are between the adjacent glycolurils. In contrast, the spectrum for C_{2v}-symmetric macrocycle **II-19** has resonances for two pairs of distereotopic protons between glycoluril and phthalhydrazide rings (H_b, H_c, H_e, and H_f, Figure 2b). The doublets for H_d and H_g appear at similar chemical shifts relative to macrocycle **II-18** corresponding to the methylene bridges that connect the two glycolurils. Finally, the ^{1}H NMR spectrum of macrocycle (±)-**II-20** which possesses a C_2 axis which gives rise to twelve doublets, some of which are overlapping (Figure 2c). Proton H_b is the ureidyl N-H proton (8.65 ppm) which is shifted upfield slightly when compared to the ureidyl N-H (8.85 ppm) of compound **II-11** in DMSO-d_6. This result can be explained by H_b being directed into the shielding region of the aromatic wall of the bis(phthalhydrazide). Most notable is the resonance for proton H_o which appears as a singlet in the ^{1}H NMR spectrum due to the fact that the methylene bridge connecting the two glycolurils (shown in green in Scheme 5) is similar to an S-shaped oligomer (**II-5**) making these protons magnetically equivalent.

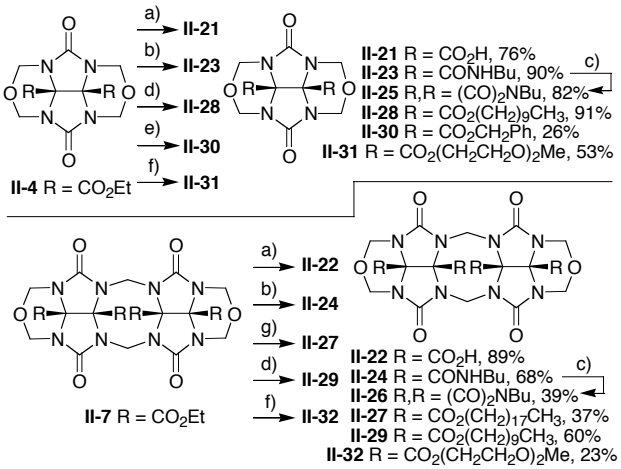

Scheme 6. Building blocks for the synthesis of CB[n] analogues. Conditions: a) i. LiOH, CH_3OH, H_2O; ii. $HClO_4$, H_2O; b) H_2NBu, neat, 78 ˚C; c) $ClCH_2CH_2Cl$, PTSA, reflux; d) $HO(CH_2)_9CH_3$, $KOCH_3$, 18-crown-6, $PhCH_3$, reflux; e) $HOCH_2Ph$, $KOCH_3$, 18-crown-6, $PhCH_3$, reflux; f) $HO(CH_2CH_2O)_2CH_3$, $KOCH_3$, 18-crown-6, $PhCH_3$, reflux; g) $HO(CH_2)_{17}CH_3$, $KOCH_3$, 18-crown-6, $PhCH_3$, reflux.

2.2.6 Synthesis of Glycoluril Building Blocks Designed to Enhance the Solubility of CB[n] Analogues

To enhance the solubility of the CB[n] analogues in aqueous and organic media, we attempted both deprotection and transesterification of the ethyl esters on the equator of macrocycles **II-18** – **II-20**. Unfortunately, the phthalhydrazide linkages of **II-18**, **II-19**, and (±)-**II-20** are sensitive to base and these reactions were not successful. Accordingly, we decided to transform the CO_2Et groups into carboxylic acid derivatives (e.g. amides, imides, esters, and acids) prior to macrocyclization (Scheme 6).[202]

For potential recognition studies in H_2O, we performed the saponification of **II-4** and **II-7** with LiOH in CH_3OH/H_2O and were able to isolate the carboxylic acids **II-21** and **II-22** in 76 and 89% yield, respectively, after acidification with $HClO_4$ and washing with ethyl acetate. To increase the solubility of the corresponding CB[n] analogues in organic media, we converted the CO_2Et groups to different esters, amides, and imides by straightforward functional group manipulations.[202] For example, amidation reactions occurred smoothly by subjecting **II-4** and **II-7** to neat butyl amine delivering **II-23** in 90% and **II-24** in 68% yield, respectively. Compounds **II-23** and **II-24** could be converted to the imides **II-25** and **II-26** in 82 and 39% yield, respectively, by heating under anhydrous acidic conditions (PTSA/$(ClCH_2)_2$, reflux). For highest solubility in organic solvents such as $CHCl_3$ and CH_2Cl_2 we performed transesterification reactions to increase the lipophilicity of the building blocks which renders the resulting CB[n] analogue soluble in nonpolar solvents. For this purpose, we selected the conditions used by Sanders for thermodynamically controlled transesterification reactions because this procedure is well established, provided good yields, and was simple to perform.[203] Accordingly, compound **II-7** was treated with 1-octadecyl alcohol to yield **II-27** in 37% (Scheme 6). We also performed the transesterification of **II-4** and **II-7** with 1-decyl alcohol which yielded **II-28** and **II-29** in 91% and 60% yields, respectively. In order to assess the generality of these transesterification reactions we tested several different alcohols and obtained **II-30**, **II-31** and **II-32** in modest yields (Scheme 6). Apparently, a fine balance of steric and electronic effects influences the efficiency of

the four-fold transesterification. All of these new building blocks possess high solubility in non-polar solvents like $CDCl_3$ commonly used for our self-assembly studies.

2.2.7 X-ray Crystal Structures of Building Blocks **II-22** and **II-26**

We obtained crystals of **II-22** and **II-26** suitable for X-ray crystal structure determination from aqueous HCl and CH_3CN, respectively (Figure 3). In this section we discuss some of the structural features of **II-22** and **II-26** that influence the preorganization of these building blocks for CB[n] analogue formation. For example, the bond angle through the glycoluril quaternary carbons of **II-22** (121.2˚) and **II-26** (116.7˚) are nearly identical to that observed for CB[6] (118.7˚).[2] The bond angle through the methylene bridges of **II-22** (105.7˚) and **II-26** (102.7˚) are somewhat smaller than the corresponding values for CB[5] (110.1˚) and CB[6] (116.4˚); we attribute this difference to the presence of 6-membered cyclic ether rings in **II-22** and **II-26** whereas CB[n] possesses 8-membered rings. The crucial O•••O distances which define the depth of the macrocycle and the width of its portals for **II-22** (5.745 and 3.242 Å) and **II-26** (5.646 and 3.236 Å) are 0.2 – 0.3 Å shorter than observed for CB[6] (6.042 and 3.417 Å). In combination, these crystallographic results suggest that building blocks **II-22** and **II-26** are preorganized to form CB[5] and/or CB[6] analogues.

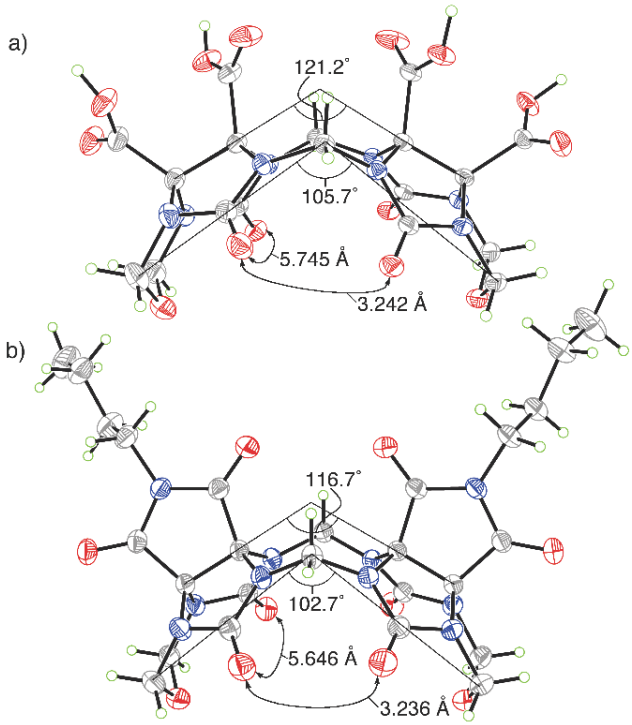

Figure 3. ORTEP plots of the X-ray crystal structures of a) **II-22** and b) **II-26** with 50% probability ellipsoids along with selected distances and angles. Solvent molecules have been omitted for clarity. Color coding: C gray, H green, N blue, O red.

2.2.8 CB[n] Analogues with Enhanced Solubility

We were pleased to find that when **II-22** is condensed with **II-17**, CB[6] analogue **II-33** is formed in 65% yield which possesses exceptional solubility (≈ 18 mM) in aqueous solutions as determined by gravimetric analysis (Scheme 7). Similarly, the condensation of **II-21** with **II-17** gave CB[5] analogue **II-34** although in a very disappointing 3% yield after extensive purification. The solubility of **II-34**

in aqueous solutions (≈ 24 mM) is slightly higher compared to **II-33**. These water soluble CB[5] and CB[6] analogues retain much of the unique binding properties of the CB[n] family with the added properties of long-wave UV/Vis and fluorescence activity which allows for easy detection of the macrocycle under a variety of conditions.[175]

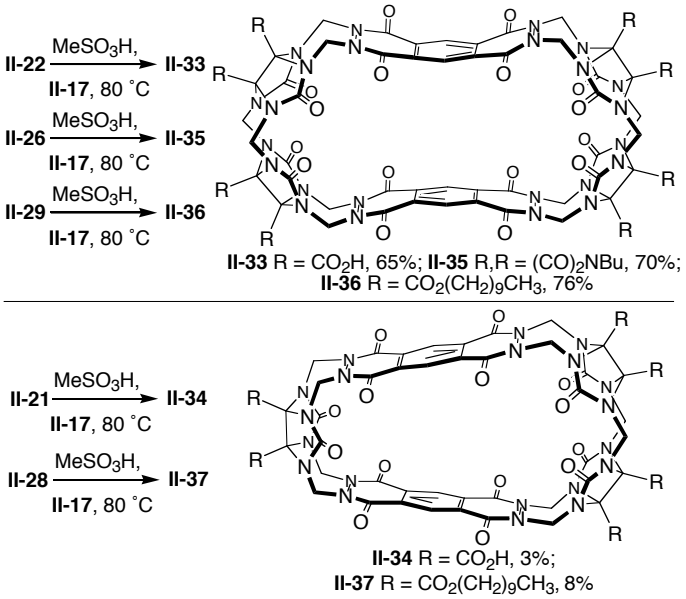

Scheme 7. Synthesis of CB[n] analogues soluble in water and organic solvents.

When we submitted **II-26** to the macrocyclic forming reaction conditions we obtained CB[6] analogue **II-35** in 70% yield which was poorly soluble in $CHCl_3$. Next, we submitted tetrakis(octadecyl ester) **II-27** to the reaction conditions and to our surprise discovered that **II-27** was not soluble in $MeSO_3H$. No CB[6] analogue could be obtained with this building block. Apparently, **II-27** is too lipophilic which does not allow it to be soluble in the polar acidic solvent ($MeSO_3H$). In contrast, the condensation reaction of tetrakis(decyl ester) **II-29** with **II-17** proceeded smoothly to give CB[6] analogue **II-36** in 76% yield (Scheme 7). A similar reaction was

performed with **II-28** and **II-17** which delivered CB[5] analogue **II-37** in 8% yield.[204] Macrocycles **II-36** and **II-37** possess excellent solubility (≈ 30 mM and ≈ 24 mM, respectively) in $CHCl_3$; solubility is comparable in CH_2Cl_2 and THF.

The purification of these new macrocycles with their enhanced characteristics is possible by simple column chromatography which is important due to the fact that CB[n] cannot be separated using SiO_2 because CB[n] are not soluble in solvents appropriate for SiO_2 columns and CB[n] are not easily detectable by UV/Vis. Therefore, more involved purification techniques, including ion-exchange (Dowex) and size-exclusion (Sephadex) resins using high boiling point solvents such as aqueous acids, have been formulated for the separation and purification of CB[n], all of which are laborious. Additionally, the solubility of these new CB[n] analogues enable studies of their molecular recognition properties in organic solvents and aqueous solution.

The relatively poor solubility of **II-35** in organic solvents proved beneficial in that crystals suitable for X-ray crystallography could be obtained from $CH_3CN/PhCH_3$. Figure 4 shows the X-ray crystal structure of **II-35**. Unlike the known cylindrical-shaped CB[n], **II-35** assumes a more elongated-oval shape with cavity dimensions of 5.90 x 11.15 x 6.92 Å. The O•••O distances on the adjacent glycolurils for **35** are 3.424 Å and are 5.930 Å on the same glycoluril respectively, which are similar to the distances observed for **II-26** (Scheme 3b) and CB[6] (3.417 and 6.042 Å). The bond angles of the adjacent glycolurils through the methylene

bridges for **II-35** (111.8˚; CB[6] = 116.4˚) and through the quaternary carbons on the glycoluril (120.2˚; CB[6] = 118.7˚) are comparable. The adjacent glycolurils appear to be slightly pinched in **II-35** to help compensate for the flat bis(phthalhydrazide) (**II-17**) incorporated into the macrocycle.

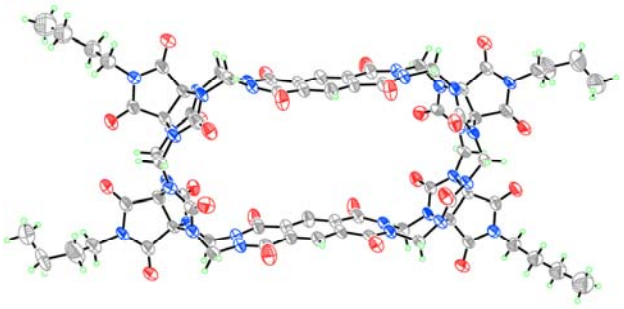

Figure 4. ORTEP plot of the X-ray crystal structure of **II-35** with 50% probability ellipsoids. Solvating CH_3CN molecules within the cavity have been omitted for clarity. Color coding: C gray, H green, N blue, O red.

2.2.9 Mechanistic Studies

We were surprised that the yields of the CB[6] analogues **II-18**, **II-33**, **II-35**, **II-36** were ≥65% given the potential complexity of the intermediates leading to their formation. This result suggests that the condensation of 2 equivalents of bis(cyclic ether) **II-38** with 1 equivalent bis(phthalhydrazide) **II-17** is not a random process and the reaction pathway must favor macrocycle formation. Scheme 8 presents a mechanistic hypothesis that details potential intermediates in CB[6] analogue formation. In a common first step, nucleophilic **II-17** reacts with electrophilic **II-38** to form **II-39** by a condensation process. Intermediate **II-39** can lead to intermediate

II-40 by reaction with **II-17** or C- and S-shaped diastereomers **II-41** and **II-42** by condensation with **II-38**. Intermediates **II-40** and **II-41** lead to a common intermediate **II-44** which is preorganized for macrocyclic formation. Alternatively, both **II-40** and **II-42** can lead to S-shaped intermediate **II-43** which is prevented from being directly converted to **II-45** by virtue of the relative stereochemistry of its two methylene bridged glycoluril dimeric subunits. Intermediates **II-42** and **II-43** are destined to form oligomers or polymers unless a change from the S-shaped to C-shaped relative orientation of the C-shaped building blocks is feasible. In this section we address key mechanistic questions that provide a rationale for the high yield of CB[6] analogues. In particular, we investigated: 1) the existence of an equilibrium between **II-41** and **II-42** and between **II-43** and **II-44** (aqua arrows), 2) the nature of these equilibria (e.g. intra- versus intermolecular; intramolecular **II-41** $\rightleftharpoons$ **II-42**, intermolecular **II-41** $\rightleftharpoons$ **II-39** + **II-17** $\rightleftharpoons$ **II-42**), and 3) the existence of an equilibrium (red arrows) between **II-44** and **II-45** (e.g kinetic *versus* thermodynamic products).

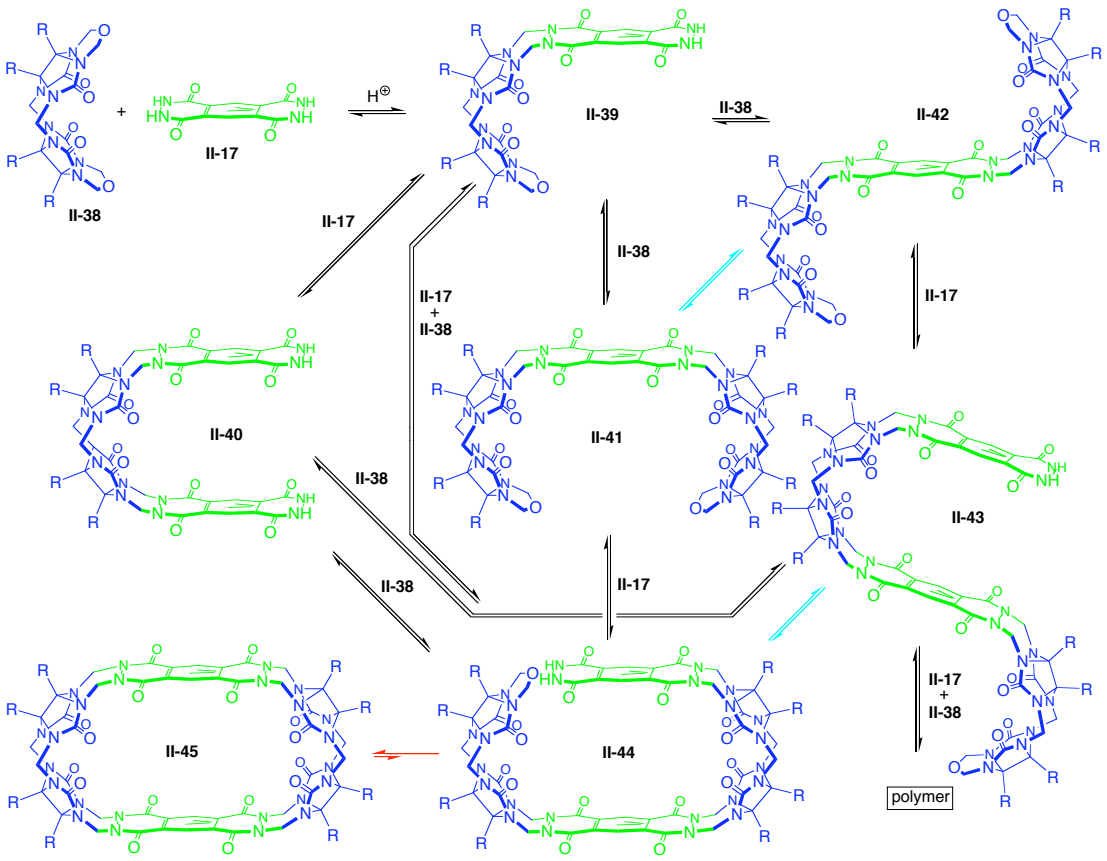

Scheme 8. Possible pathways in the formation of CB[6] analogues.

2.2.9.1 Establishment of an S- to C-Shaped Equilibrium

To address the first question – the potential presence of an equilibrium between **II-41** and **II-42** (and **II-43** and **II-44**) – we adapted a labeling experiment that we had previously used to study the mechanism of CB[n] formation.[8,191] For this purpose we reacted **II-7** and **II-46** to produce a separable mixture of **II-47C** and **II-47T** (Scheme 9a). Compounds **II-47C** and **II-47T** were separately resubmitted to the reaction conditions; in both cases we observed a 66:34 ratio of **II-47C**:**II-47T**.[205] This experiment establishes an equilibrium between **II-47C** and **II-47T** – and by

analogy suggests an equilibrium between **II-41** and **II-42** (**II-43** and **II-44**) – but does not differentiate between intra- and intermolecular S- to C-shape isomerization.

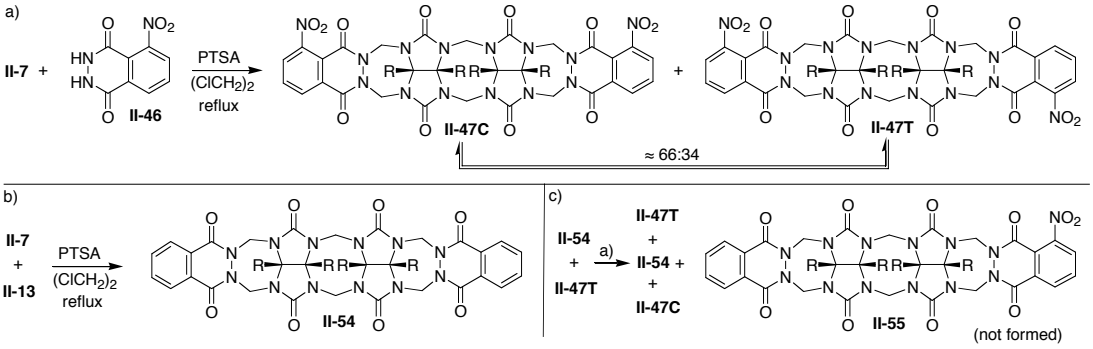

Scheme 9. a) Synthesis and isomerization of **II-47C** and **II-47T**; b) Synthesis of **II-54**, 71%; and c) evidence of mixed dimer **II-55** not being formed (R = CO_2Et). Conditions: a) PTSA, $(ClCH_2)_2$, reflux.

2.2.9.2 Differentiation Between Intramolecular and Intermolecular S- to C-Shaped Isomerization

Scheme 10 shows proposed mechanistic pathways for the intramolecular isomerization (green arrows) and the intermolecular isomerization (red arrows) for **II-47C** to **II-47T**. In brief, compound **II-47C** initially undergoes protonation and fragmentation to yield N-acyliminium ion **II-48**. Intermediate **II-48** – under our anhydrous acidic conditions – yields N-acylammonium **II-49** by intramolecular capture by the N-atom. Subsequently, **II-49** can fragment to either **II-48** or **II-50**. Intermediate **II-50** cyclizes to yield **II-51** which losses a proton to give **II-47T**. Intermolecular isomerization proceeds via intermediates **II-52** and **II-53**. To differentiate between intra- versus intermolecular processes in the S- to C-shaped conversion, we resorted to a crossover experiment. For this purpose we prepared **II-54** by the condensation of **II-7** and **II-13** (Scheme 9b). Next we allowed **II-47T** to

isomerize in the presence of **II-54** (Scheme 9c). If the equilibrium between **II-47C** and **II-47T** is an intramolecular process then we would only expect to observe homodimeric **II-54** and **II-47C**/**II-47T** at equilibrium. In contrast, if dissociation of a phthalhydrazide wall is necessary (e.g. intermolecular pathway, red arrows) then we would expect to observe the formation of **II-54**, **II-47C**, **II-47T**, and heterodimer **II-55**. In the actual experiment, we do not observe the formation of **II-55** under these conditions. This result establishes an intramolecular isomerization between **II-47C** and **II-47T** and suggests similar unimolecular isomerization between **II-41** and **II-42** (**II-43** and **II-44**; aqua arrows, Scheme 8).

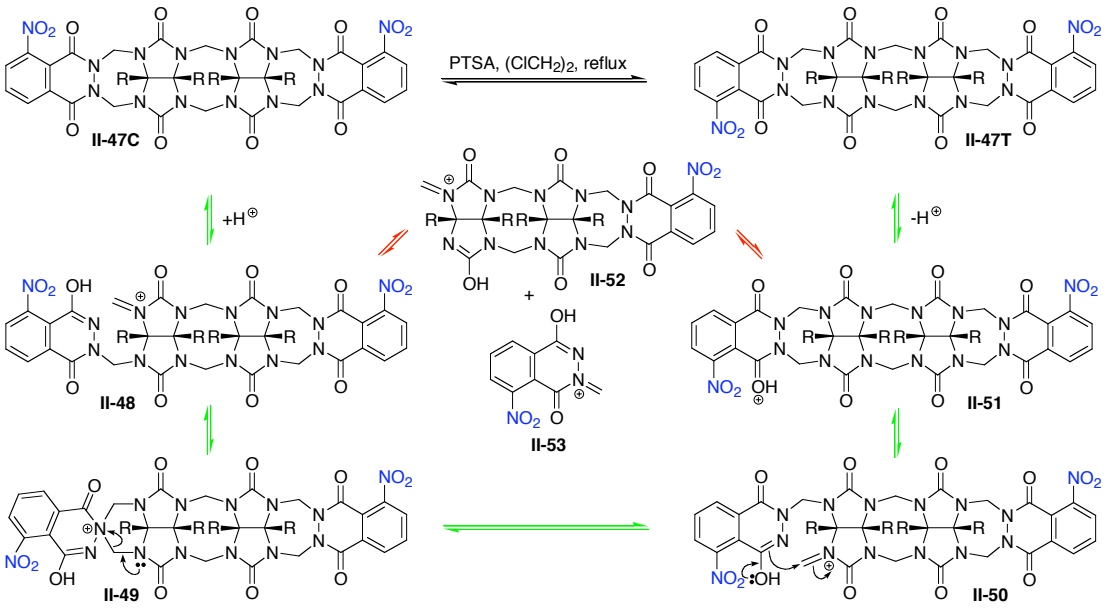

Scheme 10. Proposed mechanisms for the equilibrium between **II-47C** and **II-47T** dimers (R = CO_2Et).

2.2.10 Stability of CB[n] Analogues

CB[n] is a very robust family of macrocycles whose stabilities have been tested with several methods.[63] The incorporation of phthalhydrazides into our macrocycles gives rise to useful new properties like UV/Vis, fluorescence, and electrochemical activity. Unfortunately, the incorporation of phthalhydrazides in the macrocycle also leads to the sensitivity to basic conditions (pH > 7). In contrast, the CB[n] analogues are stable under aqueous acidic conditions. To test whether the new CB[n] analogues were kinetic or thermodynamic products, we resubmitted them to the reaction conditions ($MeSO_3H$, 80˚C, 24 h). As the solution was heated, a color change was seen from a pale yellow to a dark orange. The ^1H NMR spectrum for each CB[n] analogue showed small peaks in the downfield (H-Ar-phthalhydrazide) region of the ^1H NMR spectrum. Although we could not identify these by-products, this result establishes that **II-18**, **II-19**, and (±)-**II-20** are not thermodynamically stable under the reaction conditions and therefore, represent products formed under kinetic control. This result, in combination with the replacement reaction (**II-16** + **II-13** + **II-14**) detailed in Scheme 4 supports our suggestion that the macrocyclization reaction is reversible (red arrows, Scheme 8).

2.2.11 S-Shaped Building Blocks Break Apart During Macrocyclic Reactions

Based on the fact that C-shaped oligomers **II-7** and **II-9** form **II-18** and (±)-**II-20**, respectively, when reacted with **II-17**, we were curious to see what would happen if the S-shaped oligomers **II-5** and **II-6** were used in place of the C-shaped

oligomers. We previously established that the S-shaped **II-1** and C-shaped **II-2** are the kinetic products formed, that isomerized under forcing conditions (anh. PTSA in $ClCH_2CH_2Cl$) to yield **II-2** by an intramolecular isomerization. The reaction of phthalhydrazides with bis(cyclic ethers) is much faster than the cyclic ether dimerizing with itself. For example, in the reaction of **II-12** with **II-13** (Scheme 4) we do not detect any self-condensation occurring between two molecules of **II-12**; the formation of compound **II-14** was exclusively observed.

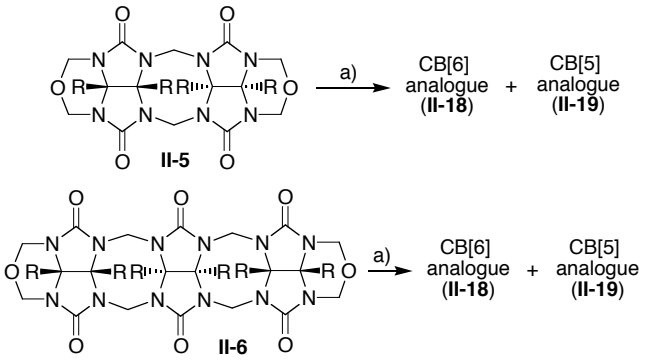

Scheme 11. S-shaped oligomers **II-5** and **II-6** yield CB[5] and CB[6] analogues (R = CO_2Et). Conditions: a) **II-17**, $MeSO_3H$, 80 ˚C.

We attempted these condensation reactions with the S-shaped isomers in order to gain further insight into the mechanism of the formation of CB[n] analogues. In the event, reaction of **II-5** or **II-6** with **II-17** in anhydrous $MeSO_3H$ yields a mixture of CB[6] analogue (**II-18**) and CB[5] analogue (**II-19**) in almost a 1:1 ratio in high overall yield based on the crude ^1H NMR spectrum (Scheme 11) which is similar to the results obtained using **II-4**, **II-7**, and **II-17** (see Scheme 5). This experiment provides indirect evidence that S-shaped compounds **II-5** and **II-6** rearrange to form C-shaped building blocks **II-4** and **II-7** which results in the formation of CB[6] and

CB[5] analogues (**II-18** and **II-19**). In contrast, attempted isomerization experiments using only **II-5** or **II-6** leads to further oligomerization rather than isomerization which was evident by broad peaks in the ^{1}H NMR spectrum of the crude reaction mixture. Under these conditions, we hypothesize that oligomerization (self-condensation) of **II-5** and **II-6** occurs faster or at similar rates relative to the isomerization required to yield the C-shaped forms **II-7** and **II-9**. Apparently, the presence of bis(phthalhydrazide) **II-17** in the reaction mixture changes the kinetics and thermodynamics of the reaction by providing an *in situ* self-protection of compounds **II-5** and **II-6** preventing further oligomerization resulting in the formation of macrocyclic products **II-18** and **II-19**.

2.2.12 Template Effects

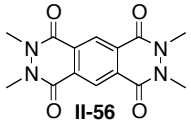

II-56

To address whether template effects are important in the formation of the CB[6] analogues we performed two experiments. First, we performed the macrocyclization in the presence of 1 equiv. of **II-56** as potential template that is unreactive under the reaction conditions. We performed a ^{1}H NMR experiment with **II-56** and **II-18** to determine whether host-guest interactions are present. From the experiment, we conclude that there are not favorable interactions between **II-56** and **II-18** in $MeSO_3H$. Even though **II-56** does not bind to **II-18** in $MeSO_3H$, it may still partake in favorable π-π interactions with intermediates **II-40** and **II-44** (see Scheme

8) which lead to **II-18** and thereby template its formation. When we conducted the reaction between **II-7** (2 eq.) and **II-17** (2 eq.) in the presence of potential template **II-56** (1 eq.), we isolated **II-18** in 59% yield which is slightly lower than that observed in its absence.[206]

As a second test for potential templation effects, we performed the macrocyclization at a series of different concentrations (147, 44, and 22 mM) to discern if **II-40** (or other intermediates) act as templates for the formation of the CB[6] analogues. In these experiments, the isolated yields of CB[6] analogue **II-18** were 78%, 74%, and 70%, respectively. There is a slight decrease in the isolated yield as the reaction concentration is decreased, but it is minimal. The combined inference of both sets of experiments is that templation effects are not important in the formation of CB[6] analogues.

2.3 Conclusion

The synthesis of CB[n] analogues – with outstanding solubility characteristics in both water and organic solution – has been presented with the focus on functionalization and mechanistic studies. C-shaped building blocks (e.g. **II-7** and **II-9**) are preorganized for macrocycle formation whereas their S-shaped diastereomers (e.g. **II-5** and **II-6**) undergo fragmentation reactions concomitant with macrocyclization. The mechanistic studies have established the intramolecular S- to

C-shaped isomerization as a key step in the synthesis of the CB[6] analogues. In contrast to the unfunctionalized cucurbiturils, the macrocyclization which delivers the CB[n] analogues is under kinetic rather than thermodynamic control and is not subject to the effects of templation. The properties of the new CB[n] analogues are enhanced by the incorporation of the bis(phthalhydrazide) walls which endow them with UV/Vis, fluorescence, and electrochemical activity.

The insights derived from our study of the mechanism of formation of the CB[6] analogues suggest methods for the expansion of the synthetic method to the production of different CB[n] analogues of greater stability and functionality. In addition, although the building block approach has only been exploited using bis(phthalhydrazide) **II-17**, we envision that longer and non-planar bis(phthalhydrazides) as well as other nucleophilic glycoluril surrogates should perform equally well in these macrocyclization reactions. The ability to increase the size of the cavity would allow for different binding properties (e.g. the formation of termolecular and higher molecularity complexes) as well as different optical properties depending on the glycoluril surrogate incorporated into the macrocycle. Currently, these new CB[6] analogues, both the aqueous and organic soluble macrocyles, are being studied to evaluate their potential for application as components of molecular machines, in self-sorting systems, and as fluorescent sensors for chemically and biologically important amines.

2.4 Experimental

2.4.1 Synthetic Procedures and Characterization

General. Starting materials were purchased from Alfa-Aesar, Acros, and Aldrich and were used without further purification. Compounds **II-1** and **II-2** were prepared by literature procedures.[191,192] TLC analysis was performed using pre-coated glass plates from E. Merck. Column chromatography was performed using silica gel (230-400 mesh, 0.040-0.063 μm) from E. Merck using eluents in the indicated v:v ratio. Melting points were measured on a Meltemp apparatus in open capillary tubes and are uncorrected. IR spectra were recorded on a Nicolet Magna spectrophotometer as KBr pellets or thin films on NaCl plates and are reported in cm^{-1}. UV/Vis spectra were recorded on an Agilent 8453 diode array spectrophotometer. NMR spectra were measured on Bruker AM-400 and DRX-400 instruments operating at 400 MHz for ^{1}H and 100 MHz for ^{13}C. Mass spectrometry was performed using a VG 7070E magnetic sector instrument by fast atom bombardment (FAB) using the indicated matrix. The matrix "magic bullet" is a 5:1 (w:w) mixture of dithiothreitol:dithioerythritol. Elemental analyses were performed by Midwest MicroLab (Indianapolis, IN).

Oligomerization of II-3: A mixture of PTSA (33.23 g, 174.7 mmol) and $ClCH_2CH_2Cl$ (500 mL) was heated at reflux for 30 min. under an addition funnel filled with molecular sieves (4Å). Compound **II-3** (10.00 g, 34.95 mmol) was added

and allowed to dissolve completely. Then, paraformaldehyde (5.25 g, 175 mmol) was added and reflux was continued for 2 h. The reaction mixture was diluted with EtOAc (800 mL), washed with sat. Na_2CO_3, dried over anh. $MgSO_4$, concentrated, and the residue was dried under high vacuum. Flash chromatography (SiO_2, $CHCl_3/CH_3CN$ 10:1) gave **II-4** (3.58 g, 9.78 mmol, 28%), **II-5** (0.394 g, 0.579 mmol, 3.3%), **II-6** (0.164 g, 0.165 mmol, 1.4%), and **II-7** (0.579 g, 0.851 mmol, 5.0%) all as white solids. The mobile phase was changed to 5:1 $CHCl_3/CH_3CN$ to give the impure **II-8** as a white solid that was recrystallized from MeOH to yield **II-8** (0.026 g, 0.037 mmol, 0.21%). Impure **II-9** was isolated as an off-white solid. The solid was washed with a small amount of EtOAc, centrifuged, and dried to give **II-9** as a white powder (0.120 g, 0.121 mmol, 1.0%).

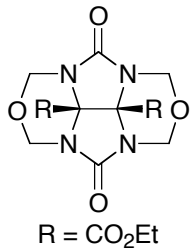

Compound II-4. M.p. 189-190 ˚C. TLC ($CHCl_3$/Hexanes/EtOAc, 1:1:1) R_f 0.38. IR ($CHCl_3$, cm^{-1}): 2940w, 2911w, 2873w, 1755s, 1735s, 1474s, 1403s, 1380s, 1294s, 1170, 1027s. ^1H NMR (400 MHz, $CDCl_3$): δ 5.53 (d, J = 11.3, 4H), 4.82 (d, J = 11.3, 4H), 4.31 (q, J = 7.2, 4H), 1.32 (t, J = 7.2, 6H). ^{13}C NMR (100 MHz, $CDCl_3$): δ 164.4, 156.7, 74.4, 72.2, 63.6, 13.7. MS (FAB, Magic Bullet): *m/z* 371 (27, $[M + H]^+$); 341 (100, $[M + H - CH_2O]^+$). HR-MS (FAB, Magic Bullet): *m/z* 371.1197 ($[M + H]^+$, $C_{14}H_{19}O_8N_4$, calcd 371.1203). X-ray crystal structure.

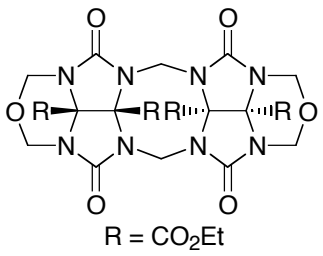

Compound II-5: M.p. 235 °C. TLC (CH_2Cl_2/CH_3CN, 10:1) R_f 0.33. IR (KBr, cm^{-1}): 3002w, 2983w, 2959w, 2897w, 1751s, 1728s, 1476m, 1425m, 1410s, 1383m, 1278s, 1239m, 1169m, 1084m, 1033m, 1010s. ^{1}H NMR (400 MHz, $CDCl_3$): 5.49 (d, J = 11.2, 4H), 5.24 (s, 4H), 4.68 (d, J = 11.2, 4H), 4.30-4.20 (m, 8H), 1.28 (t, J = 7.2, 12H). ^{13}C NMR (100 MHz, $CDCl_3$): 164.7, 163.7, 155.6, 79.2, 75.4, 72.6, 64.6, 63.9, 52.4, 13.9, 13.6. MS (FAB, Magic Bullet): *m/z* 681 (20, $[M + H]^+$), 45 (100, $C_2H_5O^+$). HR-MS (FAB, Magic Bullet): *m/z* 681.2125 ($[M + H]^+$, $C_{26}H_{33}N_8O_{14}$, calcd 681.2116). X-ray crystal structure. Crystals obtained from EtOH.

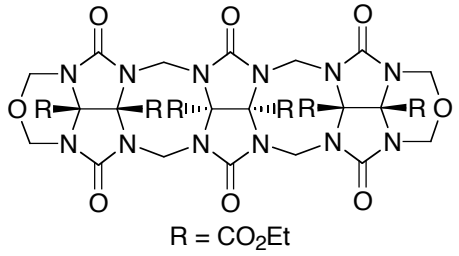

Compound II-6: M.p. 232-233 °C. TLC ($CHCl_3$/ CH_3CN, 3:1) R_f 0.22. IR (KBr, cm^{-1}): 2986w, 2936w, 1755s, 1744s, 1631w, 1472m, 1456m, 1421m, 1382m, 1293m, 1250m, 1084m, 1014m. ^{1}H NMR (400 MHz, $CDCl_3$): 5.48 (d, J = 11.0, 4H), 5.38 (d, J = 13.8, 4H), 4.98 (d, J = 13.8, 4H), 4.72 (d, J = 11.0, 4H), 4.30-4.20 (m, 8H), 4.14 (q, J = 7.2, 4H), 1.35-1.25 (m, 18H). ^{13}C NMR (100 MHz, $CDCl_3$): 164.5, 164.0, 163.5, 155.2, 154.9, 79.7, 79.5, 74.1, 72.7, 65.0, 64.4, 63.8, 51.5, 13.9, 13.8, 13.5. MS (FAB, Magic Bullet): *m/z* 991 (100, $[M + H]^+$). HR-MS (FAB, Magic Bullet): *m/z* 1123.2004 ($[M + Cs]^+$, $C_{38}H_{46}N_{12}O_{20}Cs$, calcd 1123.2006).

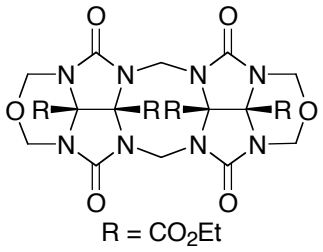

Compound II-7: M.p. 247-249 °C. TLC ($CHCl_3/CH_3CN$, 4:1) R_f 0.35. IR (KBr, cm^{-1}): 2983w, 2967w, 1759s, 1643w, 1472m, 1427m, 1367w, 1301m, 1243s. ^1H NMR (400 MHz, $CDCl_3$): 6.01 (d, J = 16.0, 2H), 5.53 (d, J = 11.0, 4H), 4.87 (d, J = 16.0, 2H), 4.73 (d, J = 11.0, 4H), 4.30-4.20 (m, 8H), 1.35-1.25 (m, 12H). ^{13}C NMR (100 MHz, $CDCl_3$): 164.8, 164.4, 155.1, 78.9, 73.7, 72.7, 64.0, 63.7, 48.2, 13.9 (only 10 of the 11 expected resonances were observed). MS (FAB, Magic Bullet): *m/z* 681 (100, $[M + H]^+$). HR-MS (FAB, Magic Bullet): *m/z* 681.2127 ($[M + H]^+$, $C_{26}H_{33}N_8O_{14}$, calcd 681.2116). Anal. Calcd for $C_{26}H_{32}N_8O_{14}$ (680.58): C 45.88, H 4.74. Found: C 45.48, H 4.62. X-ray crystal structure. Crystals obtained from a mixture of $CHCl_3/CH_3CN$ (1:1).

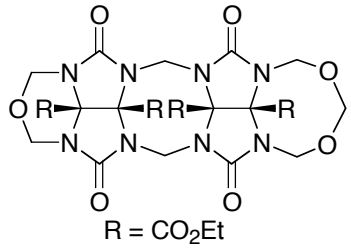

Compound II-8: M.p. 287-288 °C. TLC ($CHCl_3/CH_3CN$, 3:1) R_f 0.26. IR (KBr, cm^{-1}): 2986w, 2967w, 1751s, 1631w, 1456m, 1433m, 1293m, 1258m, 1169w, 1107m, 1087m, 1021m. ^1H NMR (400 MHz, $CDCl_3$): 6.07 (d, J = 16.0, 2H), 5.51 (d, J = 10.8, 2H), 5.42 (br. s, 2H), 4.85 (br. s, 4H), 4.73 (d, J = 10.8, 2H), 4.61 (d, J = 16.0, 2H), 4.30-4.15 (m, 8H), 1.35-1.25 (m, 12H). ^{13}C NMR (100 MHz, $CDCl_3$): 164.9, 164.7, 164.6, 164.4, 155.0, 154.5, 80.0, 78.9, 78.4, 74.1, 74.0, 72.7, 64.2, 63.8, 63.6, 63.5, 48.0, 13.9, 13.8 (only

19 of the 22 expected resonances were observed). MS (FAB, Magic Bullet): *m/z* 711 (70, $[M + H]^+$), 681 (100, $[M\text{-}CH_2CH_3]^+$). HR-MS (FAB, Magic Bullet): *m/z* 711.2240 ($[M + H]^+$, $C_{27}H_{35}N_8O_{15}$, calcd 711.2222).

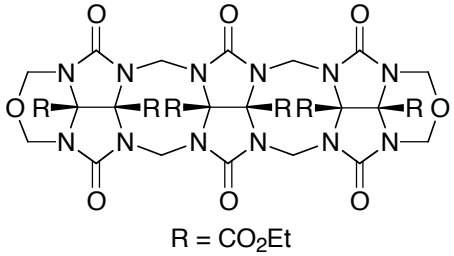

Compound II-9: M.p. 290-293 °C. TLC ($CHCl_3$/MeOH, 5:1) R_f 0.35. IR (KBr, cm^{-1}): 2963s, 2901w, 1755m, 1634w, 1437w, 1293w, 1258s, 1091s, 1021s. ^1H NMR (400 MHz, $CDCl_3$): 6.15 (d, *J* = 16.0, 4H), 5.53 (d, *J* = 10.8, 4H), 4.73 (d, *J* = 10.8, 4H), 4.72 (d, *J* = 16.0, 4H), 4.25-4.15 (m, 12H), 1.35-1.25 (m, 18H). ^{13}C NMR (100 MHz, $CDCl_3$): 164.9, 164.6, 154.8, 154.3, 79.6, 78.9, 73.9, 72.6, 64.2, 63.8, 63.5, 48.5, 13.9, 13.8 (only 14 of the 16 expected resonances were observed). MS (FAB, Magic Bullet): *m/z* 991 (100, $[M + H]^+$). HR-MS (FAB, Magic Bullet): *m/z* 1123.1971 ($[M + Cs]^+$, $C_{38}H_{46}N_{12}O_{20}Cs$, calcd 1123.2006).

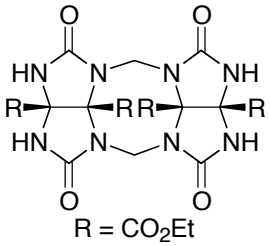

Compound II-11: Compound **II-7** (0.100 g, 0.147 mmol) and 3,5-dimethylphenol (0.450 g, 3.675 mmol) were dissolved in TFA (10 mL). The reaction mixture was stirred and heated at reflux for 24 h. The reaction mixture was concentrated and dried under high vacuum. The residue was washed with Et_2O (3 × 10 mL), centrifuged, and dried under high vacuum. The resulting powder was recrystallized from EtOH (30 mL) to give **II-11** as a white solid which was centrifuged and dried

under high vacuum (0.051 g, 0.085 mmol, 63%). M.p. > 350 ^{o}C. TLC ($CHCl_3$/CH_3OH, 5:1) R_f 0.11. IR (KBr, cm^{-1}): 3456s, 3344s, 2983w, 2936w, 1750s, 1719s, 1630w, 1448s, 1370m, 1269s, 1238s, 1160w, 1036m, 1005m. ^{1}H NMR (400 MHz, DMSO-d_6): 8.84 (s, 4H), 5.79 (d, J = 15.8, 2H), 4.22 (d, J = 15.8, 2H), 4.16 (q, J = 7.2, 4H), 4.11 (q, J = 7.2, 4H), 1.19 (t, J = 7.2, 6H), 1.17 (t, J = 7.2, 6H). ^{13}C NMR (100 MHz, DMSO-d_6): 166.9, 165.8, 156.7, 82.1, 74.7, 63.8, 63.3, 47.0, 14.1, 14.0. MS (FAB, Magic Bullet): *m/z* 597 (100, $[M + H]^+$). HR-MS (FAB, Magic Bullet): *m/z* 597.1896 ($[M + H]^+$, $C_{22}H_{29}N_8O_{12}$, calcd 597.1905).

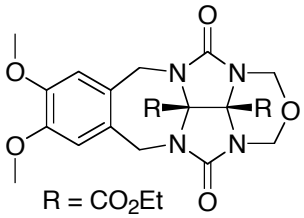

Compound II-12. 4,5-Dimethoxyxylylene glycoluril (0.270 g, 0.600 mmol) was dissolved in TFA (10 mL) and paraformaldehyde (0.078 g, 2.50 mmol of CH_2O) was added in one portion. The reaction mixture was stirred and heated at reflux for 6 h. The TFA was removed by rotary evaporation and the resulting residue was dried under high vacuum. Flash chromatography (SiO_2, $CHCl_3$) gave **II-12** (0.150 g, 0.310 mmol, 52%). M.p. 227-228 ˚C. TLC ($CHCl_3$/MeOH, 100:1) R_f 0.30. IR (KBr, cm^{-1}): 2993w, 2959w, 2940w, 2910w, 1730s, 1472m, 1450m, 1420s, 1276m, 1254m, 1097m, 1010m. ^{1}H NMR (400 MHz, $CDCl_3$): 6.85 (s, 2H), 5.37 (d, J = 11.1, 2H), 4.69 (d, J = 16.0, 2H), 4.68 (d, J = 11.1, 2H), 4.49 (d, J = 16.0, 2H), 4.35-4.25 (m, 4H), 3.84 (s, 6H), 1.35-1.25 (m, 6H). ^{13}C NMR (100 MHz, $CDCl_3$): 165.3, 165.1, 156.3, 147.9, 128.7, 113.2, 80.3, 74.1, 72.2, 63.4, 55.9,

45.3, 13.9, 13.8 (only 14 of the 15 expected resonances were observed). MS (FAB, Magic Bullet): *m/z* 491 (45, $[M + H]^+$), 206 (100, $[C_{11}H_{12}NO_3]^+$). HR-MS (FAB, Magic Bullet): *m/z* 491.1748 ($[M + H]^+$, $C_{22}H_{27}N_4O_9$, calcd 491.1778).

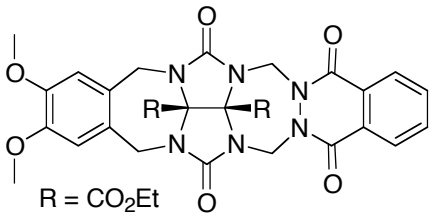

Compound II-14: *Method 1*. A mixture of PTSA (0.388 g, 2.04 mmol) and $ClCH_2CH_2Cl$ (15 mL) was heated under N_2 at reflux for 30 min. under an addition funnel filled with molecular sieves (4Å). Phthalhydrazide (**II-13**) (0.099 g, 0.612 mmol) and compound **II-12** (0.200 g, 0.408 mmol) were added and reflux was continued for 3 h. The reaction mixture was diluted with $CHCl_3$ (100 mL), washed with sat. Na_2CO_3 then brine, dried over anh. $MgSO_4$, and concentrated. Flash chromatography (SiO_2, $CHCl_3/CH_3CN$ 5:1) gave **II-14** (0.178 g, 0.280 mmol, 69%). *Method 2*. A mixture of PTSA (0.081 g, 0.428 mmol) and $ClCH_2CH_2Cl$ (5 mL) was heated under N_2 at reflux for 30 min. under an addition funnel filled with molecular sieves (4Å). Compound **II-16** (0.050 g, 0.086 mmol) and paraformaldehyde (0.013 g, 0.428 mmol) were added and reflux was continued for 24 h. Compound **II-13** (0.014 g, 0.428 mmol) was added and reflux was continued for 4 h. The reaction mixture was diluted with EtOAc (100 mL), washed with sat. Na_2CO_3 then brine, dried over anh. $MgSO_4$, and concentrated. Flash chromatography (SiO_2, $CHCl_3/CH_3CN$ 5:1) gave **II-14** (0.044 g, 0.069 mmol, 81%). M.p. > 300 ˚C (dec). TLC ($CHCl_3/CH_3CN$, 5:1) R_f 0.15. IR (KBr, cm^{-1}): 2983w, 2940w, 2851w, 1758s, 1736s, 1643s, 1608m, 1522m, 1468s, 1449s, 1429s,

1340m, 1305s, 1262s, 1150m, 1134m, 1103s, 1049m, 1025m. ^{1}H NMR (400 MHz, $CDCl_3$): 8.24 (br. s, 2H), 7.73 (br. s, 2H), 7.13 (d, *J* = 15.7, 2H), 6.74 (s, 2H), 4.70 (d, *J* = 16.0, 2H), 4.68 (d, *J* = 15.7, 2H), 4.45 (d, *J* = 16.0, 2H), 4.35-4.25 (m, 4H), 3.79 (s, 6H), 1.40-1.30 (m, 6H). ^{13}C NMR (100 MHz, $CDCl_3$): 165.2, 165.0, 156.5, 154.3, 147.9, 133.6, 128.4, 128.2, 113.3, 80.0, 64.0, 63.6, 55.9, 51.2, 45.3, 14.0, 13.9 (only 17 of the 19 expected resonances were observed). MS (FAB, Magic Bullet): *m/z* 635 (100, $[M + H]^+$). HR-MS (FAB, Magic Bullet): *m/z* 635.2112 ($[M + H]^+$, $C_{30}H_{31}N_6O_{10}$, calcd 635.2102). Anal. Calcd for $C_{30}H_{30}N_6O_{10}$ (634.59): C 56.78, H 4.76. Found: C 56.75, H 4.81.

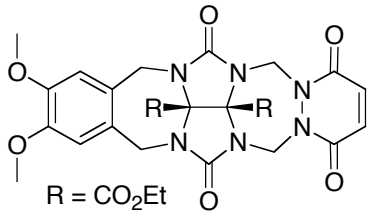

Compound II-16: Compound **II-12** (0.300 g, 0.612 mmol) and 3,6-dihydroxypyridazine (**II-15**) (0.102 g, 0.912 mmol) were dissolved in TFA (6 mL). The mixture was stirred at reflux for 48 h and then was concentrated and dried under high vacuum. The crude material was recrystallized from boiling EtOH (100 mL) to give **II-16** as a light-pink crystalline solid (0.198 g, 0.339 mmol, 55%). M.p. 281-283 ˚C. TLC ($CHCl_3$/CH_3OH, 10:1) R_f 0.35. IR (KBr, cm^{-1}): 3080w, 3002w, 2979w, 2955w, 2936w, 2920w, 1755s, 1728s, 1662s, 1522m, 1464s, 1445s, 1425s, 1336m, 1301m, 1258s, 1223m, 1107m. ^{1}H NMR (400 MHz, $CDCl_3$): 6.93 (d, *J* = 15.6, 2H), 6.78 (s, 2H), 6.75 (s, 2H), 4.71 (d, *J* = 16.0, 2H), 4.59 (d, *J* = 15.6, 2H), 4.45 (d, *J* = 16.0, 2H), 4.35-4.25 (m, 4H), 3.84 (s, 6H), 1.35-1.30 (m, 6H). ^{13}C NMR (100 MHz, $CDCl_3$): 165.0, 164.9, 155.3, 154.2, 147.9, 134.8,

128.2, 113.3, 80.1, 64.1, 63.6, 56.0, 50.6, 45.3, 14.0, 13.9 (only 16 of the 17 expected resonances were observed). MS (FAB, Magic Bullet): *m/z* 585 (73, $[M + H]^+$), 206 (100, $[C_{11}H_{12}NO_3]^+$). HR-MS (FAB, Magic Bullet): *m/z* 585.1957 ($[M + H]^+$, $C_{26}H_{29}N_6O_{10}$, calcd 585.1945). Anal. Calcd for $C_{26}H_{28}N_6O_{10}$ (584.53): C 53.42, H 4.83. Found: C 53.19, H 4.92.

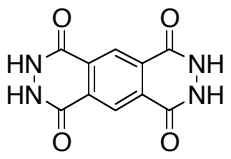

Compound II-17: This compound was prepared according to the literature procedure.[199] To a solution of pyromellitic dianhydride (5.00 g, 22.9 mmol) in hot glacial acetic acid (250 mL) was added hydrazine monohydrate (2.52 g, 50.4 mmol) in AcOH (50 mL) and heated at reflux for 1 h. The reaction mixture was cooled to RT and filtered to yield a yellow powder. This powder was dissolved in hot sodium hydroxide (1 M) and then precipitated with acetic acid (1.5 mL). The solution was filtered to give **II-17** as a pale yellow powder (4.03 g, 16.4 mmol, 71%). M.p. > 350 ˚C. IR (KBr, cm^{-1}): 2893m, 1662s, 1565m, 1518w, 1503w, 1359m, 1297m, 1184m. ^1H NMR (400 MHz,DMSO-d_6): 11.85 (br. s, 4H), 8.64 (br. s, 2H). MS (FAB, glycerol/HCl): *m/z* 247 (100, $[M + H]^+$). HR-MS (FAB, glycerol/HCl): *m/z* 247.0467 ($[M + H]^+$, $C_{10}H_7N_4O_4$, calcd 247.0466).

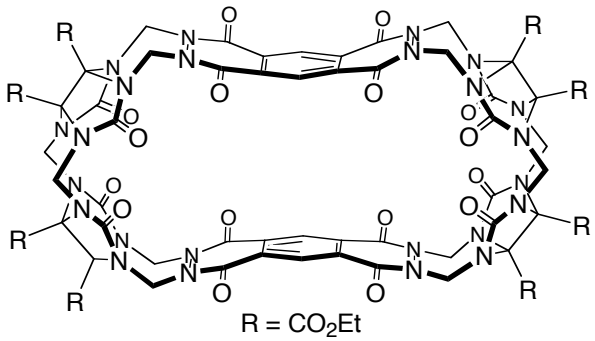

Compound II-18: To a flask containing **II-17** (0.036 g, 0.147 mmol) was added anh. $MeSO_3H$ (1 mL) and the mixture was stirred at 80 ˚C until homogeneous. Compound **II-7** (0.100 g, 0.147 mmol) was added in one portion and the flask was sealed and heated at 80 ˚C for 3 h. The reaction mixture was allowed to cool and then poured into water (10 mL). The solid was collected by centrifugation and the resulting pellet was resuspended in water (10 mL) and centrifuged again. The solid was washed with acetone and centrifuged (2 × 10 mL) and then dried under high vacuum overnight which afforded **II-18** as a pale yellow powder (0.102 g, 0.573 mmol, 78%). M.p. > 350 ˚C (dec). TLC ($CHCl_3$/MeOH, 3:2) R_f 0.16. IR (KBr, cm^{-1}): 2982w, 2928w, 2847w, 1751s, 1647s, 1464s, 1441s, 1394w, 1375w, 1285s, 1258s, 1231s, 1165m, 1115m, 1091m, 1056m, 1025m. ^1H NMR (400 MHz, DMSO-d_6): 8.69 (s, 4H), 6.84 (d, J = 15.8, 8H), 5.92 (d, J = 16.3, 4H), 5.13 (d, J = 15.8, 8H), 4.75 (d, J = 16.3, 4H), 4.31-4.24 (m, 16H), 1.29-1.21 (m, 24H). ^{13}C NMR (100 MHz, TFA/D_2O capillary): 164.0, 163.1, 156.4, 155.3, 131.9, 130.2, 78.9, 78.4, 66.3, 66.2, 52.4, 48.9, 12.3, 12.2. MS (FAB, Magic Bullet/CsI): *m/z* 1913 (100, $[M + Cs]^+$). HR-MS (FAB, Magic Bullet/CsI): *m/z* 1914.3508 ($[M + Cs]^+$, $^{12}C_{71}{}^{13}CH_{68}N_{24}O_{32}Cs$, calcd 1914.3519).

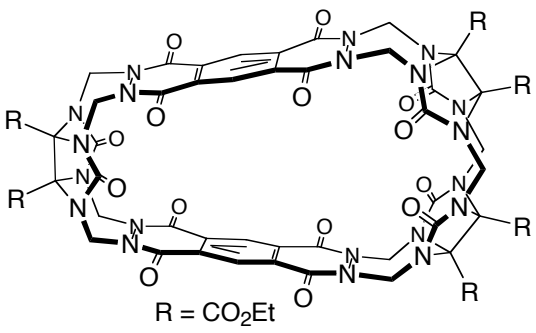

Compound II-19: To a flask containing **II-17** (0.672 g, 2.73 mmol) was added anh. $MeSO_3H$ (10 mL) and the mixture was stirred at 80 ˚C until homogeneous. Compound **II-4** (1.00 g, 2.73 mmol) was added in one portion and the flask was sealed and heated at 80 ˚C for 3 h. The reaction mixture was allowed to cool and then poured into water (100 mL). The yellow precipitate was collected by filtration over a medium fritted funnel and washed with water (50 mL) until dry. The solid was suspended in acetone (150 mL), stirred for 30 min., and filtered. The filtrate was concentrated and dried under high vacuum to yield 0.250 g of crude material. Flash chromatography (SiO_2, $CHCl_3$/MeOH 5:1) gave **II-19** as a pale yellow solid (0.125 g, 0.085 mmol, 6.3%). M.p. > 350 ˚C (dec). TLC ($CHCl_3$/MeOH, 4:1) R_f 0.11. IR (KBr, cm^{-1}): 2982w, 2963w, 2928w, 1755s, 1654s, 1460s, 1441s, 1425s, 1386m, 1371m, 1305s, 1262s, 1235s, 1153m, 1091m, 1021m. ^{1}H NMR (400 MHz, CD_3CN): 8.80 (s, 4H), 7.06 (d, J = 16.1, 4H), 7.05 (d, J = 16.1, 4H), 5.95 (d, J = 16.3, 2H), 4.92 (d, J = 16.1, 4H), 4.86 (d, J = 16.1, 4H), 4.78 (d, J = 16.3, 2H), 4.37 (q, J = 7.1, 4H), 4.34-4.27 (m, 8H), 1.36-1.26 (m, 18H). ^{13}C NMR (100 MHz, DMSO-d_6): 164.7, 164.3, 164.0, 154.4, 153.7, 153.6, 132.1, 131.6, 128.4, 78.3, 77.2, 77.1, 65.3, 65.0, 64.9, 50.2, 50.1, 48.3, 14.0, 13.9 (only 20 of the 22 expected resonances were observed). MS (FAB, Magic Bullet/PEG): *m/z* 1471 (100, $[M + H]^+$). HR-MS (FAB, Magic Bullet): *m/z* 1603.2550 ($[M + Cs]^+$, $C_{60}H_{54}N_{20}O_{26}Cs$, calcd 1603.2572).

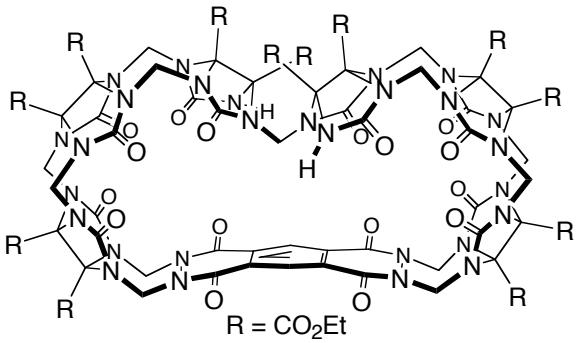

Compound (±)-II-20: To a flask containing **II-17** (36.0 mg, 0.147 mmol) was added anhydrous $MeSO_3H$ (1 mL) and the mixture was stirred at 80 ˚C until homogeneous. Compound **II-9** (0.146 g, 0.147 mmol) was added in one portion and the flask was sealed and heated at 80 ˚C for 3 h. The reaction mixture was cooled to RT and then poured into water (10 mL). The solid was collected by centrifugation and the resulting pellet was resuspended in water (10 mL) and centrifuged again. The solid was washed with water/acetone (1:1, 10 mL), centrifuged, and dried under high vacuum overnight to yield 0.140 g of impure (±)-**II-20** as a yellow solid. Flash chromatography (SiO_2, $CHCl_3$/MeOH/CH_3CN 5:1:0.5) gave (±)-**II-20** as a pale yellow solid (0.104 g, 0.0490 mmol, 67%). M.p. > 350 ˚C (dec). TLC ($CHCl_3$/MeOH CH_3CN, 5:1:0.5) R_f 0.23. IR (KBr, cm^{-1}): 2977w, 2958w, 2920w, 2848w, 1757s, 1644m, 1451s, 1259s, 1232s, 1164w, 1085m, 1017s. ^{1}H NMR (400 MHz, DMSO-d_6): 8.77 (s, 2H), 8.61 (s, 2H), 6.91 (d, J = 15.5, 2H), 6.80 (d, J = 16.0, 2H), 5.95 (d, J = 16.0, 4H), 5.86 (d, J = 16.3, 2H), 5.81 (d, J = 16.3, 2H), 5.17 (d, J = 15.5, 2H), 5.13 (d, J = 16.0, 2H), 4.78 (d, J = 16.3, 2H), 4.61 (d, J =16.0, 2H), 4.59 (s, 2H), 4.40 (d, J = 16.3, 2H), 4.29-4.14 (m, 20H), 4.09 (d, J = 16.0, 2H), 3.97 (q, J = 7.0, 4H), 1.27-1.09 (m, 36H). ^{13}C NMR (100 MHz, DMSO-d_6): 165.7, 165.6, 165.3, 165.2, 164.7, 156.2, 155.1, 154.8, 154.5, 154.2, 133.2, 132.5, 81.1, 79.6, 79.5, 78.8, 78.1, 77.1, 65.5, 64.6, 64.1, 51.2, 48.8,

14.4, 13.9 (only 25 of the 42 expected resonances were observed). ES-MS: *m/z* 1060.5 (100, $[M + 2H]^{2+}$).

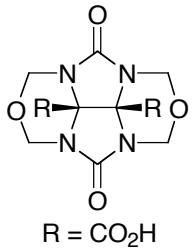

Compound II-21. A mixture of **II-4** (0.503 g, 1.35 mmol), LiOH (0.324 g, 13.51 mmol), H_2O (125 mL), and MeOH (125 mL) was heated at 70 ˚C for 24 h. The reaction mixture was concentrated and dried under high vacuum. The residue was dissolved in H_2O (20 mL) and neutralized with TFA (1.56 g, 13.65 mmol). The solution was concentrated and dried under high vacuum. The resulting solid was washed with CH_3CN (4 × 5 mL), dried under high vacuum, and redissolved in H_2O (2.5 mL). Addition of conc. HCl (2 mL) provided a precipitate that was filtered then dried under high vacuum to give **II-21** (0.322 g, 1.03 mmol, 76%) as a white solid. M.p. >300 ˚C (dec). IR (KBr, cm^{-1}): 3532s, 2960m, 1757s, 1700s, 1478m, 1379m, 1228w, 1174m, 1012s, 930s. ^1H NMR (400 MHz, DMSO-d_6): 5.32 (d, J = 11.1, 4H), 4.87 (d, J = 11.1, 4H). ^{13}C NMR (100 MHz, DMSO-d_6): 165.8, 157.2, 74.5, 72.1. MS (FAB, glycerol): *m/z* 313 (100, $[M - H]^-$). HR-MS (FAB, glycerol): *m/z* 313.0413 ($[M - H]^-$, $C_{10}H_9N_4O_8$, calcd 313.0420).

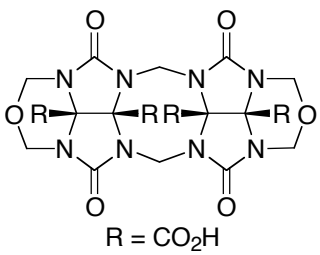

Compound II-22: To a flask containing **II-7** (0.200 g, 0.294 mmol) and LiOH (0.070 g, 2.94 mmol) was added distilled water (50 mL) and MeOH (50 mL). The flask was sealed and the reaction mixture was heated at 70 ˚C for 24 h. The reaction mixture was cooled to RT, concentrated, and dried under high

vacuum. The solid was dissolved in water (10 mL) and 70% w/w $HClO_4$ (250 μL) was added. The solution was concentrated and dried under high vacuum overnight. The solid was then washed with EtOAc and centrifuged (3 × 10 mL). After decanting the supernatant, the pellet was dried under high vacuum affording **II-22** as a white powder (0.150 g, 0.264 mmol, 89%). M.p. > 350 ˚C (dec). IR (KBr, cm^{-1}): 3239s, 2963w, 2920w, 2885w, 1748s, 1472m, 1445m, 1429m, 1371w, 1301m, 1254m, 1188w, 1122m, 1107m, 1076m, 1021m, 1006m. ^{1}H NMR (400 MHz, D_2O): 5.43 (d, *J* = 16.0, 2H), 5.24 (d, *J* = 11.2, 4H), 4.85 (d, *J* = 16.0, 2H), 4.56 (d, *J* = 11.2, 4H). ^{13}C NMR (100 MHz, D_2O): 168.5, 166.9, 156.7, 81.3, 74.9, 72.3, 48.4. MS (FAB, Magic Bullet/PEG): *m/z* 569 (100, $[M + H]^+$). HR-MS (FAB, Magic Bullet/PEG): *m/z* 569.0884 ($[M + H]^+$, $C_{18}H_{17}N_8O_{14}$, calcd 569.0864). X-ray crystal structure. Crystals obtained from H_2O.

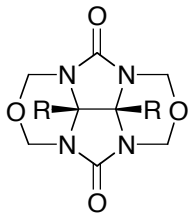

Compound II-23. A mixture of **II-4** (0.205 g, 0.554 mmol) and *n*-butylamine (10 mL) was heated at 78 ˚C for 20 h. The amine was removed by rotary evaporation and the residue was dried under high vacuum. The residue was suspended in Et_2O, filtered, and dried under high vacuum to give **II-23** (0.211 g, 0.499 mmol, 90%) as a white powder. M.p. 238-242 ˚C. TLC ($CHCl_3$/MeOH, 25:1) R_f 0.19. IR (KBr, cm^{-1}): 3286s, 2954m, 2932m, 2874m, 1766s, 1743s, 1688s, 1469m, 1410s, 1303m, 1243m, 1180m. ^{1}H NMR (400 MHz, $CDCl_3$): 6.64 (t, *J* = 5.3, 2H), 5.53 (d, *J* = 11.3, 4H), 4.59 (d, *J* = 11.3, 4H), 3.28 (m, 4H), 1.50 (m, 4H), 1.33 (m, 4H), 0.92 (t, *J* = 7.3, 6H).

^{13}C NMR (100 MHz, $CDCl_3$): 162.5, 157.2, 75.5, 72.5, 40.4, 31.1, 20.0, 13.6. MS (FAB, Magic Bullet): *m/z* 425 (100, $[M + H]^+$). HR-MS (FAB, Magic Bullet): *m/z* 425.2166 ($[M + H]^+$, $C_{18}H_{29}N_6O_6$, calcd 425.2149). Anal. calcd. for $C_{18}H_{28}N_6O_6$ (424.45): C, 50.93; H, 6.65. Found: C, 50.85; H, 6.71.

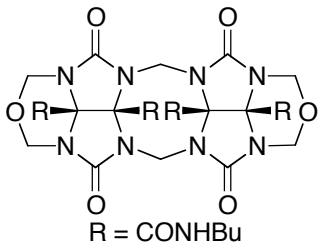

Compound II-24: A flask containing compound **II-7** (0.134 g, 0.197 mmol) was flushed with N_2 and then *n*-butylamine (26 mL) was added. The reaction mixture was sonicated and then heated at 75 ˚C for 24 h. The reaction mixture was concentrated and dried under high vacuum. The resulting residue was washed with Et_2O and dried. The less polar impurity was removed using a fritted filter funnel filled with SiO_2 ($CHCl_3$/CH_3CN 10:1). The SiO_2 containing the desired product was stirred in a mixture of $CHCl_3$/MeOH (5:1, 100 mL) for 24 h. The mixture was filtered and the filtrate was concentrated to give **II-24** as a white solid (0.105 g, 0.133 mmol, 68%). M.p. > 350 ˚C (dec). TLC ($CHCl_3$/ MeOH, 10:1) R_f 0.11. IR (KBr, cm^{-1}): 3445s, 3045w, 2963m, 2932m, 2874w, 1751s, 1697s, 1538m, 1472m, 1433s, 1375m, 1301m, 1255m, 1189w, 1118m, 1096m, 1017m, 1009m. ^{1}H NMR (400 MHz, DMSO-d_6): 8.59 (t, *J* = 5.4, 2H), 8.29 (t, *J* = 5.4, 2H), 5.61 (d, *J* = 16.0, 2H), 5.25 (d, *J* = 11.2, 2H), 4.55 (d, *J* = 16.0, 2H), 4.51 (d, *J* = 11.2, 2H), 3.05-3.00 (m, 4H), 2.95-2.90 (m, 4H), 1.40-1.30 (m, 8H), 1.25-1.15 (m, 8H), 0.86 (t, *J* = 7.2, 6H), 0.85 (t, *J* = 7.2, 6H). ^{13}C NMR (100 MHz, $CDCl_3$/MeOH (20:1)): 163.7, 161.5, 155.7, 80.6, 74.9, 72.3, 48.4, 40.7, 40.5, 31.0, 30.8, 20.2, 20.0, 13.6 (only 14 of

the 15 expected resonances were observed). MS (FAB, MNBA): *m/z* 811 (100, [M + Na]$^+$), 789 (30, ([M + H]$^+$). HR-MS (FAB, MNBA/PEG): *m/z* 789.3989 ([M + H]$^+$, $C_{34}H_{53}N_{12}O_{10}$, calcd 789.4008).

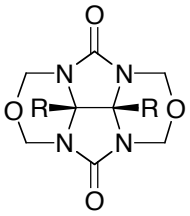

R,R = $(CO)_2NBu$

Compound II-25. A mixture of **II-23** (0.050 g, 0.118 mmol), $ClCH_2CH_2Cl$ (20 mL), and PTSA•H_2O (0.114 g, 0.589 mmol) was heated at reflux for 20 h. The solvent was removed by rotary evaporation and the residue was dried under high vacuum. The residue was washed with H_2O (3 × 8 mL) and dried under high vacuum to give **II-25** (0.034 g, 0.096 mmol, 82%) as an off-white solid. M.p. 182-184 ˚C. TLC ($CHCl_3$/EtOAc/Hexanes, 2:1:1) R_f 0.43. IR (KBr, cm^{-1}): 2959w, 1778s, 1732s, 1478m, 1465m, 1371m, 1307m, 1230m, 1200m, 1035m, 1013m. ^{1}H NMR (400 MHz, $CDCl_3$): 5.51 (d, *J* = 11.1, 4H), 5.09 (d, *J* = 11.1, 4H), 3.59 (t, *J* = 7.3, 2H), 1.59 (m, 2H), 1.30 (m, 2H), 0.92 (t, *J* = 7.3, 3H). ^{13}C NMR (100 MHz, $CDCl_3$): 167.3, 157.6, 72.4, 70.4, 39.1, 29.1, 19.7, 13.4. MS (FAB, Magic Bullet): *m/z* 352 (89, [M + H]$^+$), 322 (100). HR-MS (FAB, Magic Bullet): *m/z* 352.1268 ([M + H]$^+$, $C_{14}H_{18}N_5O_6$, calcd 352.1257). X-ray crystal structure. Anal. calcd. for $C_{14}H_{17}N_5O_6$ (351.32): C, 47.86; H, 4.88. Found: C, 48.01; H, 5.07.

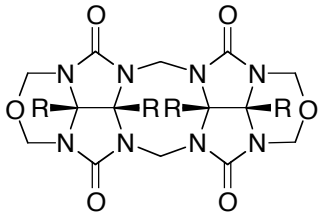

R,R = $(CO)_2NBu$

Compound II-26: To a mixture of **II-24** (0.140 g, 0.178 mmol) and PTSA (0.170 g, 0.888 mmol) was added $ClCH_2CH_2Cl$ (30 mL). The reaction mixture was heated

at reflux for 48 h, cooled, concentrated, and dried under high vacuum. The resulting residue was washed with water and dried under high vacuum. Flash chromatography (SiO_2, $CHCl_3/CH_3CN$ 10:1) gave **II-6** as a white solid (0.044 g, 0.069 mmol, 39%). M.p. > 350 °C (dec). TLC ($CHCl_3$/ CH_3CN, 10:1) R_f 0.32. IR (KBr, cm^{-1}): 2960w, 2935w, 2924w, 2874w, 1781s, 1759m, 1720s, 1472m, 1422s, 1372s, 1302s, 1263m, 1016m. ^1H NMR (400 MHz, $CDCl_3$): 5.73 (d, J = 15.5, 2H), 5.52 (d, J = 11.0, 4H), 5.30 (d, J = 15.5, 2H), 5.03 (d, J = 11.0, 4H), 3.59 (t, J = 7.4, 4H), 1.65-1.50 (m, 4H), 1.35-1.25 (m, 4H), 0.93 (t, J = 7.6, 6H). ^{13}C NMR (100 MHz, $CDCl_3$): 167.5, 166.4, 154.5, 72.7, 71.9, 70.1, 46.5, 39.5, 29.2, 20.0, 13.5. MS (FAB, Magic Bullet/PEG): *m/z* 643 (100, $[M + H]^+$). HR-MS (FAB, Magic Bullet/PEG): *m/z* 643.2229 ($[M + H]^+$, $C_{26}H_{31}N_{10}O_{10}$, calcd 643.2225). X-ray crystal structure. Crystals obtained from a mixture of CH_3CN/MeOH (5:1).

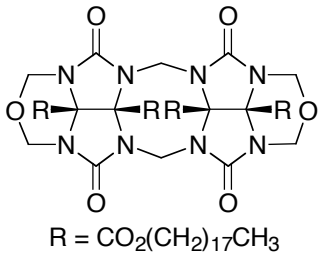

Compound II-27: A solution of **II-7** (0.100 g, 0.147 mmol) and 1-octadecanol (0.397 g, 1.47 mmol) in toluene (30 mL) was heated under N_2 at reflux for 30 min. under an addition funnel filled with molecular sieves (4Å). A pre-made solution of 18-crown-6 (0.020 g, 0.0735 mmol) and $KOCH_3$ (0.005 g, 0.0735 mmol) in toluene/CH_3OH (0.6 mL, 5:1) was added to the reaction mixture and reflux was continued for 20 h. The reaction mixture was concentrated and dried under high vacuum. Flash chromatography (SiO_2, $CHCl_3/CH_3CN$ 20:1) gave **II-27** as a white solid (0.090 g, 0.057 mmol, 37%). M.p. 161-163 °C. TLC

($CHCl_3/CH_3CN$, 20:1) R_f 0.28. IR (KBr, cm^{-1}): 2959m, 2917s, 2851s, 1767s, 1468m, 1437m, 1421m, 1297m, 1251s, 1091m, 1072m, 1017m, 1010m. ^1H NMR (400 MHz, $CDCl_3$): 5.99 (d, J = 16.0, 2H), 5.53 (d, J = 11.0, 4H), 4.86 (d, J = 16.0, 2H), 4.73 (d, J = 11.0, 4H), 4.20-4.10 (m, 8H), 1.65-1.55 (m, 8H), 1.30-1.20 (m, 120H), 0.86 (t, J = 6.8, 12H). ^{13}C NMR (100 MHz, $CDCl_3$): 165.4, 164.9, 155.5, 79.5, 77.1, 74.5, 73.2, 68.6, 68.2, 63.5, 48.7, 33.2, 32.4, 30.1, 30.1, 30.0, 29.9, 29.9, 29.8, 29.6, 29.5, 28.8, 28.5, 26.2, 26.1, 26.1, 23.1, 14.6 (only 28 of the 43 expected resonances were observed.) MS (FAB, Magic Bullet/PEG): *m/z* 1579 (100, $[M + H]^+$).

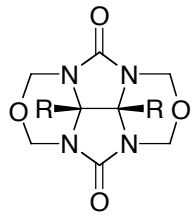

R = $CO_2(CH_2)_9CH_3$

Compound II-28: A solution of **II-4** (0.100 g, 0.273 mmol) and 1-decanol (0.52 mL, 2.73 mmol) in toluene (30 mL) was heated under N_2 at reflux for 30 min. under an addition funnel filled with molecular sieves (4Å). A pre-made solution of 18-crown-6 (0.007 g, 0.027 mmol) and $KOCH_3$ (0.002 g, 0.027 mmol) in toluene/CH_3OH (0.6 mL, 5:1) was added to the reaction mixture and reflux was continued for 20 h. The reaction mixture was concentrated and dried under high vacuum. Flash chromatography (50:1 $CHCl_3/CH_3CN$) gave **II-28** as a white solid (0.146 g, 0.245 mmol, 91%). M.p. 54-55 °C. TLC ($CHCl_3/CH_3CN$, 25:1) R_f 0.31. IR (KBr, cm^{-1}): 2959m, 2924s, 2851m, 1775s, 1748s, 1472m, 1410m, 1383s, 1297s, 1235s, 1169m, 1107m, 1068m, 1041m, 1029m, 1002m. ^1H NMR (400 MHz, $CDCl_3$): 5.53 (d, J = 11.2, 4H), 4.81 (d, J = 11.2, 4H), 4.20 (t, J = 6.9, 4H), 1.65-1.60 (m, 4H), 1.30-1.20 (m, 28H), 0.86 (t, J = 6.8, 6H). ^{13}C NMR (100 MHz, $CDCl_3$);

164.8, 156.9, 74.5, 72.5, 67.9, 31.9, 29.6, 29.5, 29.4, 29.2, 28.3, 25.8, 22.8, 14.2. MS (FAB, Magic Bullet/LiCl): *m/z* 602 (100, $[M + Li]^+$). HR-MS (FAB, Magic Bullet/LiCl): *m/z* 601.3793 ($[M + Li]^+$, $C_{30}H_{50}N_4O_8Li$, calcd 601.3789).

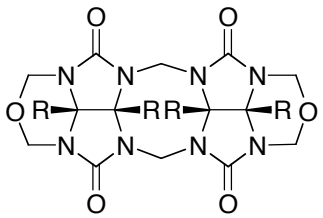

Compound II-29: A solution of **II-7** (0.100 g, 0.147 mmol) and 1-decanol (0.56 mL, 2.94 mmol) in toluene (80 mL) was heated under N_2 at reflux for 30 min. under an addition funnel filled with molecular sieves (4Å). A pre-made solution of 18-crown-6 (0.020 g, 0.074 mmol) and $KOCH_3$ (0.005 g, 0.074 mmol) in toluene/CH_3OH (0.6 mL, 5:1) was added to the reaction mixture and reflux was continued for 20 h. The reaction mixture was concentrated and dried under high vacuum. Flash chromatography (SiO_2 $CHCl_3/CH_3CN$ 40:1) gave **II-29** as a white solid (0.100 g, 0.089 mmol, 60%). M.p. 169-171 °C. TLC ($CHCl_3/CH_3CN$, 25:1) R_f 0.15. IR (KBr, cm^{-1}): 2955m, 2928s, 2854m, 1763s, 1468m, 1429m, 1414m, 1297m, 1270m, 1251s, 1087m, 1068m, 1017m, 1006m. ^1H NMR (400 MHz, $CDCl_3$): 5.99 (d, *J* = 16.0, 2H), 5.52 (d, *J* = 10.9, 4H), 4.85 (d, *J* = 16.0, 2H), 4.73 (d, *J* = 10.9, 4H), 4.20-4.10 (m, 8H), 1.65-1.60 (m, 8H), 1.30-1.20 (m, 56H), 0.86 (t, *J* = 6.6, 12H). ^{13}C NMR (100 MHz, $CDCl_3$): 165.0, 164.5, 155.1, 79.0, 74.0, 72.7, 68.1, 67.8, 48.2, 31.8, 29.5, 29.5, 29.4, 29.3, 29.2, 29.1, 29.1, 28.2, 28.1, 25.7, 25.7, 22.6, 14.1 (only 23 of the 27 expected resonances were observed). MS (FAB, Magic Bullet/CsI): *m/z* 1261 (100, $[M + Cs]^+$). HR-MS (FAB, Magic Bullet/CsI): *m/z* 1261.6061 ($[M + Cs]^+$, $C_{58}H_{96}N_8O_{14}Cs$, calcd 1261.6100).

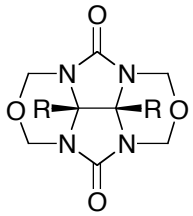

R = CO_2CH_2Ph

Compound II-30: A solution of **II-4** (0.100 g, 0.273 mmol) and benzyl alcohol (0.28 mL, 2.73 mmol) in toluene (30 mL) was heated under N_2 at reflux for 30 min. under an addition funnel filled with molecular sieves (4Å). A pre-made solution of 18-crown-6 (0.036 g, 0.140 mmol) and $KOCH_3$ (0.010 g, 0.140 mmol) in toluene/CH_3OH (0.6 mL, 5:1) was added to the reaction mixture and reflux was continued for 17 h. The reaction mixture was concentrated and dried under high vacuum. Recrystallization from toluene gave **II-30** as a white crystalline solid (0.035 g, 0.071 mmol, 26%). M.p. 176-177 °C. TLC ($CHCl_3$/CH_3CN, 25:1) R_f 0.20. IR (KBr, cm^{-1}): 3064w, 3029w, 2948w, 2924w, 2897w, 1759s, 1736s, 1472m, 1452m, 1414m, 1383m, 1309m, 1293s, 1235s, 1177m, 1103m, 1064m, 1045m, 1033m, 1017m. ^1H NMR (400 MHz, $CDCl_3$): 7.35-7.30 (m, 5H), 7.25-7.20 (m, 5H), 5.48 (d, J = 11.2, 4H), 4.94 (s, 4H), 4.72 (d, J = 11.2, 4H). ^{13}C NMR (100 MHz, $CDCl_3$): 164.3, 156.8, 133.8, 129.1, 128.8, 128.6, 74.5, 72.4, 68.8. MS (FAB, Magic Bullet/PEG): *m/z* 501 (100, $[M + Li]^+$). HR-MS (FAB, Magic Bullet/PEG): *m/z* 501.1587 ($[M + Li]^+$, $C_{24}H_{22}N_4O_8Li$, calcd 501.1598).

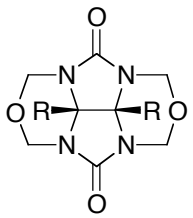

R = $CO_2(CH_2CH_2O)_2Me$

Compound II-31: A solution of **II-4** (0.100 g, 0.273 mmol) and diethylene glycol mono methyl ether (0.32 mL, 2.73 mmol) in toluene (40 mL) was heated under N_2 at reflux for 30 min. under an addition funnel filled with

molecular sieves (4Å). A pre-made solution of 18-crown-6 (0.036 g, 0.140 mmol) and $KOCH_3$ (0.010 g, 0.140 mmol) in toluene/CH_3OH (0.6 mL, 5:1) was added to the reaction mixture and reflux was continued for 13 h. The reaction mixture was diluted with ethyl acetate (200 mL), washed with sat. Na_2CO_3 then brine, dried over anh. $MgSO_4$, concentrated, and dried under high vacuum. Flash chromatography (SiO_2, EtOAc/MeOH 20:1) gave **II-31** as a colorless oil (0.075 g, 0.145 mmol, 53%). TLC (EtOAc/MeOH, 20:1) R_f 0.32. IR (KBr, cm^{-1}): 2955m, 2928m, 2889m, 2827w, 1748s, 1472m, 1455m, 1414s, 1383m, 1305s, 1234s, 1177m, 1103m, 1068m, 1014s. ^1H NMR (400 MHz, $CDCl_3$): 5.48 (d, J = 11.2, 4H), 4.86 (d, J = 11.2, 4H), 4.45-4.35 (m, 4H), 3.70-3.65 (m, 4H), 3.60-3.55 (m, 4H), 3.50-3.45 (m, 4H), 3.32 (s, 6H). ^{13}C NMR (100 MHz, $CDCl_3$): 164.6, 156.8, 74.7, 72.4, 71.8, 70.4, 68.1, 66.3, 58.9. MS (FAB, Magic Bullet): *m/z* 519 (100, $[M + H]^+$). HR-MS (FAB, Magic Bullet): *m/z* 519.1926 ($[M + H]^+$, $C_{20}H_{31}N_4O_{12}$, calcd 519.1938).

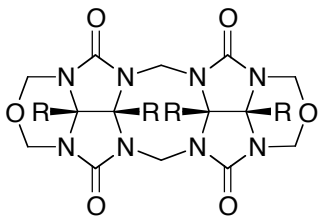

R = $CO_2(CH_2CH_2O)_2Me$

Compound II-32: A solution of **II-7** (0.185 g, 0.273 mmol) and diethylene glycol mono methyl ether (0.32 mL, 2.73 mmol) in toluene (40 mL) was heated under N_2 at reflux for 30 min. under an addition funnel filled with molecular sieves (4Å). A pre-made solution of 18-crown-6 (0.036 g, 0.140 mmol) and $KOCH_3$ (0.010 g, 0.140 mmol) in toluene/CH_3OH (0.6 mL, 5:1) was added to the reaction mixture and reflux was continued for 17 h. The reaction mixture was diluted with ethyl acetate (200 mL), washed with sat. Na_2CO_3 then brine, dried over anh.

$MgSO_4$, concentrated, and dried under high vacuum. Flash chromatography (SiO_2, $CHCl_3$/MeOH 20:1) gave **II-32** as a white solid (0.060 g, 0.061 mmol, 23%). M.p. 78-80 ˚C. TLC ($CHCl_3$/MeOH, 10:1) R_f 0.30. IR (KBr, cm^{-1}): 2959m, 2924m, 2889m, 2823w, 1760s, 1634m, 1471m, 1436m, 1417m, 1382m, 1366w, 1300s, 1250s, 1083s, 1021s. ^{1}H NMR (400 MHz, $CDCl_3$): 5.97 (d, J = 16.2, 2H), 5.49 (d, J = 11.0, 4H), 4.92 (d, J = 16.2, 2H), 4.79 (d, J = 11.0, 4H), 4.40-4.30 (m, 8H), 3.70-3.65 (m, 8H), 3.60-3.55 (m, 8H), 3.50-3.45 (m, 8H), 3.32 (s, 12H). ^{13}C NMR (100 MHz, $CDCl_3$): 165.0, 164.4, 155.1, 79.1, 74.2, 72.7, 71.8, 70.5, 68.1, 67.9, 66.8, 66.2, 59.0, 58.9, 48.3 (only 15 of the 17 expected resonances were observed). MS (FAB, Magic Bullet/CsI): *m/z* 1109 (100, $[M + Cs]^+$). HR-MS (FAB, Magic Bullet/PEG): *m/z* 1109.2570 ($[M + Cs]^+$, $C_{38}H_{56}N_8O_{22}Cs$, calcd 1109.2563).

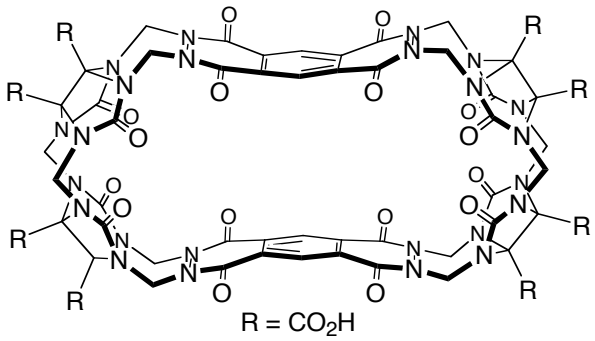

Compound II-33: To a flask containing **II-17** (17.0 mg, 0.0700 mmol) was added anh. $MeSO_3H$ (1 mL) and the mixture was stirred at 80 ˚C until homogeneous. Compound **II-22** (40.0 mg, 0.0700 mmol) was added in one portion and the flask was sealed and heated at 80 ˚C for 3 h. The reaction mixture was cooled to RT and then poured into a water/acetone mixture (1:1, 10 mL). The solid was collected by centrifugation and the resulting pellet was resuspended in acetone, centrifuged (2 × 10 mL) and then dried under high vacuum overnight which afforded **II-33** as a pale yellow powder

(35.0 mg, 0.0224 mmol, 65%). M.p. > 350 ˚C (dec). IR (KBr, cm^{-1}): 3418s, 2963w, 2932w, 2917w, 1740s, 1697m, 1685m, 1647s, 1635s, 1460m, 1417w, 1383w, 1289m, 1262m, 1239m, 1161m, 1111m, 1049m. ^{1}H NMR (400 MHz, DMSO-d_6): 8.67 (s, 4H), 6.83 (d, J = 15.8, 8H), 5.75 (d, J = 15.8, 4H), 5.04 (d, J = 15.8, 8H), 5.02 (d, J = 15.8, 4H). ^{13}C NMR (100 MHz, DMSO-d_6): 166.5, 165.7, 154.9, 154.3, 132.0, 128.2, 78.8, 77.6, 51.2, 48.2. ES-MS: *m/z* 1557 (100, $[M + H]^+$).

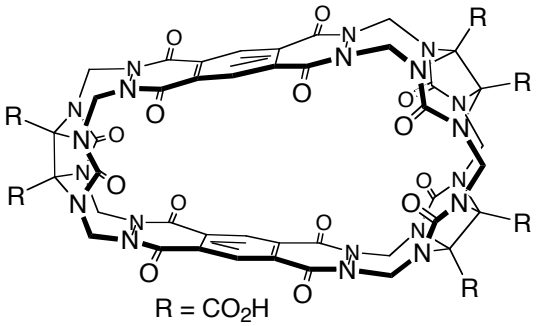

Compound II-34: A mixture of **II-17** (0.214 g, 0.870 mmol) and anh. $MeSO_3H$ (5 mL) was stirred at 80 ˚C until homogeneous. Compound **II-21** (0.540 g, 0.870 mmol) was added in one portion and the flask was sealed and heated at 80 ˚C for 3 h. The reaction mixture was cooled to RT and then poured into acetone (50 mL). The solid was collected by filtration, washed with additional acetone (50 mL), and dried under high vacuum overnight to yield crude material as a yellow solid (0.744 g). The crude material (0.300 g) was purified by ion-exchange chromatography (Cellulose-DEAE) with sodium acetate buffer (pH = 5.7, 100 mM). After loading the material on the column, increasing the NaCl gradient from 5-15% gave **II-34** contaminated with salts (NaOAc and NaCl). These salts were removed using size exclusion chromatography (Sephadex G-25) to yield **II-34** as a pale yellow solid (0.015 g, 0.012 mmol, 3%). M.p. > 350 ^{o}C (dec). IR (KBr, cm^{-1}): 2963w, 2924w, 2847w, 1732m, 1717m, 1654s, 1468m, 1386m,

1297m, 1239m, 1153w, 1103m. ^{1}H NMR (400 MHz, D_2O): 8.72 (s, 4H), 6.90 (d, J = 16.1, 4H), 6.81 (d, J = 15.9, 4H), 5.54 (d, J = 16.1, 2H), 5.00 (d, J = 16.1, 2H), 4.99 (d, J = 16.1, 4H), 4.87 (d, J = 15.9, 4H). ^{13}C NMR (100 MHz, D_2O): 168.8, 168.5, 156.7, 156.6, 156.1, 156.0, 131.8, 131.1, 128.6, 81.7, 79.6, 51.8, 50.5, 48.7 (only 14 of the 16 expected resonances were observed). MS (ESI): *m/z* 1325 (100, $[M + Na]^+$). HR-MS (ESI): *m/z* 1325.1621 ($[M + Na]^+$, $C_{48}H_{30}N_{20}O_{26}Na$, calcd 1325.1538).

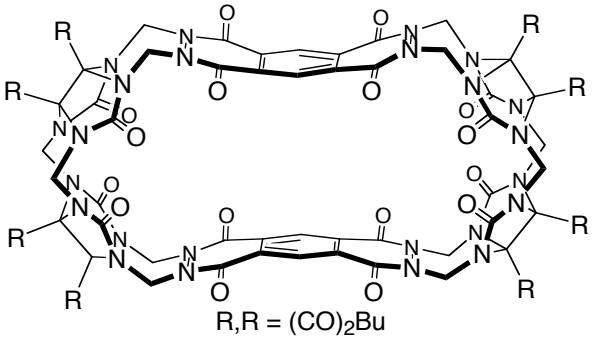

Compound II-35: To a flask containing **II-17** (12.0 mg, 0.0470 mmol) was added anh. $MeSO_3H$ (1 mL) and the mixture was stirred at 80 ˚C until homogeneous. Compound **II-26** (30.0 mg, 0.0470 mmol) was added in one portion and the flask was sealed and heated at 80 ˚C for 3 h. The reaction mixture was allowed to cool and then poured into water (10 mL). The solid was collected by centrifugation and the resulting pellet was resuspended in water (10 mL) and centrifuged again. The solid was washed with acetone and centrifuged (2 × 5 mL) and then dried under high vacuum overnight which afforded pure **II-35** as a pale yellow powder (28.0 mg, 0.0164 mmol, 70%). M.p. > 350 ˚C (dec). TLC ($CHCl_3$/MeOH, 3:1) R_f 0.18. IR (KBr, cm^{-1}): 2959w, 2932w, 2870w, 1759s, 1716s, 1643s, 1526w, 1456s, 1433s, 1386m, 1344m, 1309s, 1254s, 1173m, 1146m, 1111m, 1068m, 1048m, 1021m. ^{1}H NMR (400 MHz,

CD_3CN): 8.87 (s, 4H), 7.04 (d, J = 15.8, 8H), 5.55 (d, J = 15.8, 4H), 5.28 (d, J = 15.8, 8H), 5.13 (d, J = 15.8, 4H), 3.54 (t, J = 7.2, 8H), 1.62 (m, 8H), 1.35 (m, 8H), 0.94 (t, J = 7.2, 12H). ^{13}C NMR (100 MHz, TFA/D_2O capillary): 167.2, 165.2, 156.0, 153.7, 131.5, 129.8, 71.1, 70.6, 51.5, 46.8, 40.1, 28.2, 19.1, 11.2. MS (FAB, Magic Bullet/CsI): *m/z* 1837 (100, $[M + Cs]^+$). HR-MS (FAB, Magic Bullet/CsI): *m/z* 1837.3623 ($[M + Cs]^+$, $C_{72}H_{64}N_{28}O_{24}Cs$, calcd 1837.3703). X-ray crystal structure. Crystals obtained from CH_3CN.

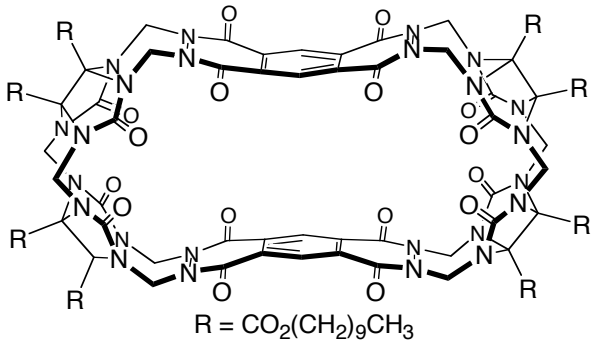

Compound II-36: A mixture of **II-17** (0.022 g, 0.147 mmol) and anh. $MeSO_3H$ (2 mL) was stirred at 80 ˚C until homogeneous. Compound **II-29** (0.100 g, 0.089 mmol) was added in one portion and the flask was sealed and heated at 80 ˚C for 3 h. The reaction mixture was cooled to RT and then poured into water (10 mL). The solid was collected by centrifugation and the resulting pellet was resuspended in water (10 mL) and centrifuged again, and then dried under high vacuum overnight to yield **II-36** as a pale yellow solid (0.090 g, 0.034 mmol, 76%). M.p. > 350 ˚C (dec). TLC ($CHCl_3$/CH_3OH, 10:1) R_f 0.10. IR (KBr, cm^{-1}): 2959m, 2924s, 2854m, 1755s, 1654s, 1645s, 1635s, 1261s, 1232m, 1165w, 1094m, 1053m, 1025m. ^{1}H NMR (400 MHz, DMSO-d_6): 8.66 (s, 4H), 6.80 (d, J = 15.4, 8H), 5.88 (d, J = 15.6, 4H), 5.10 (d, J = 15.4, 8H), 4.70 (d, J = 15.6, 4H), 4.20-4.10 (m, 16H), 1.65-1.50 (m, 16H), 1.22 (s,

112H), 0.85-0.80 (m, 24H). ^{13}C NMR (100 MHz, $CDCl_3$): 164.9, 164.7, 155.3, 153.7, 132.0, 129.6, 116.9, 78.5, 78.1, 69.2, 68.9, 53.2, 48.8, 32.3, 30.0, 29.99, 29.96, 29.88, 29.84, 29.7, 29.6, 28.6, 28.5, 26.1, 26.0, 23.1, 14.5 (only 27 of the 30 expected resonances were observed). MS (ESI): *m/z* 1362 (100, $[M + 2Na]^{2+}$).

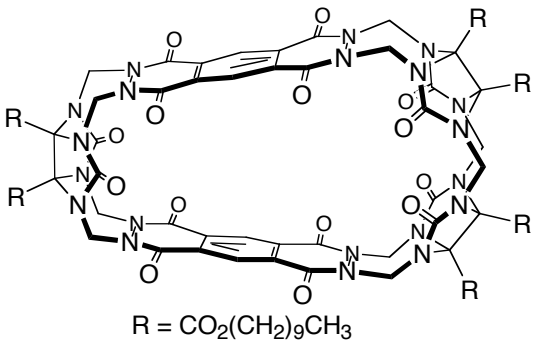

Compound II-37: A mixture of **II-17** (0.036 g, 0.147 mmol) and anh. $MeSO_3H$ (1 mL) was stirred at 80 ˚C until homogeneous. Compound **II-28** (0.130 g, 0.220 mmol) was added in one portion and the flask was sealed and heated at 80 ˚C for 3 h. The reaction mixture was cooled to RT and then poured into water (10 mL). The solid was collected by centrifugation and the resulting pellet was resuspended in water (10 mL) and centrifuged. The solid was dried under high vacuum overnight. Flash chromatography (SiO_2, $CHCl_3$/MeOH 10:1) gave **II-37** as a pale yellow solid (0.025 g, 0.0115 mmol, 8%). M.p. > 350 ˚C (dec). TLC ($CHCl_3$/CH_3CN, 10:1) R_f 0.18. IR (KBr, cm^{-1}): 2955m, 2924s, 2854m, 1759s, 1666m, 1464m, 1421m, 1383w, 1262s, 1231s, 1153m, 1099w, 1021w. ^{1}H NMR (400 MHz, $CDCl_3$): 8.92 (s, 4H), 7.18 (d, *J* = 16.0, 4H), 7.14 (d, *J* = 16.0, 4H), 6.05 (d, *J* = 16.2, 2H), 4.79 (d, *J* = 16.0, 4H), 4.74 (d, *J* = 16.0, 4H), 4.68 (d, *J* = 16.2, 2H), 4.30-4.10 (m, 12H), 1.75-1.55 (m, 12H), 1.30-1.20 (m, 84H), 0.90-0.80 (m, 18H). ^{13}C NMR (125 MHz, $CDCl_3$): 165.3, 165.0, 164.9, 155.2, 154.9, 153.6, 132.3, 132.1, 130.8, 78.9, 69.4, 69.2, 51.6, 51.2, 49.1, 32.6, 30.3, 30.2, 30.1, 29.9, 29.8, 29.0,

28.9, 28.8, 26.4, 26.3, 23.4, 14.9 (only 28 of the 44 expected resonances were observed). MS (ESI): *m/z* 2144 (100, $[M + H]^+$). HR-MS (ESI): *m/z* 2144.1139 ($[M + H]^+$, $C_{108}H_{51}N_{20}O_{26}$, calcd 2144.1108).

Compound II-47T and II-47C: A mixture of PTSA (0.279 g, 1.47 mmol) and $ClCH_2CH_2Cl$ (20 mL) was heated under N_2 at reflux for 30 min. under an addition funnel filled with molecular sieves (4Å). Compound **II-46** (0.152 g, 0.735 mmol) was added and reflux was continued for 5 min. Compound **II-7** (0.200 g, 0.294 mmol) was added and reflux was continued for 22 h. The reaction mixture was concentrated and dried under high vacuum. The reaction mixture was diluted with CH_2Cl_2 (350 mL), washed with sat. Na_2CO_3 then brine, dried over anh. $MgSO_4$, concentrated, and dried under high vacuum. Flash chromatography (SiO_2, $CHCl_3/CH_3CN$ 5:1, then $CHCl_3/CH_3CN$ 4:1) gave **II-47T** (0.115 g, 0.109 mmol, 37%), **II-47C** (0.105 g, 0.099 mmol, 34%), and a mixture of **II-47T**/**II-47C** (0.065 g, 0.061 mmol, 21%).

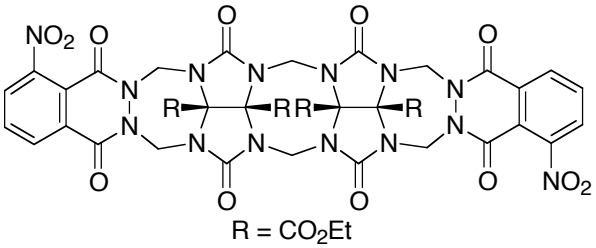

Compound II-47T: M.p. > 350 °C (dec). TLC ($CHCl_3/CH_3CN$, 1:1) R_f 0.14. IR (KBr, cm^{-1}): 3039w, 2983w, 2924w, 2851w, 1751s, 1635s, 1608m, 1546m, 1460m, 1441m, 1417m, 1383w, 1371w, 1309w, 1274s, 1258m, 1153m, 1087w, 1068w, 1052w, 1025m. ^1H NMR (400 MHz, CD_3CN):

8.30-8.25 (m, 2H), 7.95-7.85 (m, 2H), 7.80-7.75 (m, 2H), 6.96 (d, J = 16.0, 2H), 6.87 (d, J = 16.0, 2H), 5.87 (d, J = 16.2, 2H), 4.81 (d, J = 15.9, 2H), 4.79 (d, J = 15.9, 2H), 4.62 (d, J = 16.2, 2H), 4.26 (q, J = 7.13, 8H), 1.30-1.20 (m, 12H). ^{13}C NMR (100 MHz, CD_3CN): 165.7, 165.2, 154.8, 154.2, 153.9, 152.7, 149.5, 135.7, 130.8, 130.7, 128.0, 119.6, 79.2, 77.4, 65.6, 65.4, 50.8, 50.6, 48.6, 13.8, 13.7. MS (FAB, Magic Bullet): *m/z* 1081 (100, $[M + Na]^+$). HR-MS (FAB, Magic Bullet): *m/z* 1191.1415 ($[M + Cs]^+$, $C_{42}H_{38}N_{14}O_{20}Cs$, calcd 1191.1441).

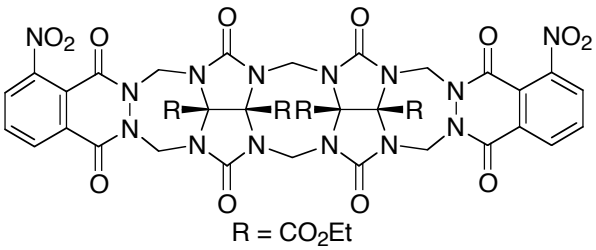

Compound II-47C: M.p. > 350 ^{o}C (dec). TLC ($CHCl_3/CH_3CN$, 1:1) R_f 0.10. IR (KBr, cm^{-1}): 3088w, 3025w, 2983w, 2936w, 1755s, 1647s, 1604w, 1546s, 1464s, 1445s, 1421m, 1375m, 1348w, 1309m, 1270s, 1173w, 1153m, 1095w, 1068w, 1021m. ^{1}H NMR (400 MHz, CD_3CN): 8.25-8.20 (m, 2H), 7.95-7.90 (m, 2H), 7.85-7.80 (m, 2H), 6.92 (d, J = 15.9, 2H), 6.89 (d, J = 16.0, 2H), 5.87 (d, J = 16.2, 1H), 5.85 (d, J = 16.2, 1H), 4.81 (d, J = 15.9, 2H), 4.80 (d, J = 16.0, 2H), 4.67 (d, J = 16.3, 1H), 4.56 (d, J = 16.3, 1H), 4.30-4.20 (m, 8H), 1.30-1.20 (m, 12H). ^{13}C NMR (100 MHz, CD_3CN): 165.7, 165.2, 154.8, 154.2, 154.1, 152.7, 149.5, 135.9, 131.0, 130.7, 128.0, 119.5, 79.2, 77.4, 65.6, 65.4, 50.8, 50.7, 48.6, 48.5, 13.8, 13.7. MS (FAB, Magic Bullet): *m/z* 1081 (100, $[M + Na]^+$). HR-MS (FAB, Magic Bullet): *m/z* 1191.1447 ($[M + Cs]^+$, $C_{42}H_{38}N_{14}O_{20}Cs$, calcd 1191.1441).

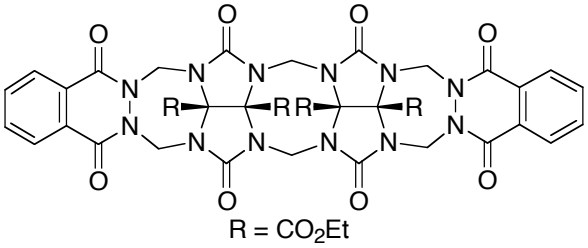

Compound II-54: A mixture of PTSA (0.069 g, 0.37 mmol) and $ClCH_2CH_2Cl$ (5 mL) was heated under N_2 at reflux for 30 min. under an addition funnel filled with molecular sieves (4Å). Phthalhydrazide (**II-13**) (0.026 g, 0.16 mmol) and compound **II-7** (0.050 g, 0.073 mmol) were added and after 4 h at reflux a precipitate formed. The reaction mixture was concentrated and dried under high vacuum. The residue was washed with water (3 × 10 mL) and centrifuged to yield **II-54** as a white solid (50.0 mg, 0.0516 mmol, 71%). M.p. 310-312 ^{o}C (dec). TLC ($CHCl_3/CH_3CN$, 10:1) R_f 0.20. IR (KBr, cm^{-1}): 2990w, 2971w, 1755s, 1635m, 1464m, 1445m, 1398w, 1371w, 1274s, 1161w, 1138m, 1091w, 1021m. ^{1}H NMR (400 MHz, DMSO-d_6): 7.80 (br. s, 4H), 7.60 (br. s, 4H), 6.70 (d, J = 15.6, 4H), 5.88 (d, J = 16.2, 2H), 5.03 (d, J = 15.6, 4H), 4.64 (d, J = 16.2, 2H), 4.30-4.20 (m, 8H), 1.26 (t, J = 7.2, 6H), 1.23 (t, J = 7.2, 6H). ^{13}C NMR (100 MHz, DMSO-d_6): 164.8, 164.2, 155.1, 153.5, 137.4, 78.5, 77.6, 65.3, 64.9, 50.4, 48.2, 14.0, 13.9 (only 13 of the 15 expected resonances were observed). MS (FAB, Magic Bullet): *m/z* 991 (100, $[M + Na]^+$), 969 (45, $[M + H]^+$). HR-MS (FAB, Magic Bullet): *m/z* 969.2802 ($[M + H]^+$, $C_{42}H_{41}N_{12}O_{16}$, calcd 969.2763).

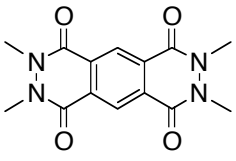

Compound II-56: To a solution of pyromellitic dianhydride (1.00 g, 4.59 mmol) in hot glacial acetic acid was added *N*, *N*'-dimethylhydrazine dihydrochloride (1.34 g, 10.09 mmol) in

AcOH (50 mL) and the reaction mixture heated at reflux for 18 h. The reaction mixture was filtered to give **II-56** as fine yellow crystals (1.00 g, 3.31 mmol, 72%). M.p. >350 °C. IR (KBr, cm^{-1}): 2963w, 2924w, 2851w, 1639s, 1355m, 1254m, 1192w, 1115w. ^{1}H NMR (400 MHz, DMSO-d_6): 8.80 (s, 2H), 3.65 (s, 12H). ^{13}C NMR (100 MHz, H_2SO_4 w/D_2O capillary): 156.6, 129.7, 129.3, 37.3. MS (EI): *m/z* 302 (100, $[M]^+$). HR-MS (EI): *m/z* 302.1017 ($[M]^+$, $C_{14}H_{14}N_4O_4$, calcd 302.1015).

Isomerization experiments: Isomerization of **II-47T**. A mixture of PTSA (0.010 g, 0.050 mmol) and $ClCH_2CH_2Cl$ (5 mL) was heated under N_2 at reflux for 30 min. under an addition funnel filled with molecular sieves (4Å). Compound **II-47T** (0.010 g, 0.010 mmol) was added and reflux was continued for 5 d. The reaction mixture was diluted with $CHCl_3$ (20 mL), washed with water, dried over $MgSO_4$, and dried under high vacuum. The crude ^{1}H NMR was taken in DMSO-d_6 and the relative ratios of the aromatic peaks at 8.36 ppm and 8.27 ppm were measured by integration to give **II-47T**/**II-47C** in a 36:64 ratio. Isomerization of **II-47C**. A mixture of PTSA (0.010 g, 0.050 mmol) and $ClCH_2CH_2Cl$ (5 mL) was heated under N_2 at reflux for 30 min. under an addition funnel filled with molecular sieves (4Å). Compound **II-47C** (0.010 g, 0.010 mmol) was added and reflux was continued for 5 d. The reaction mixture was diluted with $CHCl_3$ (20 mL), washed with water, dried over $MgSO_4$, and dried under high vacuum. The crude ^{1}H NMR was taken in DMSO-d_6 and the relative ratios of the aromatic peaks at 8.36 ppm and 8.27 ppm were measured by integration to give **II-47T**/**II-47C** in a 32:68 ratio. Crossover experiment for **II-54**

and **II-47T.** A mixture of PTSA (0.010 g, 0.050 mmol) and $ClCH_2CH_2Cl$ (5 mL) was heated under N_2 at reflux for 30 min. under an addition funnel filled with molecular sieves (4Å). Compound **II-54** (0.005 g, 0.005 mmol) and compound **II-47T** (0.005 g, 0.005 mmol) were added in one portion and reflux was continued for 5 d. The reaction mixture was diluted with $CHCl_3$ (20 mL), washed with water, dried over $MgSO_4$, and dried under high vacuum. The crude ^1H NMR was taken in DMSO-d_6 and only **II-54**, **II-47T**, and **II-47C** were observed.

III. Chapter 3: Molecular Recognition Properties of a Water Soluble Cucurbit[6]uril Analogue

3.1 Introduction

Cucurbit[6]uril (CB[6]) is a macrocyclic compound comprising twelve methylene bridges connecting six glycoluril units (Figure 1a and 1b). Since the elucidation of the structure of CB[6] by Mock in 1981, its outstanding molecular recognition properties have been described in a series of reports, most notably from the groups of Mock,[2,3,69] Buschmann,[63,99] and Kim.[5,127,190] The relative rigidity of the CB[6] framework results in highly selective recognition properties toward cationic and hydrophobic species (e.g. alkanediamines) through non-covalent interactions including ion-dipole interactions, hydrogen bonding, and the hydrophobic effect. The detection of CB[6]•guest complexes was first reported for alkylammonium ions based on experimental evidence from ^{1}H NMR,[69] UV/Vis,[4] and calorimetry.[80] Since then, the binding of CB[6] to a wide variety of species including alkali metal cations,[60] amino acids and amino alcohols,[93] and amino azabenzenes[100] has been reported.

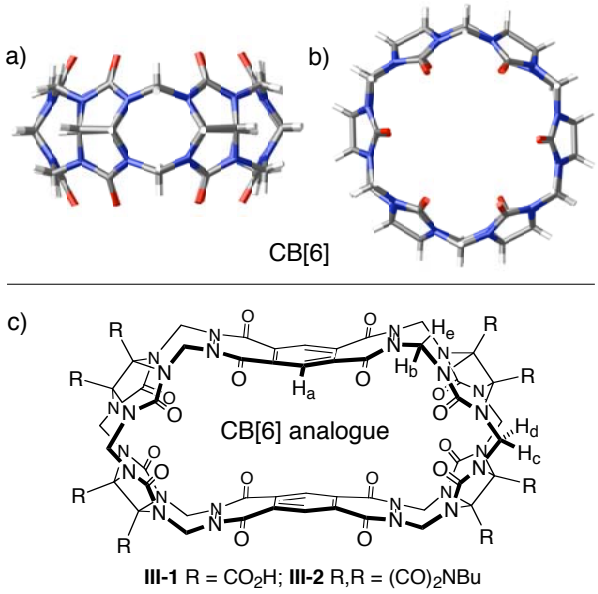

Figure 1. Representation of the X-ray crystal structure of CB[6].[7] (a) side view; (b) top view. (c) Chemical structures of CB[6] analogues **III-1** and **III-2**. The labeled hydrogens on the CB[6] analogue **III-1** are used to denote those resonances in their ^{1}H NMR spectra (*vide infra*).

Unfortunately, underivatized CB[6] is not fluorescent and, therefore, cannot be monitored directly by fluorescence spectroscopy. Incorporation of a fluorophore into the CB skeleton would result in a universal detection scheme with a potentially wide dynamic range and high sensitivity. The fluorescence experiments performed to date with CB[6] involved the use of fluorescent guests. Such experiments have been performed by the groups of Wagner,[102,103,108] Kim,[137,190] and Buschmann,[104] Nau,[207] and Kaifer.[176] For example, Wagner and Buschmann independently reported fluorescence experiments using a mixture of 1-anilinonapthalene-8-sulfonate (1,8-ANS) and CB[6] in the solid-state. A second approach towards the determination of association constants of host-guest complexes using UV/Vis or fluorescence

spectroscopy involves the use of an indicator-displacement assay that consists of a pH or solvatochromic sensitive indicator.[208-211] This indicator (usually a fluorescent dye) forms a complex with the host, but upon addition of a competitive guest, is displaced which changes its optical properties. This approach has not yet been applied in CB[n] chemistry. Our approach to CB[n] fluorescent sensors relies on the incorporation of a fluorophore into the CB skeleton which would result in a universal detection scheme with a potentially wide dynamic range and high sensitivity.[186,212]

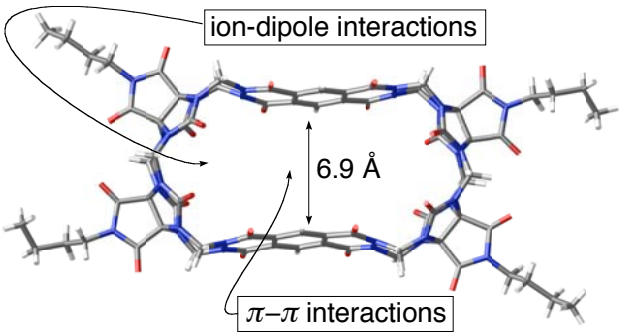

Figure 2. X-ray crystal structure of CB[6] analogue **III-2**.[186]

The synthesis of CB[n] analogues is carried out using a building block approach which allows for control over size, shape, and solubility of the resulting macrocycles.[175,186,189,197,212] The X-ray crystal structure of CB[6] analogue **III-1**, illustrates the elongated shape of the CB[6] analogues (Figure 2) with dimensions of 5.90 × 11.15 × 6.92 Å; in contrast, CB[6] has a cylindrical shaped cavity. We envisioned that the CB[n] analogues would possess unusual molecular recognition properties including tight binding, high selectivity, and slow dynamics. Furthermore,

we hoped that the CB[n] analogues would combine the desirable features of two important classes of host molecules, namely CB[n] and cyclophanes.[213-215] Due to the incorporation of aromatic walls the CB[n] analogues are structural similar to cyclophanes, but the carbonyl-lined portals resemble the CB[n] family. Since CB[n] analogues are preorganized to recognize guests molecules through a wide range of non-covalent interactions and are fluorescent. These host molecules, therefore, define a versatile platform to study the binding properties of a wide variety of chemically and biologically important guest molecules including alkyl amines, aryl amines, dyes, amino acids, peptides, and nucleotides using fluorescence spectroscopy. Furthermore, the potential to covalently attach these CB[n] analogues to a solid phase support through their carboxylic acid functional groups would allow these macrocycles to be used as fluorescent chip-based sensors in the detection of specific organic molecules such as explosives, neurotransmitters, peptides, and dyes.

In this chapter, we probe the molecular recognition properties of the water-soluble CB[6] analogue (**III-1**) and its possible application as a fluorescent sensor for chemically and biologically important amines.[175,216-218] Herein, we report the binding constants of several different types of guests toward CB[6] analogue **III-1** in aqueous solution based on results from fluorescence titration experiments. We analyze this structure-activity data to elucidate the key factors (sterics, electrostatics, hydrophobicity, etc.) influencing the ability of **III-1** to complex with organic molecules.

3.2 Results and Discussion

3.2.1 Binding Properties of CB[6] Analogue **III-1** with 1,6-hexanediamine (**III-6**)

In this section, we use 1,6-hexanediamine (**III-6**) as a model guest for **III-1** – because it is the prototypical guest for the CB[n] family – to calibrate our analytical techniques (NMR, UV/Vis, and fluorescence) before proceeding to study a wide variety of guests (*vide infra*).

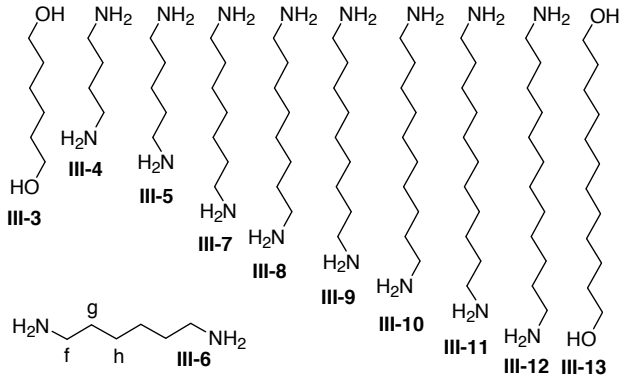

Figure 3. Alkanediamines and alkanediols used as guests for **III-1**. The hydrogens labeled on 1,6-hexanediamine (**III-6**) correspond with their ^{1}H NMR resonances in Figure 4.

3.2.1.1 ^{1}H NMR Study

The distance between the carbonyl portals of CB[6] is ≈ 6.0 Å; accordingly, alkanediamines with a commensurate N•••N distance have highest affinity toward CB[6]. For example, both 1,6-hexanediamine (**III-6**) and 1,5-pentanediamine (**III-5**)

bind with high affinity ($K_a \approx 10^6$ M^{-1}) because the hydrophobic aliphatic portion of the guest resides completely in the cavity of the CB[6].[3] The ^{1}H NMR spectrum of a 1:1 mixture of diamine and CB[6] shows characteristic upfield shifts of the aliphatic portion of **6** on the order of ≈ 0.8 ppm when bound inside the cavity of CB[6].[69] Initially we hypothesized that CB[6] analogue **III-1** would bind alkanediamines in a similar fashion with the alkane thread stretched between the two carbonyl portals. We hoped that the elongated shape of **III-1** might even allow the simultaneous binding of two alkanediamines in the hydrophobic cavity of **III-1** resulting in the formation of a ternary complex! The ^{1}H NMR spectra of **III-1**, **III-6**, and a 1:1 mixture of **III-1** and **III-6** are shown in Figure 3. The ^{1}H NMR spectrum of the mixture of **III-1** and **III-6** shows distinct upfield shifts (≈ 0.2 ppm) and broadening of the resonances corresponding to the protons on the β and γ carbons (H_g and H_h, respectively) of the aliphatic portion of guest **III-6**. Even though the protons on the α carbon (H_f) relative to the $-NH_3^+$ also show broadening, the upfield shift is not as dramatic because these methylene protons are the furthest away from the shielding region defined by the aromatic rings lining the cavity of host **III-1**. This broadening is due to the equilibrium process between free and bound 1,6-hexanediamine (**III-6**) being in the intermediate exchange regime on the chemical shift time scale. The resonances for the protons on **III-1** also show small shifts in the ^{1}H NMR spectrum upon complexation with diamine **III-6**. For example, the resonance corresponding to the aromatic protons (H_a) on the bis(phthalhydrazide) walls shifts downfield most likely because the binding of **III-6** in the cavity of **III-1** results in a geometrical change in the bis(phthalhydrazide) walls. A similar downfield shift is observed for

the resonances for the diastereotopic protons (H_b) on the methylene bridges connecting the bis(phthalhydrazide) and the glycoluril. These protons are directed toward the interior of the cavity of host **III-1**. In addition to providing information on the structure of the **III-1•III-6** complex, these shifts as a function of concentration allowed us to determine the association constant of **III-1•III-6**.

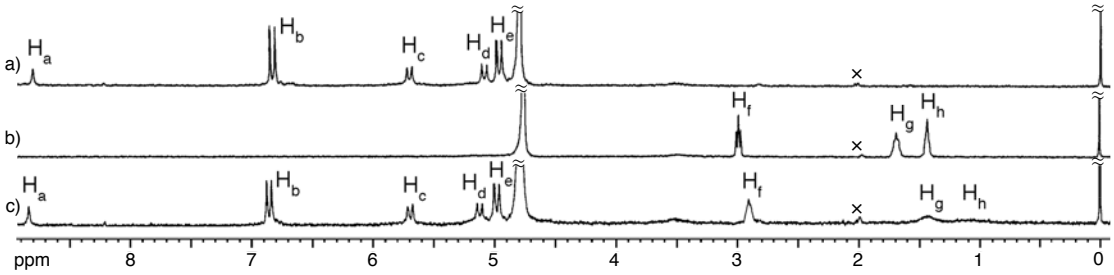

Figure 4. ^{1}H NMR spectra (400 MHz, 25 ˚C, 50 mM sodium acetate buffered D_2O, pD 4.74) for (a) **III-1** (1 mM), (b) **III-6** (1 mM), and (c) **III-1** (0.5 mM) and **III-6** (0.5 mM). × = OAc.

We performed an NMR titration experiment in which the change in the shift of the resonance corresponding to the aromatic proton (H_a) was monitored as a function of the concentration of **III-6**. When this data is fitted to a 1:1 binding model using a nonlinear least-squares analysis, we obtained $K_a = 630 \pm 40$ M^{-1} for **III-1•III-6**. Despite the fact that the titration data fitted well to a 1:1 binding model, we wanted to obtain stronger evidence for the stoichiometry of the **III-1•III-6** complex. For this purpose, we performed a Job plot analysis at a fixed total concentration of 1 mM (Figure 5). The Job plot establishes a 1:1 ratio between **III-1** and 1,6-hexanediamine (**III-6**) within their complex (e.g. **III-1•III-6**). These results

demonstrate that only a single molecule of **III-6** can complex with **III-1** at a time; putative ternary and higher order complexes are unstable due to unfavorable electrostatic or steric interactions.

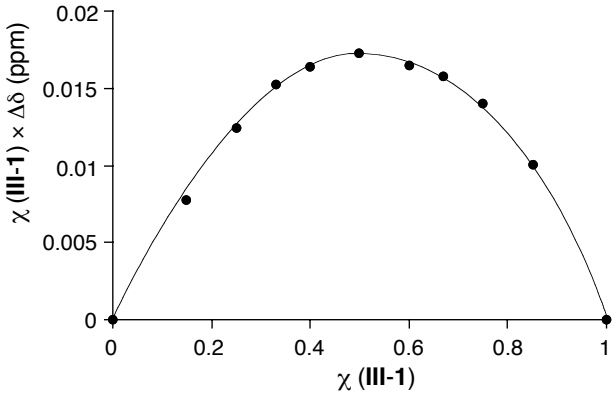

Figure 5. Job plot for CB[6] analogue (**III-1**) and 1,6-hexanediamine (**III-6**) based ^{1}H NMR experiments (400 MHz, 25 ˚C, 50 mM sodium acetate buffered D_2O, pD 4.74) monitoring the shift of the aromatic protons on the bis(phthalhydrazide) (H_a) of host **III-1**. The line in the graph is intended to act as a guide for the eye.

3.2.1.2 UV/Vis Study

Due to the incorporation of the aromatic bis(phthalhydrazide) walls into the macrocycle, host **III-1** can also be monitored directly by spectroscopic techniques such as UV/Vis and fluorescence. The ability to use optical detection methods is advantageous because the sensitivity of these techniques allows for the determination of large association constants of complexes in addition to the ability to monitor either the host or the guest, depending on the type of experiment. To assess the suitability of UV/Vis as a general method to obtain **III-1**•guest binding constants, we performed

a UV/Vis titration experiment monitoring the absorbance of the host at 330 nm (Figure 6) upon complexation with 1,6-hexanediamine (**III-6**) and compared the results to those based on the ^{1}H NMR measurements. As the concentration of **III-6** is increased in a solution containing a fixed concentration of **III-1**, a decrease in absorbance is observed. When we fitted this change in absorbance to a 1:1 binding model by non-linear least squares analysis, we obtained an association constant of 370 ± 70 M^{-1}. The isosbestic point observed at ≈ 370 nm provides strong evidence for a clear two-state equilibrium in the system comprising **III-1** and **III-6**. Although the use of UV/Vis spectroscopy to obtain association constants for **III-1** requires less material and less time than typical ^{1}H NMR titrations, the change in absorbance is small and for certain guests can prove impractical to monitor for accurate K_a determinations.

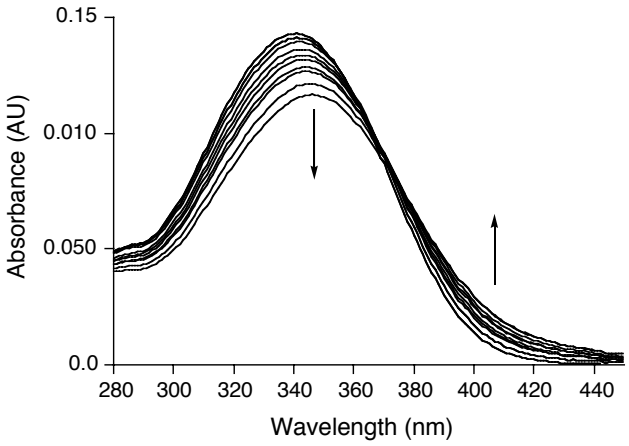

Figure 6. UV/Vis titration of **III-1** (5.2 μM, 50 mM NaOAc, pH 4.74, 25 ˚C) with 1,6-hexanediamine (**III-6**) (0 mM – 10 mM).

3.2.1.3 Fluorescence Studies

The use of fluorescence spectroscopy provides the easiest method to determine the association constants of a variety of different guests with **III-1** because very small amounts of material are needed (2.5 – 25 μM), the data can be acquired rapidly, and the fluorescence spectrum shows a large change upon injection of a wide range of guests. Accordingly, as the concentration of **III-6** is increased in a solution containing a constant concentration of **III-1**, an increase in the fluorescence emission at 525 nm is observed (Figure 7a). The change in the area under each fluorescence emission spectrum was determined by integration and then fitted to a 1:1 binding model to give an association constant of 240 ± 12 M^{-1} (Figure 7b). To further understand the factors which govern the binding of alkanediamines towards host **III-1**, we decided to examine the influence of chain length (n, $H_2N(CH_2)_nNH_2$) and functional group (e.g. –OH vs. $–NH_2$) on the strength of binding with **III-1**.

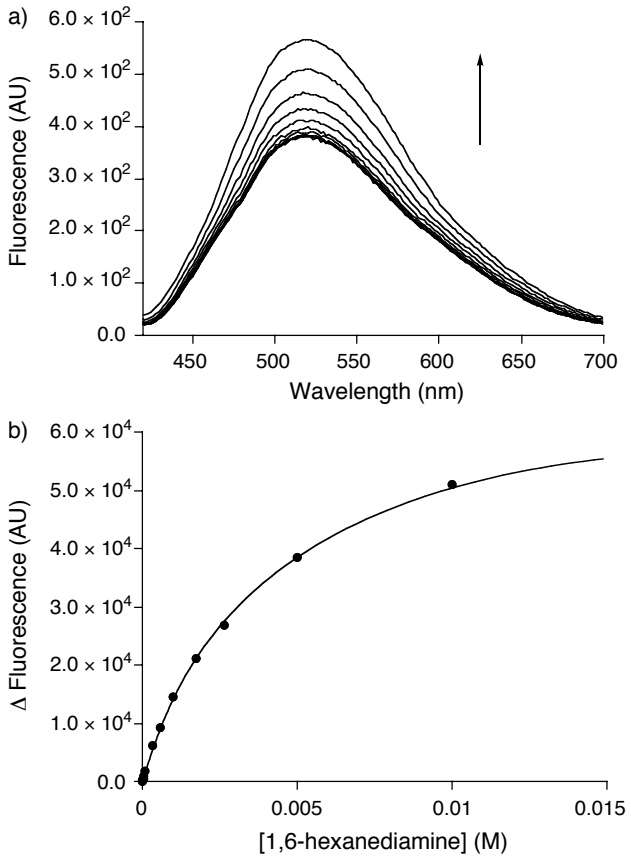

Figure 7. (a) Fluorescence titration of **III-1** (25 μM, 50 mM NaOAc, pH 4.74, 25 ˚C) with 1,6-hexanediamine (**III-6**) (0 mM – 10 mM). (b) A plot of the change in the integrated fluorescence emission of **III-1** versus [1,6-hexanediamine]; the solid line represents the best fit of the data to a 1:1 binding model with $K_a = (2.4 \pm 0.12) \times 10^2$ M^{-1}.

3.2.2 Determination of Association Constants Using Fluorescence Spectroscopy

We chose to use fluorescence spectroscopy rather than ^{1}H NMR or UV/Vis spectroscopy to determine the association constants of **III-1**•guest complexes for

several reasons: 1) the data can be acquired quickly and accurately by directly monitoring the change in emission of **III-1**, 2) the amount of material needed is minimal due to the high sensitivity of fluorescence spectroscopy, 3) the change in the fluorescence emission spectrum of **III-1** is usually large and can be easily monitored for a wide-range of guests, and 4) association constants on the order of 10^6 M^{-1} can be obtained directly.

3.2.3 Alkanediamines

In order to determine the influence of the length of the alkanediamines on the association constants, we performed fluorescence titrations with shorter and longer alkanediamines (**III-4**, **III-5**, **III-7** – **III-12**) and compared the results to those obtained for alkanediamine **III-6** (Figure 3). The general trend of decreasing binding affinity for different lengths of alkanediamines is as follows: 1,10-decanediamine (**III-10**) > 1,11-undecanediamine (**III-11**) > 1,12-dodecanediamine (**III-12**) > 1,9-nonanediamine (**III-9**) >> 1,8-octanediamine (**III-8**) > 1,7-heptanediamine (**III-7**) >> 1,6-hexanediamine (**III-6**).

Table 1. Association constants for guests **III-3** – **III-13** with **III-1**.

Guest	CB[6] analogue **III-1** K_a (M^{-1})
III-3	n.d.
III-4	n.d.
III-5	n.d.
III-6	$(2.4 \pm 0.12) \times 10^2$
III-7	$(2.8 \pm 0.12) \times 10^3$
III-8	$(5.4 \pm 0.17) \times 10^3$
III-9	$(1.8 \pm 0.05) \times 10^4$
III-10	$(2.4 \pm 0.33) \times 10^4$
III-11	$(2.3 \pm 0.27) \times 10^4$
III-12	$(2.0 \pm 0.27) \times 10^4$
III-13	n.d.

n.d. = no binding detected.

3.2.3.1 The Length of Alkanediamines Influences Their Binding Towards Host III-1

As can be seen in Table 1, as the length of the alkyl chain increases so does the binding constant. Once the length of the chain between the amines reaches ten carbons, a maximum binding constant is reached at 24,000 M^{-1}. We hypothesize that unlike CB[6], which prefers to bind shorter alkanediamines (**III-5** and **III-6**) which position their $-NH_3^+$ groups at the carbonyl-line portals, CB[6] analogue **III-1** prefers longer alkanediamines (**III-7** – **III-12**) due to the oval shape of the host which maximizes both hydrophobic and ion-dipole interactions. Based on the binding constants of **III-6** – **III-12** with CB[6] analogue **III-1**, we hypothesize that the alkyl

chain also spans the hydrophobic cavity of the CB[6] analogue as in the case of CB[6], but does so diagonally.

Figure 8 shows the results of an MMFF minimization of the **III-1•III-10** complex. The hydrophobic alkyl groups reside inside the cavity of the CB[6] analogue, shielded from the polar aqueous environment outside the cavity. As illustrated in Figure 8, the 1,10-decanediammonium is able to span across and through the cavity from one side of the macrocycle to the other in order to maximize the ion-dipole interactions between the ammonium groups and the carbonyls of the glycolurils as well as to fill the hydrophobic cavity more completely. Fluorescence titrations carried out using the shortest diamines – 1,4-butanediamine (**III-4**) and 1,5-pentanediamine (**III-5**) – with CB[6] analogue **III-1** does not result in changes in the fluorescence spectrum. Thus, we conclude that the binding constant is significantly lower than that for 1,6-hexanediamine (**III-6**) ($K_a < 240\ M^{-1}$) and outside the range of the fluorescence measurements.[219]

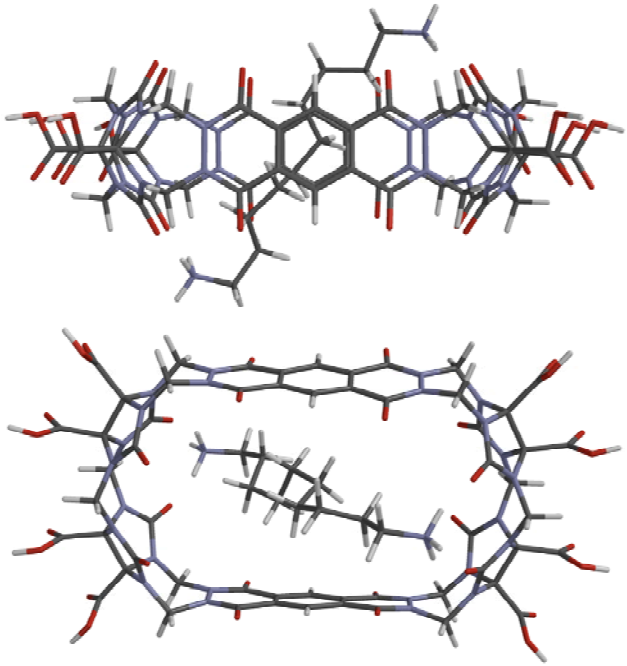

Figure 8. Minimized geometries for **III-1**•1,10-decanediammonium (**III-10**+2H$^+$) obtained from molecular mechanics calculations (MMFF). Atom colors: C, gray; N, blue; O, red; H, white.

3.2.3.2 Electrostatic Potential

Figure 9a shows the electrostatic potential energy map for CB[6];[5] the convergent C=O groups result in a highly electrostatically negative region at the two C=O lined portals. For comparison, Figure 9b shows the electrostatic potential calculated for CB[6] analogue **III-1** which indicates a less electrostatically negative portal comprising only four glycoluril carbonyl groups on each face of the macrocycle. These glycoluril carbonyl groups are important in the formation of favorable electrostatic interactions with the –NH_3^+ groups on the alkanediamine guest. The remaining four carbonyl groups associated with the bis(phthalhydrazide) portions of host **III-1** are significantly less electrostatically negative regions and are

preferentially oriented parallel to the cavity of **III-1**. It is well established that this electrostatic preorganization endows CB[6] with high selectivity towards the binding of alkanediamines. The less electrostatically negative portals of CB[6] analogue **III-1** is presumably due to the fact that the four C=O groups on each side of **III-1** do not converge upon one another as dramatically as seen for CB[6]. Accordingly, we hypothesized that ion-dipole interactions would be less important in the recognition properties of **III-1** relative to CB[6] itself. The ability of the electron deficient bis(phthalhydrazide) side walls of **III-1** to engage in π-π interactions will clearly play a prominent role in determining the affinity of **III-1** towards its guests.

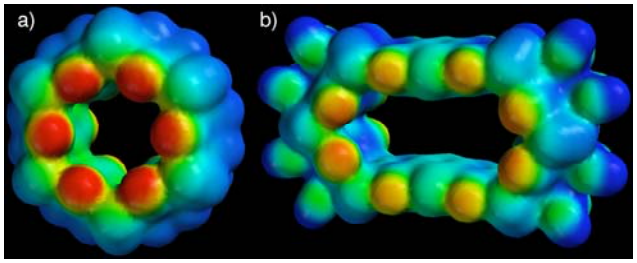

Figure 9. Electrostatic potential energy maps of: (a) CB[6] and (b) CB[6] analogue **III-1**. The red to blue color range spans –78 to +35 kcal mol^{-1}.

3.2.3.3 CB[6] Shows Greater Selectivity Towards the Binding of Alkanediamines Compared to Host III-1

A comparison of the binding constants of alkanediamines (**III-6** – **III-10**) to CB[6] analogue **1** and CB[6] are illustrated in Figure 10. From this plot, it is immediately apparent that CB[6] possesses a higher affinity for alkanediamine **III-6** with an association constant on the order of 10^6 M^{-1}. On the other hand, CB[6] analogue **III-1** possesses a larger affinity for alkanediamines **III-9** and **III-10**, but

with association constants on the order of 10^4 M^{-1}. Overall, CB[6] is a much better host for the binding of alkanediamines with association constants two orders of magnitude higher than that for CB[6] analogue **III-1**. This result is not surprising due to the fact that the shape of the cavities and portals are different. CB[6] possesses a barrel-like shape with all six electron-rich carbonyls pointed into the opening of the cavity slightly making it preorganized to engage in more favorable ion-dipole interactions with alkanediamines. In addition to its higher affinity for alkanediamines, CB[6] is also a more selective receptor than **III-1** for these compounds. The selectivity of CB[6] for alkanediamines relative to CB[6] analogue **III-1** is evident by comparing of the slope of the lines shown in Figure 10. For CB[6], the slope is much steeper (≈ 1.0 log K_a units per CH_2) than for CB[6] analogue **III-1** (≈ 0.6 log K_a units per CH_2) over a range of alkanediamines (**III-6** – **III-10**) which indicates that CB[6] displays better selectivity for shorter alkanediamines (e.g. **III-6**) versus longer alkanediamines (e.g. **III-10**) relative to host **III-1**.

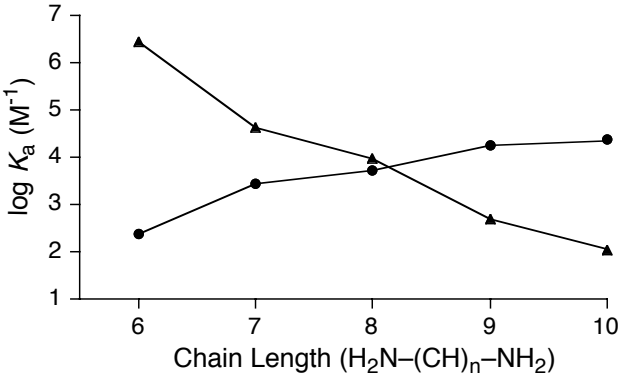

Figure 10. Relationship between the binding constant (log K_a) versus chain length n for alkanediamines **III-6** – **III-10** for CB[6] analogue **III-1** (●) and CB[6] (▲).[69]

After determining that **III-1** is capable of encapsulating alkanediamines in its cavity, we were curious to find out whether the amine groups on the alkanediamines were essential for binding to occur. Previous binding experiments with guests containing terminal hydroxy groups in place of ammonium groups have been shown to lead to a decrease in the affinity towards CB[6] of approximately 1000-fold.[3] This decrease in affinity is due to the absence of ion-dipole interactions in the case of –OH groups relative to $–NH_3^+$ groups.[69,78,80] Accordingly, we hypothesized that the affinity of **III-1** toward 1,6-hexanediol (**III-3**) would be significantly less favorable than **III-6** due to the lack of ion-dipole interactions in the complex. When the fluorescence titration experiment was carried out with host **III-1**, we did not observe a change in the fluorescence spectrum of **III-1** and thus conclude that the association constant between **III-1** and **III-3** is small; similar to what was observed for alkanediamines **III-4** and **III-5**. Finally, to further test whether the length of the alkanediamine and its resulting hydrophobicity is important in the formation of a stable host-guest complex with **III-1**, we used 1,12-dodecanediol (**III-13**). Once again, we did not observe a change in the fluorescence spectrum of **III-1** upon addition of **III-13**. Therefore, we can conclude that the ammonium groups, which interact with the carbonyl portals of host **III-1** through ion-dipole interactions, are essential in order guests to undergo tight binding in the cavity of **III-1**. The hydrophobic effect alone does not appear sufficient to induce tight binding with **III-1**. Protonated amino groups, which allow for ion-dipole interactions to occur spanning diagonally across the cavity of **III-1**, are the critical factor dictating **III-1** complexing with alkanediamines.

3.2.4 The Affinity of Substituted Aromatic Guests Towards Host **III-1**

The experimental results presented above led us to postulate that guests containing aliphatic chains are not the most favorable guests for **III-1** due to the fact that the advantageous π-π interactions between host and guest cannot occur. Therefore, we sought to determine whether CB[6] analogue **III-1** is better suited to bind larger, specifically aromatic, guests. Compared to CB[6], which does not preferentially bind large aromatic molecules in its cavity, CB[6] analogue **III-1** possesses a wider cavity as well as the potential for π-π interactions with the appropriate guests based on the incorporation of aromatic walls into the macrocycle.

Previously, we determined that the binding constant of **III-1**•benzene (**III-14**) is 6900 M^{-1}.[175] The distance between the two aromatic walls in **III-1** is 6.9 Å which results in a high level of preorganization for **III-1** to engage in favorable π-π interactions with aromatic guests (Figure 2). Based on this relatively weak binding constant relative to the long-chain alkanediamines (**III-8** – **III-11**), we hypothesized that substituents with the ability to interact with **III-1** through ion-dipole interactions and hydrogen bonds such as $–NH_3^+$ and –OH groups would increase the affinity for these types of guests toward **III-1**. Also, increasing the size of the guests and the number of aromatic rings in the guest molecule should also increase the stability of these complexes. In order to determine whether CB[6] analogue **III-1** would display enhanced affinity towards a wider range of aromatic guests, fluorescence titrations experiments were performed for several water soluble aromatic compounds (Figure 11).

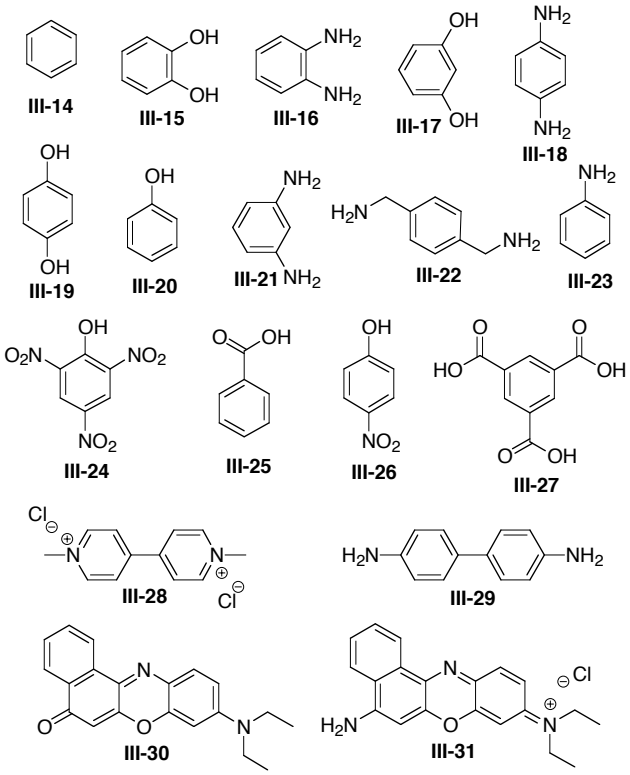

Figure 11. Aromatic guests and dyes used in fluorescence titration experiments with CB[6] analogue **III-1**.

Accordingly, several guests were studied to give insight into the electronic preferences, sterics, number of hydrogen bond donors, and the length/size of different types of aromatic guests. From monosubstituted, to disubstituted, to trisubstituted aromatic compounds, the goal was to establish a structure-activity relationship between association constants and types of substituted aromatic molecules. The association constants range from 10^3 to 10^6 M^{-1} depending on the guest studied and were all obtained directly by monitoring the change in the emission of **III-1** through the use of fluorescence spectroscopy. The order of decreasing binding affinity is as follows: catechol (**III-15**) > *o*-phenylenediamine (**III-16**) > resorcinol (**III-17**) > *p*-phenylenediamine (**III-18**) > hydroquinone (**III-19**) > phenol (**III-20**) > *m*-

phenylenediamine (**III-21**) > *p*-xylylenediamine (**III-22**) > aniline (**III-23**) > picric acid (**III-24**) > benzoic acid (**III-25**) >> benzene (**III-14**) > *p*-nitrophenol (**III-26**).

3.2.4.1 Aromatic Guests Containing One Group Capable of Donating H-Bond(s): Aniline, Phenol, Benzoic Acid

The association constant for aniline (**III-23**) is about an order of magnitude higher than benzene (**III-14**) at 4.5×10^4 M^{-1}. We hypothesize that this increased K_a is most likely due to the anilinium $-NH_3^+$ ($pK_a \approx 4.6$) group engaging in H-bonding and ion-dipole interactions with the carbonyls of **III-1** similar to the alkanediamines discussed previously. Phenol (**III-20**) also has a larger affinity towards host **1** than benzene which is most likely due to the –OH group on the aromatic ring engaging in H-bonding with the carbonyls of **III-1**. These results provide evidence that the addition of groups to the aromatic ring of the guest molecule which can form hydrogen bonds or ion-dipole interactions with the electron-rich carbonyl portals of **III-1** have a greater affinity for **III-1** with binding constants in the range of 10^4 M^{-1} which is about one order of magnitude higher than the unsubstituted benzene (**III-14**). The combination of these non-covalent interactions, which are not available with benzene (**III-14**), leads to an increase in the association constant for aniline (**III-23**) and phenol (**III-20**). On the other hand, benzoic acid (**III-25**) has a smaller association constant ($K_a = 2.5 \times 10^4$ M^{-1}) relative to aniline (**III-23**), but a larger association constant relative to benzene (**III-14**). Based on the decrease of the association constant of benzoic acid (**III-25**) relative to aniline (**III-23**) and phenol (**III-20**), we hypothesize that the $-CO_2H$ group is better solvated, making the guest less hydrophobic, which leads to less favorable host-guests interactions.[220]

Table 2. Association constants of aromatic guests **III-14** – **III-31** with CB[6] analogue **III-1**.

Guest	CB[6] analogue **III-1** K_a (M^{-1})
III-14[175]	$(6.9 \pm 1.1) \times 10^3$
III-15	$(2.9 \pm 0.60) \times 10^5$
III-16	$(2.5 \pm 0.70) \times 10^5$
III-17	$(1.3 \pm 0.20) \times 10^5$
III-18	$(8.0 \pm 1.4) \times 10^4$
III-19	$(7.6 \pm 2.0) \times 10^4$
III-20	$(7.4 \pm 1.5) \times 10^4$
III-21	$(5.6 \pm 0.80) \times 10^4$
III-22	$(5.4 \pm 0.30) \times 10^4$
III-23	$(4.5 \pm 0.70) \times 10^4$
III-24	$(3.8 \pm 0.40) \times 10^4$
III-25	$(2.5 \pm 0.50) \times 10^4$
III-26	$(2.5 \pm 0.30) \times 10^3$
III-27	n.d.
III-28	$(2.2 \pm 0.08) \times 10^4$
III-29	$(4.6 \pm 1.1) \times 10^6$
III-30[175]	$(8.2 \pm 0.50) \times 10^6$
III-31	$(1.1 \pm 0.20) \times 10^6$

n.d. = no binding detected.

3.2.4.2 Aromatic Guests Containing Two Groups Capable of Donating H-Bonds

Additional substitution on the aromatic ring of the guests generally increases the association constant towards CB[6] analogue **III-1**. Specifically, catechol (**III-15**) and *o*-phenylenediamine (**III-16**) have very favorable interactions with **III-1**, based on their association constants of 2.9×10^5 and 2.5×10^5 M^{-1}, respectively. These results provide evidence that ortho substituted aromatic rings bind preferentially in the cavity of **III-1** over para substituted aromatic rings. Based on the minimized geometries for catechol (**III-15**) obtained from molecular mechanics calculations (see Experimental Section, Figure 14), one of the –OH groups hydrogen bonds with the carbonyls of the glycolurils while the other –OH forms an intramolecular hydrogen bond. A similar geometry and enhanced K_a is observed for *o*-phenylenediamine (**III-16**) relative to *p*-phenylenediamine (**III-18**). *Meta*-substituted resorcinol (**III-17**) forms a strong complex with **III-1** ($K_a = 1.3 \times 10^5$ M^{-1}), but the K_a value for the corresponding *meta*-diamine **III-21** is reduced by half (K_a (**III-1•III-21**) $= 5.6 \times 10^4$ M^{-1}). Currently, we do not understand the origin of this difference between **III-17** and **III-21**. We would expect a higher binding constant based on the ability of **III-21** to participate in H-bonding and π-π interactions as well as the additional ion-dipole interactions due to the $–NH_3^+$ groups. On the other hand, the electron-rich aromatic ring of **III-17** can form favorable charge-transfer interactions with the electron-poor bis(phthalhydrazide) walls while inside the cavity of **III-1**.[129,131] Apparently, a fine balance exists between the various – π-π, ion-dipole, charge-transfer, and H-bonding interactions – which determine the stability of **III-1**•guest complexes.

3.2.4.3 Aromatic Guests Containing Multiple Functional Groups: Benzenetricarboxylic Acid, *p*-Nitrophenol, and Picric Acid

We chose to study the ability of trisubstituted 1,3,5-benzenetricarboxylic acid (**III-27**) to bind inside the cavity of host **III-1**. Fluorescence titration of **III-1** with **III-27** did not show a change the fluorescence emission spectrum of **III-1**. We postulate that the increase in the number of the $-CO_2H$ groups increases the solvation of the guest which makes the guest less hydrophobic, thus a decrease in the K_a with **III-1** is observed.[221-223] Therefore, the addition of two $-CO_2H$ groups on the aromatic ring dramatically decreases the association constant between **III-1** and **III-27** relative to benzoic acid (**III-25**). We postulate that benzoic acid (**III-25**) can form favorable π-π interactions in the cavity of **III-1** simply by directing the $-CO_2H$ group away from the cavity, whereas trisubstituted **III-27** does not have the ability of placing the $-CO_2H$ groups away from the carbonyls on host **III-1** and outside the hydrophobic cavity of **III-1**.

The detection of explosives in soil and groundwater have been explored using host-guest chemistry based on self-assembled monolayers functionalized with cyclodextrins.[224-227] The ability of **III-1** to bind nitrated arenes was, therefore, investigated to determine whether the CB[6] analogue **III-1** might be used in detecting explosives such as trinitrotoluene (TNT) and dinitrotoluene (DNT). We used *p*-nitrophenol (**III-26**) and picric acid (**III-24**) as surrogates for determining the relative affinity of nitrated arenes towards **III-1** because they are not highly explosive and possess better solubilities in aqueous solutions than TNT and DNT. Using fluorescence spectroscopy, we were able to determine the association constants of *p*-

nitrophenol (**III-26**) and picric acid (**III-24**) with CB[6] analogue **III-1**. The association constants for **III-26** and **III-24** are 2.5×10^3 and 3.8×10^4 M^{-1}, respectively. We hypothesize that the enhancement in binding relative to **III-26** is due to the favorable π-π interactions between the electron poor walls of the host and the electron poor arene. The size and shape of the 1,3,5-trinitro-substituted aromatic ring is a good match for the cavity of **III-1**; this result bodes well for the use of **III-1** as a fluorescent sensor for explosive devices based on TNT.

3.2.4.4 Larger Aromatic Guests Increase the Surface Area of π-π Interactions

Based on the binding constant of CB[6] analogue•guest complexes being strongly dependent on the nature (e.g. number and pattern of functional groups) aromatic properties of the guest, we decided to study guests which possess two or more aromatics rings in their structure. Methyl viologen (**III-28**) has been used previously in order to study the molecular recognition properties of both CB[7] and CB[8].[112-115,127,223] CB[7] forms a 1:1 complex with **III-28** ($K_a = 1.3 \times 10^7$ M^{-1}) which is about three orders of magnitude larger than the formation of CB[6] analogue **III-1•III-28** ($K_a = 2.2 \times 10^4$ M^{-1}). We postulate that this difference in K_a is due to CB[7] possessing an appropriately sized and shaped cavity for **III-28** which maximizes the non-covalent interactions compared to CB[6] analogue **III-1**. CB[8] forms a 1:1 complex with **III-28** ($K_a = 1.1 \times 10^5$ M^{-1}) that is less stable than CB[7]•**III-28** indicating that the distance spanning from one C=O portal to the other provides favorable ion-dipole interactions with the pyridinium rings in the formation of both 1:1 complexes (CB[7]•**III-28** and CB[8]•**III-28**), but the size of the cavity of

CB[7] accommodates guest **III-28** better resulting in the formation of a tighter complex.

Accordingly, we hypothesized that benzidine (**III-29**) would be an ideal guest for **III-1** based on molecular mechanics calculations. The distance between the $-NH_2$ groups is similar to 1,10-decanediamine (**III-10**) and the aromatic rings provide a rigidity to the guest as well as the possibility to interact with the aromatic walls of the host through π-π interactions. As can be seen in Figure 12, **III-29** is capable of spanning the hydrophobic cavity of **III-1** with favorable π-π interactions as well as ion-dipole interactions of the protonated amines with the carbonyls on the glycolurils of the macrocycle. As expected, there is a slight twist between the biphenyl rings in **III-29** as it is bound in the cavity of host **III-1**. This twist in guest **III-29** while bound in the cavity of **III-1** results in a slight twist in bis(phthalhydrazide) walls of host **III-1** to maximize the π-π interactions with **III-29**. From this minimized structure, the distance from the center of the Ar-Ar bond of the guest to the centroid of the aromatic ring of the host is ≈ 3.4 Å, which is consistent with the preferred distance for π-π interactions. After performing the fluorescence titration experiment, we discovered that the association constant for **1•III-29** was 4.6×10^6 M^{-1}. This result was consistent with previous data obtained with Nile Red (**III-30**) which binds with an association constant of 8.2×10^6 M^{-1}. Based on the strong affinity of the dye **III-30**, we decided to study a similar dye called Nile Blue Chloride (**III-31**) which resulted in a similar association constant of 1.1×10^6 M^{-1}. These results provide evidence, as expected, that increasing the surface area for π-π interactions by

increasing the size of the π-system of the guest as well as increasing the coplanarity of the guest molecule significantly increases the association constant. Accordingly, host **III-1** functions as an excellent receptor for dyes and other large, flat aromatic molecules. These results suggest that CB[6] analogue **1** will become a broadly applicable host for the detection of polycyclic aromatics with detection limits approaching or exceeding the μM range. Through the judicious selection of guests with complementary size and shape as well as electrostatic profile, it is possible to obtain host-guest complexes of **III-1** with K_a values that exceed 10^6 M^{-1}! Due to the high affinity observed for host **III-1** toward polycyclic aromatic molecules and those that possess amino groups, we thought that host **III-1** would be a prime candidate for the detection of amino acids and nucleobases.[228,229]

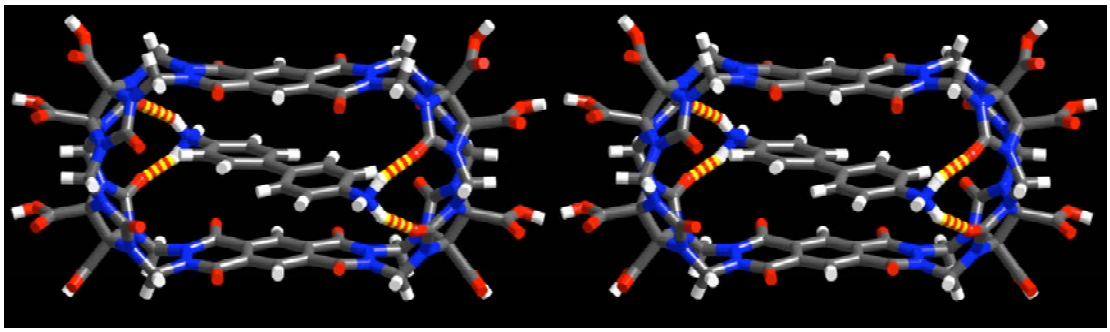

Figure 12. Cross-eyed stereoview of the MMFF-minimized structure of **III-1**•benzidinium (**III-29**+2H^+). Atom colors: C, gray; N, blue; O, red; H, white; H-bonds, red–yellow striped.

3.2.5 Biologically Relevant Guests Bind in the Cavity of Host **III-1**

Due to the high solubility of host **III-1** in aqueous solutions, its high affinity towards aromatic molecules, and the ability to detect these guest molecules at μM concentrations with fluorescence spectroscopy, we envisioned **III-1** as a potential module for the use in such applications as ion and molecular transport as well as peptide and DNA sensing.[43] Importantly, proteins and DNA do not absorb at long UV/Vis wavelengths and therefore do not interfere with the detection of host **III-1**. In order to test our hypothesis that CB[6] analogue **III-1** would associate with biological molecules, we chose to study several amino acids and nucleobases (Figure 13). These experiments were performed using fluorescence spectroscopy to monitor the change in fluorescence emission of host **III-1** as described above.

3.2.5.1 Dopamine

Based on the high affinity of **III-1** towards catechol (**III-15**) we decided to study the binding of dopamine (Figure 13, **III-32**), which is similar to **III-15**, but possesses a $-(CH_2)_2NH_2$ group on the aromatic ring. Under our experimental conditions (pH 4.74), the amino group is protonated which should enhance the K_a value for **III-1•III-32** by the combined influence of ion-dipole, hydrogen bonding, and π-π stacking interactions. In the experiment we found that the K_a value ($K_a = 7.1 \times 10^4$ M^{-1}) is comparable to that observed for **III-1•III-15**. We postulate that the geometrical preferences of the catechol (**III-15**) and ammonium region of guest **III-32** are incompatible and result in an overall decrease in the association constant. Specifically, the $-NH_3^+$ of dopamine (**III-32**) would like to position itself at

either one of the carbonyl portals of host **III-1**, similar to the alkanediamines discussed previously to maximize the ion-dipole interactions and hydrogen bonding. For this conformation of binding to occur, the complex must sacrifice more favorable π-π interactions as well as hydrogen bonding with one of the –OH groups on the aromatic portion of **III-32** (see Experimental Section, Figure 15). On the other hand, if the aromatic portion of **III-32** is positioned in the cavity in order to maximize the π-π interactions within the cavity of **III-1**, the $-NH_3^+$ group is unable to form favorable interactions with the carbonyl portal of host **III-1**. The ability of **III-1** to detect **III-32** in water has several potentially significant biological uses since dopamine is an important neurotransmitter.

3.2.5.2 Aromatic Amino Acids Form Strong Complexes With CB[6] Analogue III-1

Fluorescence titration experiments were also performed with L-phenylalanine (**III-33**), L-tyrosine (**III-34**), and L-tryptophan (**III-35**). We chose these amino acids because host **III-1** should possess good affinity for them due to the possibility of π-π stacking and ion-dipole interactions. Compounds **III-33** – **III-35** have association constants of 4.2×10^4, 5.7×10^4, and 3.2×10^6 M^{-1}, respectively (Table 3). CB[6] analogue **III-1** binds **III-35** especially tightly which is most likely due to the larger size of the indole ring compared to the monocyclic rings on amino acids **III-34** and **III-35**. Based on these initial results, we believe that CB[6] analogue **III-1** will bind to peptides and proteins containing aromatic amino acid residues which will be useful in peptide sensing applications. Interestingly, when the titration was performed using L-histidine (**III-36**) as a guest, the fluorescence emission spectrum of **III-1** does not

change. In the case of **III-36**, we hypothesize that the protonation of the imidazole ring N-atom makes the aromatic ring relatively hydrophilic. Apparently, removal of the solvating water molecules is less favorable than guest inclusion within the cavity of **III-1**. A similar result was recently reported by Urbach for complexation of **III-36** inside CB[8]•**III-28**. In this study, Urbach also reports the binding of **III-33** – **III-35** towards CB[8]•**III-28** with binding constants of 5.3×10^3, 2.2×10^3, and 4.3×10^4 M^{-1}, respectively, at 27 ˚C in sodium phosphate (10 mM, pH 7.0), respectively.[229] In combination, these experiments provide evidence that the hydrophobicity of the aromatic portion of the amino acid is essential in order to complex inside the hydrophobic cavity of **III-1**.

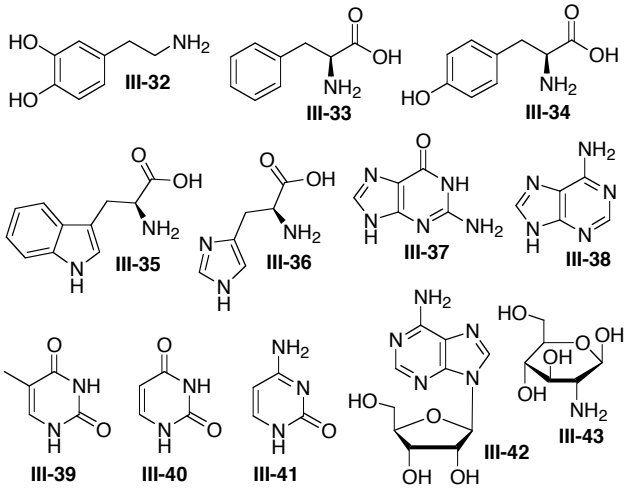

Figure 13. Biologically relevant guests used to investigate the binding properties of CB[6] analogue **III-1**.

Table 3. Association constants of biologically relevant guests **III-32** – **III-43** with CB[6] analogue **III-1**.

Guest	CB[6] analogue **III-1** K_a (M^{-1})
III-32	$(7.1 \pm 0.60) \times 10^4$
III-33	$(4.2 \pm 0.70) \times 10^4$
III-34	$(5.7 \pm 1.1) \times 10^4$
III-35	$(3.2 \pm 1.0) \times 10^6$
III-36	n.d.
III-37	n.s.
III-38	$(4.4 \pm 0.90) \times 10^4$
III-39	$(3.8 \pm 0.90) \times 10^3$
III-40	$(6.0 \pm 1.0) \times 10^3$
III-41	$(7.0 \pm 1.4) \times 10^3$
III-42	n.d.
III-43	n.d.

n.d. = no binding detected. n.s. = not soluble.

Overall, CB[6] analogue **III-1** possesses a slightly larger affinity for guests **III-33** – **III-35** compared to CB[8]•**III-28** due to **III-1** possessing two aromatic walls in the macrocycle which can participate in a sandwich-like binding (dual π-π interactions) where the aromatic walls are on both sides of the aromatic guest whereas in CB[8]•**III-28** can only interact with one side of the aromatic guest (single π-π interaction). Although the affinities of **III-1** and CB[8]•**III-28** are comparable, it may be advantageous to use **III-1** in certain cases because **III-1** – with its native fluorescence – will be responsive at sub-μM concentration where CB[8]•**III-28** will

dissociate into CB[8] and **III-28** which do not exhibit a fluorescence response to amino acids.

3.2.5.3 Nucleobases as Guests for CB[6] Analogue III-1

We were also interested in the potential binding of the building blocks of RNA and DNA, therefore we studied the ability of CB[6] analogue **III-1** to bind all five of the different nucleobases (Chart 3).[230] Unfortunately, guanine (**III-37**) was not soluble in the media used for our binding experiments (sodium acetate, 50 mM, pH 4.74, 25 ˚C) so we were unable to determine its association constant with **III-1**. However, the other purine, adenine (**III-38**), and the pyrimidines thymine (**III-39**), uracil (**III-40**), and cytosine (**III-41**) were all soluble which facilitated the determination of their affinity towards CB[6] analogue **1** (Table 3). Not surprisingly, **III-38** – with its large π-surface relative to the pyrimidines – has the largest association constant (K_a = 4.4 × 10^4 M^{-1}) of the nucleobases studied. Interestingly, adenosine (**III-42**) does not bind to host **III-1**. We postulate that sterics and solvation effects are important factors in the binding process to form stable host-guest complexes with CB[6] analogue **III-1**. The sugar residue of **III-42** most likely makes the guest too bulky as well as more hydrophilic (relative to adenine (**III-38**)) to bind efficiently in the cavity of **III-1**. To provide further evidence that sugars do not associate with host **III-1**, glucosamine (**III-43**) was injected into a solution containing **III-1**; no binding was detected by fluorescence spectroscopy. From these experiments we conclude that nucleosides as well as sugars do not possess the

appropriate shape or hydrophobicity necessary to form stable complexes with host **III-1**.

3.3 Conclusion

The incorporation of (bis)phthalhydrazide walls into the macrocycle of CB[6] analogue **III-1** gives rise to its fluorescent properties. The size and shape of **III-1** permits the binding of larger, flatter guests relative to the parent CB[6] while still retaining the ability to bind long chain alkanediamines although with different geometrical preferences. The combination of non-covalent interactions such as π-π stacking, ion-dipole, hydrogen-bonding, and the hydrophobic effect gives rise to the wide variety of guests that can be encapsulated by CB[6] analogue **III-1**.

CB[6] analogue **III-1** preferentially associates tightly with a variety of aromatic molecules with binding constants up to 10^6 M^{-1}. Aromatic guests form π-π interactions while encapsulated inside the cavity of **III-1** which is due to the preorganized structure of **III-1**. Although this paper focuses solely on monitoring the change in the fluorescence emission spectrum of **III-1**, future experiments can be performed by monitoring fluorescent guests which have the ability to be excited at different wavelengths relative to host molecule **III-1**. Therefore, the association constants can be determined either by directly monitoring the change in fluorescence of the host or the change in the fluorescence of an appropriate guest.

Furthermore, since CB[6] analogue **III-1** is highly soluble in aqueous solutions, it functions as a fluorescent sensor towards biologically important molecules with μM detection limits. The ability of **III-1** to form strong complexes with aromatic amino acids (e.g. tryptophan (**III-35**)) provides a platform for sensing peptides. The versatility of CB[6] analogue **III-1** as a host molecule allows for its potential use as a fluorescence sensor in the detection of proteins, neurotransmitters, nitroaromatics, dyes, and other aromatic guests. Additionally, the carboxylic groups on the equator can be functionalized to yield organic soluble CB[n] analogues which will display similar affinities towards aromatic guests and guests containing hydrogen-bond donating groups in non-polar, organic solutions such as $CHCl_3$ or CH_2Cl_2 which may have useful applications in nanotechnology such as micro-chip arrays. These carboxylic groups can also lead to a functionalized solid support containing CB[6] analogues which would allow the detection and separation of aromatic guests including, but not limited to, dyes, peptides, and DNA. Due to the UV/Vis, fluorescence, and electrochemical properties displayed by the CB[n] analogue family, their ease of functionality, and their ability to recognize several types of aromatic guests with affinities up to 10^6 M^{-1}, these macrocycles are poised to have a great impact towards advances in the field of supramolecular chemistry.

3.4 Experimental

3.4.1 Titration Experiments

General. Cucurbit[6]uril analogue **III-1** was synthesized and purified according to literature procedures.[177,186] All guests were purchased from commercial suppliers and were used without further purification. Solutions UV/Vis and fluorescence titrations were prepared in NaOAc buffer (pH 4.74, 50 mM). For ^{1}H NMR experiments, solutions were prepared in NaOAc buffered D_2O (pD = 4.74, 50 mM).

^{1}H NMR Spectroscopy. All spectra were recorded on a spectrometer operating at 400 MHz for ^{1}H and are referenced to external $(CH_3)_3SiCD_2CD_2CO_2H$ (δ = 0.0 ppm). The temperature was calibrated using the separation of the resonances of $HOCH_2CH_2OH$ and controlled at 22 ± 1 ˚C using a temperature control module. The chemical shifts of host **III-1** were monitored as a function of added 1,6-hexanediamine concentration and the tabulated values of chemical shift versus concentration were used to determine values of K_a by nonlinear least-squares analysis using Associate 1.6.[231] For the Job plot, the total concentration of host **III-1** and 1,6-hexanediamine was held constant at 1 mM. As the mole fraction (χ) of host **III-1** was changed from 0.0 – 1.0, the chemical shifts of the resonances for the host were monitored. The Job plot was constructed using the mole fraction (χ) of host **III-1** × the change in chemical ($\Delta\delta$) versus the mole fraction (χ) of host **III-1**.

UV/Vis Spectroscopy. All spectra were measured on a UV-Visible spectrophotometer using 1 cm path length quartz cuvettes. The temperature was held constant at 22 ± 1 ˚C using a microprocessor controlled recirculator bath. The change in absorbance of host **III-1** was monitored at 340 nm as a function of increasing 1,6-hexanediamine concentration and the change in absorbance versus concentration were used to determine values of K_a by nonlinear least-squares analysis fitting to a 1:1 binding model.

Fluorescence Spectroscopy. All spectra were measured on a fluorescence spectrophotometer with excitation and emission monochromator band-passes set at 5 nm. The temperature was held constant at 22 ± 1 ˚C using a RTE bath/circulator containing a microprocessor controller. The excitation wavelength of 360 nm was used for the fluorescence of host **III-1**. The change in fluorescence emission was monitored as a function of increasing guest concentration and the area under each spectrum was determined by integration from 450 to 600 nm. The change in area under the emission spectra versus guest concentration were used to determine values of K_a by nonlinear least-squares analysis fitting to a 1:1 binding model.

3.4.2 Molecular Mechanics Calculations (MMFF)

Computational Results. Minimized geometries obtained from molecular mechanics calculations were performed using Spartan 2002 v. 1.0.7 for Macintosh employing the MMFF force field. Electrostatic potentials were determined by single point calculations (PM3) of the MMFF minimized geometries of **III-1** and CB[6].

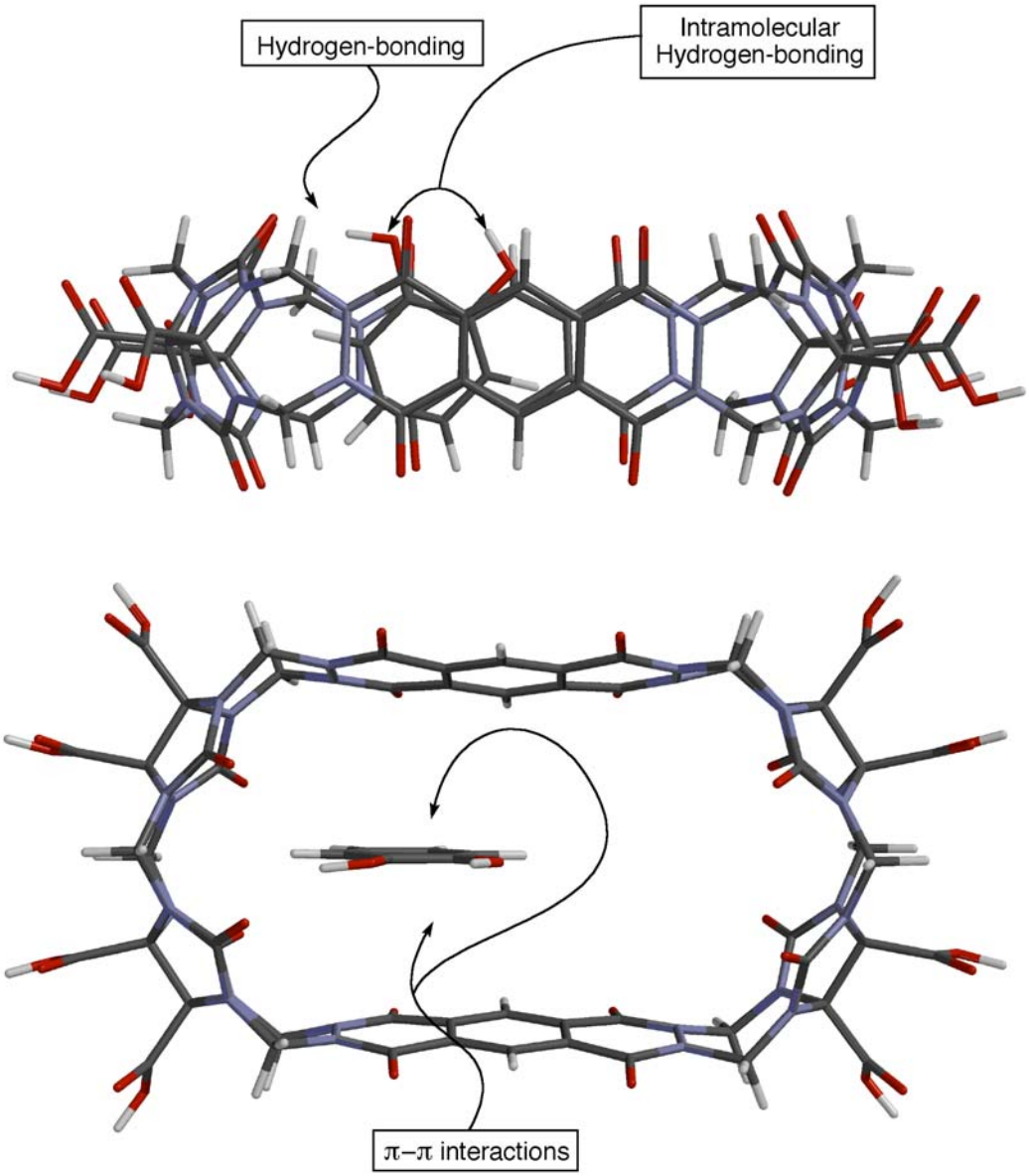

Figure 14. Minimized geometries of **III-1**•catechol (**III-15**) obtained from molecular mechanics calculations (MMFF). Atom colors: C, gray; N, blue; O, red; H, white.

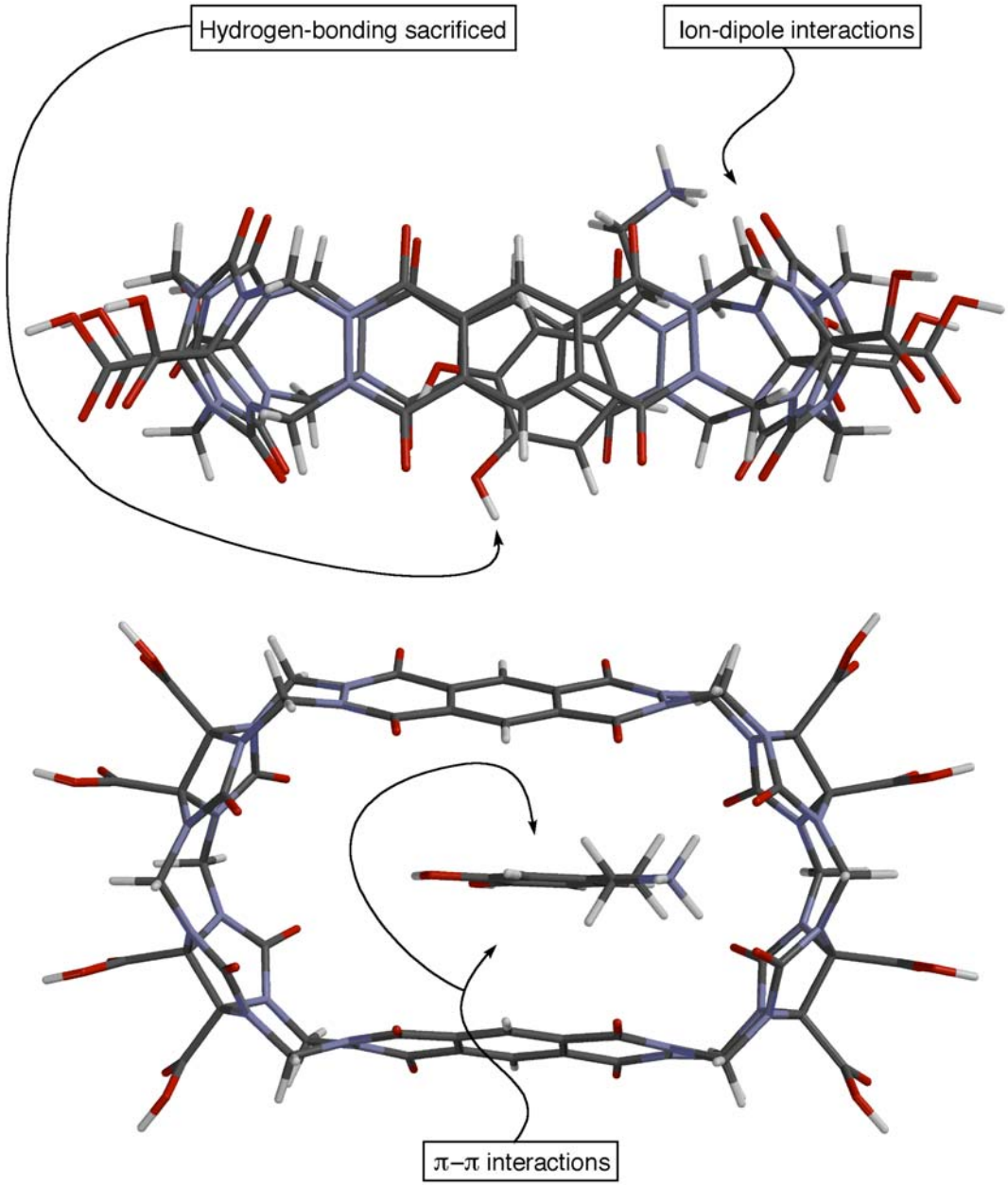

Figure 15. Minimized geometries of **III-1**•dopamine (**III-32**) obtained from molecular mechanics calculations (MMFF). Atom colors: C, gray; N, blue; O, red; H, white.

ORGANIC LETTERS

2001
Vol. 3, No. 20
3221−3224

Self-Association of Facially Amphiphilic Methylene Bridged Glycoluril Dimers

Lyle Isaacs,*,† Dariusz Witt,†,‡ and Jason Lagona†

Department of Chemistry and Biochemistry, University of Maryland, College Park, Maryland 20742, and Chemical Faculty, Technical University of Gdansk, Narutowicza St. 11/12, 80-952 Gdansk, Poland

li8@umail.umd.edu

Received August 10, 2001

ABSTRACT

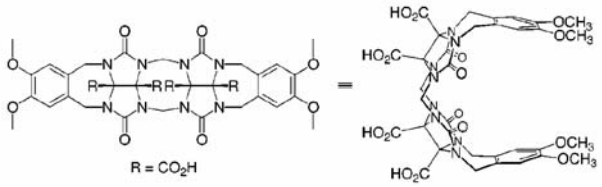

Facially amphiphilic derivatives of methylene bridged glycoluril dimers are a versatile model system for systematic studies of self-assembly in water. Thorough physical organic characterization, including analytical ultracentrifugation, a technique rarely used in synthetic self-assembly studies, allows us to conclude that this class of molecules undergoes hydrophobically driven self-association to yield tightly associated discrete dimeric assemblies.

The hydrophobic effect is widely regarded as a major driving force in a variety of molecular recognition processes including the folding of proteins into their native states, protein−protein interactions, and the formation of lipid bilayers.[1] The past decade has witnessed the increasingly sophisticated use of hydrogen bonds, $\pi-\pi$ interactions, and metal−ligand interactions to form highly structured aggregates.[2] Despite these advances, the use of the hydrophobic effect as a driving force in the self-association of nonnatural molecules into tightly associated aggregates that are well defined in terms of structure and degree of association remains a challenge.[3,4] The reason is simple: the hydrophobic effect typically involves the association in water between molecules with large apolar regions. These molecules do not typically have structural features that lend themselves to forming directional, specific intermolecular contacts that lead to stable structured aggregates in a predictable manner. We report that facially amphiphilic methylene bridged glycoluril dimers **1a** and **2a**

† University of Maryland.
‡ Technical University of Gdansk.

(1) (a) Tanford, C. *The Hydrophobic Effect*, 2nd ed.; Wiley: New York, 1980. (b) Blokzijl, W.; Engberts, J. B. F. N. *Angew. Chem., Int. Ed. Engl.* **1993**, *32*, 1545−1579. (c) Stites, W. E. *Chem. Rev.* **1997**, *97*, 1233−1250. (d) Dill, K. A. *Biochemistry* **1990**, *29*, 7133−7155.

(2) For leading reviews, see: (a) Lehn, J.-M. *Supramolecular Chemistry*; VCH: New York, 1995. (b) Philp, D.; Stoddart, J. F. *Angew. Chem., Int. Ed. Engl.* **1996**, *35*, 1155−1196. (c) Rebek, J., Jr. *Acc. Chem. Res.* **1999**, *32*, 278−286. (d) Whitesides, G. M.; Simanek, E. E.; Mathias, J. P.; Seto, C. T.; Chin, D.; Mammen, M.; Gordon, D. M. *Acc. Chem. Res.* **1995**, *28*, 37−44. (e) Leininger, S.; Olenyuk, B.; Stang, P. J. *Chem. Rev.* **2000**, *100*, 853−907.

(3) For examples of dimeric assemblies based on van der Waals interactions and/or solvophobic forces, see: (a) Wilcox, C. S.; Greer, L. M.; Lynch, V. *J. Am. Chem. Soc.* **1987**, *109*, 1865−1867. (b) Zimmerman, S. C.; Mrksich, M.; Baloga, M. *J. Am. Chem. Soc.* **1989**, *111*, 8528−8530. (c) Webb, T. H.; Suh, H.; Wilcox, C. S. *J. Am. Chem. Soc.* **1991**, *113*, 8554−8555. (d) Cram, D. J.; Choi, H.-J.; Bryant, J. A.; Knobler, C. B. *J. Am. Chem. Soc.* **1992**, *114*, 7748−7765. (e) Rowen, A. E.; Elemans, J. A. A. W.; Nolte, R. J. M. *Acc. Chem. Res.* **1999**, *32*, 995−1006. (f) Haino, T.; Rudkevich, D. M.; Shivanyuk, A.; Rissanen, K.; Rebek, J., Jr. *Chem. Eur. J.* **2000**, *6*, 3797−3805.

(4) For examples of the use of aromatic−aromatic interactions in intramolecular folding processes, see: (a) Lokey, R. S.; Iverson, B. L. *Nature* **1995**, *375*, 303−305. (b) Zych, A. J.; Iverson, B. L. *J. Am. Chem. Soc.* **2000**, *122*, 8898−8909. (c) Prince, R. B.; Barnes, S. A.; Moore, J. S. *J. Am. Chem. Soc.* **2000**, *122*, 2758−2762. (c) McKay, S. L.; Haptonstall, B.; Gellman, S. H. *J. Am. Chem. Soc.* **2001**, *123*, 1244−1245. (d) Mulla, H. R.; Cammers-Goodwin, A. *J. Am. Chem. Soc.* **2000**, *122*, 738−739. (c) Prince, R. B.; Barnes, S. A.; Moore, J. S. *J. Am. Chem. Soc.* **2000**, *122*, 2758−2762. (d) Gardner, R. R.; Christianson, L. A.; Gellman S. H. *J. Am. Chem. Soc.* **1997**, *119*, 5041−5042. (e) McKay, S. L.; Haptonstall, B.; Gellman, S. H. *J. Am. Chem. Soc.* **2001**, *123*, 1244−1245. (f) Kim, E.-I.; Paliwal, S.; Wilcox, C. S. *J. Am. Chem. Soc.* **1998**, *120*, 11192−11193.

10.1021/ol016561s CCC: $20.00
Published on Web 09/13/2001

form tightly associated, discrete dimeric aggregates **1a•1a** and **2a•2a** in water by hydrophobically driven self-association.

Nolte has pioneered the use of glycoluril-based molecular clips in molecular recognition, self-assembly, and catalysis.[3c,5,6] They have observed dimerization of molecular clips in the solid state,[5a−f] thin lamellar films,[5e,f] organic solvents,[5e,f,g] and in aqueous solution.[5h,i] We recently described a method for the synthesis of methylene bridged glycoluril dimers exemplified by **1e** and **2e**.[7] On the basis of the precedent of Nolte[5] we hypothesized that facially amphiphilic[8] compounds **1a** and **2a** that bear strictly hydrophilic carboxylate solubilizing groups on their convex face and whose concave face is defined by two roughly parallel aromatic rings might display interesting self-association behavior in water.[9] This model system combines four features that makes it well suited for systematic physical organic studies of hydrophobic self-assembly in water: (1) strong self-association, which is (2) hydrophobically driven, yielding (3) discrete dimers that (4) display slow exchange processes that can allow for structural elucidation of the aggregates.

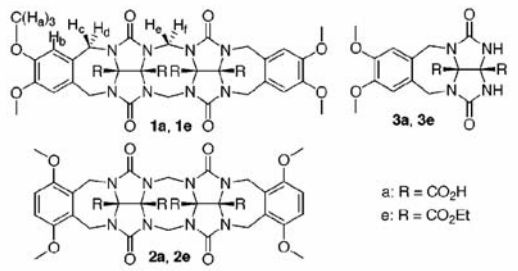

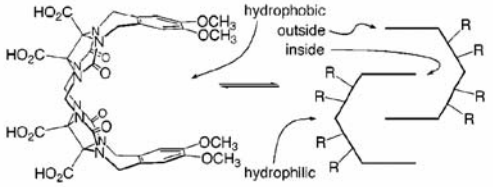

Figure 1. Three-dimensional shape of **1a** and a schematic illustration of **1a•1a** that highlights the reduction in symmetry that results upon dimerization.

Compounds **1a**−**3a** were prepared by the alkaline hydrolysis of the corresponding ethyl ester derivatives **1e**−**3e**.[7] We used isothermal titration calorimetry (ITC) dilution experiments[10] to measure association constants and thermodynamic parameters for the formation of **1a•1a** and **2a•2a**. Aggregates **1a•1a** and **2a•2a** are tightly associated at 298 K (100 mM sodium phosphate buffered D_2O, pD 7.4), and their formation is enthalpically and entropically driven (**1a•1a**, $K_d = 39\ \mu M$, $\Delta H = -3.5$ kcal mol^{-1}, $\Delta G = -6.0$ kcal mol^{-1}, $\Delta S = 8.5$ eu; **2a•2a**, $K_d = 24\ \mu M$, $\Delta H = -4.75$ kcal mol^{-1}, $\Delta G = -6.3$ kcal mol^{-1}, $\Delta S = 5.2$ eu).[11] In contrast to **1a** and **2a**, ^{1}H NMR dilution experiments indicate that **3a** (0.2−50 mM), which lacks a well-defined hydrophobic cleft, undergoes very weak self-association at room temperature ($K_a < 5\ M^{-1}$).[12] To unambiguously establish that the dimerization process was driven by the hydrophobic effect, we determined the change in heat capacity (ΔC_p) for the formation of **1a•1a** by performing ITC measurements from 288 to 328 K (Figure 2) and calculating the slope of a plot of ΔH versus T. The observed negative value of ΔC_p ($\Delta C_p = -185 \pm 6$ cal mol^{-1} K^{-1}) allows us to conclude that the formation of **1a•1a** is a hydrophobically driven event.[13]

In studies of self-association it can be challenging to unambiguously establish the degree of association. For

(5) (a) Reek, J. N. H.; Rowan, A. E.; de Gelder, R.; Beurskens, P. T.; Crossley, M. J.; De Feyter, S.; de Schryver, F.; Nolte, R. J. M. *Angew. Chem., Int. Ed. Engl.* **1997**, *36*, 361−363. (b) Jansen, R. J.; Rowan, A. E.; de Gelder, R.; Scheeren, H. W.; Nolte, R. J. M. *Chem. Commun.* **1998**, 121−122. (c) Reek, J. N. H.; Rowan, A. E.; Crossley, M. J.; Nolte, R. J. M. *J. Org. Chem.* **1999**, *64*, 6653−6663. (d) Jansen, R. J.; de Gelder, R.; Rowan, A. E.; Scheeren, H. W.; Nolte, R. J. M. *J. Org. Chem.* **2001**, *66*, 2643−2653. (e) Holder, S. J.; Elemans, J. A. A. W.; Barberá, J.; Rowan, A. E.; Nolte, R. J. M. *Chem. Commun.* **2000**, 355−356. (f) Holder, S. J.; Elemans, J. A. A. W.; Donners, J. J. J. M.; Boerakker, M. J.; de Gelder, R.; Barberá, J.; Rowan, A. E.; Nolte, R. J. M. *J. Org. Chem.* **2001**, *66*, 391−399. (g) Reek, J. N. H.; Priem, A. H.; Engelkamp, H.; Rowan, A. E.; Elemans, J. A. A. W.; Nolte, R. J. M. *J. Am. Chem. Soc.* **1997**, *119*, 9956−9964. (h) Reek, J. N. H.; Kros, A.; Nolte, R. J. M. *Chem. Commun.* **1996**, 245−247. (i) Elemans, J. A. A. W.; de Gelder, R.; Rowen, A. E.; Nolte, R. J. M. *Chem. Commun.* **1998**, 1553−1554.

(6) Compounds **1a** and **2a** are members of the class of molecules known as molecular clips and molecular tweezers. We refer to them as facial amphiphiles since this terminology fully describes their topological features and provides a rationale for the observed self-association behavior. For examples of molecular tweezers, see: (a) Chen, C.-W.; Whitlock, H. W. *J. Am. Chem. Soc.* **1978**, *100*, 4921−4922. (b) Zimmerman, S. C.; VanZyl, C. M. *J. Am. Chem. Soc.* **1987**, *109*, 7894−7896. (c) Zimmerman, S. C. *Top. Curr. Chem.* **1993**, *165*, 71−102. (d) Harmata, M.; Barnes, C. L.; Karra, S. R.; Elahmad, S. *J. Am. Chem. Soc.* **1994**, *116*, 8392−8393. (e) Maitra, U.; Potluri, V. K. *J. Org. Chem.* **2000**, *65*, 7764−7769. (f) Brown, S. P.; Schaller, T.; Seelbach, U. P.; Koziol, F.; Ochsenfeld, C.; Klärner, F.-G.; Spiess, H. W. *Angew. Chem., Int. Ed.* **2001**, *40*, 717−720. (g) Pardo, C.; Sesmilo, E.; Gutiérrez-Puebla, E.; Monge, A.; Elguero, J.; Fruchier, A. *J. Org. Chem.* **2001**, *66*, 1607−1611.

(7) Witt, D.; Lagona, J.; Damkaci, F.; Fettinger, J. C.; Isaacs, L. *Org. Lett.* **2000**, *2*, 755−758.

(8) For facial amphiphiles, see: (a) Cheng, Y.; Ho, D. M.; Gottlieb, C. R.; Kahne, D.; Bruck, M. A. *J. Am. Chem. Soc.* **1992**, *114*, 7319−7320. (b) Walker, S.; Sofia, M. J.; Kakarla, R.; Kogan. N. A.; Wierichs, L.; Longley, C. B.; Bruker, K.; Axelrod, H. R.; Midha, S.; Babu, S.; Kahne, D. *Proc. Natl. Acad. Sci. U.S.A.* **1996**, *93*, 1585−1590. (c) McQuade, D. T.; Barrett, D. G.; Desper, J. M.; Hayashi, R. K.; Gellman, S. H. *J. Am. Chem. Soc.* **1995**, *117*, 4862−4869. (d) Janout, V.; Lanier, M.; Regen, S. L. *J. Am. Chem. Soc.* **1997**, *119*, 640−647. (e) Janout, V.; Zhang, L.-H.; Staina, I. V.; Di Giorgio, C.; Regen, S. L. *J. Am. Chem. Soc.* **2001**, *123*, 5401−5406. (f) Bandyopadhyay, P.; Janout, V.; Zhang, L.-H.; Regen, S. L. *J. Am. Chem. Soc.* **2001**, *123*, 7691−7696. (g) Isaacs, L.; Witt, D.; Fettinger, J. C. *Chem. Commun.* **1999**, 2549−2550. (h) Broderick, S.; Davis, A. P.; Williams, R. P. *Tetrahedron Lett.* **1998**, *39*, 6083−6086. (i) Vandenburg, Y. R.; Smith, B. D.; Pérez-Payán, M. N.; Davis, A. P. *J. Am. Chem. Soc.* **2000**, *122*, 3252−3253. (j) Taotafa, U.; McMullin, D. B.; Lee, S. C.; Hansen, L. D.; Savage, P. B. *Org. Lett.* **2000**, *2*, 4117−4120. (k) Bharathi, P.; Zhao, H.; Thayumanavan, S. *Org. Lett.* **2001**, *3*, 1961−1964.

(9) In the crystal structure of a related C-shaped molecule[7] the distance between the tips of the aromatic rings is 7.04 Å and the angle between the aromatic rings is 18°.

(10) Burrows, S. D.; Doyle, M. L.; Murphy, K. P.; Franklin, S. G.; White, J. R.; Brooks, I.; McNulty, D. E.; Scott, M. O.; Knutson, J. R.; Porter, D.; Young, P. R.; Hensley, P. *Biochemistry* **1994**, *33*, 12741−12745.

(11) We estimate the error in the ITC derived values of ΔH and K_d to be 0.2 kcal mol^{-1} and 10%, respectively.

(12) We would have preferred to use the S-shaped diastereomer[7] of **1a** for this control experiment but it is not soluble in aqueous solution.

(13) (a) Sturtevant, J. M. *Proc. Natl. Acad. Sci. U.S.A.* **1977**, *74*, 2236−2240. (b) Murphy, K. P.; Privalov, P. L.; Gill, S. J. *Science* **1990**, *247*, 559−561. (c) Spolar, R. S.; Ha, J.-H.; Record, M. T. *Proc. Natl. Acad. Sci. U.S.A.* **1989**, *86*, 8382−8385.

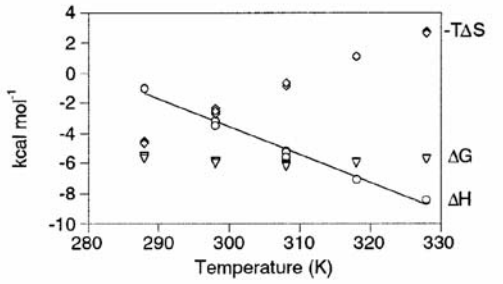

Figure 2. A plot of the ITC derived thermodynamic parameters for the formation of **1a•1a** versus temperature. ΔH (○), ΔG (▽), $-T\Delta S$ (◇).

example, ^{1}H NMR dilution experiments performed with **1a** at 55 °C in water fit well to both 2-fold and 3-fold self-association equilibrium models. To differentiate between these possibilities and provide strong evidence that **1a** undergoes controlled self-association to yield a discrete dimeric assembly in water, we turned to analytical ultracentrifugation (AUC). Sedimentation equilibrium measurements allowed a determination of the molecular weight of **1a•1a** (Figure 3) under solution-based equilibrium conditions.[14] The

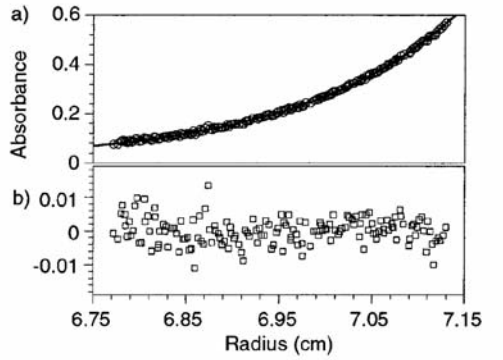

Figure 3. (a) A plot of absorbance (○) versus radius obtained for **1a** at sedimentation equilibrium. The best fit of the data to a model comprising a single homogeneous species is overlaid (—). Conditions: [**1a**] = 400 μM; 55,000 rpm; λ = 259 nm. (b) A plot of the residuals (□) versus radius for the data shown in part a.

data fit well to a model comprising a single species with a molecular weight of 1915 ± 115 (calcd MW (**1a•1a**) = 1616) with random residuals.[15] We also performed the more standard vapor pressure osmometry (VPO), gel permeation chromatography (GPC), and electrospray mass spectrometry (ES-MS) measurements. The molality of solutions of **1a** and **2a** were about half of the prepared concentrations, suggesting that **1a** and **2a** exist exclusively as the dimers **1a•1a** and **2a•2a**. In contrast, VPO showed that **3a**, which lacks a hydrophobic cleft, is monomeric in water. The ES-MS spectrum of **2a** showed the presence of [**2a•2a** − H]$^-$ and [**2a** − H]$^-$; peaks corresponding to singly or multiply charged ions of higher order aggregates were not observed. GPC measurements performed with **1a•1a** and **2a•2a** (4.1 mM) gave estimated molecular weights of 1605 and 1465, respectively. Chromatograms recorded at lower concentrations (41 μM) showed longer migration times and significant peak tailing that indicated that **1a•1a** and **2a•2a** are in equilibrium with **1a** and **2a** on the time scale of the GPC measurement. The combined inference of these four techniques provides a validation of our design hypothesis and indicates that **1a** and **2a** undergo discrete self-association processes to yield dimers.

Hydrogen bonds and metal−ligand interactions are extremely useful in self-assembly studies because they are strong and have well-defined directional preferences. Our goal is to determine similar directional preferences governing the self-association of **1a** and derivatives. Figure 4 shows

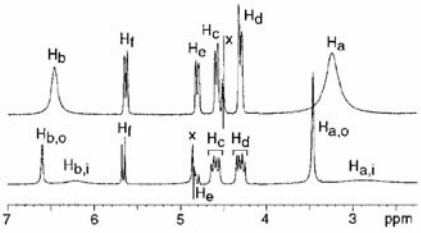

Figure 4. ^{1}H NMR spectrum of **1a** (500 MHz, 5 mM, D_2O buffer) at 324 K (top) and 294 K (bottom). The resonance marked (×) is due to incomplete suppression of residual HOD.

the ^{1}H NMR spectrum obtained for **1a•1a** at 324 and 294 K. As the temperature is decreased from 324 to 294 K, the time-averaged C_{2v} symmetry observed at higher temperature is reduced and two resonances are observed for the methoxy (H_a) and aromatic protons (H_b). We suggest that coalescence at higher temperatures results from an exchange process between protons on the inside of the aggregate ($H_{a,i}$ and $H_{b,i}$), which are upfield shifted as a result of the anisotropic effect of two aromatic rings, with those on the outside ($H_{a,o}$ and $H_{b,o}$). Although we are currently unable to determine the precise structural details of **1a•1a** because of exchange processes that are in the intermediate exchange regime on the NMR time scale, we believe that structural modifications

(14) (a) Schubert, D.; Tziatzios, C.; Schuck, P.; Schubert, U. S. *Chem. Eur. J.* **1999**, *5*, 1377−1383. (b) Laue, T. M. *Methods Enzymol.* **1995**, *259*, 427−452.

(15) We determined the density of the buffer (100 mM phosphate buffered D_2O, pD = 7.4, ρ = 1.1155 g mL^{-1}) and the partial specific volume for **1a** ($\bar{\nu}$ = 0.6137 mL g^{-1}) by making high precision density measurements on solutions of **1a** ([**1a**] = 0−10 mg mL^{-1}).

will slow the exchange processes and allow structural determinations of related dimeric aggregates.

We have presented facially amphiphilic derivatives of methylene bridged glycoluril dimers as a model system to study self-assembly in aqueous solution. This model system combines several advantageous features, namely, hydrophobically driven self-association to form tightly associated, discrete dimeric assemblies in water and sufficiently slow dynamic exchange processes that should allow for structural elucidation. We are currently studying facial amphiphiles bearing different functional groups and substitution patterns on their aromatic rings with the goal of determining the structural details and thermodynamic parameters for a series of related dimeric aggregates. By identifying trends in the structural and thermodynamic properties of this series of aggregates we plan to deduce some of the rules governing their self-association, which hopefully will be broadly applicable to other hydrophobically driven self-assembly processes.

Acknowledgment. We thank the University of Maryland, the donors of the Petroleum Research Fund, administered by the American Chemical Society (PRF 33946-G4), and the National Institutes of Health (GM61854) for generous financial support. We thank Professors Dorothy Beckett and Sandra Greer for access to the isothermal titration calorimeter and the density meter, respectively. L.I. is a Cottrell Scholar of Research Corporation.

Supporting Information Available: Experimental procedures and spectral data for **1a**−**3a** and representative data from the VPO, ES-MS, GPC, ITC, ^{1}H NMR, and AUC experiments. This material is available free of charge via the Internet at http://pubs.acs.org.

OL016561S

J|A|C|S
ARTICLES
Published on Web 06/14/2002

Diastereoselective Formation of Glycoluril Dimers: Isomerization Mechanism and Implications for Cucurbit[*n*]uril Synthesis

Arindam Chakraborty,[†] Anxin Wu,[†,‡] Dariusz Witt,[†,§] Jason Lagona,[†] James C. Fettinger,[†] and Lyle Isaacs*[,†]

Contribution from the Department of Chemistry and Biochemistry, University of Maryland, College Park, College Park, Maryland 20742, and National Laboratory of Applied Organic Chemistry, Lanzhou University, Lanzhou 730000, P. R. China

Received February 8, 2002

Abstract: Cucurbit[6]uril (**CB**[6]) is a macrocyclic compound, prepared in one pot from glycoluril and formaldehyde, whose molecular recognition properties have made it the object of intense study. Studies of the mechanism of **CB**[*n*] formation, which might provide insights that allow the tailor-made synthesis of **CB**[*n*] homologues and derivatives, have been hampered by the complex structure of **CB**[*n*]. By reducing the complexity of the reaction to the formation of S-shaped (**12*S*−18*S***) and C-shaped (**12*C*−18*C***) methylene bridged glycoluril dimers, we have been able to probe the fundamental steps of the mechanism of **CB**[*n*] synthesis to a level that has not been possible previously. For example, we present strong evidence that the mechanism of **CB**[*n*] synthesis proceeds via the intermediacy of both S-shaped and C-shaped dimers. The first experimental determination of the relative free energies of the S-shaped and C-shaped dimers indicates a thermodynamic preference (1.55−3.25 kcal mol^{-1}) for the C-shaped diastereomer. This thermodynamic preference is not because of self-association, solvation, or template effects. Furthermore, labeling experiments have allowed us to elucidate the mechanism of this acid-catalyzed equilibrium between the S-shaped and C-shaped diastereomers. The equilibration is an intramolecular process that proceeds with high diastereoselectivity and retention of configuration. On the basis of the broad implications of these results for **CB**[*n*] synthesis, we suggest new synthetic strategies that may allow for the improved preparation of **CB**[*n*] ($n > 8$) and **CB**[*n*] derivatives from functionalized glycolurils.

Introduction

In 1905, Behrend reported that the condensation reaction of glycoluril (**1a**) and formaldehyde in concentrated HCl yields an insoluble polymeric material.[1] To make the material more tractable, it was dissolved in concentrated sulfuric acid from which a crystalline substance could be obtained. In 1981, Mock et al.[2] reinvestigated Behrend's original report and discovered that the product of this reaction was cucurbituril, **CB**[6],[3] a remarkable macrocyclic compound comprising six glycoluril rings and 12 methylene bridges (Chart 1). In their syntheses of **CB**[6], neither Behrend nor Mock detected the presence of macrocyclic compounds comprising five, seven, or eight glycoluril rings (**CB**[5], **CB**[7], **CB**[8]). This result, when coupled with the high yield (82%) synthesis of **CB**[6] disclosed by Buschmann, suggested that the formation of **CB**[6] was governed by a thermodynamic preference for **CB**[6].[4] The first successful synthesis of an analogue of **CB**[6] was described by

Chart 1

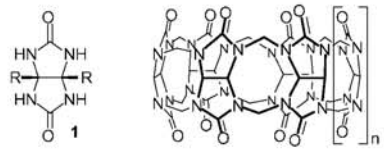

1a R = H
1b R = Me
1c R,R = $(CH_2)_4$
1d R = Ph
1e R = CO_2Et

CB[5] (n = 0)
CB[6] (n = 1)
CB[7] (n = 2)
CB[8] (n = 3)
CB[10] (n = 5)

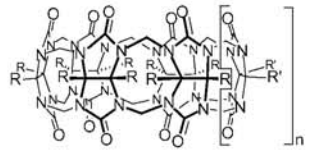

Me_{10}**CB**[5] (R = R' = Me, n = 0)
Cy_5**CB**[5] (R,R = R',R' = $(CH_2)_4$, n = 0)
Cy_6**CB**[6] (R,R = R',R' = $(CH_2)_4$, n = 1)
Ph_2**CB**[6] (R = H, R' = Ph, n=1)

* To whom correspondence should be addressed. E-mail: LI8@umail.umd.edu.
† University of Maryland.
‡ Lanzhou University.
§ Current address: Chemical Faculty, Technical University of Gdansk, Narutowicza 11/12, 80-952 Gdansk, Poland.

(1) Behrend, R.; Meyer, E.; Rusche, F. *Liebigs Ann. Chem.* **1905**, *339*, 1−37.
(2) Freeman, W. A.; Mock, W. L.; Shih, N. Y. *J. Am. Chem. Soc.* **1981**, *103*, 7367−8.
(3) Kim, J.; Jung, I.-S.; Kim, S.-Y.; Lee, E.; Kang, J.-K.; Sakamoto, S.; Yamaguchi, K.; Kim, K. *J. Am. Chem. Soc.* **2000**, *122*, 540−541.

10.1021/ja025876f CCC: $22.00

Stoddart who found that the condensation reaction between dimethylglycoluril **1b** and formaldehyde gives rise to cyclic pentameric Me_{10}**CB**[5].[5] Again, cyclic oligomers containing larger or smaller numbers of equivalents of **1b** were not detected. The belief that only a single cyclic oligomer would be accessible by the acid-catalyzed condensation reaction gained further acceptance following the suggestion by Cintas that "glycoluril directs the formation of the product and participates in the macroscopic geometry, although in this case, the template is an integral part of the structure it helps to form."[6] Since 1981, the outstanding molecular recognition properties of **CB**[6] have been described in numerous reports from the groups of Mock,[7] Buschmann,[8] Kim,[9] and others.[10−16] In light of the wide range of recognition properties of **CB**[6], many researchers have been interested in preparing derivatives of cucurbituril comprising different numbers of glycoluril rings, containing complex functional groups on their convex face, and whose methylene bridges are functionalized. Success in these endeavors has recently started to appear in the literature.[3,17−23]

Concurrent with our preliminary report[24] on the diastereoselective formation of methylene bridged glycoluril dimers, the groups of Kim[3,21] and Day[17−19] reported the preparation and characterization of homologues of cucurbituril containing five, seven, eight, and 10 glycoluril rings (**CB**[5], **CB**[7], **CB**[8], and **CB**[10]) under strongly acidic conditions (concentrated mineral acids) at moderate temperatures (75−100 °C). Kim recently extended the family of **CB**[*n*] to include Cy_5**CB**[5] and Cy_6**CB**[6] by the use of **1c** in the condensation process,[22] and Nakamura was able to isolate the partially substituted Ph_2**CB**[6].[23] These new **CB**[*n*]s possess remarkable molecular recognition properties[12,25−27] that have resulted in the synthesis of molecular Russian dolls,[28] ball bearings,[20] gyroscopes,[17] allowed the selective recognition of a charge-transfer complex,[29] and the catalysis of a [2 + 2] photoreaction.[30] Clearly, these synthetic and mechanistic studies are expanding the range of **CB**[*n*] derivatives that can be accessed and are beginning to define the scope and limitations of the cucurbituril synthesis.

The current state-of-the-art concerning the mechanism of **CB**[*n*] synthesis outlined in Scheme 1 largely follows the suggestions of Day et al.[18] The initial condensation of glycoluril with formaldehyde most likely yields a diastereomeric mixture of methylene bridged glycoluril dimers (**2*S*** and **2*C***).[24,31] We refer to these molecules as S-shaped and C-shaped, respectively, because three-dimensional depictions of these molecules resemble those letters (Chart 2). Depending on the specific conditions of the reaction, **2*S*** and **2*C*** may either equilibrate with one another or undergo further oligomerization to yield a diastereomeric mixture (**3**) of glycoluril derivatives with both S- and C-shaped methylene bridged glycoluril dimer substructures. This material, presumably related to Behrend's polymer, must now undergo equilibration to afford oligomers (**4** and **5**) containing stretches of methylene bridged dimers with the all C-shaped relative stereochemistry. This equilibration reaction

(4) Buschmann, H.-J.; Fink, H.; Schollmeyer, E. Preparation of Cucurbituril. German Patent DE 196 03 377 A1, 1997.
(5) Flinn, A.; Hough, G. C.; Stoddart, J. F.; Williams, D. J. *Angew. Chem., Int. Ed. Engl.* **1992**, *31*, 1475−1477.
(6) Cintas, P. *J. Inclusion Phenom. Mol. Recognit. Chem.* **1994**, *17*, 205−20.
(7) Mock, W. L.; Shih, N. Y. *J. Org. Chem.* **1983**, *48*, 3618−3819. Mock, W. L.; Irra, T. A.; Wepsiec, J. P.; Manimaran, T. L. *J. Org. Chem.* **1983**, *48*, 3619−3620. Mock, W. L.; Shih, N. Y. *J. Org. Chem.* **1986**, *51*, 4440−4446. Mock, W. L.; Shih, N. Y. *J. Am. Chem. Soc.* **1988**, *110*, 4706−4710. Mock, W. L.; Irra, T. A.; Wepsiec, J. P.; Adhya, M. *J. Org. Chem.* **1989**, *54*, 5302−5308. Mock, W. L.; Shih, N. Y. *J. Am. Chem. Soc.* **1989**, *111*, 2697−2699. Mock, W. L.; Pierpont, J. *J. Chem. Soc., Chem. Commun.* **1990**, 1509−1511.
(8) Buschmann, H. J.; Cleve, E.; Schollmeyer, E. *Inorg. Chim. Acta* **1992**, *193*, 93−97. Buschmann, H. J.; Schollmeyer, E. *Textilveredlung* **1993**, *28*, 182−184. Buschmann, H. J.; Schollmeyer, E. *J. Inclusion Phenom. Mol. Recognit. Chem.* **1997**, *29*, 167−174. Meschke, C.; Buschmann, H. J.; Schollmeyer, E. *Thermochim. Acta* **1997**, *297*, 43−48. Buschmann, H. J.; Jansen, K.; Schollmeyer, E. *Thermochim. Acta* **1998**, *317*, 95−98. Buschmann, H. J.; Jansen, K.; Meschke, C.; Schollmeyer, E. *J. Solution Chem.* **1998**, *27*, 135−140. Buschmann, H. J.; Jansen, K.; Schollmeyer, E. *J. Inclusion Phenom. Macrocyclic Chem.* **2000**, *37*, 231−236. Buschmann, H. J.; Jansen, K.; Schollmeyer, E. *Thermochim. Acta* **2000**, *346*, 33−36. Buschmann, H. J.; Cleve, E.; Jansen, K.; Wego, A.; Schollmeyer, E. *J. Inclusion Phenom. Macrocyclic Chem.* **2001**, *40*, 117−120. Buschmann, H. J.; Cleve, E.; Jansen, K.; Schollmeyer, E. *Anal. Chim. Acta* **2001**, *437*, 157−163. Jansen, K.; Buschmann, H. J.; Wego, A.; Dopp, D.; Mayer, C.; Drexler, H. J.; Holdt, H. J.; Schollmeyer, E. *J. Inclusion Phenom. Macrocyclic Chem.* **2001**, *39*, 357−363.
(9) Kim, H.-J.; Jeon, Y.-M.; Kim, J.; Whang, D.; Kim, K. *J. Am. Chem. Soc.* **1996**, *118*, 9790−9791. Whang, D.; Heo, J.; Park, J. H.; Kim, K. *Angew. Chem., Int. Ed.* **1998**, *37*, 78−80. Whang, D.; Park, K.-M.; Heo, J.; Ashton, P.; Kim, K. *J. Am. Chem. Soc.* **1998**, *120*, 4899−4900. Whang, D.; Jeon, Y.-M.; Heo, J.; Kim, K. *J. Am. Chem. Soc.* **1996**, *118*, 11333−11334. Roh, S.-G.; Park, K.-M.; Park, G.-J.; Sakamoto, S.; Yamaguchi, K.; Kim, K. *Angew. Chem., Int. Ed.* **1999**, *38*, 638−641. Park, K.-M.; Whang, D.; Lee, E.; Heo, J.; Kim, K. *Chem.-Eur. J.* **2002**, *8*, 498−508. Lee, J. W.; Ko, Y. H.; Park, S.-H.; Yamaguchi, K.; Kim, K. *Angew. Chem., Int. Ed.* **2001**, *40*, 746−749. Lee, E.; Heo, J.; Kim, K. *Angew. Chem., Int. Ed.* **2000**, *39*, 2699−2701. Kim, S.-Y.; Jung, I.-S.; Lee, E.; Kim, J.; Sakamoto, S.; Yamaguchi, K.; Kim, K. *Angew. Chem., Int. Ed.* **2001**, *40*, 2119−2121. Isobe, H.; Tomita, N.; Lee, J. W.; Kim, H.-J.; Kim, K.; Nakamura, E. *Angew. Chem., Int. Ed.* **2000**, *39*, 4257−4260. El Haouaj, M.; Luhmer, M.; Ko, Y. H.; Kim, K.; Bartik, K. *J. Chem. Soc., Perkin Trans. 2* **2001**, 804−807; El Haouaj, M.; Young, H. K.; Luhmer, M.; Kim, K.; Bartik, K. *J. Chem. Soc., Perkin Trans. 2* **2001**, 2104−2107.
(10) Karcher, S.; Kornmuller, A.; Jekel, M. *Water Sci. Technol.* **1999**, *40*, 425−433. Karcher, S.; Kornmueller, A.; Jekel, M. *Acta Hydrochim. Hydrobiol.* **1999**, *27*, 38−42. Karcher, S.; Kornmuller, A.; Jekel, M. *Water Res.* **2001**, *35*, 3309−3316.
(11) Sokolov, M. N.; Virovets, A. V.; Dybtsev, D. N.; Gerasko, O. A.; Fedin, V. P.; Hernandez-Molina, R.; Clegg, W.; Sykes, A. G. *Angew. Chem., Int. Ed.* **2000**, *39*, 1659−1661. Fedin, V. P.; Sokolov, M.; Lamprecht, G. J.; Hernandez-Molina, R.; Seo, M.-S.; Virovets, A. V.; Clegg, W.; Sykes, A. G. *Inorg. Chem.* **2001**, *40*, 6598−6603. Fedin, V. P.; Gramlich, V.; Woerle, M.; Weber, T. *Inorg. Chem.* **2001**, *40*, 1074−1077. Sokolov, M. N.; Virovets, A. V.; Dybtsev, D. N.; Chubarova, E. V.; Fedin, V. P.; Fenske, D. *Inorg. Chem.* **2001**, *40*, 4816−4817.
(12) Marquez, C.; Nau, W. M. *Angew. Chem., Int. Ed.* **2001**, *40*, 4387−4390. Marquez, C.; Nau, W. M. *Angew. Chem., Int. Ed.* **2001**, *40*, 3155−3160.
(13) Tuncel, D.; Steinke, J. H. G. *Chem. Commun.* **1999**, 1509−1510. Tuncel, D.; Steinke, J. H. G. *Chem. Commun.* **2001**, 253−254. Krasia, T. C.; Steinke, J. H. G. *Chem. Commun.* **2002**, 22−23.
(14) Hoffmann, R.; Knoche, W.; Fenn, C.; Buschmann, H.-J. *J. Chem. Soc., Faraday Trans.* **1994**, *90*, 1507−1511. Neugebauer, R.; Knoche, W. *J. Chem. Soc., Perkin Trans. 2* **1998**, 529−534.
(15) Wagner, B. D.; MacRae, A. I. *J. Phys. Chem. B* **1999**, *103*, 10114−10119. Wagner, B. D.; Fitzpatrick, S. J.; Gill, M. A.; MacRae, A. I.; Stojanovic, N. *Can. J. Chem.* **2001**, *79*, 1101−1104.
(16) Zhang, X. X.; Krakowiak, K. E.; Xue, G.; Bradshaw, J. S.; Izatt, R. M. *Ind. Eng. Chem. Res.* **2000**, *39*, 3516−3520.
(17) Day, A. I.; Blanch, R. J.; Arnold, A. P.; Lorenzo, S.; Lewis, G. R.; Dance, I. *Angew. Chem., Int. Ed.* **2002**, *41*, 275−277.
(18) Day, A.; Arnold, A. P.; Blanch, R. J.; Snushall, B. *J. Org. Chem.* **2001**, *66*, 8094−8100.
(19) Day, A. I.; Arnold, A. P.; Blanch, R. J. Method for Synthesis Cucurbiturils. PCT Intl. Appl. PCT/AU00/00412, 2000.
(20) Blanch, R. J.; Sleeman, A. J.; White, T. J.; Arnold, A. P.; Day, A. I. *Nano Lett.* **2002**, *2*, 147−149.
(21) Kim, K.; Kim, J.; Jung, I.-S.; Kim, S.-Y.; Lee, E.; Kang, J.-K. Cucurbituril Derivatives, Their Preparation and Uses. European Patent Appl. EP 1 094 065 A2, 2001.
(22) Zhao, J.; Kim, H.-J.; Oh, J.; Kim, S.-Y.; Lee, J. W.; Sakamoto, S.; Yamaguchi, K.; Kim, K. *Angew. Chem., Int. Ed.* **2001**, *40*, 4233−4235.
(23) Isobe, H.; Sato, S.; Nakamura, E. *Org. Lett.* **2002**, *4*, 1287−1289. For another report of partially substituted CB[*n*], see ref 19.
(24) Witt, D.; Lagona, J.; Damkaci, F.; Fettinger, J. C.; Isaacs, L. *Org. Lett.* **2000**, *2*, 755−758.
(25) Kim, H.-J.; Jeon, W. S.; Ko, Y. H.; Kim, K. *Proc. Natl. Acad. Sci. U.S.A.* **2002**, *99*, 5007−5011.
(26) Ong, W.; Gómez-Kaifer, M.; Kaifer, A. E. *Org. Lett.* **2002**, *4*, ASAP.
(27) Lorenzo, S.; Day, A.; Craig, D.; Blanch, R.; Arnold, A.; Dance, I. *CrystEngComm* **2001**, *49*, 1−7.
(28) Kim, S.-Y.; Jung, I.-S.; Lee, E.; Kim, J.; Sakamoto, S.; Yamaguchi, K.; Kim, K. *Angew. Chem., Int. Ed.* **2001**, *40*, 2119−2121.
(29) Kim, H. J.; Heo, J.; Jeon, W. S.; Lee, E.; Kim, J.; Sakamoto, S.; Yamaguchi, K.; Kim, K. *Angew. Chem., Int. Ed.* **2001**, *40*, 1526−1529.
(30) Jon, S. Y.; Ko, Y. H.; Park, S. H.; Kim, H.-J.; Kim, K. *Chem. Commun.* **2001**, 1938−1939.
(31) Wu, A.; Chakraborty, A.; Witt, D.; Lagona, J.; Damkaci, F.; Ofori, M.; Chiles, K.; Fettinger, J. C.; Isaacs, L. *J. Org. Chem.* **2002**, *67*, in press.

Scheme 1. Current Mechanistic Understanding of **CB**[*n*] Formation[a]

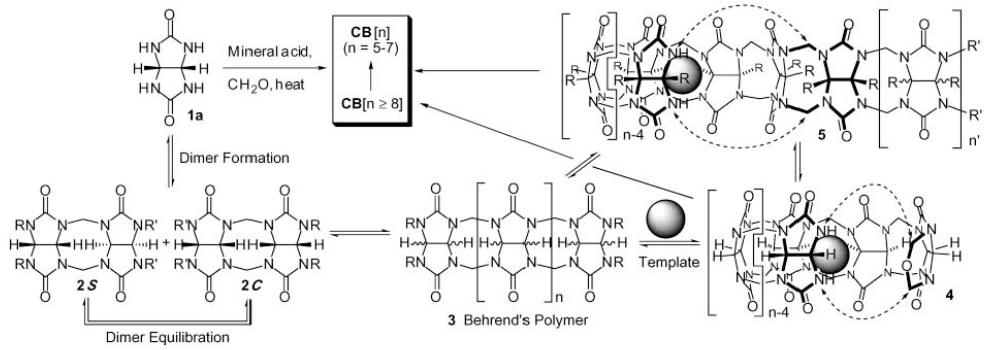

[a] The dashed arrows indicate C−N bonds that need to be formed to yield **CB**[*n*].

may, or may not, be influenced by the presence of appropriate templating molecules in the reaction medium. Day recently reported modest effects of acid type, acid concentration, reactant concentration, temperature, templating molecules, anions, and cations on the distribution of **CB**[*n*] obtained in the condensation reaction.[18,19] These oligomeric intermediates, **4** and **5**, then undergo cyclization reactions to enter the **CB**[*n*] manifold. Day also demonstrated, by elegant product resubmission experiments, that within the **CB**[*n*] manifold pure **CB**[8] is converted under the reaction conditions (concentrated HCl, 100 °C) to **CB**[5], **CB**[6], and **CB**[7], but that **CB**[5], **CB**[6], and **CB**[7] are stable under these conditions.[18]

The complexity associated with the **CB**[*n*] synthesis − formation of *n* rings, 2*n* methylene bridges, with complete control over the relative stereochemistry of *n* glycoluril rings − has frustrated experimental attempts to (1) obtain proof of the intermediacy of glycoluril dimers with the relative stereochemistry exemplified by **2*S***, (2) assess the relative thermodynamic stability of **2*S*** and **2*C***, and (3) elucidate the mechanism for the interconversion of **2*S*** and **2*C***. Our approach to the synthesis of analogues of **CB**[6] and other glycoluril derivatives with interesting molecular recognition properties[32,33] relies on the identification of the methylene bridged glycoluril dimer substructure (**2*C***) as the fundamental building block of **CB**[*n*]. Previously, we described three complementary synthetic methods that allow for the efficient synthesis of methylene bridged glycoluril dimers bearing two *o*-xylylene substituents (Chart 2). As a result of this synthetic simplification, the complexity of the reaction − the formation of one ring, two methylene bridges, and control over the relative stereochemistry of two glycoluril rings − was substantially reduced relative to the synthesis of **CB**[*n*]. As a result, we have been able to address several key mechanistic questions that have been elusive in the chemistry of **CB**[*n*] itself. In this paper, we discuss (1) the kinetic (S- and C-shaped) and thermodynamic (C-shaped) products of the dimerization reaction, (2) the ratio of the S- and C-shaped methylene bridged glycoluril dimers under equilibrium conditions, (3) potential sources of the observed preference for the C-shaped diastereomer, and (4) the mechanism of the isomerization of the S- to the C-shaped dimers. Last, we discuss the implication of these results for the synthesis of new derivatives of cucurbituril.

(32) Isaacs, L.; Witt, D. *Angew. Chem., Int. Ed.* **2002**, *41*, 1905−1907.
(33) Isaacs, L.; Witt, D.; Lagona, J. *Org. Lett.* **2001**, *3*, 3221−3224.

Results and Discussion

Previously, we reported the synthesis of a wide variety of C-shaped and S-shaped methylene bridged glycoluril dimers.[31] Chart 2 shows the structures of the compounds that we discuss in this paper. The reaction between glycoluril derivatives **6** and **7** should give rise to roughly equal amounts of S- and C-shaped methylene bridged glycoluril dimers, because the first bond-forming (stereochemical determining) step is unlikely to be highly diastereoselective.[31] We were surprised, therefore, that condensation reactions typically produced the C-shaped dimers in modest to high diastereoselectivity after 24 h.

Kinetic Formation of a Mixture of C-Shaped and S-Shaped Methylene Bridged Glycoluril Dimers. The diastereoselective formation of C-shaped methylene bridged glycoluril dimers, typified by **8*C***, suggested that thermodynamic preferences were playing a major role in the outcome of the reactions. We hypothesized that both the S- and the C-shaped diastereomers were kinetic products that were transformed into the C-shaped diastereomers under thermodynamically controlled conditions. To test this hypothesis, we performed dimerization reactions at lower temperatures and/or with shorter reaction times (Scheme 2). We choose these dimerization reactions because they represent the three different synthetic methods that we have developed and because we were not able to isolate the S-shaped diastereomers when the reactions were run to completion.[31] Gratifyingly, we found that compound **6** yields a mixture of **7e** (51%), **8*C*** (37%), and **8*S*** (7%) when the dimerization reaction is run for only 14 h; **8*C*** is formed in 88% yield as the only isolable product when the reaction is run to completion. Cyclic ether **19**, for example, is transformed into a 2:3 mixture of **12*S*** and **12*C*** when the reaction is run to 59% conversion. In contrast, **12*C*** was obtained in 87% yield to the exclusion of **12*S*** when the reaction is run to completion. Similarly, ureidyl NH compound **20** gave a mixture of cyclic ether **21** (15%), **13*S*** (7%), and **13*C*** (44%) under milder conditions. The heterodimerization reaction between (±)-**22** and cyclic ether (±)-**23** was also successful; we were able to isolate **14*ST*** (7%), (±)-**14*SC*** (6%), (±)-**14*CT*** (12%), and **14*CC*** (18%) in addition to unreacted starting materials. The *ST*, *SC*, *CT*, and *CC* descriptors denote the overall shape of the molecule (S-shaped

Chart 2. Methylene Bridged Glycoluril Dimers

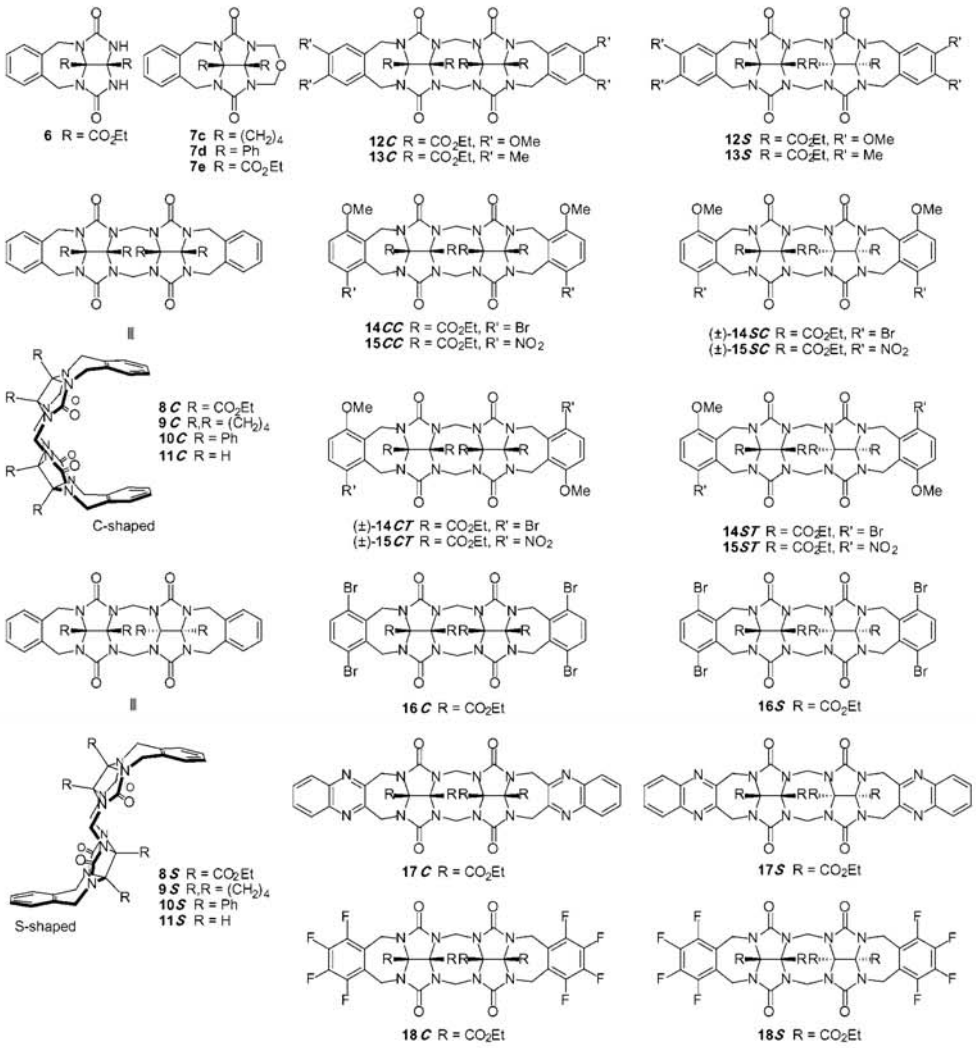

or *C*-shaped) and the relative location of the methoxy substituents (cis or trans). A similar reaction with (±)-**22** only yielded the C-shaped compounds (±)-**14*CT*** (48%) and **14*CC*** (46%).[31] These results allow us to conclude that both the C-shaped and the S-shaped diastereomers are kinetic products of the reaction, formed in comparable amounts, whereas the C-shaped diastereomers are the thermodynamic products of the reaction. These results provide strong evidence for the formation of S- and C-shaped methylene bridged glycoluril dimers, **2*S*** and **2*C***, in condensation reactions with formaldehyde and provide experimental support for the suggestion by Day et al.[18] that S-shaped intermediates initially form in the synthesis of **CB**[*n*].

Equilibration of S-Shaped and C-Shaped Diastereomers and Determination of Their Relative Free Energies. The previous section demonstrates that both the C- and the S-shaped diastereomers are kinetic products and that the C-shaped diastereomer is the thermodynamic product. Those results do not, however, allow us to conclude that these reactions have reached thermodynamic equilibrium or to assess the relative free energies of the C- and S-shaped diastereomers. To address these questions, we used the pure C-shaped and S-shaped diastereomers of six different symmetrical homodimers and separately resubmitted them to the reaction conditions (Table 1). If each set of equilibration reactions gives the same C:S ratio, then we can conclude that equilibrium has been reached and calculate a value of ΔG. Table 1 shows that similar C:S ratios were achieved in the majority of cases. Quinoxaline derivatives **17*C*** and **17*S*** did not interconvert under the reaction conditions implying that the ~2:1 ratio of **17*C***:**17*S*** obtained in their synthesis represents a slight kinetic preference for **17*C***. We attribute the lack of isomerization to preferential protonation of the quinoxaline N-atoms which competes with the protonation of the ureidyl O-atoms required for isomerization. The values of ΔG under the reaction conditions (83 °C) range from −1.55

Scheme 2. Formation of S-Shaped Compounds under Kinetically Controlled Conditions

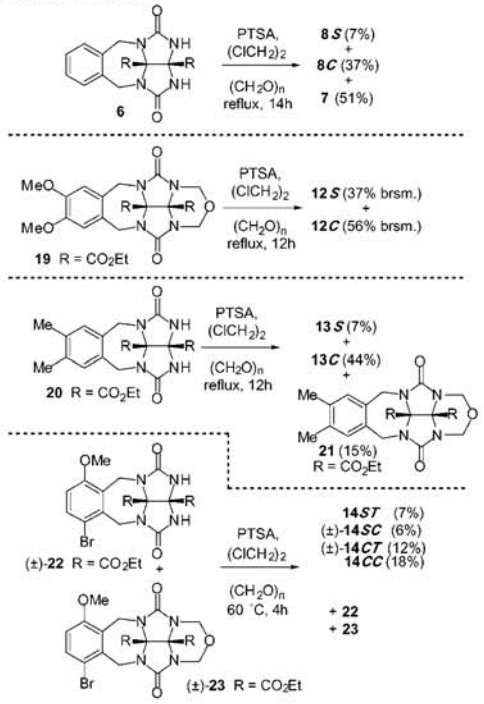

Table 1. Equilibration of C- and S-Shaped Compounds[a]

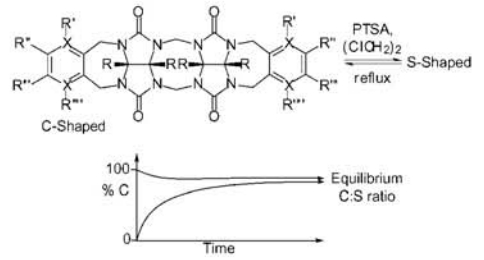

starting material	*C* → *C* + *S* *C*:*S*	*S* → *C* + *S* *C*:*S*	Δ*G* (kcal mol^{-1})
8	98:2	96:4	−2.25 to −2.75
12	98:2	98:2	~ −2.75
13	98:2	97:3	−2.46 to −2.75
16	95:5	90:10	−1.55 to −2.15
17	100:0	0:100	n.e.
18	99:1	98:2	−2.75 to −3.25

[a] n.e. = no equilibration.

to −3.25 kcal mol^{-1}. The values of Δ*G* obtained here represent the first experimental determinations of differences in free energy between S- and C-shaped glycoluril dimers; these values are of fundamental importance toward the synthesis of **CB**[*n*] and derivatives. These results suggest that it is the intrinsic preference of the methylene bridged glycoluril dimer substructure to adopt the C-shaped form that drives the formation of **CB**[*n*]. It is not necessary, although plausible, to postulate the participation of components of the reaction mixture (glycoluril, water, salts, or acid) as reaction templates to explain the formation of **CB**[*n*] (Scheme 1). A simple calculation, ignoring entropic and enhanced enthalpic contributions in the macrocyclization reaction, suggests that in a worst case scenario (**16*C***:**16*S*** = 90:10, Δ*G* = −1.55 kcal mol^{-1}) 53% ((0.9)^6) of linear glycoluril hexamers would adopt the all C shape needed for **CB**[6] formation.

Table 2. Solvent Effects on the **16*C*:16*S*** Ratio[a]

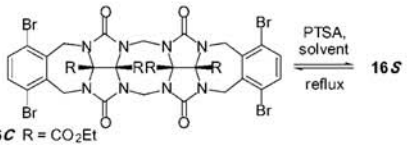

solvent	*C* → *C* + *S* **16*C*:16*S***	*S* → *C* + *S* **16*C*:16*S***	ΔΔ*G* (kcal mol^{-1})
$CHCl_3$	94:6	94:6	−1.83
CCl_4	99:1	97:3	−2.41 to −3.19
C_6F_6	99:1	97:3	−2.44 to −3.22
THF	100[b]:0	dec	n.d.
CH_3CN	100[b]:0	98.2	> −2.62
$ClCH_2CH_2Cl$	95:5	90:10	−1.55 to −2.15
CH_3NO_2	90:10	89:11	−1.55 to −1.63
$MeOCH_2CH_2OMe$	97:3	dec	n.d.

[a] n.d. = not determined. [b] S-shaped compound not detected. dec = decomposed.

Solvent Effects on the C:S Equilibrium. In an attempt to address the factors that influence the relative stability of the C- and S-shaped diastereomers, we performed the isomerization reactions of **16*C*** and **16*S*** in a variety of different solvents (Table 2). We hypothesized that different solvents might preferentially solvate either the C-shaped or the S-shaped compounds and thereby influence the C:S ratio at thermodynamic equilibrium. Alternatively, because the S-shaped and C-shaped compounds have different dipole moments, simple changes in the dielectric constant of the medium might influence their ratio at equilibrium. We choose **16*C*** and **16*S*** because it was straightforward to prepare sizable quantities of both diastereomers and because the C:S ratio determined in 1,2-dichloroethane would allow us to observe both increases and decreases in the equilibrium ratio. We were unable to study this equilibrium in solvents that undergo destructive side reactions with the iminium ion intermediates (e.g., C_6H_6). Table 2 shows the results of separate equilibration experiments that we performed in eight different solvents; these solvents range in boiling point from 61 °C ($CHCl_3$) to 101.2 °C (CH_3NO_2), have dielectric constants that range from 2.05 (C_6F_6) to 37.5 (CH_3CN), and display a range of sizes, shapes, and functional groups.[34,35] As can be seen from Table 2, the effects are neither large, nor do they follow trends based upon the dielectric constant. For example, the smallest **16*C***:**16*S*** ratio (90:10) was observed in CH_3NO_2 (ϵ = 35.9), whereas in CH_3CN (ϵ = 37.5), one of the largest ratios (98:2) was observed. Although we did not observe any dramatic effects attributable to differences in solvation in the solvents studied, we note that the two solvents with the highest **16*C***:**16*S*** ratios

(34) Laurence, C.; Nicolet, P.; Dalati, M. T.; Abboud, J.-L. M.; Notario, R. *J. Phys. Chem.* **1994**, *98*, 5807−5816.
(35) Vogel, A. I.; Furniss, B. S.; Hannaford, A. J.; Smith, P. W. G.; Tatchell, A. R. *Vogel's Textbook of Practical Organic Chemistry*, 5th ed.; Longman Scientific & Technical: Essex, U.K., 1989.

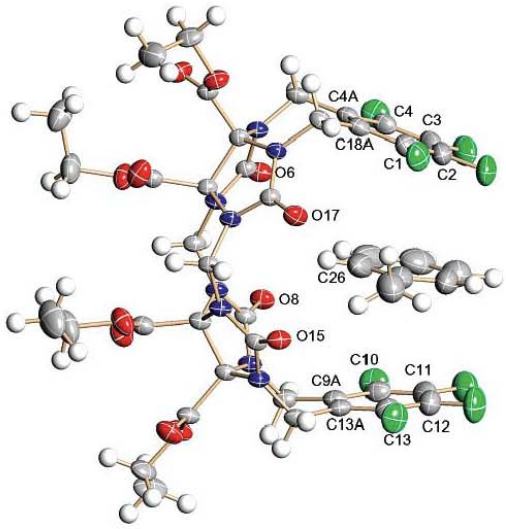

Figure 1. X-ray crystal structure of **18*C*** as the toluene solvate.

($C_6F_6$and CH_3CN) are those that we would expect to bind within the cleft of **16*C***.[31]

The X-ray crystal structure of **18*C*** (Figure 1) was obtained as the toluene solvate and depicts one possible orientation of an aromatic solvent within the cleft defined by the two tetrafluorophenyl rings. The distance between the tips of the aromatic rings, defined as the distance between the C2−C3 and C11−C12 centroids, is 6.786 Å, which represents a nearly ideal spacing for complexation of an aromatic ring. The distance between the centroids of the two tetrafluorophenyl rings is 7.228 Å. The solvating toluene assumes an offset stacked arrangement with respect to the tetrafluorophenyl rings. It is twisted by approximately 30° with respect to the tetrafluorophenyl rings; the dihedral angles from C26 through the centroids of the toluene ring, the tetrafluorophenyl ring, and the centroids of the C4A−C18A and C9A−C13A bonds amount to 2.0° and −4.9°, respectively. The molecule exhibits a slight end-to-end twist of −3.0° as defined by the dihedral angle through the centroids of the C2−C3, C4A−C18A, C9A−C13A, and C11−C12 bonds. The distances between the carbonyl oxygens of each glycoluril ring, O8−O15 and O6−O17, amount to 5.918 and 5.889 Å, respectively, values slightly smaller than those observed for **CB**[6] (5.98−6.042 Å).[2]

Self-Association Is Not the Cause of Enhanced C:S Ratios. One possible explanation for the relatively large C:S ratios is self-association. Nolte has observed a tendency for related molecules to dimerize in $CHCl_3$ and water, and we have observed strong self-association for our C-shaped molecules in water.[32,33,36−39] Self-association of the C-shaped compounds would sequester them as the dimers resulting in a shift in the equilibrium toward the C-shaped form. Such an equilibrium shift would, of course, be sensitive to concentration, solvent, temperature, and self-association constant (K_s). At the concentrations at which we perform the condensation reaction − up to 100 mM, but more typically 20 mM − relatively large values of K_s (>100 M^{-1}) would be required to drive the equilibrium. To test for self-association, we performed a dilution experiment with **12*C*** in $ClCD_2CD_2Cl$ ([**12*C***] = 200 μM to 100 mM, 298 K). We did not observe any changes in chemical shift over this concentration range, which implies that self-association is negligible for **12*C***.[40] It is unlikely, therefore, that the diastereoselective formation of the C-shaped compounds is due to self-association.

Templation of the C-Shaped Diastereomer by *p*-Toluenesulfonic Acid Is Not the Cause of Enhanced C:S Ratios. Another potential cause of the large preference for the C-shaped diastereomers is the templation of the C-shaped compounds by a molecule of PTSA. Binding of PTSA within the C-shaped cavity would result in a shift in the C to S equilibrium in favor of the C-shaped compound. A typical dimerization reaction − the formation of **12*C*** for example − results in a solution with [**12*C***] = 20 mM and [PTSA] = 100 mM. For PTSA to bind to and thereby template at least 90% of the molecules of **12*C***, a binding constant of K_a > 109 M^{-1} would be required. To test for the possibility that PTSA is acting as a template in this reaction, we performed a titration experiment with **12*C*** and PTSA in $ClCD_2CD_2Cl$ ([**12*C***] = 20 mM, [PTSA] = 0−100 mM, 70 °C). We did not observe changes in chemical shift of the aromatic protons of **12*C*** suggesting that PTSA does not bind within the cavity of **12*C*** under these conditions.[41] It is unlikely, therefore, that the diastereoselective formation of the C-shaped compounds is due to PTSA acting as a template.

AM1 Calculations Reveal a Thermodynamic Preference for the C-Shaped Diastereomer. Having excluded many of the plausible experimental causes of the diastereoselective formation of C-shaped methylene bridged glycoluril dimers, we considered the possibility that the C-shaped diastereomers are simply thermodynamically more stable than the S-shaped diastereomers. For this purpose, we decided to compute the relative heats of formation of the C-shaped and S-shaped diastereomers (Table 3).[18] Table 3 shows AM1 computational results of the heats of formation of **8**−**11**. These computations suggest a small (0.5 kcal mol^{-1}) to a quite large difference (−10.2 kcal mol^{-1}) in the heat of formation between the S- and C-shaped diastereomers. In particular, the difference calculated for ethoxycarbonyl substituted **8** (−10.2 kcal mol^{-1}) is significantly larger than the experimental value (−2.25 to −2.75 kcal mol^{-1}) determined by equilibration studies in $ClCH_2$-CH_2Cl described above. Given the large differences in the heats

(36) Holder, S. J.; Elemans, J. A. A. W.; Donners, J. J. J. M.; Boerakker, M. J.; de Gelder, R.; Barbera, J.; Rowan, A. E.; Nolte, R. J. M. *J. Org. Chem.* **2001**, *66*, 391−399.
(37) Rowan, A. E.; Elemans, J. A. A. W.; Nolte, R. J. M. *Acc. Chem. Res.* **1999**, *32*, 995−1006.
(38) Elemans, J. A. A. W.; de Gelder, R.; Rowan, A. E.; Nolte, R. J. M. *Chem. Commun.* **1998**, 1553−1554.
(39) Reek, J. N. H.; Kros, A.; Nolte, R. J. M. *Chem. Commun.* **1996**, 245−247. Elemans, J. A. A. W.; Rowan, A. E.; Nolte, R. J. M. *J. Am. Chem. Soc.* **2002**, *124*, 1532−1540.
(40) Alternatively, the observation of no changes in chemical shift could indicate a fully dimeric form over this range of concentration. When we have observed dimers for our compounds, we have invariably observed sizable upfield shifts in the NMR which we do not observe for **12*C***. We, therefore, formulate **12*C*** as the monomer in 1,2-dichloroethane. We have performed similar dilution experiments for **8*C***, **12*C***, **13*C***, **16*C***, **17*C***, and **18*C*** in the more economical solvent $CDCl_3$, and, in all cases, the self-association constants (K_s < 10 M^{-1}) were too small to be responsible for the predominance of the C-shaped diastereomer.
(41) We did, however, note small changes (~0.04 ppm) in the chemical shift of the protons on the central methylene bridges. These changes are not well described by a 1:1 binding model, but are consistent with a small conformational change of the central eight-membered ring. For a discussion of these types of conformational changes, see: Jansen, R. J.; de Gelder, R.; Rowan, A. E.; Scheeren, H. W.; Nolte, R. J. M. *J. Org. Chem.* **2001**, *66*, 2643−2653.

Scheme 3. Three Different Mechanisms for the Equilibrium between the S- and C-Shaped Diastereomers

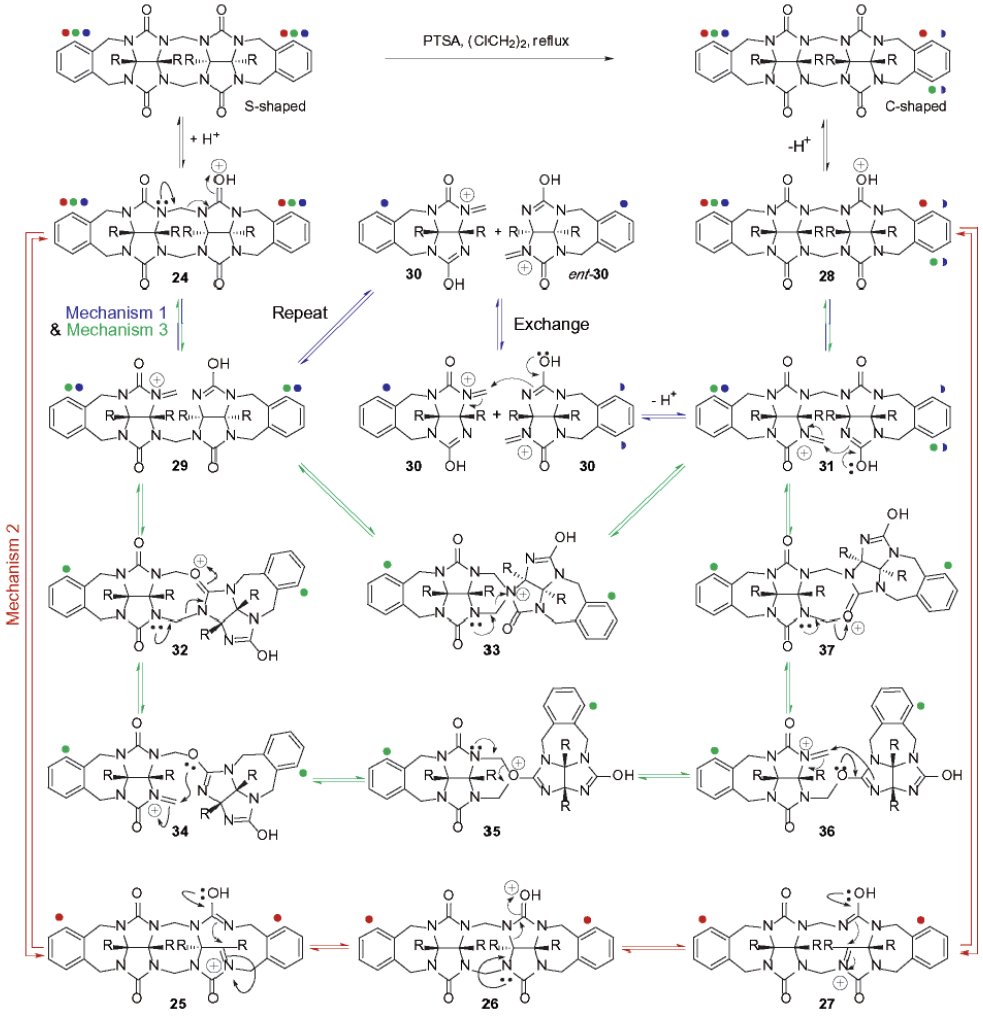

Table 3. AM1 Heats of Formation (kcal mol^{-1}) for **8**–**11**

	$\Delta H_f°$ (AM1)		
	S-shaped	C-shaped	$\Delta\Delta H_f°$ (AM1)
8[a]	−237.7 to −243.8	−246.9 to −250.1	−6.3 to −10.2
9[b]	47.6/47.3	45.3/45.2	−2.3 to −2.2
10	216.9	211.5	−5.4
11	58.2	58.7	0.5

[a] There are many different relative orientations of the four CO_2Et groups. [b] Two different relative orientations of the boat-shaped fused six-membered rings are possible.

of formation between the glycoluril dimers bearing different substituents, we are more confident in the experimental relative free energy values given in Table 1.

Mechanism of the Interconversion of the C- and S-Shaped Diastereomers. Previously, we have discussed the mechanism for the formation of methylene bridged glycoluril dimers.[31] In this section, we discuss experiments that pertain to the mechanism of the interconversion between the S- and C-shaped diastereomers. Scheme 3 describes the three different mechanistic proposals; the equilibrium arrows that connect intermediates along a single mechanistic path are color coded (mechanism 1, blue; mechanism 2, red; mechanism 3, green). All three mechanisms begin with protonation of one of the carbonyl oxygens by the acid catalyst (PTSA) giving **24**. From this point the three mechanisms diverge. In mechanism 2, one C−N bond of the glycoluril skeleton breaks, generating intermediate **25**, which has lost one stereogenic center. Reclosure of that same C−N bond can occur to generate intermediate **26**; this two-step process results in net inversion of configuration at that carbon atom. Intermediate **26** is probably prohibitively high in energy because of the trans ring junction, which disfavors mechanism 2. Repetition of this two-step process results in inversion of configuration at the second C-atom delivering intermediate **28** by way of **27**. Intermediate **28** is common to

Scheme 4. Diastereoselective Equilibration Reactions

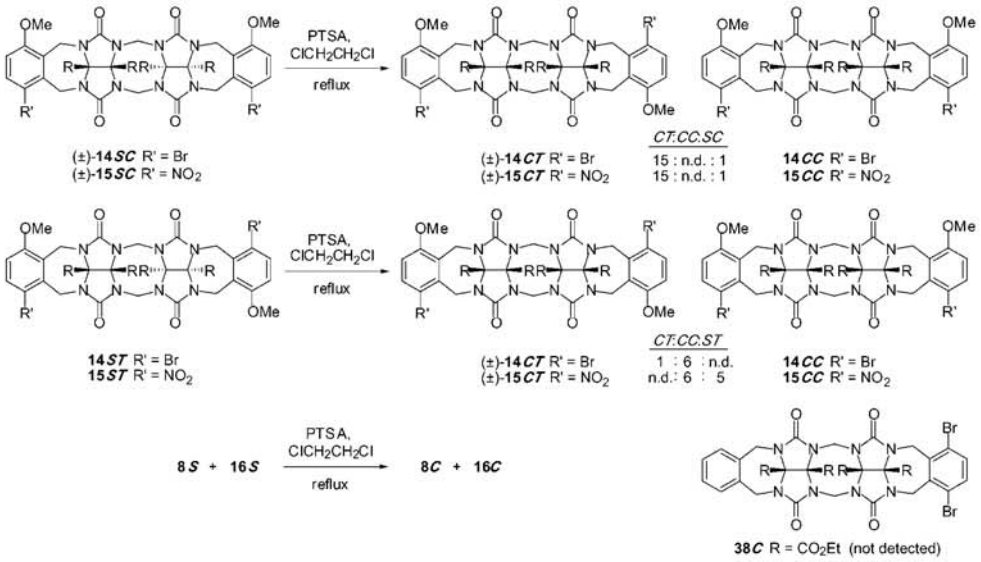

all three mechanisms; upon loss of a proton it delivers the C-shaped diastereomer. Overall, mechanism 2 is an intramolecular process that results in the inversion of configuration at two C-atoms. Mechanisms 1 and 3 diverge from mechanism 2 in the transformation of **24** into **29** by cleavage of one of the C−N bonds of a methylene bridge. Mechanisms 1 and 3 diverge from **29**. Mechanism 1 proceeds by the protonation of **29** followed by cleavage of a second C−N bond of the methylene bridge to yield the pair of intermediates (**30**). We have depicted the cleavage of **29** such that each half retains a single positive charge; the alternative pathway involving one half retaining both methylene bridges and two positive charges is also possible, but likely to be higher in energy. It is worth noting that the pair of intermediates generated in this manner from a single molecule of **29** is heterochiral, that is, the racemic mixture (±)-**30**. To generate the C-shaped product, this pair must undergo exchange with other like intermediates to generate the homochiral pair comprising two molecules of **30** or *ent*-**30**. This pair is then able to sequentially reform the C−N bonds of the two methylene bridges forming C-shaped product by way of **31** and common intermediate **28**. Overall, mechanism 1 results in breaking of the S-shaped glycoluril dimer into two heterochiral pieces that undergo exchange to generate a homochiral pair that results in formation of the C-shaped product. Mechanism 3 diverges from mechanism 1 at intermediate **29**. In mechanism 3, the iminium ion intermediate **29** is captured by the carbonyl oxygen lone pair yielding **32** or by the ureidyl nitrogen lone pair yielding intermediate **33**. Of these two options, we prefer the use of the oxygen atom lone pair because it is likely to be more nucleophilic. The overall pathway, however, is better illustrated conceptually via spiro compound **33**. The spiro compound can break down in two ways, one leading back to intermediate **29** and one leading to **31** which after deprotonation yields common intermediate **28** and then the C-shaped diastereomer. The overall process of mechanism 3 results in intramolecular swapping of partner N-atoms involved in the methylene bridges. The use of the oxygen lone pair to accomplish the same overall transformation of **29** into **31** proceeds via intermediates **32** and **34**−**37**.

Mechanisms 1−3 have different stereochemical outcomes and can be distinguished on the basis of labeling experiments. To schematically illustrate the different outcomes, two different carbon atoms of the starting S-shaped diastereomer (Scheme 3) were labeled with blue, red, and green dots. The positions of these labels are indicated as they progress through mechanisms 1, 2, and 3, respectively. As can be readily ascertained from Scheme 3, mechanism 1 (blue) leads to a scrambling of the label between two locations (blue half circles), mechanism 2 (red) does not result in any change in the relative position (cis) of the labels (red dots), and mechanism 3 (green) results in a transposition of one of the labels to the opposite side (trans) of the C-shaped diastereomer (green dots).

To realize this labeling experiment in practice, we separately performed isomerization reactions of (±)-**14*SC*** and the meso compound **14*ST*** (Scheme 4). Under mechanism 1, (±)-**14*SC*** should yield a mixture of **14*CC*** and (±)-**14*CT***, under mechanism 2 only **14*CC***, and under mechanism 3 only (±)-**14*CT***. Similarly, under mechanism 1, **14*ST*** would yield a mixture of **14*CC*** and (±)-**14*CT***, under mechanism 2 only **14*CT***, and under mechanism 3 only **14*CC***. Scheme 4 shows the results of the equilibration reactions of (±)-**14*SC***, **14*ST***, (±)-**15*SC***, and **15*ST***. The separate isomerization reactions of (±)-**14*SC*** and (±)-**15*SC*** gave *only* (±)-**14*CT*** and (±)-**15*CT***, respectively, along with small amounts of unreacted starting material. The isomerization reaction of **14*ST*** yields **14*CC*** and (±)-**14*CT*** in a 6:1 ratio, whereas the sluggish isomerization of **15*ST*** gave exclusively **15*CC*** at 55% conversion. These results provide strong evidence that mechanism 3 is the dominant pathway for the interconversion of the S-shaped and C-shaped diastereomers under our standard isomerization conditions ($ClCH_2CH_2Cl$, anhydrous

Chart 3

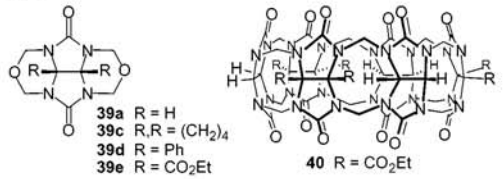

PTSA, reflux). We also performed a crossover experiment involving the isomerization of a mixture of **8*S*** and **16*S***. Under mechanism 1, we would expect the formation of **8*C***, **16*C***, and the crossover product, heterodimer **38*C***. In contrast, if mechanism 3 is dominant, then **8*C*** and **16*C*** should be the exclusive products. When this isomerization reaction was run to 78% completion, we observed the clean formation of a mixture of **8*C*** and **16*C*** providing additional support for the dominance of mechanism 3.

The fact that the isomerization of methylene bridged glycoluril dimers follows mechanism 3 is not only useful in the synthesis of our compounds, but might be important for the tailored synthesis of **CB**[*n*] and its derivatives. For example, Day and co-workers have recently shown that heating purified **CB**[8] in concentrated HCl at 100 °C results in the formation of **CB**[5], **CB**[6], and **CB**[7]. In contrast, pure **CB**[5], **CB**[6], and **CB**[7] are stable under these conditions.[18] These results require that two adjacent methylene bridges are broken and that one or more glycoluril rings are extruded. This type of reaction would likely follow a pathway related to mechanism 1. We believe that mechanism 1 is not operative in our system because we work under anhydrous acidic conditions. In aqueous acid, it is likely that H_2O can compete with the internal N and O nucleophiles of mechanism 3 for the capture of **29** (Scheme 3), effectively forcing fragmentation of the methylene bridges by a variation of mechanism 1. In the absence of competing nucleophiles, under anhydrous acidic conditions, we suggest that **CB**[*n*] ($n > 8$) and derivatives might display enhanced stability. We further suggest that the optimal synthesis of **CB**[*n*] ($n > 8$) and derivatives might be best performed in a two-step manner similar to our heterodimerization reactions, via reaction of a bis(cyclic ether) (e.g., **39a**−**39e**, Chart 3) and a functionalized glycoluril (e.g., **1a**−**1e**), followed by an isomerization step of the intermediate S- and C-shaped methylene bridged glycoluril oligomers under anhydrous acidic conditions. If this approach is fruitful, it might be possible to prepare **CB**[*n*] derivatives from two different glycoluril derivatives (e.g., **39e** and **1a**), and that those derivatives might alternate in the **CB**[*n*] derivative (e.g., **40**).[19]

Conclusions

Until recently, it has not been possible to prepare either homologues or derivatives of **CB**[*n*].[3,17−23] Even today, the synthesis of homologues mainly provides **CB**[5], **CB**[7], **CB**[8], and **CB**[10], and the synthesis of derivatives of **CB**[*n*] is limited to the smaller ring sizes (Me_{10}**CB**[5], Cy_5**CB**[5], Cy_6**CB**[6], and Ph_2**CB**[6]). Despite these limitations, it has become increasingly clear that the homologues and derivatives of **CB**[*n*] have superior characteristics.[3,17−22] The complexity of the **CB**[*n*] synthesis − the formation of *n* rings, 2*n* methylene bridges, and control over the relative stereochemistry of *n* glycoluril rings − has made investigations of the mechanism of **CB**[*n*] synthesis challenging. Such investigations can, however, provide insights that expand the scope and define the limitations of **CB**[*n*] synthesis.

The use of methylene bridged glycoluril dimers as a model system for **CB**[*n*] synthesis has reduced the complexity of the investigation to the formation of one ring, two methylene bridges, and control over the relative stereochemistry of two glycoluril rings. This reduction in complexity has allowed us to probe the mechanism of **CB**[*n*] formation at a level of detail that has not been possible to date. Specifically, we have demonstrated that the condensation reactions that connect two glycoluril rings by methylene bridges deliver both the S-shaped and the C-shaped diastereomers as kinetic products. The relative thermodynamic stability of these two diastereomers was examined by separately resubmitting the pure C- and S-shaped diastereomers to the reaction conditions. The C-shaped diastereomers are more stable than the corresponding S-shaped diastereomers by 1.55−3.25 kcal mol^{-1}. The values of ΔG are only modestly solvent dependent. These measurements represent the first experimental determinations of the driving force for the C- to S-equilibrium which is important in the conversion of the growing methylene bridged glycoluril oligomer into the all C-shaped **CB**[*n*]. The mechanism of this S- to C-interconversion was delineated by a series of labeling experiments. These experiments, performed under anhydrous conditions in $ClCH_2$-CH_2Cl, establish the intramolecular nature of the isomerization and demonstrate the retention of configuration of the two halves of the dimer. The elucidation of the mechanism of the isomerization reaction has broad implications for the improved synthesis of **CB**[*n*]. For example, the intramolecular nature of the isomerization suggests that it is the length of the growing methylene bridged glycoluril oligomer chain (**4** and **5**) that controls the size of the **CB**[*n*] oligomer. It further suggests that the substitution pattern of these intermediate oligomers might be preserved in **CB**[*n*] oligomers. For example, the heterodimerization of **39e** and **1a** could yield **CB**[*n*] derivative **40** with alternating substituents.[19] Armed with these new insights into the mechanism of **CB**[*n*] formation, it should be possible to expand the range of **CB**[*n*] homologues and **CB**[*n*] derivatives and to capitalize on their superior molecular recognition characteristics.

Experimental Section

General. Starting materials were purchased from Alfa-Aesar, Acros, and Aldrich and were used without further purification. Compounds **6*C*−10*C***, **8*S***, **12*C***, **12*S***, **13*C***, **13*S***, **14*CC***, (±)-**14*CT***, (±)-**14*SC***, **14*ST***, **15*CC***, (±)-**15*CT***, (±)-**15*SC***, **15*ST***, **16*C*−18*C***, **16*S*−18*S***, **19**, **20**, **21**, (±)-**22**, and (±)-**23** were prepared according to literature procedures.[24,31,32] THF and toluene were distilled from sodium benzophenone ketyl, and methylene chloride was distilled from CaH_2 immediately before use. TLC analysis was performed using precoated glass plates from Analtech or Merck. Column chromatography was performed using silica gel (230−400 mesh, 0.040−0.063 μm) from E. Merck using eluents in the indicated v:v ratio. Melting points were measured on a Meltemp apparatus in open capillary tubes and are uncorrected. IR spectra were recorded on a Nicolet Magna spectrophotometer as KBr pellets or thin films on NaCl plates and are reported in cm^{-1}. NMR spectra were measured on Bruker AM-400 and DRX-400 instruments operating at 400 MHz for ^1H and 100 MHz for ^{13}C. Mass spectrometry was performed using a VG 7070E magnetic sector instrument by electron impact (EI) or by fast atom bombardment (FAB) using the

indicated matrix. The matrix "magic bullet" is a 5:1 (w:w) mixture of dithiothreitol:dithioerythritol. Electrospray mass spectrometry experiments were performed on a Finnegan LCQ ion-trap mass spectrometer. Elemental analyses were performed by Midwest MicroLab (Indianapolis, IN).

Representative Procedure from Scheme 2. Synthesis of 14*ST* and (±)-14*SC*. A mixture of PTSA (737 mg, 3.88 mmol) and $ClCH_2CH_2Cl$ (30 mL) was heated under N_2 at reflux for 30 min under an addition funnel filled with molecular sieves (4 Å). Compounds (±)-**23** (418 mg, 0.78 mmol) and (±)-**22** (385 mg, 0.78 mmol) were added, and heating was continued for 4 h at 60 °C. The reaction mixture was diluted with EtOAc (500 mL), washed with saturated Na_2CO_3, dried over anhydrous $MgSO_4$, and concentrated. Flash chromatography (SiO_2, $CHCl_3/CH_3CN$, 10:1 and then 4:1) yielded **14*ST*** (27 mg, 0.03 mmol, 7%), (±)-**14*SC*** (23 mg, 0.02 mmol, 6%), (±)-**14*CT*** (48 mg, 0.05 mmol, 12%), and **14*CC*** (72 mg, 0.07 mmol, 18%) as white solids along with unreacted starting materials (±)-**23** and (±)-**22**. Compound **14*ST*** (eluted with $CHCl_3/CH_3CN$ 10:1). mp 145−147 °C. TLC ($CHCl_3/CH_3CN$ 10:1): R_f 0.24. IR (KBr, cm^{-1}): 2985m, 2935w, 2842w, 1742s, 1699s, 1457m, 1429s, 1388m, 1368w, 1268s, 1173s, 1030s. ^1H NMR (400 MHz, $CDCl_3$): 7.42 (d, J = 8.9, 2H), 6.72 (d, J = 8.9, 2H), 5.67 (d, J = 16.3, 2H), 5.52 (d, J = 16.3, 2H), 5.06 (d, J = 13.6, 2H), 4.95 (d, J = 13.6, 2H), 4.22 (d, J = 16.3, 2H), 4.19 (q, J = 7.1, 4H), 3.96 (d, J = 16.3, 2H), 3.84 (s, 6H), 3.85−3.70 (m, 4H), 1.26 (t, J = 7.1, 6H), 1.13 (t, J = 7.1, 6H). ^{13}C NMR (100 MHz, $CDCl_3$): 165.4, 164.0, 156.5, 155.2, 155.0, 137.1, 133.2, 127.1, 115.1, 113.0, 81.0, 78.7, 63.7, 63.5, 56.6, 51.9, 44.4, 36.6, 14.0, 13.6. MS (FAB, Magic Bullet): m/z 1019 (100, $[M + H]^+$). HR-MS (FAB, Magic Bullet): m/z 1149.0247 ($[M + Cs]^+$, $C_{40}H_{42}{}^{79}Br_2N_8O_{14}Cs$ calcd 1149.0242). Compound (±)-**14*SC*** (eluted with $CHCl_3/CH_3CN$ 10:1). mp 144−146 °C. TLC ($CHCl_3/CH_3CN$ 10:1): R_f 0.18. IR (KBr, cm^{-1}): 2978w, 2939m, 2842m, 1742s, 1457m, 1429m, 1388s, 1367m, 1309m, 1269s, 1078s, 1020s. ^1H NMR (400 MHz, $CDCl_3$): 7.42 (d, J = 8.9, 2H), 6.72 (d, J = 8.9, 2H), 5.64 (d, J = 16.2, 2H), 5.56 (d, J = 16.2, 2H), 5.01 (s, 2H), 4.99 (s, 2H), 4.32 (d, J = 16.2, 2H), 4.25−4.10 (m, 4H), 3.84 (s, 6H), 3.90−3.70 (m, 6H), 1.26 (t, J = 7.1, 6H), 1.14 (t, J = 7.1, 6H). ^{13}C NMR (100 MHz, $CDCl_3$): 165.4, 163.9, 156.6, 155.1, 155.0, 137.1, 133.2, 127.2, 114.9, 113.1, 80.9, 78.7, 63.7, 63.5, 56.6, 52.2, 51.5, 44.4, 36.5, 13.9, 13.6. MS (FAB, Magic Bullet): m/z 1019 (100, $[M + H]^+$). HR-MS (FAB, Magic Bullet): m/z 1149.0276 ($[M + Cs]^+$, $C_{40}H_{42}{}^{79}Br_2N_8O_{14}Cs$ calcd 1149.0242).

Representative Procedures from Table 1. Isomerization of 12*C*. A mixture of PTSA (0.042 g, 0.220 mmol) and $ClCH_2CH_2Cl$ (10 mL) was heated under N_2 at reflux for 30 min under an addition funnel filled with molecular sieves (4 Å). Compound **12*C*** (0.020 g, 0.022 mmol) was added, and reflux was continued for 72 h. The reaction mixture was diluted with EtOAc (100 mL), washed with saturated Na_2CO_3, dried over anhydrous $MgSO_4$, and concentrated. A C:S ratio of 39:1 was calculated on the basis of the integration of the resonances for **12*C*** (6.06 ppm) and **12*S*** (5.04 ppm) in the crude ^1H NMR spectrum.

Isomerization of 12*S*. A mixture of PTSA (0.051 g, 0.220 mmol) and $ClCH_2CH_2Cl$ (10 mL) was heated under N_2 at reflux for 30 min under an addition funnel filled with molecular sieves (4 Å). Compound **12*S*** (0.050 g, 0.054 mmol) was added, and reflux was continued for 6 days. The reaction mixture was diluted with EtOAc (100 mL), washed with saturated Na_2CO_3, dried over anhydrous $MgSO_4$, and concentrated. A C:S ratio of 50:1 was calculated on the basis of the integration of the resonances for **12*C*** (6.06 ppm) and **12*S*** (5.04 ppm) in the crude ^1H NMR spectrum.

General Procedures for Table 2. Isomerization of 16*C*. A mixture of PTSA (41 mg, 0.22 mmol) and solvent (6 mL) was heated under N_2 at reflux for 30 min under an addition funnel filled with molecular sieves (4 Å). Compound **16*C*** (50 mg, 0.045 mmol) was added, and reflux was continued for several days. The reaction mixture was diluted with EtOAc (100 mL), washed with saturated Na_2CO_3, dried over anhydrous $MgSO_4$, and concentrated. The **16*C***:**16*S*** ratio was calculated on the basis of the integrals of the resonances for **16*C*** (6.04 ppm) and **16*S*** (4.98 ppm) in the crude ^1H NMR spectrum.

Isomerization of 16*S*. A mixture of PTSA (41 mg, 0.22 mmol) and solvent (6 mL) was heated under N_2 at reflux for 30 min under an addition funnel filled with molecular sieves (4 Å). Compound **16*S*** (50 mg, 0.045 mmol) was added, and reflux was continued for several days. The reaction mixture was diluted with EtOAc (100 mL), washed with saturated Na_2CO_3, dried over anhydrous $MgSO_4$, and concentrated. The **16*C***:**16*S*** ratio was calculated on the basis of the integrals of the resonances for **16*C*** (6.04 ppm) and **16*S*** (4.98 ppm) in the crude ^1H NMR spectrum.

Representative Procedure from Scheme 4. Isomerization of (±)-14*SC*. A mixture of PTSA (23 mg, 0.12 mmol) and $ClCH_2CH_2Cl$ (6 mL) was heated under N_2 at reflux for 30 min under an addition funnel filled with molecular sieves (4 Å). Compound (±)-**14*SC*** (15 mg, 0.02 mmol) was added, and heating was continued for 12 days. The reaction mixture was diluted with EtOAc (100 mL), washed with saturated aqueous Na_2CO_3, dried over anhydrous $MgSO_4$, and concentrated. The ^1H NMR spectrum of the crude material was used to calculate a CT:SC ratio of 15:1 on the basis of the integrals of the resonances for (±)-**14*CT*** at 6.03 ppm and (±)-**14*SC*** at 5.01 ppm.

X-ray Crystal Structure of 18*C*. A detailed description of the data collection, solution, and refinement of the structure can be found in the Supporting Information. Crystal data for **18*C***: $[C_{38}H_{32}N_8O_{12}F_8]$-$[C_7H_8]$ (1036.85); orthorhombic, space group $Pca2(1)$; colorless block, a = 16.1489(10) Å, b = 11.4856(7) Å, c = 24.0250(15) Å; V = 4456.2(5) Å^3; Z = 4; T = 193(2) K; $R(F)$ = 0.0451; GOF on F^2 = 1.044.

AM1 Calculations. All computations were performed on a Dell Precision 620 workstation with 512 MB of RAM and dual Pentium III processors running PC Spartan Pro under Windows 2000 professional. The overall structure was created with Spartan's graphical user interface and then minimized by MMFF94 or SYBYL molecular mechanics calculations. These minimized structures served as the input files for the AM1 calculations.

Acknowledgment. We thank the National Institutes of Health (GM61854) and the University of Maryland for generous financial support. We thank Professor Bruce Jarvis for helpful discussions. L.I. is a Cottrell Scholar of Research Corp.

Supporting Information Available: Experimental procedures and spectral data for all new compounds, and details of the X-ray crystallographic analysis of **18*C*** (PDF). This material is available free of charge via the Internet at http://pubs.acs.org.

JA025876F

JOC*Article*

Methylene-Bridged Glycoluril Dimers: Synthetic Methods

Anxin Wu,[†,‡] Arindam Chakraborty,[†] Dariusz Witt,[†,§] Jason Lagona,[†] Fehmi Damkaci,[†] Marie A. Ofori,[†] Jessica K. Chiles,[†] James C. Fettinger,[†] and Lyle Isaacs*[,†]

Department of Chemistry and Biochemistry, University of Maryland, College Park, Maryland 20742, and National Laboratory of Applied Organic Chemistry, Lanzhou University, Lanzhou 730000, P. R. China

LI8@umail.umd.edu

Received May 2, 2002

Methylene-bridged glycoluril dimers are the fundamental building blocks of cucurbituril (**CB**[6]), its homologues (**CB**[*n*]), and its derivatives. This paper describes three complementary methods for the synthesis of C- and S-shaped methylene-bridged glycoluril dimers (**29**−**34** and **37**−**44**). For this purpose, we prepared glycoluril derivatives (**1a**−**d**) bearing diverse functionalities on their convex face. These glycoluril derivatives were alkylated under basic conditions (DMSO, *t*-BuOK) with 1,2-bis(halomethyl)aromatics **6**−**15** to yield **4a**−**d** and **16**−**24**, which contain a single aromatic *o*-xylylene ring and potentially nucleophilic ureidyl NH groups. Glycoluril derivatives bearing potentially electrophilic cyclic ether groups (**5a**−**f**) and **25**−**28** were prepared by various methods including condensation reactions in refluxing TFA containing paraformaldehyde. The condensation reactions of **4a**−**d** and **16**−**24** with paraformaldehyde under anhydrous acidic conditions (PTSA, $ClCH_2CH_2Cl$, reflux) give, in most cases, the C-shaped and S-shaped methylene-bridged glycoluril in good to excellent yields. In many cases, the C-shaped compound is formed preferentially with high diastereoselectivity. Cyclic ethers **5a**,**d**−**f** and **25**−**26** undergo highly diastereoselective dimerization reactions to yield methylene-bridged glycoluril dimers with the formal extrusion of formaldehyde. Last, it is possible to perform selective heterodimerization reactions using both cyclic ethers and glycoluril derivatives bearing ureidyl NH groups. These reactions deliver the desired C- and S-shaped heterodimers with low to moderate diastereoselectivities. This heterodimerization route is the method of choice in cases where the homodimerization reactions fail. The formation of side products (±)-**35b** and (±)-**35d** helps clarify the electronic requirements for a successful **CB**[*n*] synthesis. The X-ray structures of **30*C***, **38*C***, and **38*S*** allow for a discussion of the structural features of this class of compounds.

Introduction

Cucurbituril (**CB**[6]) is a an intriguing macrocyclic compound comprising six glycoluril (**1f**) rings and twelve methylene bridges whose structure was established by Mock in 1981.[1] **CB**[6] possesses a hydrophobic cavity with carbonyl-lined portals that results in remarkable molecular recognition properties (Chart 1). For example, Mock and co-workers found that **CB**[6] binds tightly ($K_d \approx 1$ μM) to alkyldiammonium ions in aqueous solution by a combination of the hydrophobic effect and ion−dipole interactions.[2] It was also demonstrated that **CB**[6] is an efficient enzyme mimic capable of catalyzing the dipolar cycloaddition between azide and acetylene-derivatized ammonium ions by their simultaneous binding within the cavity of **CB**[6].[3] The synthetic method used to prepare cucurbituril is equally impressive; simply heating glycoluril (**1a**) and formaldehyde under strongly acidic conditions (H_2SO_4, 135−145 °C) results in the formation of **CB**[6] in high yield.[4] This straightforward synthetic method has allowed the use of **CB**[6] in many elegant studies including molecular necklaces,[5] bowls,[6] polyrotaxanes,[7] DNA complexes,[8] molecular switches,[9] removal of contaminants from aqueous waste streams,[10] studies of molecular polarizability,[11] and ion and molecular complexation studies.[2,12]

In efforts to expand the range of applications, several groups have been investigating the preparation of congeners of cucurbituril that display enhanced properties. This line of inquiry was first pursued by Stoddart, who prepared Me_{10}**CB**[5] by condensation of **1e** with formaldehyde.[13] More recently, Kim and co-workers[14,15] as well as Day and co-workers[16,17] isolated homologues of cucurbituril comprising five, seven, eight, and ten glycoluril

* To whom correspondence should be addressed.
† University of Maryland.
‡ Lanzhou University.
§ Current address: Chemical Faculty, Technical University of Gdansk, Narutowicza 11/12, 80-952 Gdansk, Poland.

(1) Freeman, W. A.; Mock, W. L.; Shih, N. Y. *J. Am. Chem. Soc.* **1981**, *103*, 7367−7368.
(2) Mock, W. L.; Shih, N. Y. *J. Org. Chem.* **1983**, *48*, 3618−3819. Mock, W. L.; Shih, N. Y. *J. Org. Chem.* **1986**, *51*, 4440−4446. Mock, W. L.; Shih, N. Y. *J. Am. Chem. Soc.* **1988**, *110*, 4706−4610. Mock, W. L.; Shih, N. Y. *J. Am. Chem. Soc.* **1989**, *111*, 2697−2679.
(3) Mock, W. L.; Irra, T. A.; Wepsiec, J. P.; Manimaran, T. L. *J. Org. Chem.* **1983**, *48*, 3619−3820. Mock, W. L.; Irra, T. A.; Wepsiec, J. P.; Adhya, M. *J. Org. Chem.* **1989**, *54*, 5302−5308.
(4) Buschmann, H.-J.; Fink, H.; Schollmeyer, E. Preparation of Cucurbituril. German Patent DE 196 03 377 A1, 1997.
(5) Whang, D.; Park, K.-M.; Heo, J.; Ashton, P.; Kim, K. *J. Am. Chem. Soc.* **1998**, *120*, 4899−4900. Roh, S.-G.; Park, K.-M.; Park, G.-J.; Sakamoto, S.; Yamaguchi, K.; Kim, K. *Angew. Chem., Int. Ed.* **1999**, *38*, 638−641. Lee, E.; Kim, J.; Heo, J.; Whang, D.; Kim, K. *Angew. Chem., Int. Ed.* **2001**, *40*, 399−402.
(6) Jeon, Y.-M.; Kim, J.; Whang, D.; Kim, K. *J. Am. Chem. Soc.* **1996**, *118*, 9790−9791. Whang, D.; Heo, J.; Park, J. H.; Kim, K. *Angew. Chem., Int. Ed.* **1998**, *37*, 78−80.

10.1021/jo0258958 CCC: $22.00
Published on Web 07/03/2002

CHART 1

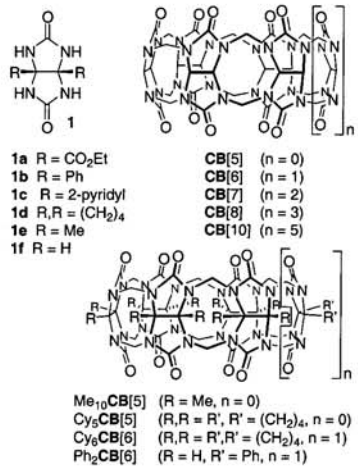

units (**CB**[5], **CB**[7], **CB**[8], and **CB**[10]) and detected other homologues by performing the condensation reaction under milder, kinetically controlled conditions. These advances have already expanded the range of molecular recognition applications[18−20] of these systems to include molecular Russian dolls,[21] ball bearings,[22] gyroscopes,[17b] the catalysis of a [2 + 2] photoreaction,[23] and the selective recognition of a charge-transfer complex.[24] Most recently, Kim's group has demonstrated that cyclohexyl-fused glycoluril **1d** is transformed into Cy_5**CB**[5] and Cy_6**CB**[6][25] whereas Nakamura's group isolated the partially substituted Ph_2**CB**[6].[26]

We have also been interested in tailoring the recognition properties of **CB**[*n*] by preparing derivatives functionalized around their equator, at their methylene bridges, or by substitution of an aromatic ring for a glycoluril ring. In contrast to the one-step syntheses of Stoddart, Kim, and Day, we have chosen to pursue a multistep synthetic approach. Such an approach, while inherently more labor intensive, affords greater structural control, may generate mechanistic insights that result in cucurbituril syntheses with enhanced scope, and offers the opportunity to study the self-assembly and molecular recognition properties of intermediates enroute to congeners of cucurbituril.[27] Our approach[28] to the synthesis of congeners of **CB**[6] relies on the identification of the methylene-bridged glycoluril dimer substructure (**2**, bold in **CB**[6]) as the essential building block for cucurbituril derivatives (Scheme 1). In this paper we present three complementary synthetic routes to methylene-bridged glycoluril dimers. We also present the X-ray crystallographic characterization of these two diastereomers.

Results and Discussion

Experimental Design. To develop flexible methods for the synthesis of derivatives of **CB**[*n*], we have initially focused our attention on the preparation of methylene-bridged glycoluril dimers (***2C*** and ***2S***) which constitute

(7) Whang, D.; Jeon, Y.-M.; Heo, J.; Kim, K. *J. Am. Chem. Soc.* **1996**, *118*, 11333−11334. Whang, D.; Kim, K. *J. Am. Chem. Soc.* **1997**, *119*, 451−452. Whang, D.; Heo, J.; Kim, C.-A.; Kim, K. *Chem. Commun.* **1997**, 2361−2362. Lee, E.; Heo, J.; Kim, K. *Angew. Chem., Int. Ed.* **2000**, *39*, 2699−2701. Lee, J. W.; Ko, Y. H.; Park, S.-H.; Yamaguchi, K.; Kim, K. *Angew. Chem., Int. Ed.* **2001**, *40*, 746−749. Park, K.-M.; Whang, D.; Lee, E.; Heo, J.; Kim, K. *Chem.−Eur. J.* **2002**, *8*, 498−508. Meschke, C.; Buschmann, H.-J.; Schollmeyer, E. *Polymer* **1998**, *40*, 945−949; Meschke, C.; Buschmann, H. J.; Schollmeyer, E. *Macromol. Rapid Commun.* **1998**, *19*, 59−63. Buschmann, H. J.; Wego, A.; Schollmeyer, E.; Dopp, D. *Supramol. Chem.* **2000**, *11*, 225−231. Buschmann, H. J.; Cleve, E.; Mutihac, L.; Schollmeyer, E. *Microchem. J.* **2000**, *64*, 99−103. Tuncel, D.; Steinke, J. H. G. *Chem. Commun.* **1999**, 1509−1510; Tuncel, D.; Steinke, J. H. G. *Chem. Commun.* **2001**, 253−254.

(8) Isobe, H.; Tomita, N.; Lee, J. W.; Kim, H.-J.; Kim, K.; Nakamura, E. *Angew. Chem., Int. Ed.* **2000**, *39*, 4257−4260.

(9) Mock, W. L.; Pierpont, J. *J. Chem. Soc., Chem. Commun.* **1990**, 1509−1511. Jun, S. I.; Lee, J. W.; Sakamoto, S.; Yamaguchi, K.; Kim, K. *Tetrahedron Lett.* **2000**, *41*, 471−475.

(10) Buschmann, H. J.; Gardberg, A.; Schollmeyer, E. *Textilveredlung* **1991**, *26*, 153−7. Buschmann, H. J.; Schollmeyer, E. *J. Inclusion Phenom. Mol. Recognit. Chem.* **1992**, *14*, 91−9; Buschmann, H. J.; Schollmeyer, E. *J. Inclusion Phenom. Mol. Recognit. Chem.* **1997**, *29*, 167−174; Buschmann, H. J.; Schollmeyer, E. *Textilveredlung* **1998**, *33*, 44−47. Karcher, S.; Kornmuller, A.; Jekel, M. *Water Sci. Technol.* **1999**, *40*, 425−433; Karcher, S.; Kornmueller, A.; Jekel, M. *Acta Hydrochim. Hydrobiol.* **1999**, *27*, 38−42; Kornmuller, A.; Karcher, S.; Jekel, M. *Water Res.* **2001**, *35*, 3317−3324. Taketsuji, K.; Tomioka, H. *Nippon Kagaku Kaishi* **1998**, 670−678.

(11) Marquez, C.; Nau, W. M. *Angew. Chem., Int. Ed.* **2001**, *40*, 4387−4390.

(12) Hoffmann, R.; Knoche, W.; Fenn, C.; Buschmann, H.-J. *J. Chem. Soc., Faraday Trans.* **1994**, *90*, 1507−11. Meschke, C.; Buschmann, H. J.; Schollmeyer, E. *Thermochim. Acta* **1997**, *297*, 43−48. Buschmann, H. J.; Jansen, K.; Meschke, C.; Schollmeyer, E. *J. Solution Chem.* **1998**, *27*, 135−140. Buschmann, H.-J.; Jansen, K.; Schollmeyer, E. *Acta Chim. Slov.* **1999**, *46*, 405−411; Buschmann, H. J.; Jansen, K.; Schollmeyer, E. *Thermochim. Acta* **2000**, *346*, 33−36. Buschmann, H. J.; Cleve, E.; Jansen, K.; Wego, A.; Schollmeyer, E. *J. Inclusion Phenom. Macrocyclic Chem.* **2001**, *40*, 117−120. Buschmann, H. J.; Cleve, E.; Jansen, K.; Schollmeyer, E. *Anal. Chim. Acta* **2001**, *437*, 157−163. El Haouaj, M.; Young, H. K.; Luhmer, M.; Kim, K.; Bartik, K. *J. Chem. Soc., Perkin Trans. 2* **2001**, 2104−2107. El Haouaj, M.; Luhmer, M.; Ko, Y. H.; Kim, K.; Bartik, K. *J. Chem. Soc., Perkin Trans. 2* **2001**, 804−807. Marquez, C.; Nau, W. M. *Angew. Chem., Int. Ed.* **2001**, *40*, 3155−3160. Neugebauer, R.; Knoche, W. *J. Chem. Soc., Perkin Trans. 2* **1998**, 529−534. Zhang, X. X.; Krakowiak, K. E.; Xue, G.; Bradshaw, J. S.; Izatt, R. M. *Ind. Eng. Chem. Res.* **2000**, *39*, 3516−3520. Wagner, B. D.; Fitzpatrick, S. J.; Gill, M. A.; MacRae, A. I.; Stojanovic, N. *Can. J. Chem.* **2001**, *79*, 1101−1104.

(13) Flinn, A.; Hough, G. C.; Stoddart, J. F.; Williams, D. J. *Angew. Chem., Int. Ed. Engl.* **1992**, *31*, 1475−1477.

(14) Kim, K.; Kim, J.; Jung, I.-S.; Kim, S.-Y.; Lee, E.; Kang, J.-K. Cucurbituril Derivatives, Their Preparation and Uses. European Patent Appl. EP 1 094 065 A2, 2001.

(15) Kim, J.; Jung, I.-S.; Kim, S.-Y.; Lee, E.; Kang, J.-K.; Sakamoto, S.; Yamaguchi, K.; Kim, K. *J. Am. Chem. Soc.* **2000**, *122*, 540−541.

(16) Day, A. I.; Arnold, A. P.; Blanch, R. J. Method for Synthesis Cucurbiturils. PCT Intl. Appl. PCT/AU00/00412, 2000.

(17) (a) Day, A.; Arnold, A. P.; Blanch, R. J.; Snushall, B. *J. Org. Chem.* **2001**, *66*, 8094−8100. (b) Day, A. I.; Blanch, R. J.; Arnold, A. P.; Lorenzo, S.; Lewis, G. R.; Dance, I. *Angew. Chem., Int. Ed.* **2002**, *41*, 275−277.

(18) Lorenzo, S.; Day, A.; Craig, D.; Blanch, R.; Arnold, A.; Dance, I. *CrystEngComm* **2001**, *49*, 1−7.

(19) Ong, W.; Gómez-Kaifer, M.; Kaifer, A. E. *Org. Lett.* **2002**, *4*, 1791−1794.

(20) Kim, H.-J.; Jeon, W. S.; Ko, Y. H.; Kim, K. *Proc. Natl. Acad. Sci. U.S.A.* **2002**, *99*, 5007−5011.

(21) Kim, S.-Y.; Jung, I.-S.; Lee, E.; Kim, J.; Sakamoto, S.; Yamaguchi, K.; Kim, K. *Angew. Chem., Int. Ed.* **2001**, *40*, 2119−2121.

(22) Blanch, R. J.; Sleeman, A. J.; White, T. J.; Arnold, A. P.; Day, A. I. *Nano Lett.* **2002**, *2*, 147−149.

(23) Jon, S. Y.; Ko, Y. H.; Park, S. H.; Kim, H.-J.; Kim, K. *Chem. Commun.* **2001**, 1938−1939.

(24) Kim, H.-J.; Heo, J.; Jeon, W. S.; Lee, E.; Kim, J.; Sakamoto, S.; Yamaguchi, K.; Kim, K. *Angew. Chem., Int. Ed.* **2001**, *40*, 1526−1529.

(25) Zhao, J.; Kim, H.-J.; Oh, J.; Kim, S.-Y.; Lee, J. W.; Sakamoto, S.; Yamaguchi, K.; Kim, K. *Angew. Chem., Int. Ed.* **2001**, *40*, 4233−4235.

(26) Isobe, H.; Sato, S.; Nakamura, E. *Org. Lett.* **2002**, *4*, 1287−1289.

(27) Isaacs, L.; Witt, D.; Lagona, J. *Org. Lett.* **2001**, *3*, 3221−3224.

(28) Witt, D.; Lagona, J.; Damkaci, F.; Fettinger, J. C.; Isaacs, L. *Org. Lett.* **2000**, *2*, 755−758.

SCHEME 1. Retrosynthetic Analysis of CB[*n*]

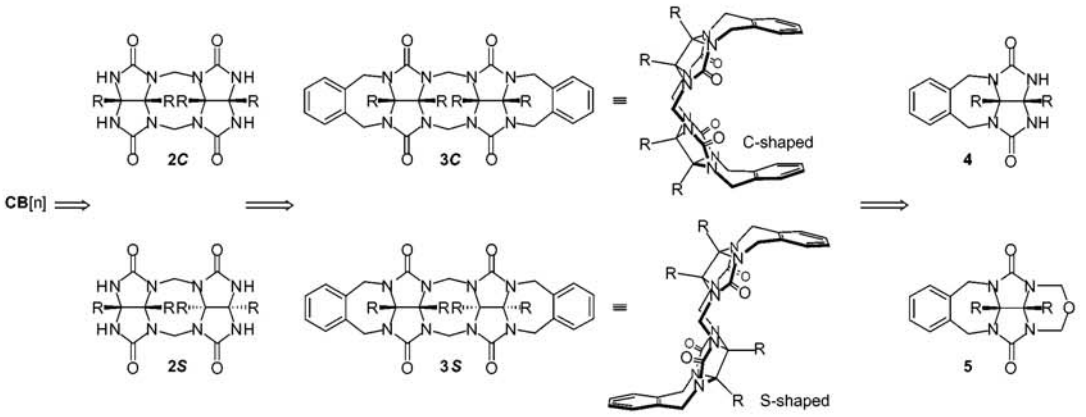

the fundamental structural unit of cucurbituril (Scheme 1). To minimize the synthetic challenges posed by the presence of four ureidyl NH groups in **2*C*** and **2*S***, we further restrict the present study to the preparation of derivatives of **2*C*** and **2*S*** comprising a single set of methylene bridges and bearing two *o*-xylylene groups (**3*C*** and **3*S***). We use the suffixes ***C*** and ***S*** throughout this paper to distinguish between these two diastereomers because their three-dimensional structures resemble those letters (Scheme 1). A successful synthesis of congeners of cucurbituril requires control over the relative stereochemistry of each pair of methylene-bridged glycoluril dimers. For example, consideration of the pair of diastereomers **3*C*** and **3*S*** reveals that only the C-shaped diastereomer **3*C*** is capable of being transformed into a derivative of cucurbituril, since the S-shaped diastereomer **3*S*** possesses the wrong relative stereochemistry. An important objective of the present work, therefore, is the development of methods that allow the diastereoselective formation of **3*C***. Our retrosynthetic analysis of **3*C*** and **3*S*** leads to ureidyl NH compound **4** and cyclic ether **5**. We envisioned that condensation reactions between **4** and **5** would proceed under acidic conditions where the nucleophilic tautomer of **4** could react with the iminium ion generated after protonation of **5**. To investigate the scope and limitations of the dimerization reaction used to prepare methylene-bridged glycoluril dimers, we needed to prepare derivatives of **4** and **5** bearing a range of solubilizing substituents on their convex faces and on their aromatic rings.

Synthesis of Glycoluril Building Blocks. Compounds **1a**−**d** were prepared by literature procedures.[29−33] We chose these four building blocks because (1) they were easily prepared, (2) they broadly represented the range of glycoluril derivatives typically encountered (alkyl, carboxylic acid derivative, aromatic, and heteroaromatic), and (3) they provided good solubility characteristics. The majority of glycoluril derivatives used in this paper, however, are derived from **1a**, which possesses two ethyl ester groups on its convex face. This choice is based on our interest in preparing water soluble methylene-bridged glycoluril dimers[27,34] and the fact that glycoluril derivatives bearing ethoxycarbonyl groups dimerize in high yield.

Synthesis of 1,2-Bis(halomethyl)aromatic Compounds. In their pioneering studies of molecular recognition, self-assembly, and catalysis, the groups of Nolte[35,36] and Rebek[37,38] have devised many practical synthetic methods for the preparation of derivatives of glycoluril. An important step in many of these syntheses involves the nucleophilic addition of glycoluril anions to 1,2-bis(halomethyl)aromatics to generate glycoluril derivatives bearing *o*-xylylene rings on one or both sides of the glycoluril skeleton.[39] Chart 2 shows the structures of 10 alkylating agents (**6**−**15**) that we have used in our synthetic studies. Of these 10 alkylating agents, **6** and **14** were commercially available, **7**,[40] **8**,[41,42] **10**,[43] **11**,[44] and **15**[45] were prepared by literature procedures, and **9**, **12**,

(29) Branda, N.; Grotzfeld, R. M.; Valdéz, C.; Rebek, J. J. *J. Am. Chem. Soc.* **1995**, *117*, 7.
(30) Reek, J. N. H.; Kros, A.; Nolte, R. J. M. *Chem. Commun.* **1996**, 245−247.
(31) Butler, A. R.; Leitch, E. *J. Chem. Soc., Perkin Trans. 2* **1980**, 103−105.
(32) Gompper, R.; Nöth, H.; Rattay, W.; Schwarzensteiner, M.-L.; Spes, P.; Wagner, H.-U. *Angew. Chem., Int. Ed. Engl.* **1987**, *26*, 1039−1041.
(33) Kutepov, D. F.; Potashnik, A. A.; Khokhlov, D. N.; Tuzhilkina, V. A. *J. Gen. Chem. USSR* **1959**, *29*, 840−842.
(34) Isaacs, L.; Witt, D. *Angew. Chem., Int. Ed.* **2002**, *41*, 1905−1907.
(35) Rowan, A. E.; Elemans, J. A. A. W.; Nolte, R. J. M. *Acc. Chem. Res.* **1999**, *32*, 995−1006.
(36) Sijbesma, R. P.; Nolte, R. J. M. *Top. Curr. Chem.* **1995**, *175*, 25−56.
(37) Rebek, J., Jr. *Chem. Soc. Rev.* **1996**, *25*, 255−264.
(38) Rebek, J., Jr. *Acc. Chem. Res.* **1999**, *32*, 278−286.
(39) (a) Valdéz, C.; Spitz, U. P.; Toledo, L. M.; Kubik, S. W.; Rebek, J. J. *J. Am. Chem. Soc.* **1995**, *117*, 12733−12745. (b) Wyler, R.; de Mendoza, J.; Rebek, J., Jr. *Angew. Chem., Int. Ed. Engl.* **1993**, *32*, 1699−1701. (c) O'Leary, B. M.; Szabo, T.; Svenstrup, N.; Schalley, C. A.; Luetzen, A.; Schaefer, M.; Rebek, J., Jr. *J. Am. Chem. Soc.* **2001**, *123*, 11519−11533. (d) Reek, J. N. H.; Kros, A.; Nolte, R. J. M. *Chem. Commun.* **1996**, 245−247. (e) Elemans, J. A. A. W.; de Gelder, R.; Rowan, A. E.; Nolte, R. J. M. *Chem. Commun.* **1998**, 1553−1554. (f) Jansen, R. J.; Rowan, A. E.; de Gelder, R.; Scheeren, H. W.; Nolte, R. J. M. *Chem. Commun.* **1998**, 121−122.
(40) Diederich, F.; Jonas, U.; Gramlich, V.; Herrmann, A.; Ringsdorf, H.; Thilgen, C. *Helv. Chim. Acta* **1993**, *76*, 2445−2453.
(41) Ardecky, R. J.; Kerdesky, F. A. J.; Cava, M. P. *J. Org. Chem.* **1981**, *46*, 1483−1485.
(42) Kang, J.; Hilmersson, G.; Santamaría, J.; Rebek, J. J. *J. Am. Chem. Soc.* **1998**, *120*, 3650−3656.
(43) Shahak, I.; Bergmann, E. D. *J. Chem. Soc. C* **1966**, 1005−1009.

CHART 2

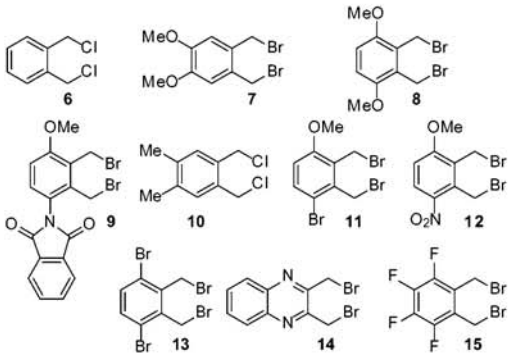

and **13** were prepared by bromination of the corresponding *o*-xylylene derivatives with *N*-bromosuccinimide in CCl_4.[46,47]

Synthesis of Glycoluril Derivatives Bearing Two Ureidyl NH Groups and a Single *o*-Xylylene Group. For the preparation of glycoluril derivatives bearing a single substituted *o*-xylylene sidewall, we adapted chemistry developed by the groups of Rebek and Nolte.[39] Treatment of glycoluril derivatives **1a**−**d** with *t*-BuOK in DMSO results in nucleophilic species that react with bis(halomethyl)aromatics **6**−**15** yielding glycoluril derivatives **4a**−**d** and **16**−**24** (Chart 3 and Table 1) in low to moderate yields. Entries 1−4 (Table 1) illustrate the effect of the four different solubilizing groups (CO_2Et, Ph, 2-pyridyl, and $(CH_2)_4$) on the alkylation reaction with a single alkylating agent (**6**). The nature of the solubilizing group significantly affects the yield of the alkylation reaction, and in our hands, the alkylation of **1a** proceeds most smoothly, since the anion generated by treatment with *t*-BuOK is nicely soluble in DMSO and shows a lower tendency to form gels which lower yields significantly. Entries 1 and 5−13 illustrate the effect of the alkylating agent on the alkylation reaction; compounds **16**−**24** have been arranged from electron rich to electron poor. The electronic nature of the substituents on the aromatic ring does not have a discernible effect on the efficiency of the alkylation reaction, although we have noticed that extended reaction times lead to decreased yields in the case of the more electron deficient alkylating agents. Compounds (±)-**18**, (±)-**20**, and (±)-**21** are chiral because of the unsymmetrical arrangements of functional groups on their aromatic rings; these compounds are synthesized and used in this paper as the racemic mixture.

Synthesis of Cyclic Ethers by Acid-Catalyzed Condensation with Paraformaldehyde. Having secured a range of potentially nucleophilic glycoluril derivatives (**4a**−**d** and **16**−**24**) bearing a range of solubilizing groups on their convex faces and substituents on their aromatic rings, we turned to the problem of creating a series of potentially electrophilic glycoluril derivatives (**5a**−**f** and **25**−**28**). For this purpose, we turned to the work of Nolte, who has developed a methodology utilizing glycoluril-derived cyclic ethers, chloromethyl groups, acetoxymethyl groups, and hydroxymethyl groups for the generation of iminium ions that undergo efficient electrophilic aromatic substitution reactions.[48−52] For our purposes, the more stable cyclic ethers (Chart 4) were preferable. The Nolte cyclic ether synthesis[53] calls for sequential treatment with NaOH and formaldehyde in aq DMSO, followed by reflux in HCl at pH 1. We anticipated that these basic and aqueous acidic conditions might pose problems with substrates bearing ethoxycarbonyl groups. We, therefore, developed a one-step procedure that proceeds under anhydrous acidic conditions (TFA, reflux) using paraformaldehyde (Table 2). These reactions proceed in moderate to good yield and offer an alternative to Nolte's procedure when working with compounds containing potentially sensitive functional groups. The lowest yield (20%) was obtained for 2-pyridyl-substituted glycoluril **5c**. This result is not surprising, since the pyridyl ring is protonated in TFA, which probably raises the energy of the intermediates leading to **5c**, resulting in a reduced reaction rate or side reactions.

Synthesis of Methylene-Bridged Glycoluril Dimers. After preparing a series of glycoluril derivatives bearing potentially nucleophilic ureidyl NH groups (**4a**−**d** and **16**−**24**) and potentially electrophilic cyclic ether groups (**5a**−**f** and **25**−**28**), we turned our attention toward their condensation reactions that lead to methylene-bridged glycoluril dimers. Chart 5 gives a summary of the compounds (**29*C***−**44*C*** and **29*S***−**44*S***) that are discussed in this paper. There are three synthetic methods that lead from the two sets of building blocks to methylene-bridged glycoluril dimers: (1) the reaction of 2 equiv of **4** with a source of formaldehyde, (2) the condensation of **4** with cyclic ether **5**, and (3) the reaction of 2 equiv of **5** with the formal extrusion of formaldehyde. In each case, we propose that the reaction proceeds through a common set of intermediates (Scheme 2), although many subtle variations are possible and we do not have evidence to exclude those possibilities in this discussion. Compound **4** can tautomerize into nucleophile (±)-**45**, which after reaction with formaldehyde, proton transfer, loss of water, and tautomerization leads to the racemic mixture (±)-**47**. Similarly, protonation of cyclic ether **5** followed by extrusion of formaldehyde also leads to racemic mixture (±)-**47**. At this stage, two different scenarios are possible: **47** can react with a molecule of like handedness (**45**) or it can react with a molecule of opposite handedness (*ent*-**45**). Reaction between **47** and **45** gener-

(44) Goldberg, Y.; Bensimon, C.; Howard, A. *J. Org. Chem.* **1992**, *57*, 6374−6376.
(45) Coe, P. L.; Croll, B. T.; Patrick, C. R. *Tetrahedron* **1967**, *23*, 505−508.
(46) Knölker, H. J.; Bauermeister, M.; Pannek, J. B. *Tetrahedron* **1993**, *49*, 841−862.
(47) Lai, Y.-H.; Yap, A. H.-T. *J. Chem. Soc., Perkin Trans. 2* **1993**, 1373−1377.
(48) Smeets, J. W. H.; Sijbesma, R. P.; Niele, F. G. M.; Spek, A. L.; Smeets, W. J. J.; Nolte, R. J. M. *J. Am. Chem. Soc.* **1987**, *109*, 928−929.
(49) Niele, F. G. M.; Zwikker, J. W.; Nolte, R. J. M. *Tetrahedron Lett.* **1986**, *27*, 243−246.
(50) Smeets, J. W. H.; Sijbesma, R. P.; van Dalen, L.; Spek, A. L.; Smeets, W. J. J.; Nolte, R. J. M. *J. Org. Chem.* **1989**, *54*, 3710−3717.
(51) Sijbesma, R. P.; Nolte, R. J. M. *Recl. Trav. Chim. Pays-Bas* **1993**, *112*, 643−647.
(52) Reek, J. N. H.; Elemans, J. A. A. W.; Nolte, R. J. M. *J. Org. Chem.* **1997**, *62*, 2234−2243.
(53) Niele, F. G. M.; Nolte, R. J. M. *J. Am. Chem. Soc.* **1988**, *110*, 172−177.

CHART 3

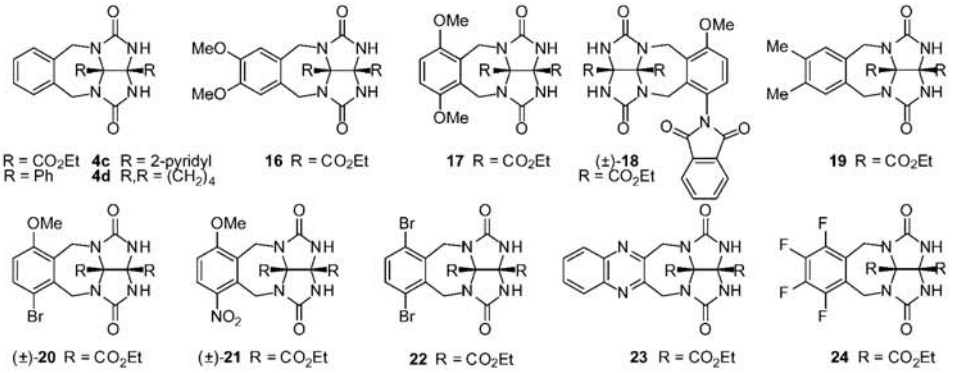

TABLE 1. Synthesis of 4b–d and 16–24

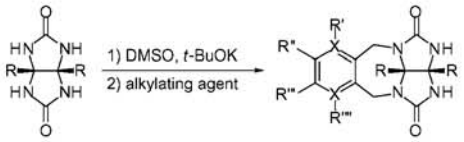

entry	R	alkylating agent	product	yield (%)
1	CO_2Et	**6**	**4a**	84[a]
2	Ph	**6**	**4b**	62
3	2-pyridyl	**6**	**4c**	43
4	$(CH_2)_4$	**6**	**4d**	31
5	CO_2Et	**7**	**16**	45
6	CO_2Et	**8**	**17**	47
7	CO_2Et	**9**	**18**	22
8	CO_2Et	**10**	**19**	68
9	CO_2Et	**11**	**20**	62
10	CO_2Et	**12**	**21**	32
11	CO_2Et	**13**	**22**	37
12	CO_2Et	**14**	**23**	26
13	CO_2Et	**15**	**24**	45

[a] Ref 39a.

ates intermediate **48*S***, which is transformed into **49*S*** and ultimately into the S-shaped product **3*S***. Conversely, reaction between **47** and *ent*-**45** generates intermediate **48*C***, which leads to the C-shaped methylene-bridged glycoluril dimer via intermediate **49*C***. Since a highly diastereoselective reaction is not expected between intermediates **45** and **47**, one would expect to isolate a mixture of the S-shaped and C-shaped methylene-bridged glycoluril dimers if the reaction is run under kinetically controlled conditions. If, however, the reaction is run under thermodynamically controlled conditions, the ratio of the two products will be dictated solely by the relative free energies of the S- and C-shaped diastereomers.

Homodimerization Reactions of Ureidyl NH Compounds. The most straightforward synthesis of methylene-bridged glycoluril dimers involves the condensation reaction between 2 equiv of **4** and 2 equiv of formaldehyde. Our standard procedure (Scheme 3) involves heating the reactants at reflux in 1,2-dichloroethane containing *p*-toluenesulfonic acid as acid catalyst under anaddition funnel filled with molecular sieves for at least 1 day. Table 3 summarizes 12 homodimerization reactions that we have performed. In all cases, we observe a moderate

CHART 4

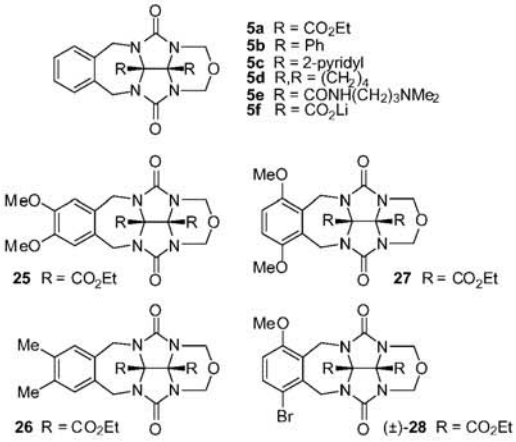

TABLE 2. Synthesis of Cyclic Ethers under Anhydrous Acidic Conditions

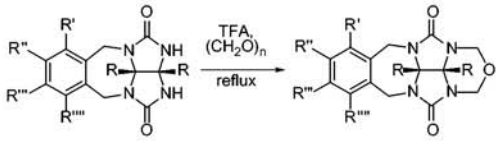

entry	R	starting material	product	yield (%)
1	CO_2Et	**4a**	**5a**	44
2	2-pyridyl	**4c**	**5c**	20
3	$(CH_2)_4$	**4d**	**5d**	63
4	CO_2Et	**16**	**25**	52
5	CO_2Et	**17**	**27**	56
6	CO_2Et	**19**	**26**	55
7	CO_2Et	**20**	**28**	34

to large preference for the formation of the C-shaped diastereomers. Such a preference, if general, would explain the high yields obtained in the synthesis of **CB**[*n*].

Entries 1–4 (Table 3) illustrate the pronounced influence of the solubilizing groups on the convex face of the glycoluril ring on the dimerization reaction. For example,

CHART 5. Chemical Structures of Methylene-Bridged Glycoluril Dimers

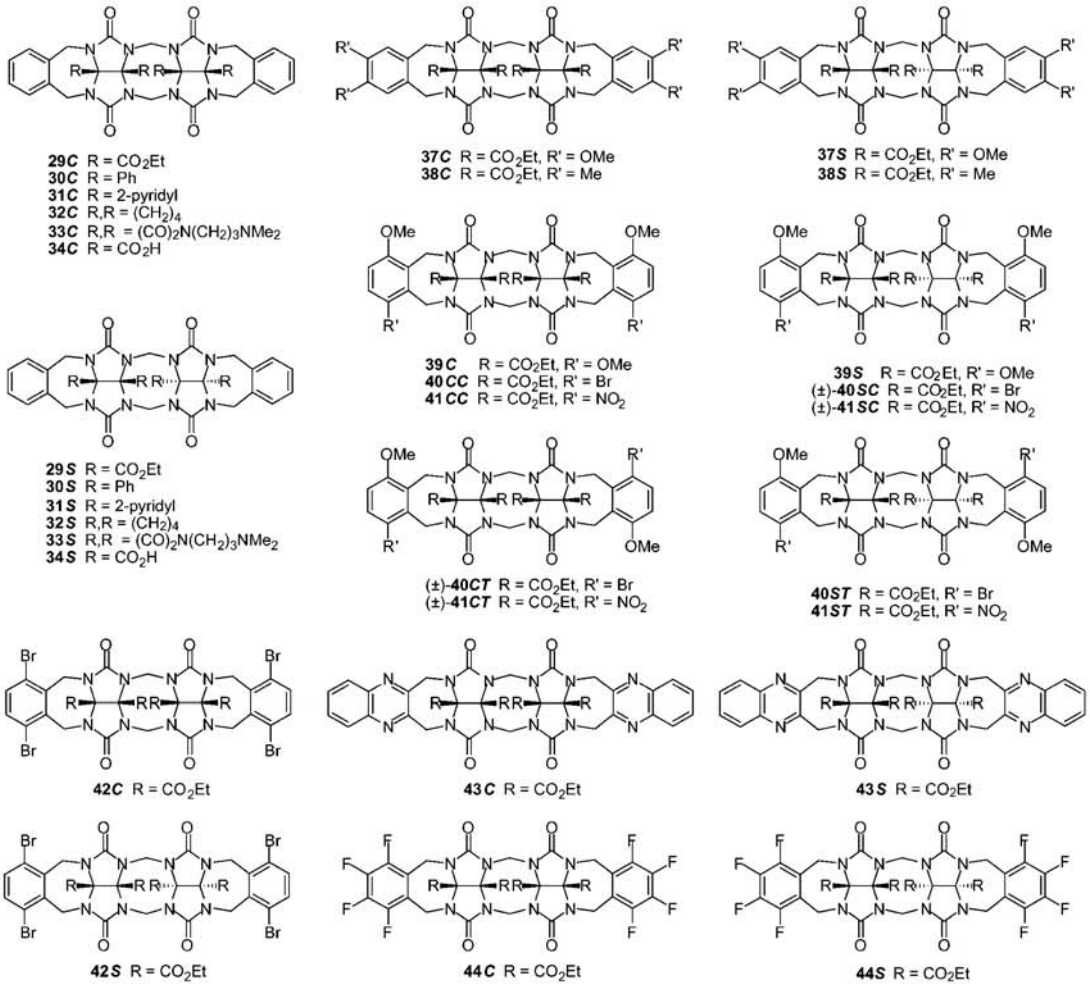

the dimerization reaction with ethoxycarbonyl-substituted glycoluril **4a** (entry 1) furnishes only the C-shaped diastereomer **29*C***, whereas cyclohexyl- and phenyl-substituted glycolurils **4d** and **b** (entries 4 and 2) proceed in lower yield and with the formation of side products **35** and **36**. For **4c**, with 2-pyridyl solubilizing groups, we did not detect either **31*C*** or **31*S*** by ^{1}H NMR. These changes in yield and product distribution cannot be explained by steric differences. Below, we present a mechanistic rationale for these changes based on the electronic nature of the solubilizing groups.

The remaining entries in Table 3 focus on the chemistry of glycoluril derivatives bearing ethoxycarbonyl solubilizing groups, since those substrates result in efficient dimerization reactions. Entries 5 and 7−12 illustrate that the dimerization reaction tolerates a variety of different substituents on their aromatic rings (OMe, Br, NO_2, F, and heteroaromatics). The nature and location of substituents can, however, significantly influence the rate and yield of the reaction. For example, simply changing the location of two methoxy groups (compare entries 5 and 6) resulted in decomposition rather than dimerization, and the presence of a quinoxaline ring (entry 11) lowers the yield and greatly reduces the reaction rate presumably because of the protonation of the quinoxaline ring N-atom.

As mentioned above, compounds (±)-**20** and (±)-**21** are chiral and racemic because of the unsymmetrical arrangements of substituents on their *o*-xylylene rings. In the dimerization reaction of (±)-**21** (Table 3, entries 9), two C-shaped and two S-shaped diastereomers were isolated and characterized. We denote these compounds as **41*CC*** (*C*-shaped, OMe groups *cis*), (±)-**41*CT*** (*C*-shaped, OMe groups *trans*), (±)-**41*SC*** (*S*-shaped, OMe groups *cis*), and **41*ST*** (*S*-shaped, OMe groups *trans*). Compounds **41*CC*** and **41*ST*** result from the dimerization of two molecules of opposite handedness and are achiral *meso* compounds, whereas the racemic mixtures (±)-

SCHEME 2. Outline of Three Pathways to Methylene-Bridged Glycoluril Dimers[a]

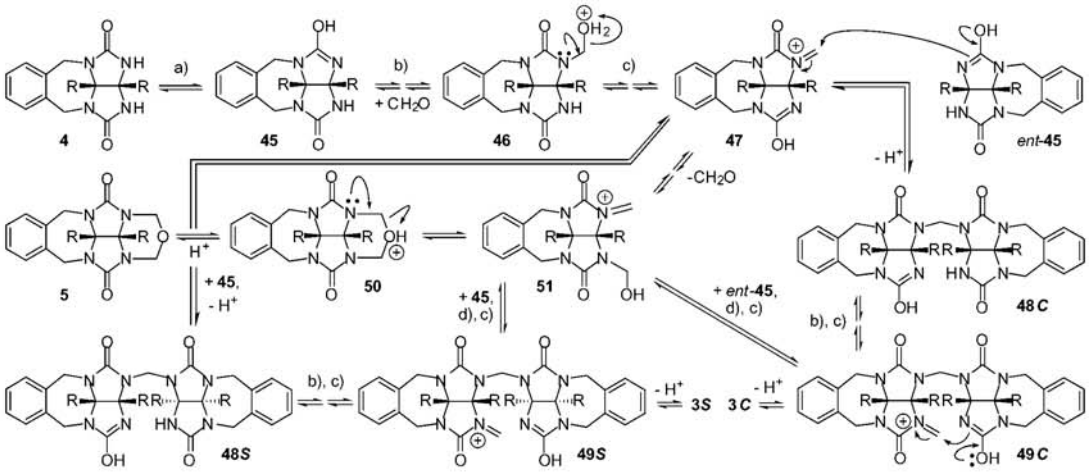

[a] Mechanistic steps: (a) tautomerization, (b) nucleophilic addition (+CH_2O) and proton transfer, (c) loss of water and tautomerization, (d) proton transfer.

SCHEME 3. Dimerization of Glycoluril Derivatives with Ureidyl NH Compounds

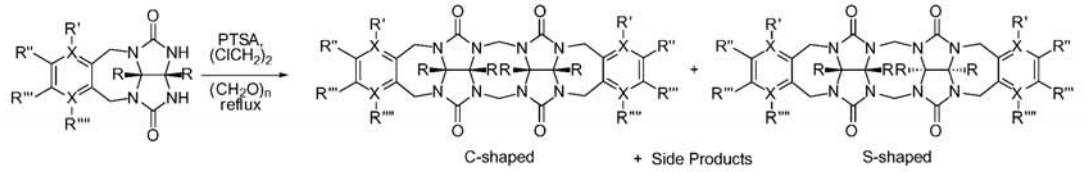

TABLE 3. Dimerization of Glycoluril Derivatives Bearing Ureidyl NH Groups

entry	R	starting material	C-shaped (yield, %)		S-shaped (yield, %)		side product(s) (yield, %)
1	CO_2Et	**4a**	**29*C***	(88)	**29*S***	(nd)	
2	Ph	**4b**	**30*C***	(19)	**30*S***	(nd)	**35b** (26), **36b** (2)
3	2-pyridyl	**4c**	**31*C***	(nd)[a]	**31*S***	(nd)	
4	$(CH_2)_4$	**4d**	**32*C***	(57)	**32*S***	(nd)	**35d** (9), **36d** (5)
5	CO_2Et	**16**	**37*C***	(87)	**37*S***	(nd)	
6	CO_2Et	**17**	**39*C***	(nd)	**39*S***	(nd)	
7	CO_2Et	**19**	**38*C***	(75)	**38*S***	(6)	
8	CO_2Et	**20**	**40*CC***	(46)	**40*SC***	(nd)	
			40*CT*	(48)	**40*ST***	(nd)	
9	CO_2Et	**21**	**41*CC***	(28)	**41*SC***	(21)	
			41*CT*	(24)	**41*ST***	(22)	
10	CO_2Et	**22**	**42*C***	(47)	**42*S***	(10)	
11	CO_2Et	**23**	**43*C***	(35)	**43*S***	(18)	
12	CO_2Et	**24**	**44*C***	(44)	**44*S***	(3)	

[a] nd = not detected.

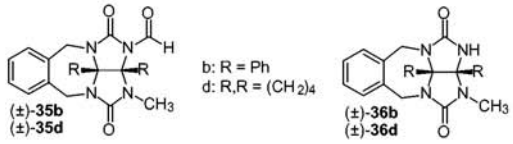

41*CT* and (±)-**41*SC*** result from the dimerization of **21** of like handedness. In this example, a nearly statistical distribution of the four stereoisomers was obtained. In contrast, the dimerization of (±)-**20** yielded exclusively the C-shaped diastereomers **40*CC*** and (±)-**40*CT*** in 94% combined yield.

Separation, Identification, and X-ray Crystallographic Characterization of the C-Shaped and S-Shaped Diastereomers. Gratifyingly, the separation of the crude reaction mixtures described in Table 3 was possible using simple silica gel chromatography. The conformationally rigid C-shaped diastereomers have higher dipole moments, lower R_f values, and lower solubilities in common organic solvents than the corresponding S-shaped diastereomers ($\mu = 0$ D by symmetry arguments), which facilitate their purification. Spectroscopic identification of the C-shaped and S-shaped diastereomers is based on a combination of ^{1}H and ^{13}C NMR spectroscopy and symmetry arguments. Consider, for example, the C-shaped and S-shaped diastereomers **38*C*** and **38*S*** (Table 3, entry 7). The C-shaped diastereomer **38*C*** is C_{2v}-symmetric, whereas **38*S*** has time-averaged C_{2h}-symmetry. These symmetry differences manifest themselves in the number of resonances expected for the newly formed methylene bridges; for **38*C*** we expect and observe a pair of doublets for the diastereotopic methylene protons (6.02 and 4.58 ppm), whereas for **38*S*** we expect and observe a singlet (5.00 ppm) for the chemically equivalent methylene protons. These symmetry considerations are sufficient to allow complete spectroscopic identification of methylene-bridged glycoluril dimers prepared from two achiral building blocks. A peculiar but particularly diagnostic feature of the ^{1}H NMR spectra of

all of the S-shaped diastereomers that we have prepared to date is the significant upfield shift observed for only one of the two chemically nonequivalent CH_2 groups of the $CO_2CH_2CH_3$ solubilizing groups. For example, for **38*S*** the two methylene groups resonate at 4.19 and 3.58 ppm, whereas for **38*C*** both resonate at 4.17 ppm. The X-ray crystal structure of **38*S*** (Figure 1) provides an explanation for this observation. In each of two rapidly equilibrating S-shaped conformations of **38*S***, one of the methylene groups of the internal CO_2Et groups is in the shielding region of the aromatic ring of the opposing sidewall, leading to the observed upfield shift. A similarly diagnostic feature of the S-shaped versus the C-shaped diastereomers is the ^{13}C NMR chemical shifts of the central methylene bridges. For **38*C*** these carbon atoms resonate at 47.8 ppm, whereas for **38*S*** they resonate at 51.8 ppm. In general, the C-shaped diastereomers resonate at ≈47−48 ppm, and the S-shaped diastereomers resonate at 51−52 ppm.[17] These three criteria and symmetry arguments allow complete structural assignments of even the most complicated C_s-, C_2-, and C_1-symmetric methylene-bridged glycoluril dimers (examples: **41*CC***, (±)-**41*CT***, (±)-**41*SC***, and **41*ST***).

The structural assignments of the C-shaped and S-shaped diastereomers based on ^1H and ^{13}C NMR and symmetry arguments described above have been further corroborated by X-ray crystallography of many of our compounds. Figure 1 shows the X-ray structures determined for **30*C***, **38*C***, and **38*S***. Compounds **30*S*** and **38*C*** assume C-shaped conformations with their *o*-xylylene rings roughly parallel. All four solubilizing groups (Ph and CO_2Et) are displayed on one face of the molecule, resulting in an amphiphilic topology. Compound **38*C*** crystallized as the CH_3CN solvate; one of the solvating CH_3CN molecules fills its cleft with the CH_3 group oriented toward the glycoluril rings. The distances between the centers of the *o*-xylylene rings of **30*C*** and **38*C***, defined as the C1−C2−C3−C4−C4A−C18A and C9A−C10−C11−C12−C13−C13A centroids, are 7.366 and 7.588 Å, respectively. Because of the slight tapering of the cleft, the distances between the tips of the *o*-xylylene rings, defined as the distance between the centroids of the C2−C3 and C11−C12 bonds, are 6.951 and 7.258 Å for **30*C*** and **38*C***, respectively. The mean planes of the aromatic rings of **30*C*** and **38*C*** intersect each other with angles of 21.8° and 17.1°, respectively. There is a slight overall end-to-end twist of the C-shaped molecules of **30*C*** (−4.0°) and **38*C*** (−3.3°), as measured by the dihedral angle through the centroids of the C2−C3, C4A−C18A, C9A−C13A, and C11−C12 bonds. The substituents on the convex face of **30*C*** and **38*C*** are nearly eclipsed; the C5B−C5A−C6A−C6B and C7B−C7A−C8A−C8B dihedral angles measure 9.6° and 3.4° (**30*C***) and −1.6° and 1.4° (**38*C***), respectively. The substituents at C6A and C7A on the convex face of the molecules are nearly collinear; the C6B−C6A−C7A and C7B−C7A−C6A angles amount to 95.0° and 94.7° (**30*C***) and 96.5° and 95.0° (**38*C***), respectively. The separations between these substituents, as measured by the C6B−C7B distance, are 3.985 Å (**30*C***) and 3.984 Å (**38*C***), indicating that they are not in van der Waals contact. The N6−C7−N7 and N16−C16−N15 bond angles of the methylene bridges amount to 116.2° and 118.3° (**30*C***) and 114.8° and 115.0° (**38*C***). These values are larger than the tetrahedral bond angle, as are those observed for Me_{10}**CB**[5] (114.0°−115.4°)[13] and **CB**[5] (113.2°−114.7°), **CB**[6] (112.9°−

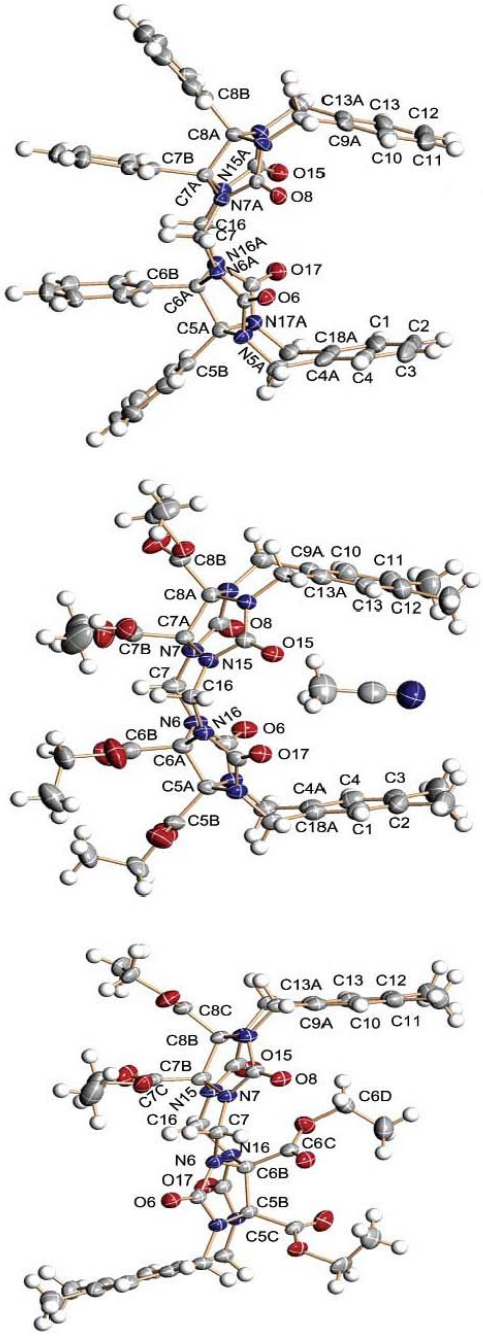

FIGURE 1. X-ray crystal structures of **30*C***, **38*C***, and **38*S***. The solvating $CHCl_3$ and toluene molecules have been removed from the structure of **30*C***.

SCHEME 4. Dimerization Reactions of Glycoluril-Derived Cyclic Ethers

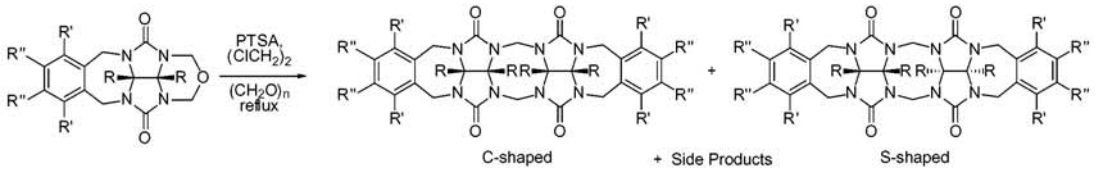

TABLE 4. Dimerization Reactions of Glycoluril-Derived Cyclic Ethers

entry	R	starting material	C-shaped (yield, %)		S-shaped (yield, %)		side product(s) (yield, %)
1	CO_2Et	**5a**	**29*C***	(92)	**29*S***	(nd)	
2	Ph	**5b**	**30*C***	(nd)[a]	**30*S***	(nd)	**35b** (42)
3	2-pyridyl	**5c**	**31*C***	(nd)	**31*S***	(nd)	
4	$(CH_2)_4$	**5d**	**32*C***	(34)	**32*S***	(nd)	**35d** (16), **36d** (12)
5	$CONH(CH_2)_3NMe_2$	**5e**	**33*C***	(85)	**33*S***	(nd)	
6	CO_2Li	**5f**	**34*C***	(85)	**34*S***	(nd)	
7	CO_2Et	**25**	**37*C***	(93)	**37*S***	(nd)	
8	CO_2Et	**26**	**38*C***	(87)	**38*S***	(3)	
9	CO_2Et	**27**	**39*C***	(nd)	**39*S***	(nd)	

[a] nd = not detected.

115.0°), **CB**[7] (112.7°−114.5°), and **CB**[8] (113.0°−113.6°).[1,15] The ureidyl N atoms involved in the central eight-membered ring do not show significant deviations from planarity; the sum of the three bond angles around N6A, N7A, N15A, and N16A of **30*C*** amount to 358.3°, 359.9°, 359.5°, and 359.8°, whereas those around N6, N7, N15, and N16 of **38*C*** amount to 359.0°, 359.9, 359.0°, and 360°, respectively. The distances between the carbonyl oxygens (O6−O17 and O8−O15) of a single glycoluril ring are 5.611 and 5.653 Å (**30*C***) and 5.755 and 5.785 (**38*C***), distances that are slightly larger than those observed for related molecules containing a single glycoluril ring[48−50] but smaller than those observed for **CB**[5] (6.176−6.217 Å), **CB**[6] (5.98−6.042 Å), **CB**[7] (5.913−6.114 Å), and **CB**[8] (6.041−6.171 Å).[1,15] The distances between oxygen atoms of adjacent glycoluril rings (O6−O8 and O15−O17) are 3.405 and 3.309 Å (**30*C***) and 3.424 and 3.389 Å (**38*C***), respectively. These distances are larger than those observed in the crystal structures of Me_{10}**CB**[5] (average, 3.177 Å; range, 3.141−3.218 Å)[13] and **CB**[5] (average, 3.310 Å; range, 3.184−3.602 Å), comparable to those of **CB**[6] (average, 3.4025 Å; range, 3.138−3.624 Å), and shorter than those of **CB**[7] (average, 3.627 Å; range, 3.405−3.859 Å) and **CB**[8] (average, 3.810 Å; range, 3.695−3.906 Å).[1,15]

In constrast to **30*C*** and **38*C***, diastereomer **38*S*** crystallizes in an S-shaped conformation that displays two ethoxycarbonyl groups on each face of the molecule. One of the most interesting features of the crystal structure of **38*S*** is the close proximity of methylene carbon atom C6D to the centroid of the aromatic ring defined by C9A−C10−C11−C12−C13−C13A (3.713 Å). One of the protons attached to C6D is a mere 2.951 Å from the centroid of this aromatic ring. The close proximity of this proton to the center of the aromatic ring places it in its shielding region, which provides an explanation for the observation of the significant upfield shifts observed for these protons in the ^{1}H NMR of the S-shaped diastereomers. The most notable structural effect of the relative stereochemistry of the S-shaped diastereomers is present in the central eight-membered ring. For example, the sums of the bond angles around ureidyl nitrogen atoms N6, N7, N15, and N16 of **38*S*** amount to 350.1°, 357.9°, 359.9°, and 346.3°. N atoms N6 and N16 are decidedly nonplanar, suggesting the presence of strain relative to C-shaped diastereomers **30*C*** (average, 359.4°; range, 358.3°−359.9°) and **38*C*** (average, 359.5°; range, 359.0°−360°) and cucurbiturils Me_{10}**CB**[5] (average, 359.7°; range, 359.5°−360), **CB**[5] (average, 358.7°; range, 357.3°−359.9°), **CB**[6] (average, 358.8°; range, 356.0°−360°), **CB**[7] (average, 358.1°; range, 354.9°−359.9°), and **CB**[8] (average, 357.3°; range, 355.3°−358.2°).[1,13,15] Other structural features are comparable between the C- and S-shaped diastereomers. For example, the N6−C7−N7 and N15−C16−N16 bond angles measure 110.9° and 113.9°, values only slightly smaller than those observed for **30*C*** and **38*C***. The substituents on the convex face of the glycoluril rings are once again nearly eclipsed with C5C−C5B−C6B−C6C and C7C−C7B−C8B−C8C dihedral angles of −5.0° and −5.5°.

Homodimerization Reactions of Cyclic Ethers. The mechanistic rationale proposed in Scheme 2 suggests that cyclic ethers should also participate in this dimerization reaction (Scheme 4). Table 4 shows the results of the dimerization reactions from cyclic ethers that we have performed to date. Entries 1−6 illustrate the influence of the solubilizing groups on the convex face of the glycoluril skeleton on the dimerization reaction. Substrates **5a**, **e**, and **f** (entries 1, 5, and 6) that bear electron withdrawing carboxylic acid derivatives on their convex face are efficient substrates yielding only the C-shaped diastereomers in high yield. As in the case of the dimerization from the ureidyl NH compounds (Table 3), the substrates bearing Ph, fused-cyclohexyl, and 2-pyridyl substituents are poor substrates for the reaction (Table 4, entries 2−4), and both **5b** and **5d** lead to side products (±)-**35** and (±)-**36**. Compounds bearing functionalized *o*-xylylene rings are also acceptable substrates for this reaction (Table 4, entries 1, 7, and 8). Interestingly, we could not detect either **39*C*** or **39*S*** in the dimerization reaction with **27**. Similar behavior was observed in the dimerization reaction of **17** (Table 3, entry 6).

SCHEME 5. Dimerization Reactions from Ureidyl NH and Cyclic Ether Compounds

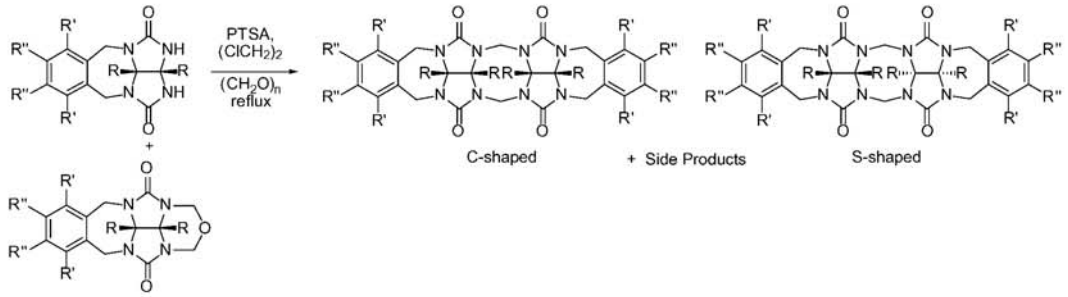

The survey of the substrates that participate effectively in this reaction is not as extensive as that described in Table 3 because the cyclic ethers themselves must be derived from the corresponding compounds containing ureidyl NH groups. Additionally, a comparison of the results obtained by these two methods (Table 3, entries 1−7 versus Table 4, entries 1−4 and 7−9) indicates that dimerization occurs in comparable yield in most cases. The single exception is the dimerization reaction of phenyl glycoluril (**5b**), a poor substrate for our reaction, which yields **30*C*** only from **4b** (Table 3, entry 2 versus Table 4, entry 2). These considerations suggest that the method described in Table 3 is preferable, since the cyclic ether substrates are themselves derived from the ureidyl NH compounds in only moderate yield (Chart 4, Table 2).

Heterodimerization Reactions of Ureidyl NH Compounds and Cyclic Ethers. The dimerization reactions described in Tables 3 and 4 offer two routes to the preparation of methylene-bridged glycoluril dimers. Of these two methods, the direct dimerization of the ureidyl NH compounds is preferable. On the basis of the mechanism of the dimerization reaction proposed in Scheme 2, we considered the possibility of performing a selective heterodimerization reaction by the reaction between 1 equiv of ureidyl NH compound and 1 equiv of cyclic ether (Scheme 5). The success of this method, the selective synthesis of a dimer comprising two different *o*-xylylene rings, requires a fast reaction between intermediates **45** and **51** (Scheme 2) and that the equilibria connecting those intermediates (via **46** and **47**) that result in the scrambling of the methylene bridges are slow relative to methylene-bridged glycoluril dimer formation.

Initially, we choose to study reactions between ureidyl NH compounds and cyclic ethers that would result in homodimeric species to limit the potential complexity of the reaction. Table 5 summarizes the results of the experiments that we performed. The effects of the solubilizing groups on the convex face of the glycoluril on the dimerization reaction (Table 5, entries 1−4) are similar to those observed for the direct dimerization of **4a−d** (Table 3) or **5a−d** (Table 4). Glycoluril derivatives bearing electron withdrawing ethoxycarbonyl groups (Table 5, entry 1) dimerized much more readily than those bearing phenyl or fused cyclohexyl groups (entries 2 and 4), and those bearing the readily protonated pyridyl substituents (entry 3) were resistant to dimerization. Those glycoluril derivatives bearing ethoxycarbonyl solubilizing groups that undergo smooth homodimerization also yield dimers by the heterodimerization route (Table 5, entries 5 and 7; Table 4, entries 7 and 8; Table 3, entries 5 and 7). There are situations, however, where the heterodimerization reaction is preferable to either of the two homodimerization pathways. For example, even though neither homodimerization pathway allowed the detection of either **39*C*** or **39*S*** (Table 3, entry 6; Table 4, entry 9), the heterodimerization pathway (Scheme 5) allowed the isolation of **39*C*** in good yield (Table 5, entry 6). In those cases, where direct dimerization reactions fail, the heterodimerization route offers a viable alternative.

TABLE 5. Dimerization Reactions from Ureidyl NH and Cyclic Ether Compounds

entry	R	starting material	C-shaped (yield, %)	S-shaped (yield, %)	side product(s) (yield, %)
1	CO_2Et	**4a** + **5a**	**29*C*** (89)	**29*S*** (2)	
2	Ph	**4b** + **5b**	**30*C*** (16)	**30*S*** (nd)	**35b** (70)
3	2-pyridyl	**4c** + **5c**	**31*C*** (nd)[a]	**31*S*** (nd)	
4	$(CH_2)_4$	**4d** + **5d**	**32*C*** (30)	**32*S*** (nd)	**35d** (12), **36d** (10)
5	CO_2Et	**16** + **25**	**37*C*** (91)	**37*S*** (2)	
6	CO_2Et	**17** + **27**	**39*C*** (56)	**39*S*** (nd)	
7	CO_2Et	**19** + **26**	**38*C*** (90)	**38*S*** (3)	

[a] nd = not detected.

To fully demonstrate the synthetic utility of the heterodimerization reaction (Scheme 5), it was necessary to prepare true heterodimers, methylene-bridged glycoluril dimers comprising two different *o*-xylylene rings, and show that these heterodimers are produced selectively at the expense of the corresponding homodimers. Table 6 shows the results of three heterodimerization reactions that we have performed. Entry 1 shows the heterodimerization of dimethoxyxylylene ureidyl NH compound **16** and xylylene cyclic ether **5a**. In theory, six dimers might be formed (homodimers **29*C***, **29*S***, **37*C***, and **37*S*** and heterodimers **52*C*** and **52*S***); in practice, we isolate the two heterodimers and the two C-shaped homodimers. The desired heterodimers **52*C*** and **52*S*** were obtained in high combined yield (81%), with a modest level of diastereoselectivity favoring the C-shaped diastereomer **52*C***. This level of diastereoselectivity was particularly surprising, considering the fact that the relative stereochemistry of the product is set during the first covalent bond forming reaction between the two reaction partners (Scheme 2, (±)-**45** + (±)-**51**). In a separate report, we present a mechanistic rationale for the enhanced yield of the

TABLE 6. Heterodimerization Reactions

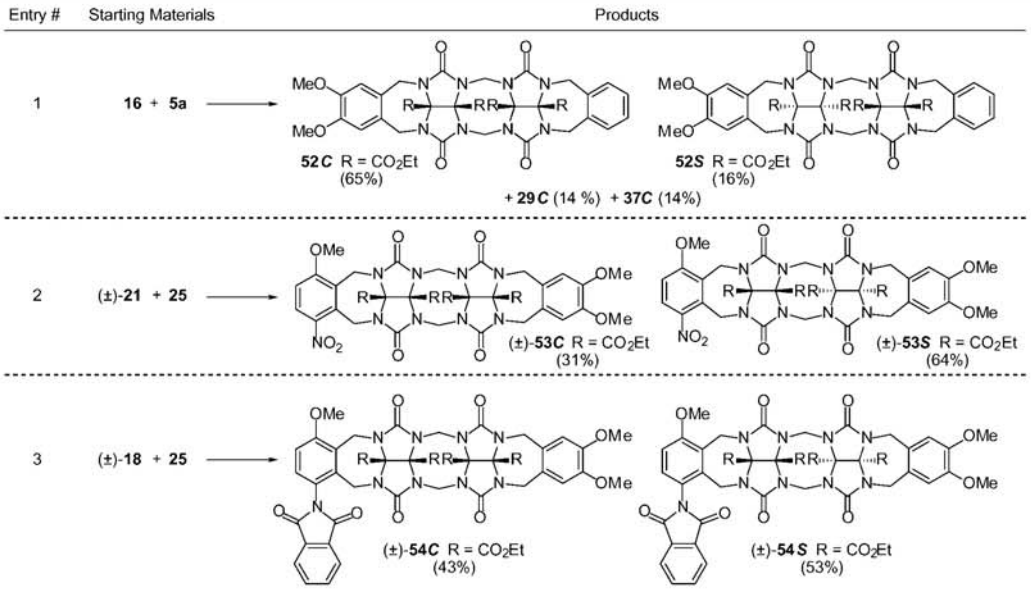

C-shaped heterodimer.[54] Table 6 (entries 2 and 3) shows the reactions of the racemic ureidyl NH compounds (±)-**21** and (±)-**18** with the dimethoxyxylylene cyclic ether **25**. In these cases, of the six possible products, we observe only two, the desired heterodimers, and isolate them in excellent combined yield. In contrast to entry 1 (Table 6), these two heterodimerization reactions produce the S-shaped diastereomers with modest diastereoselectivities. These three experiments and the results of Tables 3−5 that demonstrate a preference for the C-shaped diastereomers suggest that the formation of the mixture of C- and S-shaped diastereomers occurs under kinetic control (Table 6, entries 2 and 3) and that the preference for the C-shaped heterodimer (Table 6, entry 1) reflects thermodynamic control.[54]

Substituent Effects on the Mechanism of the Dimerization Reaction and Implications for CB[*n*] Synthesis. To date, **CB**[*n*] and fully substituted derivatives have been synthesized using glycolurils **1d**−**f**.[1,4,13−17,21] These three glycoluril derivatives represent only one of the four main classes of commonly encountered glycolurils (alkyl, aromatic, heteroaromatic, and carboxylic acid derivative). We were surprised by the lack of success in the synthesis of **CB**[*n*] derivatives using other glycoluril derivatives. The formation of cyclohexyl- and phenyl-substituted dimers **32*C*** and **30*C***, in sharp contrast to the dimerization reactions involving ethoxycarbonyl-substituted glycolurils, proceeds in modest yields and with the formation of side products **35** and **36**. These side products provide clues for the lack of success in the synthesis of fully substituted **CB**[*n*] from **1b**. Scheme 6 shows a mechanistic proposal for the formation of side products (±)-**35**. This mechanistic proposal is illustrated for the dimerization reactions of cyclic ethers **5**, but the mechanisms of all three types of dimerization reactions potentially involve common intermediates (Scheme 2).

SCHEME 6. Proposed Mechanism for the Formation of (±)-35 in the Dimerization Reactions

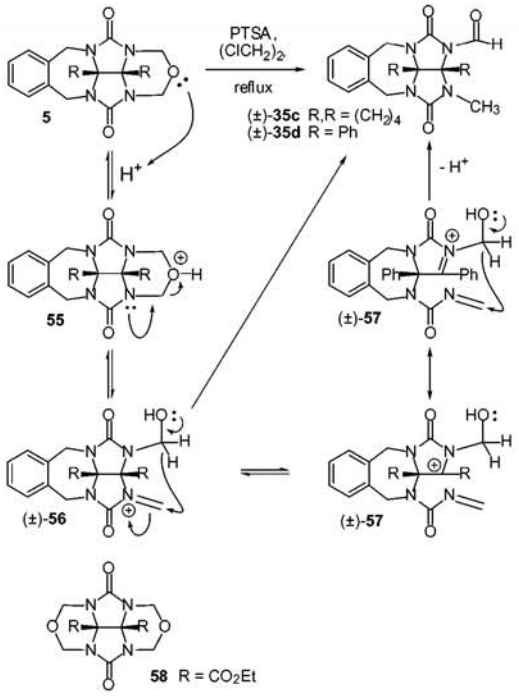

(54) Chakraborty, A.; Wu, A.; Witt, D.; Lagona, J.; Fettinger, J. C.; Isaacs, L. *J. Am. Chem. Soc.* **2002**, *124*, 8297−8306.

Cyclic ether **5** undergoes protonation on its ether oxygen (**55**), followed by ring opening to yield iminium ion (±)-**56**. Formally, the conversion of (±)-**56** into the observed products (±)-**35** occurs by a hydride shift. Formulation of the reaction as a hydride shift from (±)-**56** ignores the fact that only phenyl and cyclohexyl glycolurils generate these side products, since one would also expect ethoxycarbonyl-substituted glycolurils to generate similar side products. We have never observed aldehydic side products in the dimerization of ethoxycarbonyl-substituted glycoluril derivatives. Alternatively, one can postulate the formation of intermediates (±)-**57**. One would expect that intermediates (±)-**57** would be favored when R,R = $(CH_2)_4$ and R = Ph because of the ability of these groups to stabilize adjacent carbocations but disfavored when R = CO_2Et, since this group would destabilize an adjacent positive charge. The conversion of (±)-**57** into (±)-**35** is then formulated as an ene reaction of a cationic *N*-acyl iminium ion with an imine.[55] The lower yield obtained in the synthesis of **30*C*** than in that of **32*C*** can be explained by the fact that the phenyl substituents are better able to stabilize the adjacent positive charge in (±)-**57**, thereby leading to the enhanced yield of (±)-**35b** compared to (±)-**35d**. These observations have implications for the synthesis of derivatives of **CB**[*n*]. They suggest that the **CB**[*n*] synthesis is likely to be most successful in the case of glycoluril derivatives bearing electron withdrawing substituents on their convex face and least successful in the case of electron donating substituents that are able to stabilize adjacent positive charges. The recent report of the synthesis of Cy_6**CB**[6] and Cy_5**CB**[5] in 2% and 16% yields, respectively, suggests that alkyl groups may be borderline substituents for the synthesis of **CB**[*n*].[21] However, if it is desired to use a glycoluril derivative containing electron donating groups on its convex face (e.g. **1b** or **d**) for **CB**[*n*] synthesis, then it would be prudent to perform such a reaction using heterodimerization conditions (Tables 5 and 6),[16,26] involving the reaction of **1b** or **d** with, for example, **58** which is not prone to form aldehydic side products.

Conclusions

The outstanding molecular recognition properties of cucurbituril, its homologues **CB**[*n*], and its derivatives (Me_{10}**CB**[5], Cy_5**CB**[5], Cy_6**CB**[6], and Ph_2**CB**[6]) have prompted several groups to broaden the scope and define the limitations of cucurbituril synthesis. We have taken a multistep synthetic organic approach based on the identification of methylene-bridged glycoluril dimers **2*C*** and **2*S*** as the fundamental building blocks in **CB**[*n*] synthesis. We examined condensation reactions between glycoluril derivatives bearing one *o*-xylylene wall and either free ureidyl NH groups (**4a**–**d** and **16**–**24**) or cyclic ether (**5a**–**f** and **25**–**27**) groups. Three different methods, the condensation reactions of **4a**–**d** and **16**–**24** with paraformaldehyde (Table 3), the homodimerization of cyclic ethers **5a**–**f** and **25**–**27** (Table 4), and the heterodimerization reactions (Tables 5 and 6) of cyclic ethers and ureidyl NH compounds, all deliver the C- and S-shaped diastereomers in good to excellent yields with glycoluril derivatives bearing electron withdrawing carboxylic acid derivatives on their convex face. The C-shaped compound is usually formed preferentially in diastereoselective reactions. Of these three synthetic methods, we prefer the direct dimerization reaction of the ureidyl NH compounds (Scheme 3, Table 3), since it produces the C- and S-shaped dimers in similar yields and diastereoselectivities to those of the dimerization of cyclic ethers (Scheme 4, Table 4) but involves fewer synthetic steps. The heterodimerization reactions (Tables 5 and 6) are most useful when it is necessary to access methylene-bridged glycoluril dimers bearing differentially substituted rings or when substrates undergo low yielding homodimerization reactions. Glycoluril derivatives bearing phenyl and fused cyclohexyl groups are poor substrates for the dimerization reactions because they are able to stabilize adjacent positive charges leading to aldehydic side products. The development of synthetic methods for the synthesis of methylene-bridged glycoluril dimers offers the opportunity to study the fundamental steps in **CB**[*n*] synthesis[54] and the potential to expand the range of **CB**[*n*] homologues and derivatives.

Experimental Section

General. Starting materials were purchased from commercial suppliers and were used without further purification. Compounds **5a**, **b**, **e**, and **f**, **25**, **27**, **29*C***, **33*C***, **34*C***, **37*C***, **37*S***, **39*C***, **52*C***, **52*S***,[28] **29*S***,[54] as well as **12**, (±)-**21**, (±)-**53*S***, and (±)-**53*C***[64] were prepared according to literature procedures. THF and toluene were distilled from sodium benzophenone ketyl, and methylene chloride was distilled from CaH_2 immediately before use. TLC analyses were performed using precoated glass plates from Analtech or E. Merck. Column chromatography was performed using silica gel (230–400 mesh, 0.040–0.063 μm) from E. Merck using eluents in the indicated v/v ratio. Melting points were measured on a Meltemp apparatus in open capillary tubes and are uncorrected. IR spectra were recorded on a spectrophotometer as KBr pellets or thin films on NaCl plates and are reported in inverse centimeters. NMR spectra were measured at 400 MHz for ^{1}H and 100 MHz for ^{13}C. Fast atom bombardment (FAB) mass spectra were obtained using the indicated matrix. The matrix "magic bullet" is a 5:1 (w/w) mixture of dithiothreitol–dithioerythritol. Elemental analyses were performed by Midwest MicroLab (Indianapolis, IN).

Representative Experimental Procedure from Table 1 (19). Glycoluril **1a** (8.00 g, 28.0 mmol) was dissolved in anhyd DMSO (100 mL) under N_2, and *t*-BuOK (5.91 g, 52.7 mmol) was added. After stirring for 15 min, 1,2-bis(chloromethyl)-4,5-dimethylbenzene (1.26 g, 6.20 mmol) was added in one portion, and stirring was continued for 3 h. The reaction mixture was poured into 0.1 N HCl (1 L) and extracted with EtOAc (3 × 400 mL). The extracts were washed with brine (2 × 300 mL) and dried over anhyd $MgSO_4$. After filtration and rotary evaporation, the residue was purified by flash chromatography (SiO_2, $CHCl_3$/MeOH 25:1) to give **19** (1.76 g, 4.22 mmol, 68%) as a white solid. Mp 236 °C. TLC ($CHCl_3$/MeOH, 25:1) R_f 0.23. IR (KBr, cm^{-1}): 3217 s, 3019 m, 2940 m, 1710 s, 1464 m, 1368 m, 1270 m, 1145 m, 1034 s. ^{1}H NMR (400 MHz, DMSO-d_6): 8.38 (s, 2H), 6.99 (s, 2H), 4.48 (d, J = 15.8, 2H), 4.32 (d, J = 15.8, 2H), 4.19 (q, J = 7.1, 2H), 4.09 (q, J = 7.1, 2H), 2.12 (s, 6H), 1.19 (t, J = 7.1, 3H), 1.16 (t, J = 7.1, 3H). ^{13}C NMR (100 MHz, DMSO-d_6): 167.0, 166.6, 157.5, 135.6, 135.0, 130.9, 82.9, 74.4, 63.1, 62.9, 43.9, 19.2, 14.2, 14.2. MS

(55) Borzilleri, R. M.; Weinreb, S. M. *Synthesis* **1995**, 347–360. The conversion of (±)-**57d** into (±)-**35d** could also conceivably deliver the compound with the *trans*-fused glycoluril derivative, whereas this transformation would be precluded by the cyclohexyl ring of (±)-**35c**. In either case, the comparatively high energy *trans*-fused ring system has never, to the best of our knowledge, been observed in glycoluril derivatives.

(FAB, magic bullet): *m/z* 417 (100, $[M + H]^+$). HRMS (FAB, magic bullet): *m/z* 417.1774 ($[M + H]^+$, $C_{20}H_{25}N_4O_6$, calcd 417.1774). Anal. Calcd for $C_{20}H_{24}N_4O_6$ (416.17): C, 57.68; H, 5.81. Found: C, 57.66; H, 5.78.

Representative Procedure from Table 2 (5d). A mixture of **4d** (435 mg, 1.46 mmol) and paraformaldehyde (438 mg, 14.6 mmol) in TFA (5 mL) was stirred and heated at reflux for 20 h. After rotary evaporation, the residue was dissolved in EtOAc (150 mL), washed with saturated aq Na_2CO_3, dried over anhyd $MgSO_4$, and concentrated. The residue was purified by flash chromatography (SiO_2, $CHCl_3$/MeOH 50:1) to give **5d** (314 mg, 0.924 mmol, 63%) as a white solid. Mp 245−246 °C. TLC ($CHCl_3$/MeOH 50:1) R_f 0.33. IR (KBr, cm^{-1}): 2949 m, 2911 m, 2876 m, 1707 s, 1472 s, 1446 s, 1239 s, 1005 s, 740 s. ^1H NMR (400 MHz, $CDCl_3$): 7.40−7.35 (m, 2H), 7.25−7.20 (m, 2H), 5.30 (d, J = 11.3, 2H), 4.67 (d, J = 15.8, 2H), 4.54 (d, J = 11.3, 2H), 4.35 (d, J = 15.8, 2H), 2.19 (br m, 2H), 2.08 (br m, 2H), 1.66 (br m, 4H). ^{13}C NMR (100 MHz, $CDCl_3$): 157.4, 136.9, 129.8, 128.1, 71.8, 70.9, 44.0, 25.3, 24.3, 14.9, 14.8. (12 resonances expected, 11 observed). MS (FAB, magic bullet): *m/z* 341 (100, $[M + H]^+$). HRMS (FAB, magic bullet): *m/z* 341.1626 ($[M + H]^+$, $C_{18}H_{21}N_4O_3$, calcd 341.1614).

Representative Procedure for Table 3 (38*C* and 38*S*). A mixture of PTSA (0.168 g, 0.884 mmol) and $ClCH_2CH_2Cl$ (10 mL) was heated under N_2 at reflux for 30 min under an addition funnel filled with molecular sieves (4 Å). Compound **19** (92.0 mg, 0.221 mmol) and paraformaldehyde (20.0 mg, 0.663 mmol) were added, and reflux was continued for 48 h. The reaction mixture was diluted with EtOAc (150 mL), washed with saturated Na_2CO_3, dried over anhyd $MgSO_4$, and concentrated. Flash chromatography (SiO_2, $CHCl_3$/CH_3CN 20:1) gave **38*C*** (67.0 mg, 0.0782 mmol, 75%) and **38*S*** (5.2 mg, 0.0061 mmol, 6%) as white solids. Compound **38*C***: mp > 300 °C. TLC ($CHCl_3$/CH_3CN 15:1) R_f 0.22. IR (KBr, cm^{-1}): 2965 w, 1747 s, 1456 m, 1256 m, 1021 m. ^1H NMR (400 MHz, $CDCl_3$): 6.99 (s, 4H), 6.02 (d, J = 16.0, 2H), 4.79 (d, J = 16.0, 4H), 4.58 (d, J = 16.0, 2H), 4.32 (d, J = 16.0, 4H), 4.17 (m, 8H), 2.12 (s, 12H), 1.29 (t, J = 7.2, 6H), 1.24 (t, J = 7.2, 6H). ^{13}C NMR (100 MHz, $CDCl_3$): 165.7, 165.0, 154.6, 136.4, 133.5, 131.1, 80.1, 78.7, 63.7, 63.3, 47.8, 44.9, 19.2, 13.9, 13.9. MS (FAB, magic bullet): *m/z* 857 (27, $[M + H]^+$), 174 (100, $[C_{11}H_{12}NO]^+$). HRMS (FAB, magic bullet): *m/z* 857.3440 ($[M + H]^+$, $C_{42}H_{49}N_8O_{12}$, calcd 857.3470). X-ray crystal structure. Anal. Calcd for $C_{42}H_{48}N_8O_{12}$ (856.88): C, 58.87; H, 5.65. Found: C, 58.74; H, 5.60. Compound **38*S***: mp 297−299 °C. TLC ($CHCl_3$/CH_3CN 20:1) R_f 0.20. IR (KBr, cm^{-1}): 2980 w, 1766 s, 1742 s, 1720 s, 1456 s, 1424 m, 1387 s, 1308 m, 1250 m, 1157 m, 1020 m. ^1H NMR (400 MHz, $CDCl_3$): 7.07 (s, 4H), 5.00 (s, 4H), 4.74 (d, J = 16.0, 4H), 4.26 (d, J = 16.0, 4H), 4.19 (q, J = 7.1, 4H), 3.58 (q, J = 7.1, 4H), 2.16 (s, 12H), 1.25 (t, J = 7.1, 6H), 1.04 (t, J = 7.1, 6H). ^{13}C NMR (100 MHz, $CDCl_3$): 165.4, 164.2, 155.3, 136.4, 133.4, 131.1, 81.8, 78.5, 63.6, 51.8, 44.9, 19.1, 13.9, 13.6 (15 resonances expected, 14 observed). MS (FAB, magic bullet): *m/z* 857 (30, $[M + H]^+$), 174 (100, $[C_{11}H_{12}NO]^+$). HRMS (FAB, magic bullet): *m/z* 857.3490 ($[M + H]^+$, $C_{42}H_{49}N_8O_{12}$, calcd 857.3470). X-ray crystal structure. Anal. Calcd for $C_{42}H_{48}N_8O_{12}$ (856.88): C, 58.87; H, 5.65. Found: C, 58.69; H, 5.58.

Representative Procedure for Table 4 (32*C*, (±)-35d, and (±)-36d). A mixture of PTSA (760 mg, 4.00 mmol) and $ClCH_2CH_2Cl$ (5 mL) was heated at reflux for 30 min under an addition funnel filled with molecular sieves (4 Å). Compound **5d** (136 mg, 0.400 mmol) was added in one portion, and reflux was continued for 20 h. The reaction mixture was diluted with EtOAc (50 mL), washed with saturated aq Na_2CO_3, dried over anhyd $MgSO_4$, and concentrated. The residue was purified by flash chromatography (SiO_2, $CHCl_3$/MeOH 25:1) to yield **32*C*** (42.5 mg, 0.0685 mmol, 34%), (±)-**35d** (21.2 mg, 0.0624 mmol, 16%), and (±)-**36d** (14.8 mg, 0.0474 mmol, 12%) all as white solids. Compound **32*C***: mp 370 °C dec. TLC ($CHCl_3$/MeOH 25:1) R_f 0.09. IR (KBr, cm^{-1}): 2948 w, 2875 w, 1709 s, 1464 s, 1422 m, 1308 m, 1225 m, 759 m, 737 m. ^1H NMR (400 MHz, CF_3COOH, D_2O-cap.): 7.40−7.35 (br m, 8H), 6.00 (d, J = 16.6, 2H), 4.92 (d, J = 16.2, 4H), 4.73 (d, J = 16.2, 4H), 4.67 (d, J = 16.6, 2H), 2.60−2.50 (m, 8H), 2.00−1.85 (br m, 8H). ^{13}C NMR (100 MHz, CF_3COOH, D_2O-cap.): 160.8, 136.4, 131.5, 131.1, 82.4, 79.9, 46.3, 46.1, 26.0, 25.6, 16.5, 16.0. MS (FAB, magic bullet): *m/z* 621 (100, $[M + H]^+$). HRMS (FAB, magic bullet): *m/z* 621.2968 ($[M + H]^+$, $C_{34}H_{37}N_8O_4$, calcd 621.2938). Compound (±)-**35d**: mp 223−225 °C. TLC ($CHCl_3$/MeOH 50:1) R_f 0.37. IR (KBr, cm^{-1}): 2948 w, 2875 w, 1738 s, 1706 s, 1457 s, 1417 m, 1306 m, 758 m. ^1H NMR (400 MHz, $CDCl_3$): 8.93 (s, 1H), 7.40−7.30 (m, 2H), 7.30−7.20 (m, 2H), 4.79 (d, J = 15.6, 1H), 4.72 (d, J = 15.8, 1H), 4.41 (d, J = 15.6, 1H), 4.30 (d, J = 15.8, 1H), 2.86 (s, 3H), 2.50−2.20 (m, 3H), 2.10−2.00 (m, 1H), 1.70−1.50 (br m, 4H). ^{13}C NMR (100 MHz, $CDCl_3$): 160.8, 156.8, 152.9, 136.8, 135.6, 130.0, 129.3, 128.5, 128.2, 76.8, 76.2, 43.6, 43.4, 27.4, 24.7, 23.9, 14.9, 14.5. MS (FAB, magic bullet): *m/z* 341 (60, $[M + H]^+$), 55 (100). HRMS (FAB, magic bullet): *m/z* 341.1601 ($[M + H]^+$, $C_{18}H_{21}N_4O_3$, calcd 341.1614). Compound (±)-**36d**: mp 314 °C dec. TLC ($CHCl_3$/MeOH 25:1) R_f 0.27. IR (KBr, cm^{-1}): 3219 m, 2948 m, 1718 s, 1697 s, 1483 s, 1416 m, 764 m. ^1H NMR (400 MHz, $CDCl_3$): 7.35−7.10 (m, 4H), 6.06 (br s, 1H), 4.66 (d, J = 15.7, 1H), 4.64 (d, J = 15.7, 1H), 4.30 (d, J = 15.7, 1H), 4.28 (d, J = 15.7, 1H), 2.59 (s, 3H), 2.25−2.15 (m, 1H), 2.10−1.70 (m, 3H), 1.70−1.50 (m, 4H). ^{13}C NMR (100 MHz, $CDCl_3$): 158.2, 157.4, 137.3, 136.9, 129.8, 129.2, 127.9, 127.8, 77.5, 74.1, 43.6, 43.1, 27.9, 26.0, 24.5, 16.5, 16.2. MS (FAB, magic bullet): *m/z* 313 (100, $[M + H]^+$). HRMS (FAB, magic bullet): *m/z* 313.1660 ($[M + H]^+$, $C_{17}H_{21}N_4O_2$, calcd 313.1664).

Representative Procedure for Table 5 (30*C* and (±)-35b). A mixture of PTSA (5.000 g, 26.3 mmol) in $ClCH_2CH_2Cl$ (25 mL) was heated at reflux for 30 min under an addition funnel filled with molecular sieves (4 Å). Compounds **4b** (1.042 g, 2.63 mmol) and **5b** (922.7 mg, 2.11 mmol) were added, and reflux was continued for 5 days. The reaction mixture was diluted with EtOAc (100 mL), washed with saturated aq Na_2CO_3, dried over anhyd $MgSO_4$, and concentrated. The residue was purified by flash chromatography (SiO_2, $CHCl_3$/MeOH 50:1) to yield **30*C*** (282.7 mg, 0.35 mmol, 16%) and (±)-**35b** (642 mg, 1.47 mmol, 70%) as white solids. Compound **30*C***: mp 384 °C dec. TLC ($CHCl_3$/hexanes/EtOAc/MeOH 25:10:2:1) R_f 0.16. IR (KBr, cm^{-1}): 3062 w, 3034 w, 2962 w, 1734 s, 1450 s, 1426 m, 1286 m, 753 m, 697 m. ^1H NMR (400 MHz, $CDCl_3$): 7.40−7.30 (m, 8H), 7.10−6.95 (m, 6H), 6.95−6.80 (m, 10H), 6.55−6.50 (m, 4H), 5.89 (d, J = 15.4, 2H), 4.70 (d, J = 15.5, 4H), 4.03 (d, J = 15.5, 4H), 3.76 (d, J = 15.4, 2H). ^{13}C NMR (100 MHz, $CDCl_3$): 156.5, 136.4, 133.4, 132.0, 129.7, 128.8, 128.6, 128.4, 127.8, 127.6, 127.6, 86.1, 84.0, 47.7, 45.0 (16 resonances expected, 15 observed). MS (FAB, magic bullet): *m/z* 817 (30, $[M + H]^+$), 91 (100, $C_7H_7^+$). HRMS (FAB, magic bullet): *m/z* 817.3226 ($[M + H]^+$, $C_{50}H_{41}N_8O_4$, calcd 817.3251). Compound (±)-**35b**: mp 310−312 °C dec. TLC (hexanes/EtOAc 4:1) R_f 0.23. IR (KBr, cm^{-1}): 3061 w, 3024 w, 2925 w, 1746 s, 1711 s, 1461 m, 1450 m, 1303 m, 1285 m. ^1H NMR (400 MHz, $CDCl_3$): 9.19 (s, 1H), 7.40−6.90 (m, 13H), 6.75−6.60 (m, 1H), 4.95 (d, J = 15.6, 1H), 4.86 (d, J = 15.6, 1H), 4.29 (d, J = 15.6, 1H), 4.18 (d, J = 15.6, 1H), 2.93 (s, 3H). ^{13}C NMR (100 MHz, $CDCl_3$): 160.3, 157.8, 154.2, 136.6, 135.3, 132.6, 131.4, 130.0, 129.4, 129.3, 129.0, 128.8, 128.7, 128.6, 128.5, 128.2, 127.6, 127.5, 126.6, 85.9, 84.3, 45.3, 45.2, 29.5. MS (FAB, magic bullet): *m/z* 439 (72, $[M + H]^+$), 91 (100, $C_7H_7^+$). HRMS (FAB, magic bullet): *m/z* 439.1812 ($[M + H]^+$, $C_{26}H_{23}N_4O_3$, calcd 439.1770).

Representative Procedure for Table 6 ((±)-54*C* and (±)-54*S*). A mixture of PTSA (0.410 g, 2.15 mmol) in $ClCH_2CH_2Cl$ (20 mL) was heated under N_2 at reflux for 30 min under an addition funnel filled with molecular sieves (4 Å). Compound **25** (0.210 g, 0.43 mmol) and (±)-**21** (0.240 g, 0.43 mmol) were added, and heating was continued for 24 h. The reaction mixture was diluted with EtOAc (100 mL), washed with saturated Na_2CO_3, dried over anhyd $MgSO_4$, and concentrated. Flash chromatography (SiO_2, $CHCl_3$/ CH_3CN 4:1) gave (±)-

54*S* (0.24 g, 0.23 mmol, 53%) and (±)-**54*C*** (0.19 g, 0.19 mmol, 43%). Compound (±)-**54*S***: mp > 330 °C dec. TLC ($CHCl_3/CH_3CN$ 4:1) R_f 0.40. IR (KBr, cm^{-1}): 2983 w, 2936 w, 2835 w, 1717 s, 1452 s, 1390 s, 1270 s. ^1H NMR (400 MHz, $CDCl_3$): 8.00−7.95 (m, 1H), 7.90−7.80 (m, 1H), 7.80−7.70 (m, 2H), 7.13 (d, J = 8.8, 1H), 6.96 (d, J = 8.8, 1H), 6.82 (s, 1H), 6.79 (s, 1H), 5.75 (d, J = 16.2, 1H), 5.16 (d, J = 13.6, 1H), 5.07 (d, J = 13.6, 1H), 4.97 (d, J = 13.6, 1H), 4.75−4.60 (m, 4H), 4.34 (d, J = 16.2, 1H), 4.30−4.00 (m, 6H), 3.95−3.85 (m, 3H), 3.89 (s, 3H), 3.82 (s, 3H), 3.80 (s, 3H), 3.60−3.50 (m, 1H), 3.40−3.30 (m, 1H), 1.30−1.00 (m, 9H), 0.96 (t, J = 7.1, 3H). ^{13}C NMR (100 MHz, $CDCl_3$): 168.0, 167.0, 165.2, 165.1, 164.0, 163.9, 157.4, 155.3, 155.1, 154.8, 147.8, 136.3, 134.5, 134.3, 131.9, 131.3, 129.2, 128.6, 126.2, 124.1, 123.6, 122.5, 113.0, 112.9, 111.8, 81.6, 81.0, 78.8, 78.2, 64.1, 63.6, 63.4, 56.4, 55.9, 51.8, 44.7, 39.6, 36.3, 13.8, 13.6, 13.5, 13.4 (49 resonances expected, 42 observed). MS (FAB, magic bullet): m/z 1036 (100, $[M + H]^+$). HRMS (FAB, magic bullet): m/z 1036.3284 ($[M + H]^+$, $C_{49}H_{50}N_9O_{17}$, calcd 1036.3325). Compound (±)-**54*C***: mp > 330 °C dec. TLC ($CHCl_3/CH_3CN$ 4:1) R_f 0.19. IR (KBr, cm^{-1}): 2975 w, 2940 w, 2839 w, 174e, 1717 s, 1456 s, 1270 s, 1014 m, 909 m. ^1H NMR (400 MHz, $CDCl_3$): 7.95−7.90 (m, 1H), 7.85−7.80 (m, 1H), 7.70−7.60 (m, 2H), 7.13 (d, J = 8.8, 1H), 6.88 (d, J = 8.8, 1H), 6.74 (s, 1H), 6.71 (s, 1H), 6.05 (d, J = 16.0, 1H), 5.92 (d, J = 16.0, 1H), 5.62 (d, J = 16.0, 1H), 4.78 (d, J = 16.0, 1H), 4.73 (d, J = 16.5, 1H), 4.72 (d, J = 16.0, 1H), 4.64 (d, J = 16.0, 1H), 4.48 (d, J = 16.0, 1H), 4.34 (d, J = 16.0, 1H), 4.33 (d, J = 16.0, 1H), 4.25 (d, J = 16.5, 1H), 4.25−4.00 (m, 9H), 3.80 (s, 3H), 3.79 (s, 3H), 3.78 (s, 3H), 1.30−1.10 (m, 12H). ^{13}C NMR (100 MHz, $CDCl_3$): 167.8, 166.5, 165.5, 165.4, 164.7, 164.6, 157.0, 154.5, 154.4, 154.4, 154.2, 147.6, 147.5, 135.7, 134.1, 134.0, 131.5, 131.1, 129.2, 128.3, 128.2, 125.3, 123.9, 123.3, 122.1, 112.7, 112.6, 111.4, 79.9, 79.5, 78.6, 63.5, 63.3, 63.2, 56.1, 55.6, 55.5, 47.7, 47.5, 44.8, 39.8, 36.4, 13.7, 13.7, 13.6, 13.6 (49 resonances expected, 46 observed). MS (FAB, magic bullet): m/z 1036 (100, $[M + H]^+$). HRMS (FAB, magic bullet): m/z 1036.3359 ($[M+H]^+$, $C_{49}H_{50}N_9O_{17}$, calcd 1036.3325).

X-ray Crystal Structures for 30*C*, 38*C*, and 38*S*. Detailed descriptions of the data collection, solution, and refinement of the structures can be found in the Supporting Information. Crystal data for **30*C***: $[C_{50}H_{40}N_8O_4][CHCl_3]\cdot[C_7H_8]_2$ (1120.54); triclinic, space group $P\bar{1}$; colorless block, a = 14.4877(12) Å, b = 14.8574(12) Å, c = 15.1182(12) Å; V = 2787.7(4) Å^3; Z = 2; T = 193(2) K; $R(F)$ = 0.0654; GOF on F^2 = 1.082. Crystal data for **38*C***: $[C_{42}H_{48}N_8O_{12}][NCCH_3]_2$ (938.99); orthorhombic, space group $Pna2_1$; colorless block, a = 10.7933(9) Å, b = 26.350(2) Å, c = 16.7931(14) Å; V = 4776.1(7) Å^3; Z = 4; T = 193(2) K; $R(F)$ = 0.0586; GOF on F^2 = 1.065. Crystal data for **38*S***: $[C_{42}H_{48}N_8O_{12}]$ (856.88); monoclinic, space group $P2_1/c$; colorless block, a = 20.9952(17) Å, b = 16.8963(13) Å, c = 11.9470(9) Å; V = 4083.8(6) Å^3; Z = 4; T = 193(2) K; $R(F)$ = 0.0774; GOF on F^2 = 1.087.

Acknowledgment. We thank the National Institutes of Health (GM61854), the donors of the Petroleum Research Fund, administered by the American Chemical Society (33946-G4), and the University of Maryland for generous financial support. We thank the Howard Hughes Medical Institute (M.O. and J.C.) and the Dreyfus Foundation (M.O., Jean Dreyfus Boissevain Undergraduate Scholarship for Excellence in Chemistry) for undergraduate research fellowships. L.I. is a Cottrell Scholar of Research Corporation.

Supporting Information Available: Experimental procedures and spectral data for all new compounds and details of the X-ray crystal structures of **30*C***, **38*C***, and **38*S***. This material is available free of charge via the Internet at http://pubs.acs.org.

JO0258958

References

(1) Behrend, R.; Meyer, E.; Rusche, F. *Liebigs Ann. Chem.* **1905**, *339*, 1-37.

(2) Freeman, W. A.; Mock, W. L.; Shih, N. Y. *J. Am. Chem. Soc.* **1981**, *103*, 7367-7368.

(3) Mock, W. L. *Top. Curr. Chem.* **1995**, *175*, 1-24.

(4) Hoffmann, R.; Knoche, W.; Fenn, C.; Buschmann, H.-J. *J. Chem. Soc., Faraday Trans.* **1994**, *90*, 1507-1511.

(5) Lee, J. W.; Samal, S.; Selvapalam, N.; Kim, H.-J.; Kim, K. *Acc. Chem. Res.* **2003**, *36*, 621-630.

(6) Kim, K. *Chem. Soc. Rev.* **2002**, *31*, 96-107.

(7) Kim, J.; Jung, I.-S.; Kim, S.-Y.; Lee, E.; Kang, J.-K.; Sakamoto, S.; Yamaguchi, K.; Kim, K. *J. Am. Chem. Soc.* **2000**, *122*, 540-541.

(8) Day, A. I.; Arnold, A. P.; Blanch, R. J.; Snushall, B. *J. Org. Chem.* **2001**, *66*, 8094-8100.

(9) Day, A. I.; Blanch, R. J.; Arnold, A. P.; Lorenzo, S.; Lewis, G. R.; Dance, I. *Angew. Chem., Int. Ed.* **2002**, *41*, 275-277.

(10) Hubin, T. J.; Kolchinski, A. G.; Vance, A. L.; Busch, D. H. *Adv. Supramol. Chem.* **1999**, *5*, 237-357.

(11) Elemans, J. A. A. W.; Rowan, A. E.; Nolte, R. J. M. *Ind. Eng. Chem. Res.* **2000**, *39*, 3419-3428.

(12) Buschmann, H.-J.; Mutihac, L.; Jansen, K. *J. Inclusion Phenom. Macrocyclic Chem.* **2001**, *39*, 1-11.

(13) Kihara, N.; Takata, T. *Yuki Gosei Kagaku Kyokaishi* **2001**, *59*, 206-218.

(14) Robinson, T.; McMullan, G.; Marchant, R.; Nigam, P. *Bioresour. Technol.* **2001**, *77*, 247-255.

(15) Schollmeyer, E.; Buschmann, H. J.; Jansen, K.; Wego, A. *Prog. Colloid Polym. Sci.* **2002**, *121*, 39-42.

(16) Wagner, B. D. In *Handbook of Photochemistry and Photobiology*, 2003; Vol. 3, pp 1-57.

(17) Cintas, P. *J. Inclusion Phenom. Mol. Recognit. Chem.* **1994**, *17*, 205-220.

(18) Mock, W. L. In *Comprehensive Supramolecular Chemistry, Vol. 2*; Vogtle], E. F., Ed.; Pergamon: Oxford, 1996, pp 477-493.

(19) Buschmann, H. J. *Biol. Abwasserreinig.* **1997**, *9*, 101-129.

(20) Kim, K. *Perspect. Supramol. Chem.* **1999**, *5*, 371-402.

(21) Park, K.-M.; Heo, J.; Roh, S.-G.; Jeon, Y.-M.; Whang, D.; Kim, K. *Mol. Cryst. Liq. Cryst. A* **1999**, *327*, 65-70.

(22) Heo, J.; Kim, S.-Y.; Roh, S.-G.; Park, K.-M.; Park, G.-J.; Whang, D.; Kim, K. *Mol. Cryst. Liq. Cryst. A* **2000**, *342*, 29-38.

(23) Fedin, V. P.; Geras'ko, O. A. *Priroda (Moscow)* **2002**, 3-8.

(24) Gerasko, O. A.; Samsonenko, D. G.; Fedin, V. P. *Russ. Chem. Rev.* **2002**, *71*, 741-760.

(25) Han, B.-H.; Liu, Y. *Youji Huaxue* **2003**, *23*, 139-149.

(26) Sokolov, M. N.; Dybtsev, D. N.; Fedin, V. P. *Russ. Chem. Bull.* **2003**, *52*, 1041-1060.

(27) Hardie, M. J. *Struct. Bonding (Berlin)* **2004**, *111*, 139-174.

(28) Fedin, V. P. *Russ. J. Coord. Chem.* **2004**, *30*, 151-158.

(29) Kim, K.; Selvapalam, N.; Oh, D. H. *J. Inclusion Phenom. Macrocyclic Chem.* **2004**, *50*, 31-36.

(30) Buschmann, H. J.; Fink, H.; *Ger. Offen.* (Germany): DE 4001139, **1990** [*Chem. Abstr.* **1991**, *114*, 253475].

(31) Buschmann, H.-J.; Jonas, C.; Saus, W.; *Ger. Offen.* (Germany): DE 4412320, **1995** [*Chem. Abstr*. **1996**, *124*, 65677].

(32) Buschmann, H.-J.; Fink, H.; Schollmeyer, E.; *Ger. Offen.* (Germany): DE 19603377, **1997** [*Chem. Abstr.* **1997**, *127*, 205599].

(33) Day, A. I.; Arnold, A. P.; Blanch, R. J.; *PCT Int. Appl.* (Unisearch Limited, Australia): WO 2000068232, **2000** [*Chem. Abstr*. **2000**, *133*, 362775].

(34) Taketsuji, K.; Ito, R.; *Jpn. Kokai Tokkyo Koho* (Hakuto Co., Ltd., Japan): JP 2001146690, **2001** [*Chem. Abstr.* **2001**, *135*, 6819].

(35) Blum, H.; Sick, S.; Salow, H.; Kaussen, M.; *Eur. Pat. Appl.* (Germany): EP 1210966, **2002** [*Chem. Abstr*. **2002**, *137*, 21835].

(36) Richter, A. M.; Felicetti, M.; *PCT Int. Appl.* (Germany): WO 2002096553, **2002** [*Chem. Abstr*. **2003**, *138*, 8757].

(37) Richter, A. M.; Felicetti, M.; *Ger. Offen.* (Germany): DE 10040242, **2002** [*Chem. Abstr*. **2002**, *136*, 200050].

(38) Kim, K.; Jeon, Y. J.; Kim, S.-Y.; Ko, Y. H.; *PCT Int. Appl.* (Postech Foundation, S. Korea): WO 2003024978, **2003** [*Chem. Abstr*. **2003**, *138*, 264767].

(39) Kim, K.; Zhao, J.; Kim, H.-J.; Kim, S.-Y.; Oh, J.; *PCT Int. Appl.* (Postech Foundation, S. Korea): WO 2003004500, **2003** [*Chem. Abstr.* **2003**, *138*, 89832].

(40) Miyahara, Y.; *Jpn. Kokai Tokkyo Koho* (Sangaku Rentai Kiko Kyushu K. K., Japan),: JP 2003212877, **2001** [*Chem. Abstr.* **2001**, *135*, 6819].

(41) Doering, S.; Kainz, S.; Roesmann, R.; *PCT Int. Appl.* (Henkel Commanditgesellschaft Auf Aktien, Germany). WO 2004055258, **2004** [*Chem. Abstr.* **2004**, *141*, 90461].

(42) Geckeler, K. E.; Constabel, F. In *U.S. Pat. Appl. Publ.*; *U.S. Pat. Appl. Publ.* (S. Korea). US 2004167328, **2004** [*Chem. Abstr*. **2004**, *141*, 207239].

(43) Kim, K.; Balaji, R.; Oh, D.-H.; Ko, Y.-H.; Jon, S.-Y.; *PCT Int. Appl.* (Postech Foundation, S. Korea). WO 2004072151, **2004** [*Chem. Abstr.* **2004**, *141*, 207238].

(44) Lehn, J.-M. *Angew. Chem., Int. Ed. Engl.* **1988**, *27*, 89-112.

(45) Cram, D. J. *Angew. Chem., Int. Ed. Engl.* **1988**, *27*, 1009-1020.

(46) Pedersen, C. J. *Angew. Chem., Int. Ed. Engl.* **1988**, *27*, 1021-1027.

(47) *Comprehensive Supramolecular Chemistry, Vol. 1 Molecular Recognition: Receptors for Cationic Guests* (Ed.: G. W. Gokel), Pergamon, Oxford, **1996**.

(48) *Comprehensive Supramolecular Chemistry, Vol. 2 Molecular Recognition: Receptors for Molecular Guests* (Ed.: F. Vogtle), Pergamon, Oxford, **1996**.

(49) *Comprehensive Supramolecular Chemistry, Vol. 3 Cyclodextrins* (Eds.: J. Szejtli, T. Osa), Pergamon, Oxford, **1996**.

(50) Hill, D. J.; Mio, M. M.; Prince, R. B.; Hughes, T. S.; Moore, J. S. *Chem. Rev.* **2001**, *101*, 3893-4011.

(51) Cheng, R. P.; Gellman, S. H.; DeGrado, W. F. *Chem. Rev.* **2001**, *101*, 3219-3232.

(52) Wulff, W. *Chem. Rev.* **2002**, *102*, 1-27.

(53) Epstein, J. R.; Walt, D. R. *Chem. Soc. Rev.* **2003**, *32*, 203-214.

(54) Lavigne, J. J.; Anslyn, E. V. *Angew. Chem., Int. Ed.* **2001**, *40*, 3118-3130.

(55) Marquez, C.; Huang, F.; Nau, W. M. *IEEE Trans. Nanobioscience* **2004**, *3*, 39-45.

(56) Pichierri, F. *Chem. Phys. Lett.* **2004**, *390*, 214-219.

(57) Marquez, C.; Hudgins, R. R.; Nau, W. M. *J. Am. Chem. Soc.* **2004**, *126*, 5808-5816.

(58) Buschmann, H.-J.; Cleve, E.; Jansen, K.; Wego, A.; Schollmeyer, E. *Mater. Sci. Eng., C* **2001**, *C14*, 35-39.

(59) Germain, P.; Letoffe, J. M.; Merlin, M. P.; Buschmann, H. J. *Thermochim. Acta* **1998**, *315*, 87-92.

(60) Buschmann, H. J.; Cleve, E.; Schollmeyer, E. *Inorg. Chim. Acta* **1992**, *193*, 93-97.

(61) Szejtli, J. *Chem. Rev.* **1998**, *98*, 1743-1753.

(62) Trotta, F.; Zanetti, M.; Camino, G. *Polym. Degrad. Stab.* **2000**, *69*, 373-379.

(63) Buschmann, H. J.; Jansen, K.; Meschke, C.; Schollmeyer, E. *J. Solution Chem.* **1998**, *27*, 135-140.

(64) Zhang, G.-L.; Xu, Z.-Q.; Xue, S.-F.; Zhu, Q.-J.; Tao, Z. *Wuji Huaxue Xuebao* **2003**, *19*, 655-659.

(65) Jansen, K.; Buschmann, H. J.; Wego, A.; Dopp, D.; Mayer, C.; Drexler, H. J.; Holdt, H. J.; Schollmeyer, E. *J. Inclusion Phenom. Macrocyclic Chem.* **2001**, *39*, 357-363.

(66) Honig, B.; Nicholls, A. *Science* **1995**, *268*, 1144-1149.

(67) Houk, K. N.; Leach, A. G.; Kim, S. P.; Zhang, X. *Angew. Chem., Int. Ed.* **2003**, *42*, 4872-4897.

(68) Rekharsky, M.; Inoue, Y. *Chem. Rev.* **1998**, *98*, 1875-1917.

(69) Mock, W. L.; Shih, N. Y. *J. Org. Chem.* **1986**, *51*, 4440-4446.

(70) Buschmann, H. J.; Jansen, K.; Schollmeyer, E. *Thermochim. Acta* **2000**, *346*, 33-36.

(71) Fujiwara, H.; Arakawa, H.; Murata, S.; Sasaki, Y. *Bull. Chem. Soc. Jpn.* **1987**, *60*, 3891-3894.

(72) Izatt, R. M.; Terry, R. E.; Haymore, B. L.; Hansen, L. D.; Dalley, N. K.; Avondet, A. G.; Christensen, J. J. *J. Am. Chem. Soc.* **1976**, *98*, 7620-7626.

(73) Buschmann, H. J.; Cleve, E.; Jansen, K.; Schollmeyer, E. *Anal. Chim. Acta* **2001**, *437*, 157-163.

(74) Buschmann, H. J.; Cleve, E.; Jansen, K.; Wego, A.; Schollmeyer, E. *J. Inclusion Phenom. Macrocyclic Chem.* **2001**, *40*, 117-120.

(75) Buschmann, H. J.; Jansen, K.; Schollmeyer, E. *Inorg. Chem. Commun.* **2003**, *6*, 531-534.

(76) Zhang, X. X.; Krakowiak, K. E.; Xue, G.; Bradshaw, J. S.; Izatt, R. M. *Ind. Eng. Chem. Res.* **2000**, *39*, 3516-3520.

(77) Mock, W. L.; Shih, N. Y. *J. Org. Chem.* **1983**, *48*, 3618-3619.

(78) Mock, W. L.; Shih, N. Y. *J. Am. Chem. Soc.* **1988**, *110*, 4706-4710.

(79) Mock, W. L.; Shih, N. Y. *J. Am. Chem. Soc.* **1989**, *111*, 2697-2699.

(80) Meschke, C.; Buschmann, H. J.; Schollmeyer, E. *Thermochim. Acta* **1997**, *297*, 43-48.

(81) Virovets, A. V.; Blatov, V. A.; Shevchenko, A. P. *Acta Crystallogr., Sect. B* **2004**, *B60*, 350-357.

(82) Marquez, C.; Nau, W. M. *Angew. Chem., Int. Ed.* **2001**, *40*, 3155-3160.

(83) Jeon, Y.-M.; Kim, J.; Whang, D.; Kim, K. *J. Am. Chem. Soc.* **1996**, *118*, 9790-9791.

(84) El Haouaj, M.; Young, H. K.; Luhmer, M.; Kim, K.; Bartik, K. *J. Chem. Soc., Perkin Trans. 2* **2001**, 2104-2107.

(85) Whang, D.; Heo, J.; Park, J. H.; Kim, K. *Angew. Chem., Int. Ed.* **1998**, *37*, 78-80.

(86) Flinn, A.; Hough, G. C.; Stoddart, J. F.; Williams, D. J. *Angew. Chem.* **1992**, *104*, 1550-1552.

(87) Zhang, H.; Paulsen, E. S.; Walker, K. A.; Krakowiak, K. E.; Dearden, D. V. *J. Am. Chem. Soc.* **2003**, *125*, 9284-9285.

(88) Shen, Y.; Xue, S.; Zhao, Y.; Zhu, Q.; Tao, Z. *Chin. Science Bull.* **2003**, *48*, 2694-2697.

(89) Rudkevich, D. M. *Angew. Chem., Int. Ed.* **2004**, *43*, 558-571.

(90) Kellersberger, K. A.; Anderson, J. D.; Ward, S. M.; Krakowiak, K. E.; Dearden, D. V. *J. Am. Chem. Soc.* **2001**, *123*, 11316-11317.

(91) Rockwood, A. L.; Van Orman, J. R.; Dearden, D. V. *J. Am. Soc. Mass Spectrom.* **2004**, *15*, 12-21.

(92) Miyahara, Y.; Abe, K.; Inazu, T. *Angew. Chem., Int. Ed.* **2002**, *41*, 3020-3023.

(93) Buschmann, H. J.; Jansen, K.; Schollmeyer, E. *Thermochim. Acta* **1998**, *317*, 95-98.

(94) Buschmann, H.-J.; Meschke, C.; Schollmeyer, E. *Ann. Quim. Int. Ed.* **1998**, *94*, 241-243.

(95) Jansen, K.; Wego, A.; Buschmann, H.-J.; Schollmeyer, E. *Vom Wasser* **2000**, *94*, 177-190.

(96) Jansen, K.; Wego, A.; Buschmann, H.-J.; Schollmeyer, E. *Vom Wasser* **2000**, *95*, 229-236.

(97) Jansen, K.; Buschmann, H. J.; Zliobaite, E.; Schollmeyer, E. *Thermochim. Acta* **2002**, *385*, 177-184.

(98) Buschmann, H. J.; Schollmeyer, E.; Mutihac, L. *Thermochim. Acta* **2003**, *399*, 203-208.

(99) Buschmann, H. J.; Schollmeyer, E. *J. Inclusion Phenom. Mol. Recognit. Chem.* **1997**, *29*, 167-174.

(100) Neugebauer, R.; Knoche, W. *J. Chem. Soc., Perkin Trans. 2* **1998**, 529-534.

(101) El Haouaj, M.; Luhmer, M.; Ko, Y. H.; Kim, K.; Bartik, K. *J. Chem. Soc., Perkin Trans. 2* **2001**, 804-807.

(102) Wagner, B. D.; MacRae, A. I. *J. Phys. Chem. B* **1999**, *103*, 10114-10119.

(103) Wagner, B. D.; Fitzpatrick, S. J.; Gill, M. A.; MacRae, A. I.; Stojanovic, N. *Can. J. Chem.* **2001**, *79*, 1101-1104.

(104) Buschmann, H.-J.; Wolff, T. *J. Photochem. Photobiol., A* **1999**, *121*, 99-103.

(105) Liu, S.-M.; Wu, X.-J.; Liang, F.; Yao, J.-H.; Wu, C.-T. *Gaodeng Xuexiao Huaxue Xuebao* **2004**, *25*, 2038-2041.

(106) Mukhopadhyay, P.; Wu, A.; Isaacs, L. *J. Org. Chem.* **2004**, *69*, ASAP.

(107) Ma, P.; Dong, J.; Xiang, S.; Xue, S.; Zhu, Q.; Tao, Z.; Zhang, J.; Zhou, X. *Sci. China, Ser. B: Chem.* **2004**, *47*, 301-310.

(108) Wagner, B. D.; Stojanovic, N.; Day, A. I.; Blanch, R. J. *J. Phys. Chem. B* **2003**, *107*, 10741-10746.

(109) Zhang, K.-C.; Mu, T.-W.; Liu, L.; Guo, Q.-X. *Chin. J. Chem.* **2001**, *19*, 558-561.

(110) Choi, S.; Park, S. H.; Ziganshina, A. Y.; Ko, Y. H.; Lee, J. W.; Kim, K. *Chem. Commun.* **2003**, 2176-2177.

(111) Kim, H.-J.; Jeon, W. S.; Ko, Y. H.; Kim, K. *Proc. Natl. Acad. Sci. USA* **2002**, *99*, 5007-5011.

(112) Ong, W.; Gomez-Kaifer, M.; Kaifer, A. E. *Org. Lett.* **2002**, *4*, 1791-1794.

(113) Ong, W.; Kaifer, A. E. *Angew. Chem., Int. Ed.* **2003**, *42*, 2164-2167.

(114) Ong, W.; Kaifer, A. E. *J. Org. Chem.* **2004**, *69*, 1383-1385.

(115) Moon, K.; Kaifer, A. E. *Org. Lett.* **2004**, *6*, 185-188.

(116) Blanch, R. J.; Sleeman, A. J.; White, T. J.; Arnold, A. P.; Day, A. I. *Nano Lett.* **2002**, *2*, 147-149.

(117) Ong, W.; Kaifer, A. E. *Organometallics* **2003**, *22*, 4181-4183.

(118) Lorenzo, S.; Day, A.; Craig, D.; Blanch, R.; Arnold, A.; Dance, I. *CrystEngComm* **2001**, 49.

(119) Yan, K.; Huang, Z.-x.; Liu, S.-m.; Feng, L.; Wu, C.-t. *Wuhan Univ. J. Nat. Sci.* **2004**, *9*, 99-101.

(120) Wheate, N. J.; Day, A. I.; Blanch, R. J.; Arnold, A. P.; Cullinane, C.; Collins, J. G. *Chem. Commun.* **2004**, 1424-1425.

(121) Sindelar, V.; Moon, K.; Kaifer, A. E. *Org. Lett.* **2004**, *6*, 2665-2668.

(122) Marquez, C.; Nau, W. M. *Angew. Chem., Int. Ed.* **2001**, *40*, 4387-4390.

(123) Mohanty, J.; Nau, W. M. *Photochem. Photobiol. Sci.* **2004**, *3*, 1026-1031.

(124) Marquez, C.; Pischel, U.; Nau, W. M. *Org. Lett.* **2003**, *5*, 3911-3914.

(125) Constabel, F.; Geckeler, K. E. *Tetrahedron Lett.* **2004**, *45*, 2071-2073.

(126) Xu, L.; Liu, S.-M.; Wu, C.-T.; Feng, Y.-Q. *Electrophoresis* **2004**, *25*, 3300-3306.

(127) Jeon, W. S.; Kim, H.-J.; Lee, C.; Kim, K. *Chem. Commun.* **2002**, 1828-1829.

(128) Mu, T. W.; Liu, L.; Zhang, K. C.; Guo, Q. X. *Chin. Chem. Lett.* **2001**, *12*, 783-786.

(129) Kim, H.-J.; Heo, J.; Jeon, W. S.; Lee, E.; Kim, J.; Sakamoto, S.; Yamaguchi, K.; Kim, K. *Angew. Chem., Int. Ed.* **2001**, *40*, 1526-1529.

(130) Lee, J. W.; Kim, K.; Choi, S.; Ko, Y. H.; Sakamoto, S.; Yamaguchi, K.; Kim, K. *Chem. Commun.* **2002**, 2692-2693.

(131) Jeon, Y. J.; Bharadwaj, P. K.; Choi, S. W.; Lee, J. W.; Kim, K. *Angew. Chem., Int. Ed.* **2002**, *41*, 4474-4476.

(132) Liu, J.-X.; Tao, Z.; Xue, S.-F.; Zhu, Q.-J.; Zhang, J.-X. *Wuji Huaxue Xuebao* **2004**, *20*, 139-146.

(133) Chubarova, E. V.; Samsonenko, D. G.; Sokolov, M. N.; Gerasko, O. A.; Fedin, V. P.; Platas, J. G. *J. Inclusion Phenom. Macrocyclic Chem.* **2004**, *48*, 31-35.

(134) Kim, S.-Y.; Jung, I.-S.; Lee, E.; Kim, J.; Sakamoto, S.; Yamaguchi, K.; Kim, K. *Angew. Chem., Int. Ed.* **2001**, *40*, 2119-2121.

(135) Balzani, V.; Credi, A.; Raymo, F. M.; Stoddart, J. F. *Angew. Chem., Int. Ed.* **2000**, *39*, 3348-3391.

(136) Mock, W. L.; Pierpont, J. *J. Chem. Soc., Chem. Commun.* **1990**, 1509-1511.

(137) Jun, S. I.; Lee, J. W.; Sakamoto, S.; Yamaguchi, K.; Kim, K. *Tetrahedron Lett.* **2000**, *41*, 471-475.

(138) Lee, J. W.; Kim, K.; Kim, K. *Chem. Commun.* **2001**, 1042-1043.

(139) Lee, J. W.; Choi, S.; Ko, Y. H.; Kim, S.-Y.; Kim, K. *Bull. Korean Chem. Soc.* **2002**, *23*, 1347-1350.

(140) Jon, S. Y.; Ko, Y. H.; Park, S. H.; Kim, H.-J.; Kim, K. *Chem. Commun.* **2001**, 1938-1939.

(141) Ziganshina, A. Y.; Ko, Y. H.; Jeon, W. S.; Kim, K. *Chem. Commun.* **2004**, 806-807.

(142) Mock, W. L.; Irra, T. A.; Wepsiec, J. P.; Adhya, M. *J. Org. Chem.* **1989**, *54*, 5302-5308.

(143) Mock, W. L.; Irra, T. A.; Wepsiec, J. P.; Manimaran, T. L. *J. Org. Chem.* **1983**, *48*, 3619-3620.

(144) Kolb, H. C.; Finn, M. G.; Sharpless, K. B. *Angew. Chem., Int. Ed.* **2001**, *40*, 2004-2021.

(145) Tuncel, D.; Steinke, J. H. G. *Chem. Commun.* **1999**, 1509-1510.

(146) Tuncel, D.; Steinke, J. H. G. *Macromolecules* **2004**, *37*, 288-302.

(147) Tuncel, D.; Steinke, J. H. G. *Chem. Commun.* **2002**, 496-497.

(148) Krasia, T. C.; Steinke, J. H. G. *Chem. Commun.* **2002**, 22-23.

(149) Kim, K.; Jeon, W. S.; Kang, J.-K.; Lee, J. W.; Jon, S. Y.; Kim, T.; Kim, K. *Angew. Chem., Int. Ed.* **2003**, *42*, 2293-2296.

(150) Buschmann, H. J.; Gardberg, A.; Schollmeyer, E. *Textilveredlung* **1991**, *26*, 153-157.

(151) Buschmann, H. J.; Rader, D.; Schollmeyer, E. *Textilveredlung* **1991**, *26*, 157-160.

(152) Buschmann, H. J.; Gardberg, A.; Rader, D.; Schollmeyer, E. *Textilveredlung* **1991**, *26*, 160-162.

(153) Buschmann, H. J.; Carvalho, C.; Driessen, U.; Schollmeyer, E. *Textilveredlung* **1993**, *28*, 176-179.

(154) Buschmann, H. J.; Gardberg, A.; Rader, D.; Schollmeyer, E. *Textilveredlung* **1993**, *28*, 179-182.

(155) Buschmann, H. J.; Schollmeyer, E. *Textilveredlung* **1994**, *29*, 58-60.

(156) Buschmann, H. J.; Schollmeyer, E. *Textilveredlung* **1997**, *32*, 249-252.

(157) Buschmann, H. J.; Schollmeyer, E. *Textilveredlung* **1998**, *33*, 44-47.

(158) Buschmann, H. J. *Wiss. Ber. Zentralinst. Festkoerperphys. Werkstofforsch.* **1990**, *44*, 114-122.

(159) Buschmann, H. J.; Schollmeyer, E. *WLB, Wasser, Luft Boden* **1991**, *35*, 40-41.

(160) Buschmann, H. J.; Schollmeyer, E. *Textilveredlung* **1993**, *28*, 182-184.

(161) Buschmann, H. J.; Schollmeyer, E. *WLB, Wasser, Luft Boden* **1993**, *37*, 50-51.

(162) Buschmann, H. J. *Vom Wasser* **1995**, *84*, 263-269.

(163) Dantz, D. A.; Otyakmaz, O.; Buschmann, H.-J.; Schollmeyer, E. *Vom Wasser* **1998**, *91*, 305-314.

(164) Buschmann, H. J.; Schollmeyer, E. *J. Inclusion Phenom. Mol. Recognit. Chem.* **1992**, *14*, 91-99.

(165) Dantz, D. A.; Meschke, C.; Buschmann, H.-J.; Schollmeyer, E. *Supramol. Chem.* **1998**, *9*, 79-83.

(166) Karcher, S.; Kornmueller, A.; Jekel, M. *Biol. Abwasserreinig.* **1997**, *9*, 131-152.

(167) Karcher, S.; Kornmueller, A.; Jekel, M. *Acta Hydrochim. Hydrobiol.* **1999**, *27*, 38-42.

(168) Karcher, S.; Kornmuller, A.; Jekel, M. *Water Sci. Technol.* **1999**, *40*, 425-433.

(169) Karcher, S.; Kornmuller, A.; Jekel, M. *Water Res.* **2001**, *35*, 3309-3316.

(170) Kornmuller, A.; Karcher, S.; Jekel, M. *Water Res.* **2001**, *35*, 3317-3324.

(171) Taketsuji, K.; Tomioka, H. *Nippon Kagaku Kaishi* **1998**, 670-678.

(172) Taketsuji, K. *Res. Rep. Fac. Eng., Mie Univ.* **1999**, *24*, 119-120.

(173) Isobe, H.; Tomita, N.; Lee, J. W.; Kim, H.-J.; Kim, K.; Nakamura, E. *Angew. Chem., Int. Ed.* **2000**, *39*, 4257-4260.

(174) Lim, Y.-B.; Kim, T.; Lee, J. W.; Kim, S.-M.; Kim, H.-J.; Kim, K.; Park, J.-S. *Bioconjugate Chem.* **2002**, *13*, 1181-1185.

(175) Wagner, B. D.; Boland, P. G.; Lagona, J.; Isaacs, L. *J. Phys. Chem. B* **2005**, *109*, 7686-7691.

(176) Sindelar, V.; Cejas, M. A.; Raymo, F. M.; Kaifer, A. E. *New J. Chem.* **2005**, *29*, 280-282.

(177) Lagona, J.; Mukhopadhyay, P.; Chakrabarti, S.; Isaacs, L. *Angew. Chem., Int. Ed.* **2005**, *44*, 4844-4870.

(178) Pattabiraman, M.; Natarajan, A.; Kaanumalle, L. S.; Ramamurthy, V. *Org. Lett.* **2005**, *7*, 529-532.

(179) Kim, K.; Kim, D.; Lee, J. W.; Ko, Y. H.; Kim, K. *Chem. Commun.* **2004**, 848-849.

(180) Meschke, C.; Buschmann, H. J.; Schollmeyer, E. *Macromol. Rapid Commun.* **1998**, *19*, 59-63.

(181) Tuncel, D.; Steinke, J. H. G. *Chem. Commun.* **2001**, 253-254.

(182) Jeon, J. J.; Kim, H.; Jon, S.; Selvapalam, N.; Oh, D. H.; Seo, I.; Park, C.-S.; Jung, S. R.; Koh, D.-K.; Kim, K. *J. Am. Chem. Soc.* **2004**, *126*, 15944-15945.

(183) Moon, K.; Grindstaff, J.; Sobransingh, D.; Kaifer, A. E. *Angew. Chem., Int. Ed.* **2004**, *43*, 5496-5499.

(184) Liu, S.-M.; Xu, L.; Wu, C.-T.; Feng, Y.-Q. *Talanta* **2004**, *64*, 929-934.

(185) Wei, F.; Liu, S.; Xu, L.; Wu, C.; Feng, Y. *Sepu* **2004**, *22*, 476-478.

(186) Lagona, J.; Fettinger, J. C.; Isaacs, L. *Org. Lett.* **2003**, *5*, 3745-3747.

(187) Zhao, J.; Kim, H.-J.; Oh, J.; Kim, S.-Y.; Lee, J. W.; Sakamoto, S.; Yamaguchi, K.; Kim, K. *Angew. Chem., Int. Ed.* **2001**, *40*, 4233-4235.

(188) Isobe, H.; Sato, S.; Nakamura, E. *Org. Lett.* **2002**, *4*, 1287-1289.

(189) Day, A. I.; Arnold, A. P.; Blanch, R. J. *Molecules* **2003**, *8*, 74-84.

(190) Jon, S. Y.; Selvapalam, N.; Oh, D. H.; Kang, J.-K.; Kim, S.-Y.; Jeon, Y. J.; Lee, J. W.; Kim, K. *J. Am. Chem. Soc.* **2003**, *125*, 10186-10187.

(191) Chakraborty, A.; Wu, A.; Witt, D.; Lagona, J.; Fettinger, J. C.; Isaacs, L. *J. Am. Chem. Soc.* **2002**, *124*, 8297-8306.

(192) Wu, A.; Chakraborty, A.; Witt, D.; Lagona, J.; Damkaci, F.; Ofori, M. A.; Chiles, J. K.; Fettinger, J. C.; Isaacs, L. *J. Org. Chem.* **2002**, *67*, 5817-5830.

(193) Wu, A.; Chakraborty, A.; Fettinger, J. C.; Flowers, R. A.; Isaacs, L. *Angew. Chem., Int. Ed.* **2002**, *41*, 4028-4031.

(194) Wu, A.; Isaacs, L. *J. Am. Chem. Soc.* **2003**, *125*, 4831-4835.

(195) Ko, Y. H.; Kim, K.; Kang, J.-K.; Chun, H.; Lee, J. W.; Sakamoto, S.; Yamaguchi, K.; Fettinger, J. C.; Kim, K. *J. Am. Chem. Soc.* **2004**, *126*, 1932-1933.

(196) The formation of macrocycles using bis(cyclic ethers) **II-4**, **II-7**, or **II-9** alone or in combination requires the formal extrusion of formaldehyde from the reaction mixture. Since there are too many CH_2 groups present in **II-4**, **II-7**, and **II-9**, the equilibrium may not favor the formation of CB[n] derivatives.

(197) Zhao, Y.; Xue, S.; Zhu, Q.; Tao, Z.; Zhang, J.; Wei, Z.; Long, L.; Hu, M.; Xiao, H.; Day, A. I. *Chin. Sci. Bull.* **2004**, *49*, 1111-1116.

(198) The function of 3,5-dimethylphenol (**II-10**) in the reaction illustrated in Scheme 3 is to act as a formaldehyde scavenger. The CH2 group of the bis(cyclic ether) portion of **II-7** is transferred to the aromatic ring

through an electrophilic aromatic substitution mechanism. The Me groups in the 3,5-positions of the aromatic ring block cyclization reactions which would create a stable *o*-xylylene glycoluril derivative and thereby promote removal of the CH_2-O-CH_2 residues.

(199) Drew, H. D. K.; Pearman, F. H. *J. Chem. Soc.* **1937**, 586-592.

(200) Compound **II-17** is soluble in hot $MeSO_3H$, but is not soluble in refluxing $ClCH_2CH_2Cl$/PTSA. Therefore, we cannot perform these macrocyclization reactions with $ClCH_2CH_2Cl$/PTSA.

(201) Although (±)-**II-20** could be chromatographed on SiO_2 with high recovery, there were significant losses of **II-19** during SiO_2 chromatography.

(202) Burnett, C. A.; Lagona, J.; Wu, A.; Shaw, J. A.; Coady, D.; Fettinger, J. C.; Day, A. I.; Isaacs, L. *Tetrahedron* **2003**, *59*, 1961-1970.

(203) Brady, P. A.; Bonar-Law, R. P.; Rowan, S. J.; Suckling, C. J.; Sanders, J. K. M. *Chem. Commun.* **1996**, *3*, 319-320.

(204) The crude reaction mixture contains approximately 30% compound **II-37**.

(205) Analysis of the ^{1}H NMR spectra as well as TLC provides evidence that only three products result from this reaction: **II-47C**, **II-47T**, and **II-54**. This result establishes that the isomerization of the **II-47C** and **II-47T** occurs though an intramolecular mechanism because an intermolecular pathway would result in the formation of mixed dimer **II-55**.

(206) The experiments detailed here do not provide evidence of template effects operating in the formation of CB[6] analogues. An alternative rationale for the high yields observed for this 4-component macrocyclization lies in the preorganized shape of the building blocks. For example, the structural features of **II-7** and **II-17** (e.g. bond and torsional angles) are such that mixtures of these building blocks have few choices other than macrocyclization.

(207) Marquez, C. H., F.; Nau, W. M. *IEEE Trans Nanobioscience* **2004**, 39-45.

(208) Zhu, L.; Zhong, Z.; Anslyn, E. V. *J. Am. Chem. Soc.* **2005**, *127*, 4260-4269.

(209) Folmer-Andersen, J. F.; Lynch, V. M.; Anslyn, E. V. *Chem. Eur. J.* **2005**, *11*, 5319-5326.

(210) Folmer-Andersen, J. F.; Lynch, V. M.; Anslyn, E. V. *J. Am. Chem. Soc.* **2005**, *127*, 7986-7987.

(211) Houk, R. J. T.; Tobey, S. L.; Anslyn, E. V. *Top. Curr. Chem.* **2005**, *255*, 199-229.

(212) Lagona, J.; Fettinger, J. C.; Isaacs, L. *J. Org. Chem.* **2005**, *70*, in press.

(213) Smithrud, D. B.; Diederich, F. *J. Am. Chem. Soc.* **1990**, *112*, 339-343.

(214) Ngola, S. M.; Dougherty, D. A. *J. Org. Chem.* **1996**, *61*, 4355-4360.

(215) Abe, H.; Mawatari, Y.; Teraoka, H.; Fujimoto, K.; Inouye, M. *J. Org. Chem.* **2004**, *69*, 495-504.

(216) Feuster, E. K.; Glass, T. E. *J. Am. Chem. Soc.* **2003**, *125*, 16174-16175.

(217) Greene, N. T.; Morgan, S. L.; Shimizu, K. D. *Chem. Commun.* **2004**, 1172-1173.

(218) Zhang, C.; Suslick, K. S. *J. Am. Chem. Soc.* **2005**, *127*, 11548-11549.

(219) The lack of a change in the fluorescence spectrum does not rule out complex formation since host and host•guest complex could accidentally be identical. In order to provide further evidence that 1,4-butanediamine (**III-4**) does not form a stable complex with host **III-1** under our experimental conditions, a ^{1}H NMR experiment was performed. Upon mixing **III-4** and **III-1**, there were no shifts in the resonances for either **III-4** or **III-1** in the NMR spectrum.

(220) Alternatively, the less electron-rich aromatic ring may engage in more favorable π-π interactions with **III-1** relative to **III-14**.

(221) Alternatively, **27** will be partially anionic at pH 4.74; electrostatic interactions are known to strongly influence the affinity of CB[n]•guest interactions.

(222) Jeon, W. S.; Moon, K.; Park, S. H.; Chun, H.; Ko, Y. H.; Lee, J. Y.; Lee, E. S.; Samal, S.; Selvapalam, N.; Rekharsky, M. V.; Sindelar, V.; Sobransingh, D.; Inouye, Y.; Kaifer, A. E.; Kim, K. *J. Am. Chem. Soc.* **2005**, *127*, 12984-12989.

(223) Liu, S.; Ruspic, C.; Mukhopadhyay, P.; Chakrabarti, S.; Zavalij, P. Y.; Isaacs, L. *J. Am. Chem. Soc.* **2005**, *127*, ASAP.

(224) Swanson, B. I.; Shi, J.; Johnson, S.; Yang, X. *Proc. SPIE Int. Soc. Opt. Eng.* **1998**, *3270*, 25-31.

(225) Sheremata, T. W.; Hawari, J. *Hazard. Ind. Wastes* **2000**, *32*, 455-456.

(226) Sheremata, T. W.; Hawari, J. *Environ. Sci. Technol.* **2000**, *34*, 3462-3468.

(227) Yang, X.; Du, X. X.; Shi, J.; Swanson, B. *Talanta* **2001**, *54*, 439-445.

(228) Sindelar, V. C., M. A.; Raymo, F. M.; Chen, W.; Parker, S. E.; Kaifer, A. E. *Chem. Eur. J.* **2005**, *11*, 1-7.

(229) Bush, M. E.; Bouley, N. D.; Urbach, A. R. *J. Am. Chem. Soc.* **2005**, *127*, 14511-14517.

(230) Kim, K.; Balaji, R.; Oh, D.-H.; Ko, Y.-H.; Jon, S.-Y.; *PCT Int. Appl.* (Postech Foundation, S. Korea). WO 2004072151, **2004** [*Chem. Abstr.* **2004**, *141*, 207238].

(231) Peterson, B. R., Ph.D.Dissertation, University of California, Los Angeles, CA, 1994.